IMPROVING PERFORMANCE OF PORTLAND-LIMESTONE CEMENTS IN SULFATE EXPOSURES USING SUPPLEMENTARY CEMENTING MATERIALS

Seyed Sajjad Mirvalad

A Thesis
In the Department
of
Building, Civil and Environmental Engineering

Presented in Partial Fulfillment of the Requirements
For the Degree of
Doctor of Philosophy (Civil Engineering) at
Concordia University
Montreal, Quebec, Canada
November 2013

© Seyed Sajjad Mirvalad, 2013

CONCORDIA UNIVERSITY
SCHOOL OF GRADUATE STUDIES

This is to certify that the thesis prepared

By: **Seyed Sajjad Mirvalad**

Entitled: **Improving performance of Portland-limestone cements in sulfate exposures using supplementary cementing materials**

and submitted in partial fulfillment of the requirements for the degree of

Doctor of Philosophy (Civil Engineering)

Complies with the regulations of the University and meets the accepted standards with respect to originality and quality.

Signed by final examining committee

_____ Chair
Dr. Martin Pugh

_____ External Examiner
Dr. Yixin Shao

_____ External to Program
Dr. Mamoun Medraj

_____ Examiner
Dr. Lucia Tirca

_____ Examiner
Dr. Ashutosh Bagchi

_____ Thesis Supervisor
Dr. Michelle Nokken

Approved by

_____
Chair of Department or Graduate Program Director

_____ 2014

_____
Dean of Faculty

ABSTRACT

Improving performance of Portland-limestone cements in sulfate exposures using supplementary cementing materials

Seyed Sajjad Mirvalad, Doctor of Philosophy,

Concordia University, 2013

Portland limestone cement (PLC) is a recent addition to North America, promoted for its environmental benefits while maintaining suitable properties in both the fresh and hardened state. However, due to concerns regarding the degradation of concrete in sulfate exposure, especially in cold environments, its use is currently limited. In Canada, this type of cement was first introduced in 2008, but its practice in sulfate exposure was prohibited according to CSA A23.1. In 2010, CSA A3001 introduced physical requirements and suggested minimum amounts of supplementary cementing materials (SCMs) to be used for a blended PLC to be considered in sulfate exposure. Alongside, CSA A3004-C8, the standard test method for evaluating performance of cement in sulfate exposure, was revised.

In this study, different SCMs available in Canada were used in binary and ternary PLC blends in order to achieve sulfate resistance. For all PLC blends, ettringite sulfate attack (ESA) and thaumasite sulfate attack (TSA) were studied. It was found that the PLC blends containing the standard recommended amounts of SCMs were not resistant against TSA. However, when the SCM amount was increased in the blend, the desired resistance was achieved. Ternary blends of slag and fly ash were found to be the most resistant.

In addition, mass changes in ESA and TSA as well as compressive strength and ultrasonic velocity in mortar samples were studied. Moreover, a combined differential scanning calorimetry and X-ray diffraction study were performed on samples in TSA and indicated formation of thaumasite in the deteriorated samples as well as on the surface of the intact ones. Interestingly, the mortar samples of the ternary PLC blend containing 40% slag and 20% fly ash were the only ones that did not show formation of thaumasite after a two-year TSA study.

Overall, SCMs were found effective in improving the resistance of PLC blends in sulfate exposure. Additionally, it was found that, in general, the increase in the SCM content in a PLC blend promoted its resistance.

Acknowledgments

I would like to sincerely thank my advisor, Dr. Michelle Nokken, for her continuous support, valuable advice, and her nice attitude through the past four years of my life as a student at Concordia University. She never doubted my abilities and always motivated me with her patience and confidence in my efforts. A meeting with her was always a good solution for my concerns about my research; for this I am grateful to her.

I would like to thank all the people who have helped me in my life. I extend my special thanks to Dorina Banu who helped me with the differential scanning calorimetry tests. Definitely, I benefited from her knowledge and inspiration. I am also thankful of my friends in Canada and back home who supported me with their nice and meaningful words.

I am truly grateful to have an incredible family. I am sincerely thankful of my kind, caring, and wonderful parents who have always supported me in all aspects of my life. My brothers are the best brothers in the world; thank you Javad and Hossein for being what you are. I feel blessed to have a truly kind wife who has always supported me with her nice words and help; thank you dear Zahra.

Table of Contents

List of Tables

List of Figures

List of Abbreviations and Symbols

ASTM	ASTM International
CSA	Canadian Standard Association
BRE	Building and Research Establishment
CSH	Calcium Silicate Hydrate
ESA	Ettringite Sulfate Attack
FA	Fly Ash
GU	General Use Portland Cement
GUL	General Use Portland-limestone Cement
HEL	High Early Strength Portland-limestone Cement
LHL	Low Heat of Hydration Portland-limestone Cement
MHL	Moderate Heat of Hydration Portland-limestone Cement
MK	Metakaolin
NDT	Non-destructive Test
PLC	Portland-limestone Cement
S	Slag
SF	Silica Fume
SFI	Intermediate Silica Fume
SCM	Supplementary Cementing Material
TEG	Thaumasite Expert Group
TSA	Thaumasite Sulfate attack
UPV	Ultrasonic Pulse Velocity

1- Introduction

1-1- Sustainable development and Portland cement industry

Sustainable development has been an integral issue during the past few decades in all aspects of the world development, especially for large industries and production processes. Concrete is the most used construction material in the world, thus the Portland cement manufacturing industry is a principal target regarding the sustainable development issue (Mehta-2002).

Portland cement principally consists of ground clinker. Clinker is a material produced in a rotary kiln in a cement factory by mixing and heating limestone (calcareous materials), clay (argillaceous materials), and silica and iron oxide-bearing materials together. High temperature in the kiln that reaches over 1450°C leads to chemical reactions between the raw materials and formation of a new material that is called clinker (Neville and Brooks-1987).

A considerable amount of carbon dioxide is emitted during Portland cement production in factories due to fuel combustion and limestone calcination throughout chemical processes in the kiln. Therefore, one of the best ways toward greening concrete industry is to reduce the amount of cement used in construction practices or to decrease clinker component of Portland cement. During the past decades, different supplementary cementing materials have been used in concrete preparation in order to reduce the amount of cement usage in concrete.

Supplementary cementing materials (SCMs) are materials that can contribute in cementing reactions when partially replaced with cement in concrete. SCMs such as different types of natural pozzolans, slag, fly ash, silica fume and metakaolin are

beneficial in term of reducing Portland cement consumption therefore improvement of sustainable development and reduction in CO_2 emissions. Additionally, SCMs are effective in improving durability characteristics as well as fresh and hardened properties of concrete. Moreover, some SCMs are by-products of industries and their consumption in concrete enhances the sustainability of those industries.

Limestone powder is a material that even though it does not have cementing properties like SCMs, is nowadays getting widely used in Portland cements. In comparison to supplementary cementing materials, limestone powder has an additional sustainability characteristic that is its availability to all cement plants as these plants are always located beside limestone quarries (Tennis et al.-2011). Schmidt (1992) performed an investigation on three different cement manufacturing plants in Germany and reported an average of 12% reduction of CO_2 emissions by replacing 15% of clinker with limestone (Schmidt-1992; Schmidt et al.-2010). Accordingly, partially replacing cement with limestone powder can have substantial effect on reducing global CO_2 emissions and sustaining the environment.

1-2- Portland-limestone cement

Portland-limestone cement (PLC) is a cementitious material produced by either blending Portland cement with limestone ($CaCO_3$) powder or inter-grinding clinker with limestone in cement plants. This type of cement is progressively becoming widely used in the world. The key reason for developing such a cementitious material is its economical benefits and interesting sustainability characteristics since manufacturing involves lower fuel consumption and lower greenhouse gas emissions in comparison to ordinary Portland cement. Generally, cement specifications permit up to 5% limestone content in

general types of Portland cement, and classify Portland-limestone cement with higher contents of limestone.

1-3- History of using Portland-limestone cement

European countries have a long experience in using limestone powder incorporation with Portland cement since the 1960s. Portland-limestone cements are now used more than any other type of cement in European Union countries (Hooton et al.-2007). In the past few decades, several studies on production and utilization of limestone containing concrete have been performed in European countries specifically in Germany, France and England. The first standardization of limestone containing cement by the European standard was in 1987 when EN197 specified a type of cement called PKZ which consisted of 15 ± 5% limestone and 85 ± 5% clinker (Schmidt-1992). Years later, the profound practice on utilization of limestone powder in cement led to delineating different types of Portland-limestone cement by the European standard, EN197-1 (European Committee for Standardization-2000), in 2000. This standard allows replacement of Portland cement with limestone powder up to 35% by weight (EN197-1-2000). In all European countries, certain limitations for usage of Portland-limestone cement in sulfate attack conditions are defined because of poor performance of such cement against sulfate ions. For instance, in the UK, the Thaumasite Expert Group (TEG) declares "those cements in which the amount of limestone filler can range from 6% to 35%, should not be permitted in conditions where sulfate concentrations in the groundwater are in excess of 0.4 g/L" (Crammond-2003).

In North America, the concept of addition of ground limestone to Portland cement is rather new in comparison to Europe. The Canadian standard CSA A5 (Standard

specifications for Portland cement) allowed using up to 5% limestone as filler in Type 10 Portland cement (Type GU in current standard) since 1983. In 2008, CSA A3001 (CSA-2008b) introduced a new category of cement (Portland-limestone cement) containing up to 15% ground limestone, which is allowed to be used in all conditions other than sulfate exposure (CSA A23.1-2009; Thomas and Hooton-2010). This kind of Portland-limestone cement, designated as GUL in CSA A3001 (CSA-2010b), is now practically prepared with 12% to 13% limestone filler in the cement plants in Canada (Hooton et al.-2010). In the United States, the use of limestone powder in concrete was allowed for the first time in 2004 by ASTM, but up to replacement of 5% of Portland cement (ASTM C150-2004a). In 2012, ASTM C595 (ASTM-2012) introduced Portland-limestone cement with 15% replacement of clinker with limestone in the process of cement manufacture, but it is not permitted to use this type of cement as moderate sulfate resistant or high sulfate resistant cement. It should be noted that same limitation is defined by American Association of State Highway and Transportation Office in AASHTO M240.

Besides the growth in production of Portland-limestone cement in Europe and North America, utilization and production of this type of cement has been studied and practiced in many other countries with regards to amendment of cement standards. For example, Australia and New Zealand (NZS 3125) have also allowed use of 15% limestone in specific types of cements (Schneider et al.-2011). In Mexico, NMX C-414 has defined blended cements that may contain 6% to 35% limestone, and South Africa refers to EN197-1 and practices the Portland-limestone cements defined in this standard (Tennis et al.-2011).

1-4- Portland-limestone cement in the Canadian Standard

As mentioned before, 5% limestone filler was allowed in the Canadian standard in 1983 for the first time and only for ordinary Portland cement. In the current standard (CSA A3001), 5% limestone filler is allowed in all types of Portland cement including the ordinary type of Portland cement that is called general use cement (GU). Moreover, new types of Portland-limestone cements with contents of up to 15% limestone, named GUL, MHL, HEL, and LHL are introduced. These types of Portland-limestone cements, presented in Table 1-1, are typically manufactured in cement plants by inter-grinding limestone with the corresponding cement clinker. According to the Canadian concrete standard (CSA A23.1-09), none of the categorized Portland-limestone cements are allowed to be used in an environment subjected to sulfate exposure. This reflects concerns about durability of Portland-limestone cements in a sulfate environment, which is also taken into account in the European countries as well as the United States.

Table 1-1: Different types of cement defined by CSA A3001-10

Portland cement type	Blended hydraulic cement type		Portland-limestone cement type	Name – Application
GU	GUb	GULb	GUL	General use cement
MS	MSb	MSLb	-----	Moderate sulfate-resistant cement
MH	MHb	MHLb	MHL	Moderate heat of hydration cement
HE	HEb	HELb	HEL	High early-strength cement
LH	LHb	LHLb	LHL	Low heat of hydration cement
HS	HSb	HSLb	-----	High sulfate-resistant cement

1-5- Sulfate attack and performance of Portland-limestone cement

Sulfate attack is basically known as a deterioration mechanism in which sulfate ions react with calcium hydroxide and calcium aluminate hydrates, which are results of cementing reactions, and form gypsum and ettringite. This process of deterioration is

known as ordinary sulfate attack, conventional sulfate attack or ettringite sulfate attack (ESA), and typically occurs at temperatures above 15°C. This process of deterioration does not target the calcium silicate hydrates in the hydrated cement matrix. The main problem with this kind of deterioration is expansion inside the hydrated cement matrix resulting in cracks and deformation.

Another form of sulfate attack, known as thaumasite sulfate attack (TSA), targets the main part of the hydrated cement matrix, which is CSH gel, and turns it to a white non-cohesive substance called thaumasite ($3CaO•SiO_2•SO_3•CO_2•15H_2O$). This kind of attack is more severe than the other types of sulfate attack (Shi et al.-2012) and can completely disintegrate the cement paste matrix ending in incoherence of hydrated cement paste and a whole concrete structure failure. Concrete attacked by severe thaumasite sulfate attack "can be crumbled by a hammer, or even by hand" (Shi et al.-2012). Usually, the initial visual sign of thaumasite sulfate attack is formation of sub-parallel cracks filled with a white substance (Shi et al.-2012). Severe thaumasite sulfate attack in hydrated cement paste only occurs in cold (<15°C) conditions in presence of moisture, sulfate ions, carbonate ions, and active form of alumina, e.g. ettringite (Crammond-2003; Report of the Thaumasite Expert Group-1999; Sharp-2006), and when the temperature rises above 15°C, its rate of attack considerably decreases (Bensted-1999). Generally, thaumasite can form at temperatures from 15°C to 25°C but with much slower rate of formation (Report of the Thaumasite Expert Group-1999).

Normally, the predominant mode of sulfate attack to any type of Portland cement at ordinary temperatures (higher than 15°C) is ettringite sulfate attack. Sulfate ions attack calcium hydroxide and aluminate hydrates inside the hydrated cement paste and form

gypsum and ettringite, respectively. When carbonate ions are present in the system it is likely that minor amounts of thaumasite form in the paste due to thaumasite sulfate attack (Report of the Thaumasite Expert Group-1999). In cold conditions, when the temperature drops bellow 15°C, the mode of sulfate attack tends to switch to TSA depending on the amount of carbonates available in the pore solution of hydrated cement. Portland-limestone cements are highly susceptible to thaumasite sulfate attack at low temperatures because of the carbonate content of limestone powder. In such conditions, sulfate ions react with calcium silicate hydrates, carbonate ions, and water and form thaumasite (Bensted-1999). Generally, formation of thaumasite in ordinary Portland cements or general use cements is negligible because of lack of carbonate bearing components inside the system, but carbonation, ingress of carbonate ions into the hydrated cement paste, and addition of minor amounts of limestone (5% – allowed in standards) can result in formation of minor amounts of thaumasite. It should be noted that such thaumasite formation in ordinary types of cements is naturally much less destructive than cases of Portland-limestone cement. Therefore, researchers focus on TSA in Portland-limestone cements.

1-6- Decreasing the negative effects of thaumasite sulfate attack

Generally, developing concrete quality is beneficial on improving the performance against any kind of deterioration process. Therefore, lowering water to binder ratio, increasing amount of cement in the concrete mixture, improving the concrete compaction, and properly curing concrete helps in decreasing problems with thaumasite sulfate attack (Bensted-1999; Crammond-2003). All of these solutions can effectively

reduce the permeability of concrete so they minimize the possibility of seepage of destructive ions and moisture inside the concrete.

Additionally, it has been found in different research that mineral admixtures, also called supplementary cementing materials (SCMs), can impede or retard thaumasite formation in carbonate bearing concrete and mortar samples, and improve their performance against thaumasite sulfate attack (Tsivilis et al.-2003; Higgins and Crammond-2003; Mulenga et al.-2003; Skaropoulou et al.-2009; Ramezanianpour and Hooton-2013a). The principal effect of supplementary cementing materials is the refinement of the hydrated cement matrix by taking part in pozzolanic reactions and formation of secondary calcium silicate hydrate (CSH) gels. Formation of secondary CSH gels improves bonding as well as density of hydrated cement paste and reduces its porosity and permeability thus improves its resistance against ingress of ions inside the cement paste. This phenomenon can effectively develop resistance versus any type of sulfate attack. Moreover, replacement of cement with specific types of SCMs can reduce alumina content of cement, which helps formation of lower amounts of ettringite in the process of sulfate attack. In addition, pozzolanic reactions reduce the amount of calcium hydroxide ($Ca(OH)_2$) in hydrated cement paste and therefore decrease possibility of formation of gypsum and ettringite in sulfate attack.

Supplementary cementing materials are specifically beneficial in reducing the problems occurring from thaumasite sulfate attack. Pozzolans, when added to cement, react with calcium hydroxide in the hydrated cement paste and lower the calcium to silicon ratio in the CSH phase. Hydrated cement phases with lower amounts of calcium hydroxide are more resistant against thaumasite sulfate attack. Therefore, addition of

supplementary cementing materials is effectively advantageous in preparing resistant mixtures against TSA (Bellmann and Stark-2007; 2008).

1-7- Research objectives

The objectives of this research are as follows:

- Evaluate and compare performance of different Portland-limestone cements, produced in Canada, in combination with different supplementary cementing materials exposed to ettringite sulfate attack as well as thaumasite sulfate attack.
- Evaluate CSA A3001-10 recommendations for addition of SCMs to Portland-limestone cement in order to achieve high sulfate resistant PLC.
- Study effect of SCMs, available in Canada, on performance of Canadian Portland-limestone cements, and introduce sulfate resistant binary and ternary blended Portland-limestone cements.
- Assessment of the limitations assigned by the Canadian standard for expansions of prismatic mortar samples in sulfate exposures.
- Study strength development of mortar samples of blended PLC in combination with SCMs in thaumasite sulfate attack.
- Investigating deterioration inside mortar samples, prepared with blended Portland-limestone cement, during exposure to sulfate environment using UPV, DSC, and XRD techniques.

2- Literature review

Considering the fact that the focus of this experimental study is on ettringite and thaumasite sulfate attack to Portland-limestone cements blended with supplementary cementing materials, it is essential to first understand the nature and types of sulfate attack to concrete and the consequence of each mechanism of deterioration. Second, it is crucial to investigate effect of carbonates in concrete on different types of sulfate attack. Third, the role of SCMs in different mechanisms of sulfate attack is necessary to be studied. Finally, methods for detecting and studying the process of sulfate attack in concrete and mortar should be taken into consideration. In this section, previous published research on the mentioned fields is reviewed in order to establish a comprehensive state of the art for launching new research in the field.

2-1- Sulfate attack

"Sulfate attack is the term used to describe a series of chemical reactions between sulfate ions and the components of hardened concrete, principally the cement paste, caused by exposure of concrete to sulfates and moisture" (Skalny et al.-2002). It is usually known as a process of deterioration that targets concrete durability by expansion, degradation and decomposition of hydrated cement paste. In this mechanism of deterioration, sulfate ions, depending on their cation type, take part in different chemical reactions with hydrated compounds inside cement paste and result in formation of different compounds such as gypsum, monosulfoaluminate (also called monosulfate), ettringite, and thaumasite. Sulfate solutions containing Ca, Na, Mg, and Fe as the cation are the most usual types in sulfate attack (Santhanam et al.-2001).

With respect to the source of ions, sulfate attack can be characterized as internal sulfate attack and external sulfate attack. The internal sulfate attack occurs when sulfates are present inside concrete during manufacture. Cement, supplementary cementing materials, aggregates, chemical admixtures, and water are different possible sources of sulfate ions for internal sulfate attack. The other type of sulfate attack, external sulfate attack, is the most common one. In this process, sulfate solutions from various sources such as ground water, soil, solid and liquid industrial wastes, fertilizers, and atmospheric SO_3 penetrate into hydrated cement paste and start reactions associated with sulfate attack (Skalny et al.-2002).

On the other hand, external sulfate attack can be categorized as physical sulfate attack and chemical sulfate attack. Physical sulfate attack, also called salt crystallization, occurs when sodium sulfate decahydrate ($Na_2SO_4.10H_2O$) is formed in concrete pores and is followed by recrystallization as sodium sulfate anhydrite (Na_2SO_4) and vice versa. These reactions are depicted in Eq. 2-1 (a and b). The repeated recrystallization in the system leads to fatigue in the cement paste and subsequent loss of cohesion (Skalny et al.-2002). Chemical sulfate attack is the mechanism of chemical reactions between sulfate ions and concrete components. Physical sulfate attack occurs in unsaturated concrete exposed to air, often just above grade; while chemical sulfate attack occurs below grade. Chemical sulfate attack is the most recognized in the literature and is differentiated in two types; Ettringite sulfate attack (ESA) and thaumasite sulfate attack (TSA).

Eq. 2-1: $2Na^{+} + SO_4^{2-}$ ----------> $Na_2SO_4 \bullet 10H_2O$ **(a) (Skalny et al.-2002)**

(Solution) Evaporation (Solid)

$Na_2SO_4 \bullet 10H_2O$ <----------> Na_2SO_4 **(b) (Skalny et al.-2002)**

Repeated recrystallization

2-1-1- Ettringite sulfate attack (ordinary sulfate attack – conventional sulfate attack)

Ettringite sulfate attack is the most common mechanism of sulfate deterioration in which sulfate bearing solutions react with the hydrated cement matrix. Generally, the result of this type of deterioration is formation of gypsum and ettringite (Santhanam et al.-2001). The typical reactions associated with formation of gypsum and ettringite are presented in Eq. 2-2 and Eq. 2-3. Basically, sulfate ions react with calcium hydroxide and form gypsum. Following that reaction, gypsum itself reacts with calcium aluminate hydrates inside the hydrated cement paste and results in formation of ettringite. Both gypsum and ettringite are larger in volume than the reactants in this process; therefore, their formation is expansive. Accordingly, the main problem with ordinary sulfate attack lies in expansion, cracks and deformation inside the hydrated cement paste that might cause serious problems in structural concrete. Evidently, formation of cracks during this process increases the pace of deterioration by increasing concrete permeability and facilitating more sulfate bearing solution to penetrate into concrete (Santhanam et al.-2003b). Examples of formation of ettringite in hydrated cement paste are shown in Fig. 2-1, Fig. 2-2, and Fig. 2-3.

Eq. 2-2: $Ca(OH)_2 + SO_4^{2-} + 2H_2O$ ----> $CaSO_4 \bullet 2H_2O + 2OH^-$ (Hime and Mather-1999)

(Gypsum)

Eq. 2-3: $3(CaSO_4 \bullet 2H_2O) + 3CaO \bullet Al_2O_3 + 26H_2O$ ----> $3CaO \bullet Al_2O_3 \bullet 3CaSO_4 \bullet 32H_2O$

(Hime and Mather-1999)

Gypsum + tricalcium aluminate + water ----> ettringite

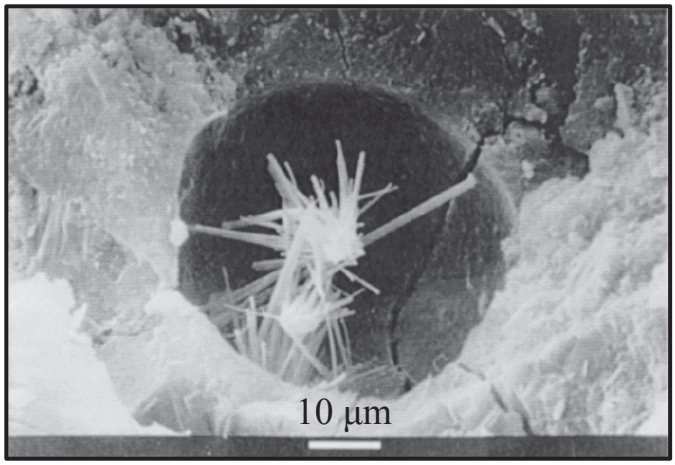

Fig. 2-1: Scanning Electron Microscopy (SEM) image depicting a crack and ettringite needles on the fractured surface of a mortar sample (After Zelić et al.-1999)

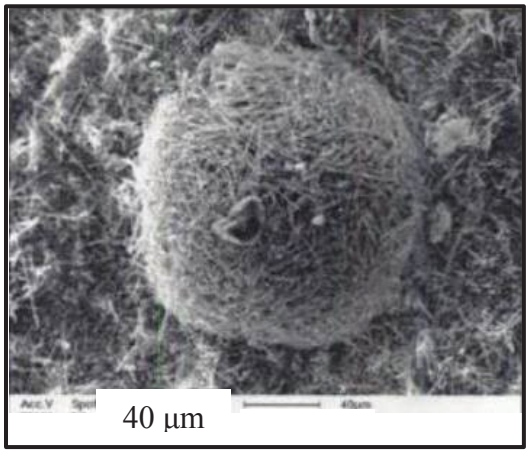

Fig. 2-2: Entrained air bubble filled with needles of ettringite – 400X

(After Scrivener and Skalny-2002)

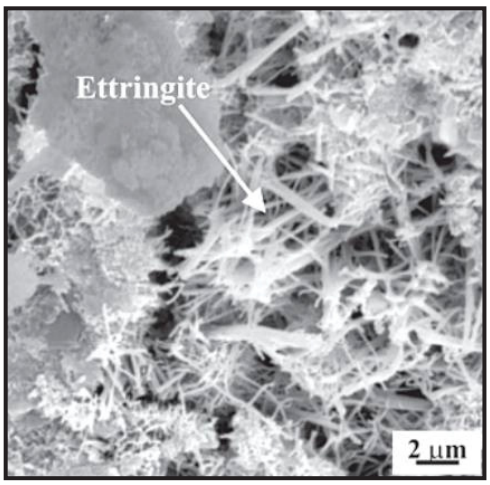

Fig. 2-3: SEM image of ettringite crystals in cement paste (Gemelli et al.-2004)

Practically, different types of sulfates such as sodium, magnesium, and potassium sulfates may be involved in ordinary sulfate attack to concrete structures. The deleterious sulfate attack reactions may be different for various types of sulfates. In the following sections, the deterioration process when different types of sulfates are present in ordinary sulfate attack is briefly discussed.

2-1-1-1- Alkali sulfate attack - Na_2SO_4 and K_2SO_4

Sodium sulfate and potassium sulfate when penetrated into concrete react with monosulfate that is formed through hydration of Portland cement. The result of this reaction is formation of ettringite (Eq. 2-4). The source of Ca^{2+} in this process is calcium hydroxide, also called Portlandite, which is produced when C_3S and C_2S (two main components of clinker) react with water through cement hydration. The main problem in this type of deterioration is expansion due to formation of ettringite. However, at high alkali sulfate concentrations, it is possible that when calcium hydroxide is consumed, the CSH gel starts to decompose to supply Ca^{2+} for further reactions (Skalny et al.-2002). In a such condition, in addition to expansion, cement paste starts to gradually lose bonding.

On the other hand, if aluminates originating from C_3A are consumed, gypsum rather than ettringite starts to be formed which is depicted in Eq. 2-5 (Skalny et al.-2002).

Eq. 2-4: $2SO_4^{2-} + Ca_4Al_2(OH)_{12}\bullet SO_4\bullet 6H_2O + 2Ca^{2+} \text{-----> } Ca_6Al_2(OH)_{12}(SO_4)_3\bullet 26H_2O$

(Monosulfate) (Ettringite)

(Skalny et al.-2002)

Eq. 2-5: $SO_4^{2-} + Ca^{2+} + 2H_2O \text{-----> } CaSO_4\bullet 2H_2O$ **(Skalny et al.-2002)**

(Gypsum)

2-1-1-2- $CaSO_4$ attack

In some areas water can contain calcium sulfate, typically from dissolved anhydrite or gypsum, and then migrate into concrete, which can cause deterioration (Skalny et al.-2002). In such situations, calcium sulfate reacts with monosulfate existing in hydrated cement paste and forms ettringite (Eq. 2-6). Unlike alkali sulfate attack, Ca^{2+} is available in the sulfate solution so portlandite or calcium silicate hydrates do not decompose. Accordingly, in this type of sulfate attack, CSH matrix remains intact.

Eq. 2-6: $4CaO\bullet Al_2O_3\bullet SO_3\bullet 12H_2O + 2Ca^{2+} + SO_4^{2-} + 24H_2O \text{----> } 6CaO\bullet Al_2O_3\bullet SO_3\bullet 32H_2O$

(Monosulfate) (Ettringite)

(Skalny et al.-2002)

2-1-1-3- $MgSO_4$ attack

Magnesium sulfate attack primarily targets calcium hydroxide in the hydrated cement paste, and forms magnesium hydroxide (Brucite) and gypsum (Eq. 2-7). Magnesium hydroxide is insoluble in water; therefore, its formation causes reduction in alkalinity of the system. CSH gel is unstable in low pH conditions, so formation of brucite leads to decomposition of CSH gel to calcium hydroxide in order to maintain

equilibrium pH in the system. As long as magnesium sulfate is available, calcium hydroxide will be attacked and this can ultimately result in a complete decomposition of calcium silicate hydrate gel and complete loss of bonding in concrete. Hence, magnesium sulfate is more deleterious than alkali sulfates when attacking concrete material. Besides formation of gypsum and brucite, ettringite can be formed in the system with presence of gypsum and monosulfate, but the main cause of deterioration is disintegration of concrete and loss of strength due to decomposition of CSH matrix rather than expansions due to formation of ettringite and gypsum (Skalny et al.-2002).

Eq. 2-7: $Mg^{2+} + SO_4^{2-} + Ca(OH)_2 + 2H_2O \text{ -----> } Mg(OH)_2 + CaSO_4 \bullet 2H_2O$

(Skalny et al.-2002)

2-1-2- Thaumasite sulfate attack

Thaumasite sulfate attack (TSA) is a term attributed to decomposition of calcium silicate hydrates of hydrated cement paste in presence of sulfate ions, carbonate ions and moisture, preferably at low temperatures (Skalny et al.-2002). In this process, CSH gel, which bonds the concrete material, gradually and constantly transforms into a soft white non-cohesive mass (Fig. 2-4 and Fig. 2-5). Consequently, in a severe form of this attack, concrete will totally disintegrate and serious structural failures may occur. Thaumasite is structurally similar to ettringite. In thaumasite, in comparison with ettringite structure, $Al(OH)_6^{3-}$ ions are replaced with $Si(OH)_6^{2-}$ ions and $(3SO_4^{2-} + 2H_2O)$ are replaced with $(2CO_3^{2-} + 2SO_4^{2-})$, (Skalny et al.-2002). Similar to ettringite, using scanning electron microscopy (SEM), thaumasite crystals could be found in cement paste (Fig. 2-6 and Fig. 2-7). Formation of these crystals as prismatic needles can cause expansion inside the hydrated cement paste. According to Bickley et al. (1994), formation of thaumasite is an

expansive reaction and, compared to ettringite formation, can be more accelerated and larger in extent.

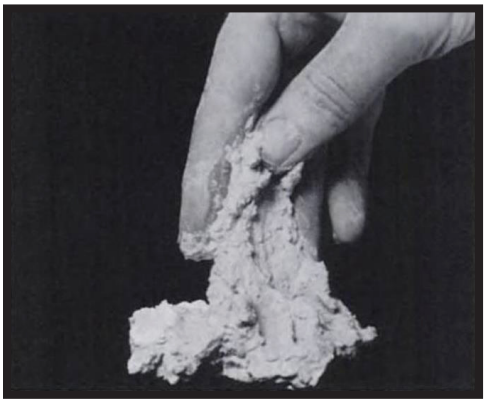

Fig. 2-4: Conversion of hardened concrete to a non-cohesive substance (Scrivener and Young-1997)

Fig. 2-5: Mortar cubes completely converted to thaumasite (Hooton-2010)

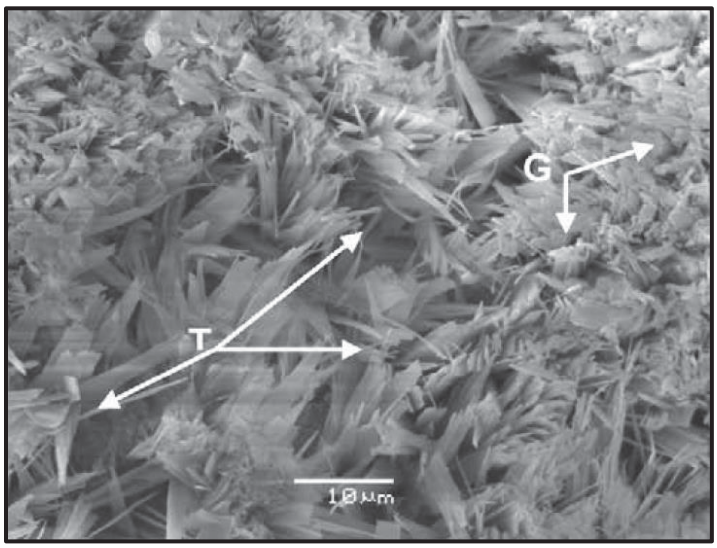

Fig. 2-6: SEM image of thaumasite sulfate attack to a cement paste during an exposure to magnesium sulfate attack at 5°C (T: thaumasite and G: gypsum) (Skaropoulou et al.-2009b)

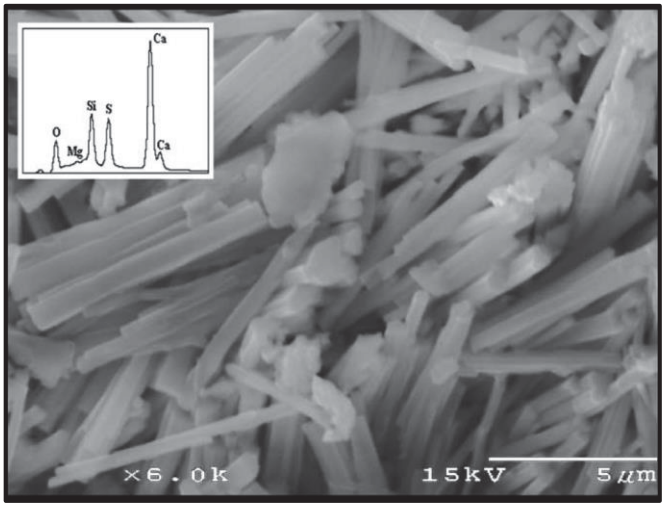

Fig. 2-7: SEM image of thaumasite crystals filling air voids of a concrete aqueduct in Manitoba (Thomas et al.-2003)

Thaumasite is a mineral found in nature with approximate composition of $3CaO•SiO_2•SO_3•CO_2•15H_2O$ (Skalny et al.-2002). This mineral was well known in the beginning of 20th century, and it was named from a Greek word that means, "to be surprised". Apparently, the scientists were surprised by its chemical composition and

crystal structure (Sharp-2006). Its occurrence in structural concrete as thaumasite sulfate attack (TSA) was first detected in 1965 (Erlin and Stark-1966), but serious concerns about it arose only after 1998, when several cases of this kind of attack were reported in buried concrete structures in the UK (Crammond-2003; Brueckner et al.-2012). Obviously, this was not a specific problem to UK, and thaumasite sulfate attack has been reported in other countries such as USA, Canada, Denmark, Italy, Hungary, Switzerland, China, and South Africa. One of the most severe TSA deterioration has been reported in the Canadian Arctic (Bickley et al.-1994; Crammond-2003). Serious concerns about thaumasite sulfate attack in recent years has led to several studies in this field of concrete deterioration in order to define restrictions in use of carbonate containing aggregates and carbonate containing cements in concrete. As an instance of these limitations, in 2001 the UK's Building Research Establishment (BRE) prohibited use of Portland-limestone cements containing more than 5% limestone filler in concrete structures exposed to groundwater with sulfate ions concentration of more than 0.4 g/L (BRE Special Digest-2001). Similar limitations were implemented in Canada (CSA A23.1-09) and in the US (ASTM C595-12).

2-1-2-1- Examples of occurrence of thaumasite formation in the world

- Eastern Transvaal, South Africa (Oberholster et al.-1984)

Thaumasite formation was identified in concrete bricks, used in construction of residential houses, in a white powdery form causing deterioration. The concrete brickwork was "made with a carbonaceous, sulfide-bearing Cummingtonite slate aggregate". Although there was no mobile water and the temperature was higher than

15°C, thaumasite sulfate attack occurred with internally available sulfate and carbonates ions.

- Formazza Valley, Italy (Berra and Baronio-1987)

The concrete lining of the diversion tunnel of the Ponte hydroelectric power station in the upper Formazza valley was affected by thaumasite sulfate attack so rigorously that concrete at some parts were completely disintegrated and detached from the surface and turned to a whitish plastic mass. Investigations showed that the temperature range inside the tunnel was constantly between 4°C and 6°C, and the humidity was almost 100%. In addition, sulfate and carbonate ions were found in water seeping in the faults of rocks of the tunnel. Consequently, overall conditions were totally favorable for formation of thaumasite.

- Resolute Bay, Canadian Arctic (Bickley et al.-1994; Bickley-1999)

Severe concrete deterioration in supporting piers of a building and parts of a slab-on-grade of a hangar, constructed in 1988, was found only after two years of casting due to thaumasite sulfate attack. Typically, the temperature in the region is below zero for 10 months in a year. It was found that carbonate bearing fine aggregates and high levels of sulfate ions in the ground water as well as cold climate resulted in a severe thaumasite sulfate attack.

- Gloucestershire, UK (Longworth-2003)

In 1998, deterioration in the concrete foundations of 30-year-old motorway bridges in Gloucestershire was found owing to thaumasite sulfate attack. “The concrete was affected to a depth of up to 50 mm”, and the surface was “transformed into a soft white mush” (Fig. 2-8).

In soil adjacent to the bridges, considerable amount of sulfate ions was found that were mostly formed due to oxidation of pyrite (FeS_2), which was present in the regional soil. The construction practice (excavation and backfilling) and soil disturbance had led to more oxidation of pyrite and development of more sulfate ions. The aggregates used in the construction were carbonate rich aggregates holding calcium carbonate and dolomite; besides, the affected areas were wet. Subsequently, "a soft white crystalline mush, composed mostly of thaumasite" was found around aggregates in TSA affected zones (Fig. 2-9).

Fig. 2-8: Damage due to TSA at the base of a 30-year old bridge column (Longworth-2003)

Fig. 2-9: Formation of thaumasite around dolomite aggregates
(Modified image – Report of the Thaumasite Expert Group-1999)

- Budapest, Hungary (Révay and Gável-2003)

The first concerns about the condition of Ferenc Puskás stadium in Budapest, constructed during 1947 to 1953, were raised in the mid-sixties, when it was found that the strength of the concrete had started to gradually decrease. The cement used in the concrete structure was produced in Hungary, and in its production limestone was added to the clinker to produce a type of Portland-limestone cement with 15% limestone filler. The deterioration due to thaumasite sulfate attack was observed in major parts of the structure. A typical damage to a concrete beam is presented in Fig. 2-10. The reinforcement is exposed on most of the parts of the beam due to disintegration of concrete.

In total, presence of considerable amounts of sulfate ions in the rainwater due to the surrounding air pollution, usual cold weather (less than 15°C), and carbonate ions presence in the concrete structure helped progress of thaumasite sulfate attack. Due to the extent of deterioration, the stadium was completely demolished in 2000.

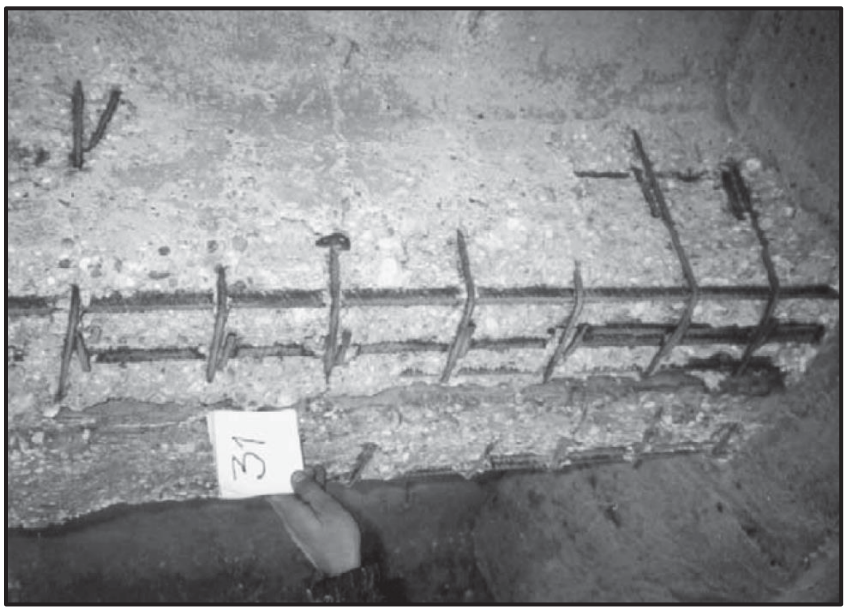

Fig. 2-10: Severe damage of concrete beam due to thaumasite sulfate attack – Ferenc Puskás stadium (Révay and Gável-2003)

- Chatham, Ontario, Canada (Thomas et al.-2003)

Extensive cracking and deterioration was found in a 33-year old concrete pavement in Ontario due to simultaneous effects of freezing and thawing and thaumasite sulfate attack. Formation of thaumasite in the form of white chalky stains was found in core samples obtained from site. Thaumasite had extensively filled the air void system in the hydrated cement matrix as can be seen in Fig. 2-11. The de-dolomitization process in dolostone coarse aggregate supplied enough carbonates, and presence of sulfide in the shale used as fine aggregate provided sulfur for development of thaumasite in the concrete pavement.

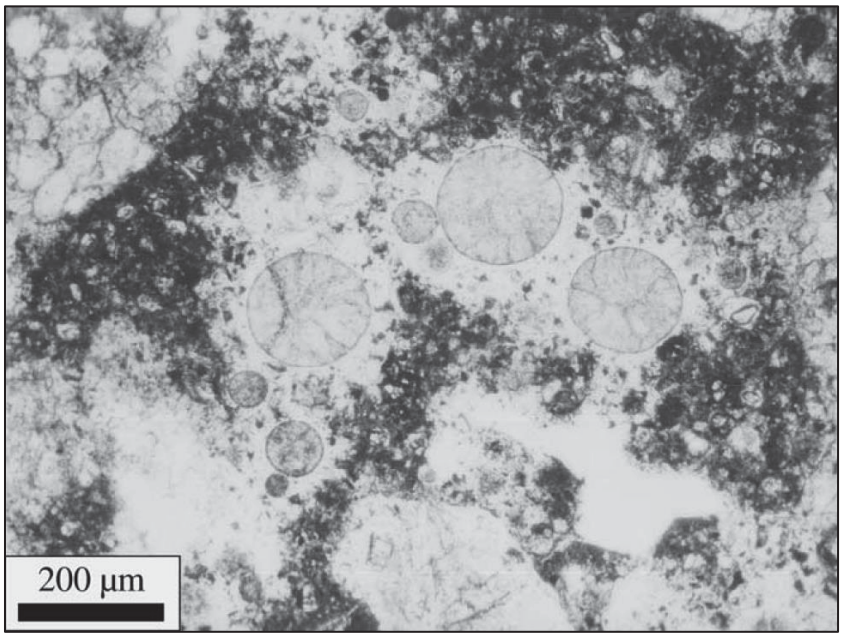

Fig. 2-11: A section of the pavement concrete sample showing formation of thaumasite in hydrated cement paste and air voids (Thomas et al.-2003)

- Manitoba, Canada (Thomas et al.-2003)

Thaumasite sulfate attack was identified in a 156-km long concrete aqueduct in Manitoba, which was built between 1915 and 1919. Thaumasite was found to form inside cracks occurred due to deterioration and the air voids near cracks. Sulfate ions in ground water adjacent to the structure as well as carbonate ions present inside concrete because of the usage of carbonate dust as aggregate filler were the main causes of thaumasite sulfate attack to the structure.

- Copenhagen, Denmark (Eriksen-2003)

Serious signs of attack were found in concrete columns and stairs of the waterworks in Marbjerg near Copenhagen in Denmark in 1997 (Fig. 2-12). During inspections, spalling and exfoliation was found in parts of the concrete structure that were

wet. A whitish to brownish soft and greasy material was found on the surface of concrete, which could be easily peeled off by hand.

Thaumasite sulfate attack was found to be the main cause for deterioration. The surrounding humid air temperature was constantly 5°C to 8°C in the structure, and it was found that hydrogen sulfide in the surrounding air was the source of sulfate ions which took part in reactions leading to formation of thaumasite.

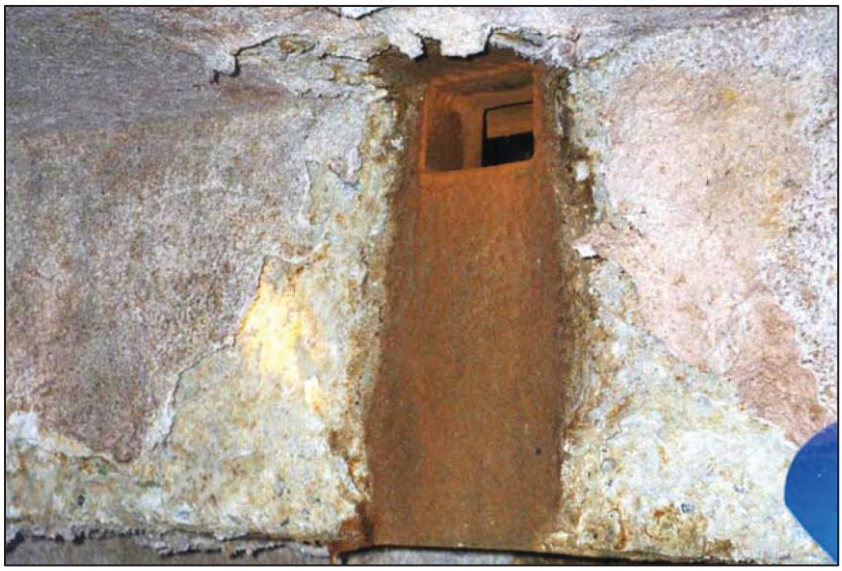

Fig. 2-12: Concrete spalling due to thaumasite sulfate attack in waterworks construction in Copenhagen, Denmark (Eriksen-2003)

- Switzerland (Romer et al.-2003)

Several deteriorated tunnel constructions in Switzerland were investigated by Romer et al. (2003). It was detected that generally deterioration in shotcrete linings of tunnels occurred due to presence of sulfate bearing ground water. Thaumasite formation was found mainly where the sulfate and carbonate bearing ground water was in contact with porous concrete. Many cases of deterioration due to thaumasite sulfate attack were spotted near the drainage system as can be seen in Fig. 2-13.

Fig. 2-13: Concrete altered into a soft mush like material on base of a tunnel lining in contact with drainage water (Romer et al.-2003)

- Lanzhou, China (Ma et al.-2006)

A tunnel in the Bapanxia hydraulic power plant, constructed in 1970's, in China was investigated and deterioration owing to thaumasite sulfate attack was found in drainage channels where expansion, cracking and softening in concrete was observed. At some points concrete lost its integrity completely and "cement paste transformed into a white, pulpy mass with no strength" as seen in Fig. 2-14. Groundwater in the region contains noticeable amounts of sulfate and carbonate ions. The relative humidity in the tunnel is more than 85%, and the temperature within the tunnel ranges between 4°C to 10°C. Carbonation on surface of concrete was found as another source for carbonate ions. All the visual observations and field investigations along with laboratory study on site samples confirmed severe thaumasite sulfate attack in the structure.

Fig. 2-14: Thaumasite sulfate attack found in drainage channels in form of development of a white pulpy mass (Ma et al.-2006)

- Xingjiang, China (Mingyu et al.-2006)

Thaumasite sulfate attack was found in the concrete slabs of Yongan dam in Xingjiang, which were in contact with groundwater. In less than a year after construction finished, "it was found that the slabs had became grey and mushy throughout the thickness where they contacted with groundwater". An image of a typical degradation of the concrete slabs is shown in Fig. 2-15. According to XRD analysis, thaumasite sulfate attack was found to be the primary type of attack to the concrete.

The main reasons found for such fast deterioration were usage of an ordinary Portland cement containing 9% limestone filler in construction of the dam, presence of great amounts of sulfate salts in the region's soil as well as the mixing water, and frequent low temperature in the area. All these factors were in favor of an intense thaumasite sulfate attack.

Fig. 2-15: Concrete slab of Yongan dam damaged by TSA (Mingyu et al.-2006)

- Chuxiong, China (Long et al.-2011)

Thaumasite sulfate attack was detected in the severely deteriorated concrete lining of a tunnel constructed in 1960's in the form of soft, white, mushy powder and a light grey mud (Fig. 2-16 and Fig. 2-17). Sulfate ions were found available in groundwater in contact with the concrete as well as coal powder scattered in tunnel due to movement of trains loading coal through the tunnel. The annual average temperature in the area was 12°C, and the environment was humid, making favorable condition for formation of thaumasite and causing swelling and flaking on concrete surface.

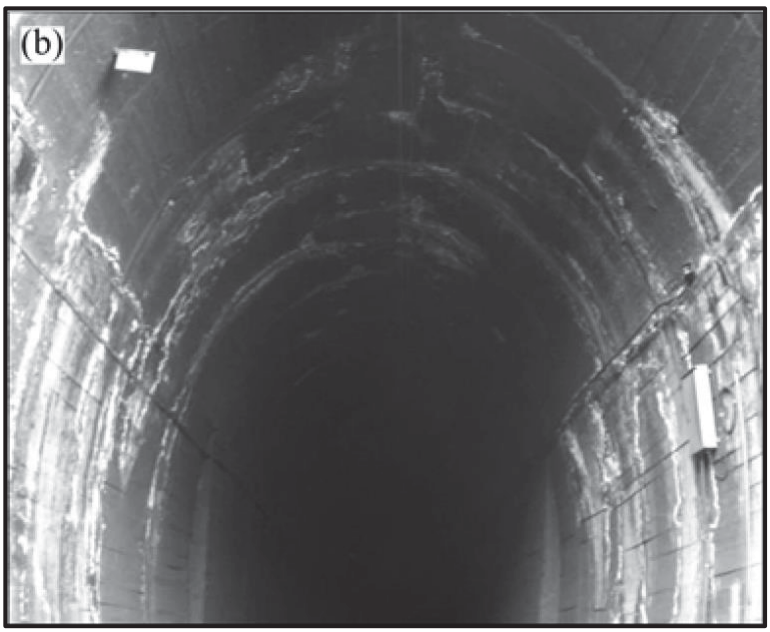

Fig. 2-16: General image of deteriorated tunnel in Chuxiong, China (Long et al.-2011)

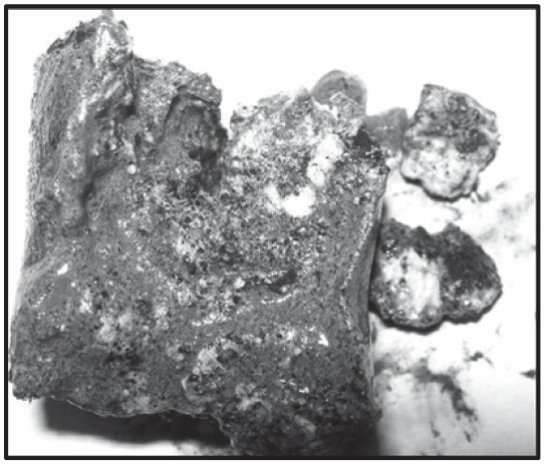

Fig. 2-17: Development of whitish soft material in core sample due to thaumasite sulfate attack (Long et al.-2011)

2-1-2-2- Reactions associated with thaumasite sulfate attack

It has been shown and proven that formation of thaumasite is associated with formation of ettringite in cement paste. Thus, presence of alumina in cement paste helps the reactions through formation of thaumasite. Thaumasite and ettringite have almost similar chemical structures. As mentioned previously, thaumasite can form from

ettringite by the interchange of [Si] for [Al] and [CO_3^{2-} + SO_4^{2-}] for [SO_4^{2-} + H_2O] (Eq. 2-8). It should be noted that sometimes a part of aluminum can be present in the final structure of thaumasite (Bensted-1999). Because of the similarity in mineral structure of ettringite and thaumasite, thaumasite can nucleate on surface of ettringite and grow to large volume very fast (Köhler et al.-2006). When thaumasite forms, the aluminum ion is released and can take part in formation of ettringite. The chemical interchange and thaumasite nucleation explained, this triggers formation of thaumasite in the paste and pore solution, and thaumasite sulfate attack can progress regardless of further existence of ettringite. In other words, ettringite is only needed for initial nucleation of thaumasite (Crammond-2003). Although formation of ettringite is helpful in nucleation of thaumasite, it can be formed directly in presence of CSH, Ca^{2+}, SO_4^{2-}, CO_2, and water as shown in Eq. 2-9 (Bensted-1999), but it is believed that formation of thaumasite without presence of ettringite is extremely slow, and "ettringite considerably controls the rate of thaumasite formation" (Köhler et al.-2006).

Eq. 2-8: $Ca_6[Al(OH)_6]2(SO_4)_3 \bullet 26H_2O + Ca_3Si_2O_7 \bullet 3H_2O + CaCO_3 + CO_2 + xH_2O$ ----> $Ca_6[Si(OH)_6]_2(CO_3)_2(SO_4)_2 \bullet 24H_2O + CaSO_4 \bullet 2H_2O + Al_2O_3 \bullet xH_2O + 3Ca(OH)_2$ **(Bensted-1999)**

Eq. 2-9: $Ca_3Si_2O_7 \bullet 3H_2O + 2\{CaSO_4 \bullet 2H_2O\} + CaCO_3 + CO_2 + 23H_2O$ ----> $2Ca_6[Si(OH)_6]_2(CO_3)_2(SO_4)_2 \bullet 24H_2O$ **(Bensted-1999)**

Commonly, sulfate ions, when diffused inside concrete, can take part in chemical reactions resulting in formation of gypsum, ettringite, monosulfate, and thaumasite. At cold temperatures (preferably lower than 15°C) and in presence of sulfate ions, carbonate or bicarbonate ions, calcium ions, silicate ions, and moisture, thaumasite can theoretically

start to form (Bensted-1999). Thaumasite is very insoluble at cold temperatures (Crammond-2003). Accordingly, considering the fact that its formation involves the depletion of $Ca(OH)_2$ in pore solution, it reduces the pH of the paste and results in instability of CSH gel. Therefore, CSH gel, which is the main part of cement paste providing bonding, dissolves in the lowered pH pore solution. This phenomenon along with depletion of CSH gel due to chemical reactions that end in formation of thaumasite, results in disintegration of the cement paste. This disintegration lasts as long as sources of carbonates and sulfates are available in the system and a cold, moist environment is maintained (Crammond-2003).

2-2- Standard tests for evaluation of sulfate resistance of concrete

Sulfate attack is a complicated deterioration process that appears in various forms and modes and may emerge with different visual signs. Chemical reactions, compounds formed, and physical property changes through sulfate attack depend on the exposure condition, materials used in concrete, and the sulfate cation that attacks concrete. Additionally, sulfate attack to concrete may result in several characteristic changes such as mass loss, change in compressive strength, dimensional changes, and visual condition alterations. Correspondingly, it is not practical to devise a unique test procedure for studying and evaluating sulfate attack on concrete. In order to have a brief overview of the standards tests' criteria, in the following paragraphs standard tests on sulfate attack developed by ASTM International and Canadian Standards Association (CSA) are reviewed.

ASTM C452 (ASTM-2006) test method is a fast one in comparison to the other standard test methods on sulfate attack, and studies sulfate attack to solely Portland

cement when sulfates are internally available. In this test, 25x25x285 mm mortar prisms are prepared with Portland cement that is mixed with gypsum in such proportion that the whole mixture contains 7.0% sulfur trioxide (SO_3) by mass. After 22-23 hours, samples are removed from molds and immersed in water at 23°C for 14 days. The length change of the samples after 14 days is an indicator of resistance of cement against sulfates. The ASTM C150 (ASTM-2007) has a defined expansion limit (0.040%) for sulfate resistant Portland cement (Type V). The limitation of the test is that it is only applicable to Portland cement, and it studies internal sulfate attack, which is not the case in majority of sulfate attack instances. Considering these limitations, ASTM C150 refers to this test only for evaluating suitability of Type V Portland cement.

ASTM C1012 (ASTM-2004b) is a test measuring the length change of 25x25x285 mm prismatic mortar samples immersed in 5% sodium or magnesium sulfate solutions. The test specifies particular intervals for measuring the length of the samples and renewing the sulfate solution. Considering this test, ASTM C1157 (ASTM-2008b) assigns expansion limitations for moderate sulfate resistant Portland cement and high sulfate resistant Portland cement (Table 2-1). Also, ASTM C595 (ASTM-2008a) specifies limitations for expansion of moderate and high sulfate resistant blended cements (Table 2-2).

Table 2-1: Expansion limitations for ASTM C1012 test (ASTM C1157-08)

	Moderate Sulfate Resistant Cement	High Sulfate Resistant Cement
6 months (%)	0.10	0.05
12 months (%)	…	0.10

Table 2-2: Expansion limitations for ASTM C1012 test (ASTM C595-08)

	Moderate Sulfate Resistant Blended Cement Type IS* and IP**	High Sulfate Resistant Blended Cement Type IS* and IP**
6 months (%)	0.10	0.05
12 months (%)	…	0.10

*** Type IS—Portland blast-furnace slag cement**

**** Type IP—Portland-pozzolan cement**

The sulfate attack tests introduced by ASTM only target expansion of mortar samples at 23°C. Therefore, these tests evaluate ettringite sulfate attack and do not quantify the thaumasite sulfate attack that is only dominant at low temperatures, particularly lower than 15°C (Crammond-2003). The Canadian standard CSA A3004-C8 (CSA-2010c) has resolved this shortcoming in April 2010. CSA A3004-C8-10 presents two procedures for testing of sulfate attack. The first one, procedure A, is sulfate attack at standard temperature (23°C). This procedure determines the resistance against formation of ettringite and gypsum as these are the dominant materials formed during the process of sulfate attack at temperatures above 15°C. The second one, procedure B, is performed at 5°C, and evaluates the resistance against thaumasite sulfate attack. It should be mentioned that the most favorable temperature for formation of thaumasite is found around 5°C (Bensted-1999 and Skalny et al.-2002). Both procedures A and B are practically the same as ASTM C1012, and the most integral difference is the defined ambient temperature.

According to CSA A3004-C8, the 25x25x285 mm prismatic mortar samples are cured in their molds for 24 hours at 35 ± 3°C and thereafter in limewater at 23°C until the compressive strength of 50x50x50 mm mortar cubes, prepared at the same time, reaches

20±1 MPa. Then, the samples are placed in 50 g/L sodium sulfate solution at 23°C (Procedure A) and 5°C (Procedure B). The length of the samples are initially measured prior to the exposure to sodium sulfate solution, and the following measurements will be at 1, 2, 3, 4, 8, 13, 15 weeks followed by 4, 6, 9, 12, 15, 18, 21, and 24 months after placement in the solution. At each length change measurement, the solution is renewed.

Similar to ASTM, the Canadian standard has defined sulfate resistant cements according to the expansion test method. CSA A3001-10 has defined expansion limitations for blended hydraulic cements, and blended Portland-limestone cements when tested according to CSA A3004-C8. These limitations are shown in Table 2-3.

Table 2-3: Expansion limitations for mortar samples studied according to test CSA A3004-C8 (CSA A3001-10)

	MSb and MSLb*	HSb and HSLb*	Reference
Maximum expansion at 6 months (%)	**0.10**	**0.05**§	**CSA A3004-C8 Procedure A**
Maximum expansion at 18 months (%)	**0.10****	**0.10****	**CSA A3004-C8 Procedure B**

*: MSb stands for moderate sulfate resistant blended hydraulic cement
HSb stands for high sulfate resistant blended hydraulic cement
MSLb stands for moderate sulfate resistant blended Portland limestone cement
HSLb stands for high sulfate resistant blended Portland limestone cement
**: If the increase in expansion between 12 and 18 months exceeds 0.03%, the sulfate expansion at 24 months shall not exceed 0.10% in order for the cement to be deemed to have passed the sulfate resistance requirement.
§: If the expansion is greater than 0.05% at 6 months but less than 0.10% at 1 year, the cement shall be considered to have passed.

2-3- Review of Sulfate attack to concrete containing limestone filler or aggregates

As mentioned before, sulfate attack can be extremely deleterious when carbonates are available in the system and conditions favor thaumasite formation. In this section,

research on sulfate attack to concrete containing carbonates in the form of aggregates or cement is to be reviewed as well as the effect of supplementary cementing materials on sulfate attack to concrete material. Also, there will be a review on the ways of improving concrete resistance against thaumasite sulfate attack.

2-3-1- Thaumasite sulfate attack in presence of carbonate bearing aggregates in concrete

Many researchers have investigated the effect of carbonate bearing aggregates on the onset and progress of thaumasite sulfate attack. As carbonates are a part of process of thaumasite formation, now it is clear that carbonate bearing aggregates effectively increase formation of thaumasite in concrete attacked by sulfate ions.

Crammond and Nixon (1993) showed that even with carbonate free cements, thaumasite sulfate attack could initiate and progress in presence of carbonate containing aggregates. In order to investigate the effect of limestone aggregates on thaumasite sulfate attack, they obtained sound concrete samples prepared with sulfate resistant cement and limestone aggregates from a pile exposed to sulfate bearing soil and stored the samples in 1.8% magnesium sulfate solution as well as 1.8% sodium sulfate solution at 5°C. The deterioration due to thaumasite sulfate attack was found after 8 months of exposure in form of cracks. “The degradation process continued in a rapid rate and after 18 months storage at 5°C about a quarter of each of the samples had eroded away to form a fine-grained sludge on the bottom of the storage containers”. Crammond and Nixon (1993) also prepared 10x40x160 mm mortar samples with sulfate resistant Portland cement and two different types of fine aggregates (pure quartz and limestone crushed aggregate) in order to investigate thaumasite sulfate attack. After demoulding, samples

were water cured for 14 days then immersed in 1.8% magnesium sulfate solution at 5°C. After a year of thaumasite sulfate attack, mortar samples containing quartz aggregate were found visually intact while the ones prepared with limestone aggregate were completely disintegrated. The results of this study indicate that sulfate resistant cement was insufficient to prevent TSA. It should be noted that sulfate resistant Portland cements are resistant against ordinary sulfate attack and formation of ettringite as amount of C_3A is reduced in such cements. However, in formation of thaumasite, calcium silicate hydrates are attacked instead of aluminates. Therefore, in general, sulfate resistant cement will not be effective in resistance against TSA.

Brueckner et al. (2012) studied thaumasite sulfate attack on cylindrical concrete samples prepared with limestone aggregates in combination with regular Portland cement immersed in 1.8% magnesium sulfate solution at 5°C for 27 months. In their research, the onset of TSA in samples was reported after a dormant period of 6 months. Accordingly, TSA is possible to occur in the presence of limestone aggregates in concrete. Sotiriadis et al. (2012) examined durability characteristics of concrete cubes when limestone aggregate and limestone filler are simultaneously present in concrete. Different concrete mixes containing 0% (PC), 15% (LC1), and 35% (LC2) limestone powder were prepared in the lab by inter-grinding clinker, limestone, and gypsum. The concrete cubes were immersed in 2% magnesium sulfate solution for 24 months at 5°C, and visual condition, compressive strength, and mass loss of concrete cubes were inspected periodically. Evolution of thaumasite was found in all samples during the 24-month study. Also, it was evident that increase in limestone content resulted in more severe deterioration from the point of view of visual condition, mass loss, and compressive strength loss. Fig. 2-18

shows the visual condition of concrete cubes, and Fig. 2-19 depicts the mass changes during the 2-year immersion in magnesium sulfate solution at 5°C.

Fig. 2-18: Deterioration of concrete specimens containing limestone as aggregate and filler during 24 months of exposure to magnesium sulfate solution at 5°C (Sotiriadis et al.-2012)

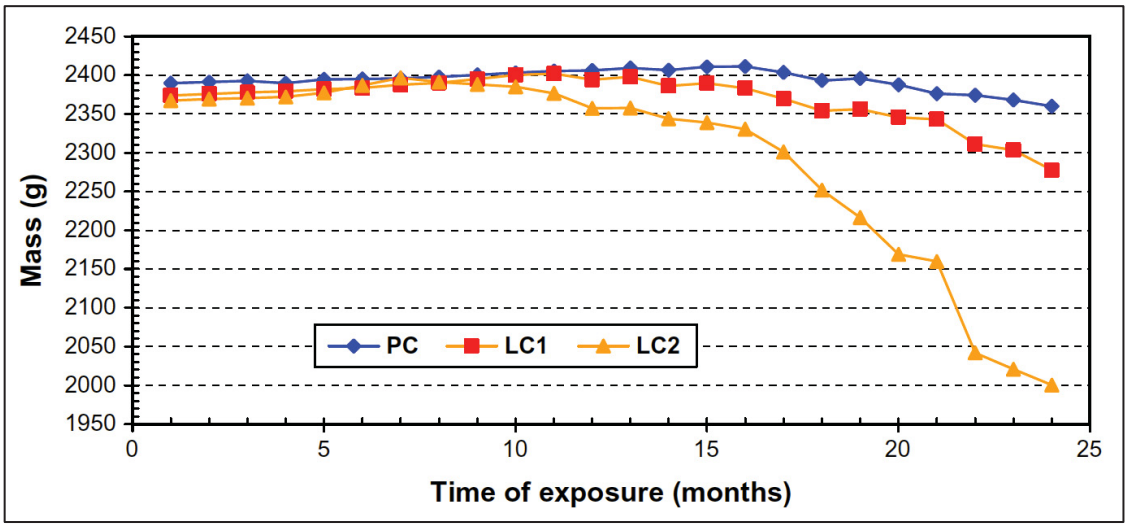

Fig. 2-19: Mass changes of concrete specimens containing limestone as aggregate and filler during 24 months of exposure to magnesium sulfate solution at 5°C (Sotiriadis et al.-2012)

2-3-2- Thaumasite sulfate attack and ettringite sulfate attack in presence of ground limestone filler in concrete

As the tendency in usage of limestone filler has increased in recent years, several researchers have focused on ettringite and thaumasite formation in mortar and concrete containing limestone filler. Matthews (1994) indicated that at 20°C the mode of sulfate attack in concrete prepared with 25% of different types of limestone filler is predominantly related to ettringite formation rather than thaumasite formation. So, the amount of C_3A in cement was found to be the main factor ruling the deterioration due to sulfate attack at 20°C. Therefore, Matthews (1994) concluded that limestone addition to cement does not have a consistent effect on the performance of concrete against sulfate attack at ordinary temperatures. Limestone addition to cement, depending on many factors, can slightly improve or worsen concrete performance in ordinary sulfate exposures.

Gonzalez and Irassar (1998) studied effect of addition of limestone filler (10% and 20%) on resistance of mortars against ettringite sulfate attack. Mortar prisms were prepared with Type II and Type V cement, and their expansion was measured according to ASTM C1012 for one year (Fig. 2-20). They concluded that addition of 20% limestone powder to both sulfate resistant cement and Type II cement leads to a considerable increase in expansion of mortar prisms, but 10% addition does not have such effect. In addition, their experiments showed 40% and 20% reduction in compressive strength of 25 mm mortar cubes after a one-year exposure to sodium sulfate solution for Type II cement containing 20% and 10% limestone filler, respectively.

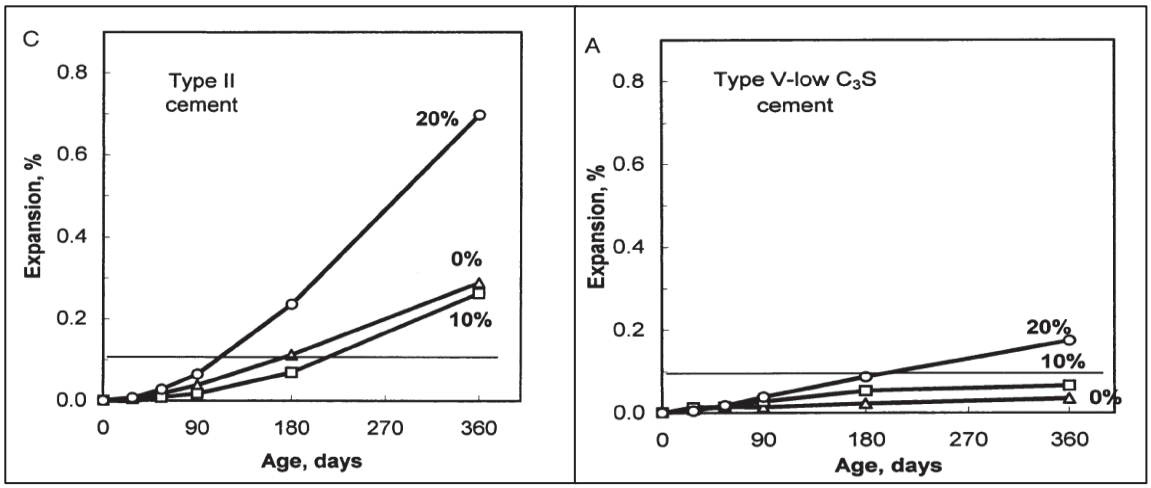

Fig. 2-20: Mortars expansions – ASTM C1012 (Gonzalez and Irassar-1998)

Barker and Hobbs (1999) found that presence of limestone filler in cement can change the mode of sulfate attack from ESA to TSA. In their research, they investigated both ettringite sulfate attack and thaumasite sulfate attack. They used a sulfate resistant Portland cement, a Portland cement with 10% C_3A by mass, and two inter-blended cements containing 15% by mass of a carboniferous and an oolitic limestone in preparation of 40x40x160 mm mortar prisms. The mortar prisms were immersed in either sodium sulfate or magnesium sulfate solution at 5°C for 12 months after 28 days of curing in water at 20°C. According to X-ray diffraction, Barker and Hobbs (1999) reported that both ettringite and thaumasite formed in Portland-limestone cement samples and mode of sulfate attack to these samples was TSA while Portland cement samples were mainly attacked by ettringite and gypsum formation and their mode of deterioration was ESA.

Torres et al. (2003) studied sulfate attack to 40x40x160 mm mortar prisms made by mixing Portland cement with limestone powder at 5%, 15%, and 35% replacement by mass and reported formation of thaumasite. In their research, the samples were water

cured for 28 days, then some of them were exposed to air at 5°C and 20°C and others submerged in 1.8% magnesium solution at 5°C for 5 years (the samples in solution were let to gradually dry in the last year of the study). Their visual inspections showed that samples immersed in magnesium sulfate solution experienced "progressive deterioration which increases with limestone content" (Fig. 2-21). Using X-ray diffraction, infrared spectroscopy, and scanning electron microscopy (SEM) tests, the researchers characterized thaumasite in all samples immersed in sulfate solution at 5°C. As an instance, in Fig. 2-22 thaumasite crystals formed in samples containing 5% limestone filler are depicted.

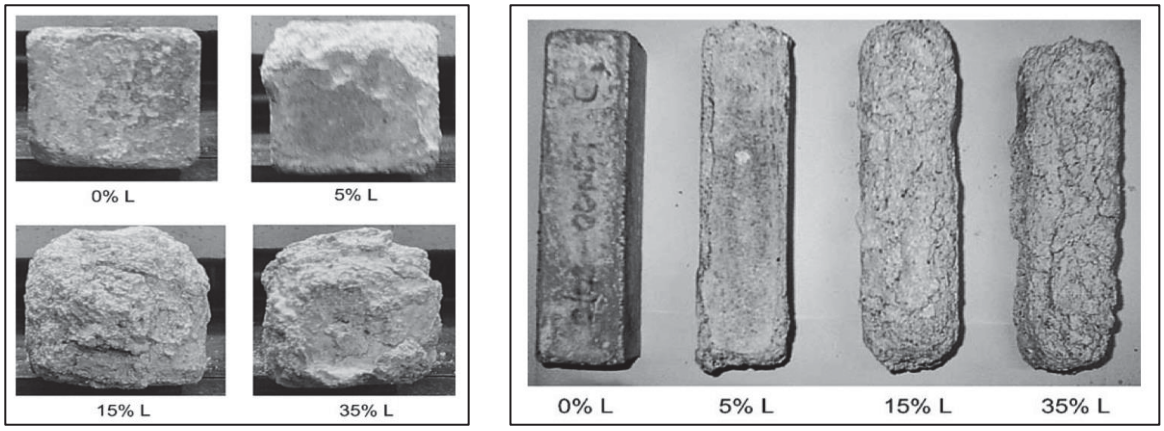

Fig. 2-21: Section view and top view of mortar prisms stored in 1.8% $MgSO_4$ at 5°C for 5 years (L: limestone) (Torres et al.-2003)

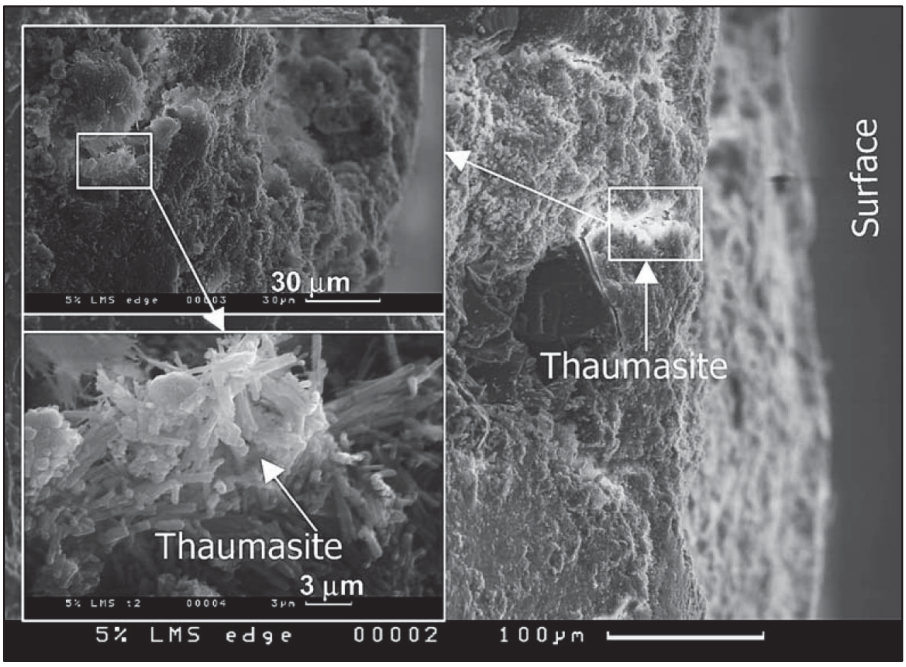

Fig. 2-22: SEM image showing thaumasite in a fracture surface of mortar containing 5% limestone filler replacement (Torres et al.-2003)

Senhadji et al. (2010) studied sulfate attack to 50x50x50 mm cubic mortar samples, containing Type I Portland cement, replaced with 0, 10, 20, and 30% limestone filler. After 27 days of water curing, samples were immersed in 5% magnesium sulfate solution for one year at 5°C and 23°C. According to visual inspections performed by Senhadji et al. (2010), the signs of TSA deterioration as cracks on the corners of the samples were detected in the samples after only 5 months. Also, the extent of deterioration was reported higher for samples with higher amounts of limestone filler. In addition, according to the compressive strength tests performed on the cubic samples, the researchers indicated that the loss in compressive strength was higher for the samples experiencing thaumasite sulfate attack in comparison to those for ordinary sulfate attack. Moreover, an increase in the amount of limestone filler resulted in more compressive strength loss in normal and low temperature sulfate exposures.

Ramezanianpour and Hooton (2013b) reported severe thaumasite sulfate attack to mortar samples prepared with a laboratory interground Portland-limestone cement with limestone content of 21.8%. They studied thaumasite sulfate attack to mortar prisms at 5°C in accordance with CSA A3004-C8 – Procedure B. Thaumasite sulfate attack was found extremely destructive to Portland-limestone cement compared to ordinary Portland cement. Only 3 months after immersion in 5% sodium sulfate solution, a complete decomposition was found in PLC mortar prisms while such decomposition was observed after a year in Type I Portland cement samples (Fig. 2-23). Using X-ray diffraction, Ramezanianpour and Hooton (2013b) confirmed formation of ettringite and gypsum along with thaumasite, and they inferred that gypsum and ettringite formation physically enhance thaumasite formation. “In fact, the opening up of the microstructure, caused by extensive cracking of the samples at the early stages of the attack, seems to be a prerequisite for the formation of thaumasite”.

Fig. 2-23: Disintegration of mortar prisms in TSA: Type I cement after one year (left), Laboratory ground PLC after three months (right) (Ramezanianpour and Hooton-2013b)

2-3-3- Effect of supplementary cementing materials on ettringite sulfate attack to limestone containing cements

According to many experimental studies, it is well known that generally supplementary cementing materials enhance resistance of Portland cement against ettringite sulfate attack. In recent years, with increase in utilization of Portland-limestone cements in the world, some experimental studies have been conducted on samples of PLC containing SCMs in ettringite sulfate attack to evaluate its performance against sulfate ions in ordinary conditions. As expected, in ettringite sulfate attack, SCMs generally reduce formation of ettringite and gypsum in Portland-limestone cement samples.

Ghrici et al. (2007) studied performance of concrete samples prepared with natural pozzolan and limestone filler. The blended cements for this study were prepared by partially replacing an ordinary Portland cement with a local natural pozzolan and limestone filler up to 30% and 20% by mass, respectively. Ghrici et al. (2007) showed that samples containing 15% limestone filler had almost the same sorptivity as those with ordinary Portland cement, and sorptivity was reduced by partially replacing PLC with natural pozzolan. Hence, preparing concrete with a mixture of Portland cement, limestone filler and natural pozzolan is beneficial in reducing permeability and improving durability of concrete. ASTM C1012 was also performed on mortar samples. It was shown that replacing Portland cement with 20% natural pozzolan and 10% limestone filler reduces the expansion of the samples against sodium and magnesium sulfate attack at 23°C. Accordingly, one can expect improvement in durability of ternary cements containing a mix of Portland cement, limestone powder, and natural pozzolan.

Zelić et al. (1999) tested mortar samples, containing 15% limestone by mass and different percentages of silica fume (2, 5, 8, 11, and 15%), in sodium and magnesium sulfate solutions according to ASTM C452. Their results show that by partially replacing Portland-limestone cements with silica fume, the resistance of the samples against sulfate attack considerably improves. According to the authors, this is due to formation of monocarboaluminate-hydrate during cement hydration in presence of limestone powder and silica fume, which prevents formation of calcium monosulfate-hydrate. İnan Sezer (2012) studied effect of addition of limestone powder and silica fume to Portland cement on performance of mortars through ASTM C1012. Different mixtures of ordinary Portland cement, silica fume, and limestone powder were prepared according to Table 2-4. She found that an increase in the amount of silica fume and limestone added to the samples results in reduction of the expansion of mortar samples cured in sodium sulfate solution as well as magnesium sulfate solution at room temperature. The replacement of cement with 35% limestone and 15% silica fume resulted in the lowest expansions among all studied blends. Therefore, İnan Sezer (2012) concludes that simultaneous use of silica fume and limestone is beneficial in performance of mortars in sulfate attack, and presence of limestone powder in the mixture which increases the workability compensates the reductions in flow due to adding silica fume to the mixture. Accordingly, by utilizing limestone in cement it is possible to take advantage of using higher percentages of silica fume in cement mixtures.

Table 2-4: Mixture proportions (İnan Sezer-2012)

Mixture	Cement (%)	Limestone (%)	Silica fume (%)
Control	100	0	0
5L	95	5	0
20L	80	20	0
35L	65	35	0
5S	95	0	5
10S	90	0	10
15S	85	0	15
5L5S	90	5	5
5L10S	85	5	10
5L15S	80	5	15
20L5S	75	20	5
20L10S	70	20	10
20L15S	65	20	15
35L5S	60	35	5
35L10S	55	35	10
35L15S	50	35	15

Hooton et al. (2010) reported the positive effect of slag on performance of Portland-limestone cement against ettringite sulfate attack. They found that addition of 30% and 50% slag to Portland-limestone cement considerably reduces the expansions of the ASTM C1012 prismatic mortar samples in ettringite sulfate attack. Addition of 50% slag was found to be more effective than 30% in improving the performance of Portland-limestone cement in ordinary sulfate attack. Ramezanianpour and Hooton (2013a) also assessed replacing a portion of PLC with slag. They found that different Portland-limestone cements, made with high C_3A clinker, when partially replaced with 30% or 50% slag, were highly resistant to ettringite sulfate attack, considering the CSA A3001-10 requirements for sulfate resistance of PLC (For high sulfate resistant blended PLC the expansion limit after 6 months is 0.05%). The samples' expansion up to 2 years is presented in Fig. 2-24 and Fig. 2-25. According to their results, "the positive effect of slag in improving the resistance against sulfate attack could be attributed to reducing the

permeability of the samples as well as diluting the C_3A content of the system and reducing the amount of portlandite by transforming it to CSH".

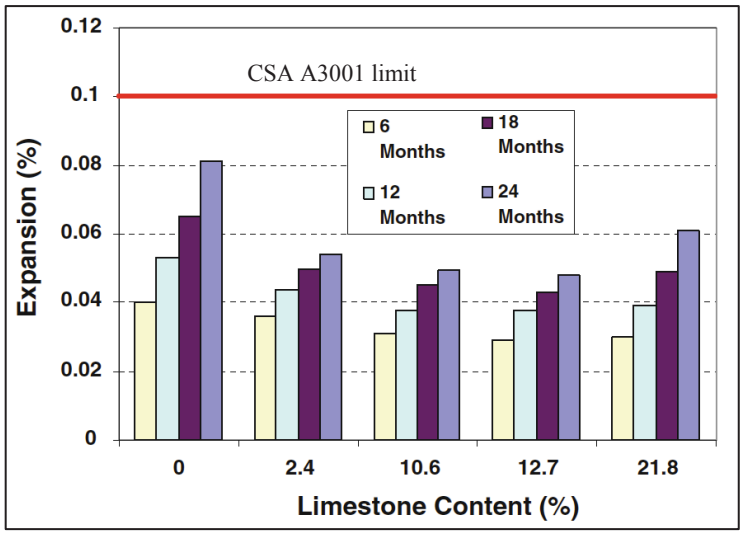

Fig. 2-24: Expansion of mortar bars made with 70% cement and 30% slag according to CSA A3004-C8 procedure A – 23°C (modified from Ramezanianpour and Hooton-2013a)

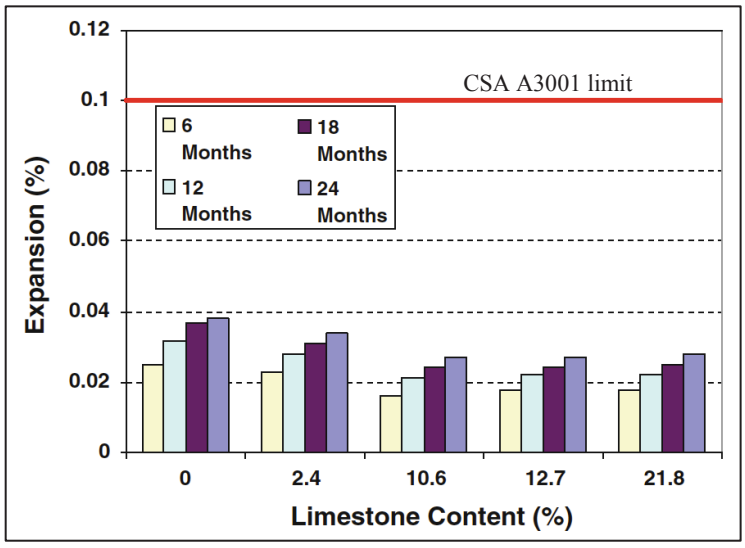

Fig. 2-25: Expansion of mortar bars made with 50% cement and 50% slag according to CSA A3004-C8 procedure A – 23°C (modified from Ramezanianpour and Hooton-2013a)

2-3-4- Effect of supplementary cementing materials on thaumasite sulfate attack to limestone containing cements

Numerous experimental studies on the positive effects of supplementary cementing materials has been directed to research focusing on effect of these materials on the TSA performance of concrete and mortar prepared with Portland-limestone cement in the past decade. Recent studies deliberate the effect of various types of supplementary cementing materials on resistance of PLC against thaumasite sulfate attack.

Generally, replacing a part of cement with ground granulated blast furnace slag can improve the performance of susceptible concretes to thaumasite sulfate attack. Crammond (2003) has reported that addition of 70% slag to Portland cement significantly increased the resistance of concrete prepared with limestone aggregates against thaumasite formation in sulfate exposures. Hooton et al. (2010) and Ramezanianpour and Hooton (2013a) studied partially replacing PLC with slag, and found a considerable contribution of slag in resistance against thaumasite sulfate attack. In their experimental research, 6 different types of Portland-limestone cements were prepared by inter-grinding a CSA GU Portland cement clinker (containing 12% C_3A) with limestone at levels of 0%, 2.4%, 10.6%, 12.7%, and 21.8% by weight. Then, the Portland-limestone cements were partially replaced by slag at levels of 0%, 30%, and 50%. It was found that replacement of Portland-limestone cement with 50% slag was more effective than 30% replacement in reducing the mortar prisms expansions during thaumasite sulfate attack, and considering the CSA A3001-10 requirements for sulfate resistance of PLC, the examined PLC when partially replaced with 50% slag would be categorized as high sulfate resistant blended Portland-limestone cement (HSLb). The expansion of samples is presented in Fig. 2-26.

Moreover, according to X-ray diffraction (XRD), Hooton et al. (2010) reported that no thaumasite formation was detected in Portland-limestone cement samples prepared incorporating slag.

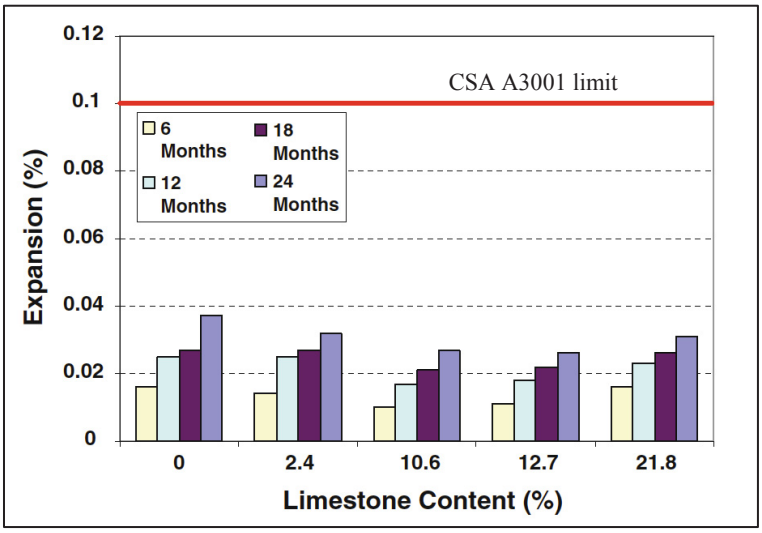

Fig. 2-26: Expansion of mortar bars made with 50% cement and 50% slag according to CSA A3004-C8 procedure B – 5°C (after Ramezanianpour and Hooton-2013a)

Smallwood et al. (2003) monitored performance of concrete samples prepared with metakaolin and dolomitic limestone aggregates in thaumasite sulfate attack during 280 days immersion sulfate solution at 5°C. Their results showed that the expansions of sample prisms were reduced by adding 7% metakaolin to cement (by weight). Also, they showed that the concrete samples, prepared with Portland cement that was partially replaced with metakaolin, maintain compressive strength for longer periods of time when exposed to thaumasite sulfate attack.

To investigate effect of fly ash on thaumasite sulfate attack, Thomas et al. (2003) studied various marine-exposed concrete samples for 10 years. Thaumasite, observed by XRD, was formed on surface of the 10 cm concrete cubes prepared with ordinary

Portland cement, while concrete specimens containing 30% and 50% fly ash were resistant against formation of thaumasite. The source of carbonate ions was found to be carbonates in seawater and carbonates from surface carbonation of concrete.

Bellmann and Stark (2007) studied the effect of fly ash and silica fume on thaumasite sulfate attack. In their research, 40x40x160 mm mortar prisms were prepared with incorporation of fly ash, silica fume, and limestone in different mixes, and exposed to sulfate solution at 8°C (SO_4^{2-} = 1500 mg/L) for 4.5 years. Their results showed that the calcium/silica ratio in CSH phases of samples prepared without supplementary cementing materials was about 1.7, which could be reduced to 1.1 by addition of pozzolanic materials. Bellmann and Stark (2007) indicated that CSH phase in samples with calcium/silicon ratio of 1.7 could be transformed to thaumasite at very low sulfate concentrations while those with lower calcium/silicon ratio could resist against transformation to thaumasite at much higher sulfate concentrations. This finding confirms the positive effect of supplementary cementing materials on improving performance of Portland cements and Portland-limestone cements against thaumasite sulfate attack. Accordingly, addition of sufficient amounts of supplementary cementing materials in order to consume the calcium hydroxide in the hydrated cement paste and reduce the calcium to silicon ratio in the CSH phases is recommended by Bellmann and Stark (2007) to prevent the formation of thaumasite in hydrated cement pastes during exposures to sulfate environment at low temperatures.

Zhang et al. (2011) studied the effect of addition of fly ash on TSA by using different mixes of cement, limestone, and fly ash in preparation of 40x40x40 mm mortar samples (Table 2-5). All the samples were water cured for 28 days then immersed in

magnesium sulfate solution (33,800 ppm mass concentration of SO_4^{2-}) at 5 ± 2°C. After 15 weeks, the surface of the samples was subjected to XRD. According to XRD results, no trace of thaumasite is reported on the surface of the samples containing 30%, 45%, and 60% fly ash. Therefore, the authors conclude that fly ash is effective in preventing thaumasite sulfate attack in limestone cements. In their study, the percentage of limestone is changed in different mixtures so it is not possible to draw a conclusion from Zhang's results regarding the optimum usage of fly ash for a specific type of Portland-limestone cement, and declare that to what extent the addition of fly ash would be effective in prevention of thaumasite formation. In addition, the study is only for 15 weeks exposure so the state of the proposed samples is not clear for longer periods of exposure to sulfate attack, and it is not possible to conclude if fly ash can totally hinder the formation of thaumasite in Portland-limestone cement or not.

Table 2-5: Mixture proportions (g) (Zhang et al.-2011)

No.	Cement	Limestone	Fly ash	Water
C	650	350	-	450
F3	552.5	297.5	150	450
F4	455	245	300	450
F5	357.5	192.5	450	450
F6	260	140	600	450

Crammond et al. (2003) performed a parallel laboratory and field visual study on performance of concrete samples prepared with different types of cement, aggregates and supplementary cementing materials in thaumasite sulfate attack. It was found that, in thaumasite sulfate attack, binary blended cements containing 25% metakaolin, 10% silica

fume, or 40% slag perform satisfactory in concrete prepared with different aggregate types including carbonate aggregates.

Skaropoulou et al. (2009b) performed a comprehensive 5-year study on effect of addition of natural pozzolan, blast furnace slag, fly ash (Type C), and metakaolin on performance of limestone cement mortars, containing 15% limestone powder by weight, in thaumasite sulfate attack. Mortar samples with dimensions of 40x40x53 mm were prepared with siliceous and calcareous sands and different mixes of limestone cement with supplementary cementing materials (Table 2-6). The samples were immersed in 1.8% magnesium sulfate solution at 5°C and 25°C, 28 days after preparation.

Table 2-6: Codes and compositions of cement mixes (Skaropoulou et al.-2009b)

Code	Composition of samples
LC1	Portland limestone cement (clinker: 85% w/w, limestone: 15% w/w) (gypsum: 5% of clinker by mass)
LPC	LC1: 80% w/w, natural pozzolana (P): 20% w/w
LFC	LC1: 70% w/w, fly ash (F): 30% w/w
LSC	LC1: 50% w/w, ggbs (S): 50% w/w
LMC	LC1: 90% w/w, metakaolin (M): 10% w/w

The visual condition of samples kept at 5°C prepared with siliceous sand at different ages is shown in Fig. 2-27. Obviously, the samples prepared with metakaolin and slag showed better performance against sulfate attack at 5°C. The researchers reported no visual damage for the samples cured at 25°C. This shows the extent of the deleterious effect of thaumasite sulfate attack in comparison with ordinary sulfate attack. The compressive strength test at the first day of the exposure to sulfate solution and 9 months later gave the same idea as the visual inspection results, and showed that adding slag and metakaolin to limestone cement had effectively reduced formation of thaumasite

and protected the samples from strength loss during the first 9 months. Ultrasonic pulse velocity (UPV) and mass loss gave results in this study in agreement with the compressive strength test. Finally, Skaropoulou et al. (2009b) concluded that incorporation of slag and metakaolin could considerably improve the performance of limestone cement. Fly ash was not as effective as slag and metakaolin, but it might retard formation of thaumasite. The natural pozzolan used was found not helpful in preventing deterioration, as it needed longer moist curing time to participate in pozzolanic reactions.

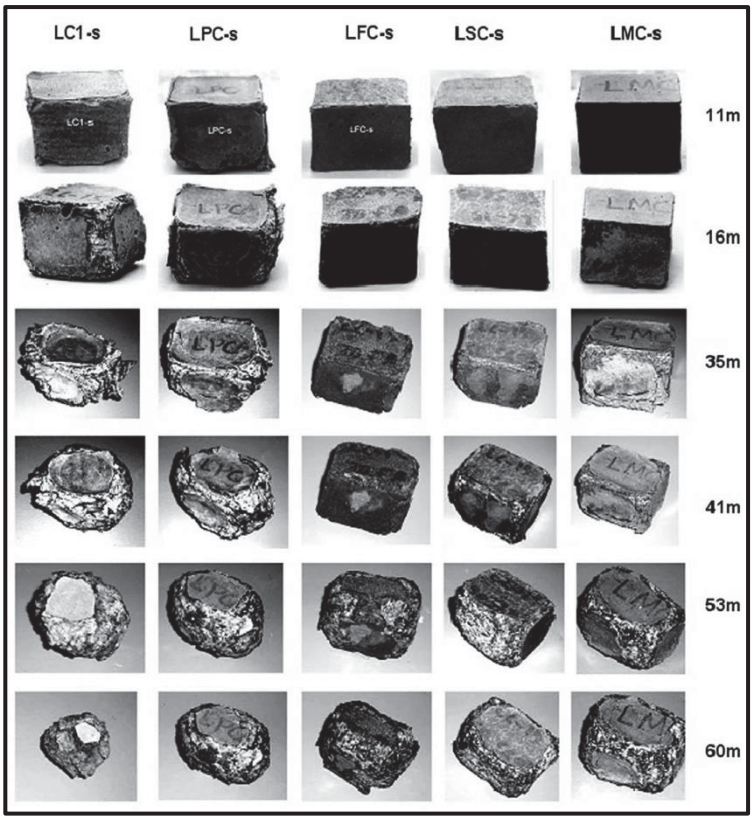

Fig. 2-27: Samples prepared with siliceous sand, cured for 11, 16, 35, 41, 53, 60 months in a 1.8% $MgSO_4$ solution at 5°C (Skaropoulou et al.-2009b)

Qu and Zhang (2012) studied compressive strength of ternary Portland-limestone cement (30% limestone filler) mortar samples prepared with combination of slag and

silica fume or slag and fly ash. Mortar samples were immersed in 2% magnesium sulfate solution at 5°C, and the compressive strength was studied for one year. It was found that ternary blends of Portland-limestone cement were more sustainable in maintaining compressive strength than control cement. The ternary mortar prepared with mixing Portland-limestone cement, slag and fly ash (25% slag and 15% fly ash) showed around 20% reduction in compressive strength while the control mortar sample lost more than 70% of the compressive strength. The same observation was reported for mortar sample prepared with mixture of limestone cement, slag and silica fume (25% slag and 5% silica fume).

2-3-5- Reducing problems with thaumasite sulfate attack by improving concrete quality

It is well known that improvement in the quality of concrete enhances its performance in different aspects including durability characteristics. Crammond (2003) reported that improving concrete quality by lowering water/cement ratio, increasing the amount of cement, improving the concrete compaction, and proper curing helps in decreasing the problems with thaumasite sulfate attack.

Smallwood et al. (2003) studied performance of concrete samples containing metakaolin against thaumasite sulfate attack and reported that reducing water to binder ratio in concrete samples results in reduction in expansion of samples experiencing thaumasite sulfate attack. Furthermore, they showed that concrete samples, prepared with lower water to binder ratio, maintain compressive strength for longer periods of time when exposed to thaumasite sulfate attack in comparison with samples prepared with higher water to binder ratio.

Brueckner et al. (2012) also reported that by decreasing water/cement ratio or increasing cement content, the rate of thaumasite sulfate attack decreased in concrete samples prepared with limestone aggregates and immersed in magnesium sulfate solution at 5°C for 27 months.

2-4- Using thermal analysis methods in detecting sulfate attack

Differential Scanning Calorimetry (DSC) is one of the tests using thermal analysis in detecting different compounds; it has been utilized in research fields of cement and concrete chemical analysis. In this test, small amounts of powdered samples are slowly heated with a constant rate of temperature increase in a controlled atmosphere. The heat required to maintain the temperature of the sample as compared to a reference is measured and presented in a graph as an output data. Accordingly, this technique depicts different exothermic and endothermic peaks of dehydration and decomposition for different compounds. By knowing these peaks for different compounds, it is possible to characterize present compounds in the hydrated cement paste.

Abdelrazig et al. (1992), used DSC on ordinary Portland cement paste samples and reported an endothermic peak around 105°C due to ettringite and CSH gel dehydration, an endothermic peak at 145°C relating to gypsum dehydration, and also an endothermic peak in the range of 440-480°C due to calcium hydroxide dehydroxylation. Hartshorn et al. (1999) used DSC along with XRD to study the lab made Portland-limestone cement paste samples immersed in sodium sulfate solution as well as magnesium sulfate solution at 5°C. Regarding the DSC curves, they identified a strong endothermic peak for dehydroxylation of calcium hydroxide at 420°C in unaffected parts of samples as well as a wide endothermic peak related to ettringite, gypsum, and CSH gel

between 60°C and 140°C. Moreover, they found a strong endothermic peak at 115°C attributed to thaumasite in the deteriorated parts of Portland-limestone paste sample (Fig. 2-28 and Fig. 2-29).

Santhanam et al. (2003a) stated, "The dehydration peaks for ettringite and gypsum occur at 80 – 100°C and 110 – 135°C, respectively." and "The peak for pure thaumasite occurs between 100°C and 120°C". Accordingly, using the DSC technique during research on sodium sulfate attack to ordinary Portland cement and C_3S mortars, they showed increases in the amounts of gypsum and ettringite in Portland cement paste and an increase in the amount of gypsum in C_3S paste. Gao et al. (2010) studied sodium sulfate attack to concrete samples at 20°C for a year and reported endothermic peaks between 83.2°C and 104.2°C for dehydration of ettringite and between 429.6°C and 449.1°C for dehydroxylation of $Ca(OH)_2$.

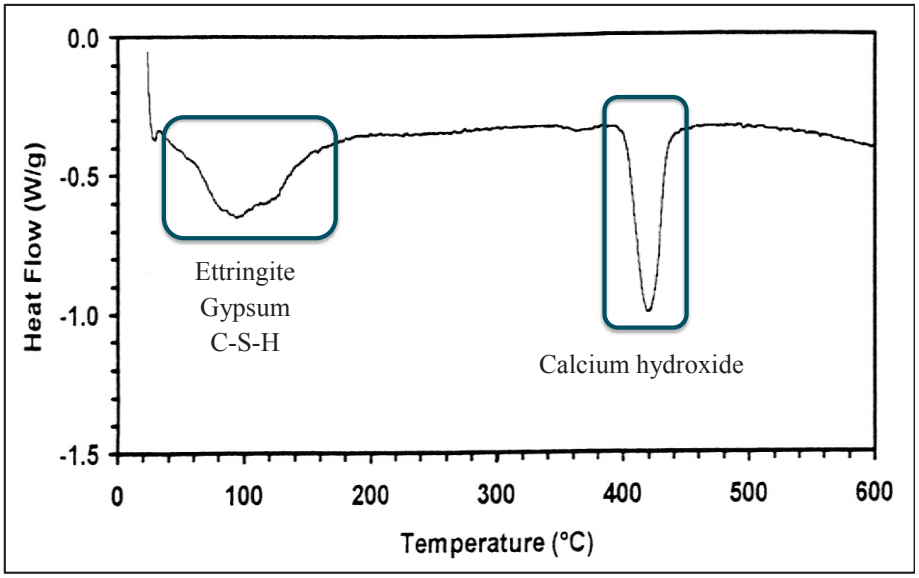

Fig. 2-28: DSC curve for unaffected part of Portland-limestone cement paste sample stored in sulfate solution at 5°C for 196 days (modified graph from Hartshorn et al.-1999)

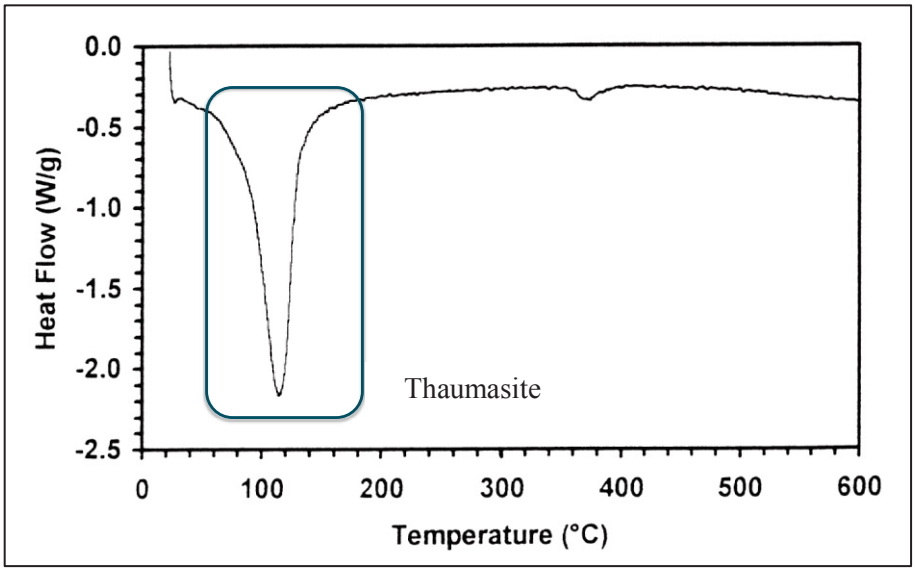

Fig. 2-29: DSC curve for deteriorated part of Portland-limestone cement paste sample stored in sulfate solution at 5°C for 196 days (modified graph from Hartshorn et al.-1999)

Differential thermogravimetry (DTG) is a technique, which is almost similar to DSC, but it is based on the changes of the weight of components when temperature changes. A differential thermogravimetry peak corresponds to a loss of the weight of the components that is associated with an endothermic or exothermic reaction thus this peak can also be detected in differential scanning calorimetry.

Bensted and Varma (1974) obtained mineral samples of thaumasite and through a thermal analysis study found a peak for dehydration of thaumasite that starts at 110°C. Vuk et al. (2002) reported a strong peak at 145°C in DTG related to thaumasite and ettringite in Portland-limestone paste samples immersed in magnesium sulfate solution at 5°C. Additionally, they reported a peak at 100°C related to the CSH dehydration. Skaropoulou et al. (2006) studied thaumasite sulfate attack to lab made Portland-limestone cement mortars, immersed in 1.8% magnesium sulfate solution at 5°C, during one year by XRD, SEM and differential thermogravimetry. They characterized

thaumasite and gypsum in a double peak in the range of 100-130°C (Fig. 2-30). Pipilikaki et al. (2008) also studied the DTG curve resulted from Portland-limestone mortar samples immersed in 5% sodium sulfate solution at 5°C and deteriorated due to thaumasite formation. They identified a peak around 130°C attributed to the dehydration of thaumasite. For dehydroxylation of calcium hydroxide Vedalakshmi et al. (2008) found a peak around 465°C during thermal analysis on concrete samples stored in 10% magnesium sulfate solution.

Ou et al. (2011) studied the products of an ordinary Portland cement hydration with FT-IR, thermal analysis, and XRD techniques. At the first hours of hydration, they found peaks for gypsum and calcium hydroxide at 120°C and 413°C, respectively; after longer periods of hydration, they reported a peak at 95°C for both ettringite and CSH gels. Patsikas et al. (2012) studied ettringite sulfate attack to PLC with 15% limestone powder content. Using DTG, they found a peak around 130°C attributed to dehydration of ettringite and a peak at 450°C related to consumption of $Ca(OH)_2$.

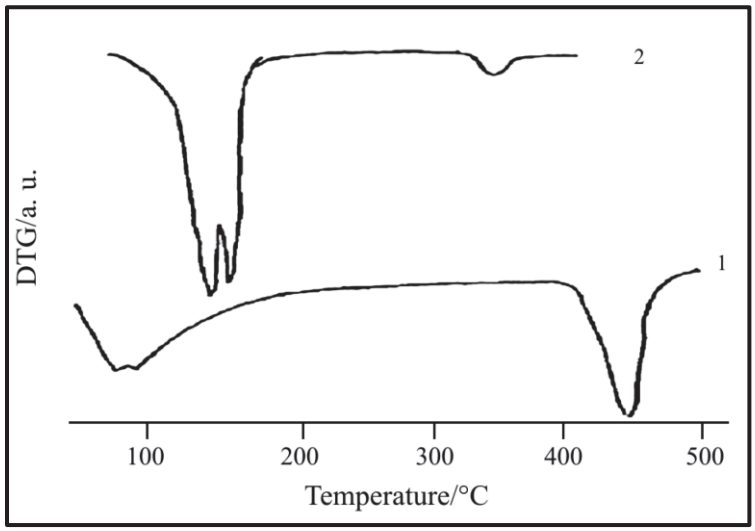

Fig. 2-30: DTG graph of Portland-limestone mortar under thaumasite sulfate attack (1: unaffected area, 2: deteriorated area) (Skaropoulou et al.-2006)

A summary of the reviewed research on adopting thermal analysis for characterization of compounds inside the hydrated cement paste is presented in Table 2-7. According to the table, generally, dehydration peaks for calcium silicate hydrates and ettringite are quite close. The dehydration of CSH and ettringite could be found in a single endothermic peak according to Abdelrazig et al. (1992) and Ou et al. (2011). Generally, dehydration of ettringite is found between 80°C and 105°C (in one study a peak at 130°C is reported (Patsikas et al.-2012)), and the peak related to calcium silicate hydrate can take place in range of 95-105°C. The peaks confirming thaumasite dehydration are found between 100°C and 130°C according to the literature that is reviewed. Also, the gypsum peak is reported between 100°C and 145°C. Finally, considering the thermal analysis studies presented, calcium hydroxide dehydroxylation occurs at elevated temperatures in comparison to ettringite, CSH, thaumasite, and gypsum. Its endothermic peak is reported in the range of 413-480°C. Consequently, it is possible to detect thaumasite, ettringite, and gypsum in distinct thermal peaks in a hydrated cement paste affected by sulfate attack.

Table 2-7: The thermal peaks detected for ettringite, CSH, thaumasite, gypsum and $Ca(OH)_2$ in various thermal analysis studies

			Peak/interval temperature				
Reference	Analyzed sample	Method	Ettringite	CSH	Thaumasite	Gypsum	$Ca(OH)_2$
Bensted and Varma (1974)	Mineral thaumasite	DTG			Starts at 110°C		
Abdelrazig et al. (1992)	OPC paste	DSC	105°C	105°C		145°C	440-480°C
Hartshorn et al. (1999)	PLC paste	DSC			115°C		420°C
Vuk et al. (2002)	PLC paste	DTG		100°C			
Santhanam et al. (2003a)	OPC and C_3S	DSC	80-100°C			110-135°C	
Santhanam et al. (2003a)	Pure thaumasite	DSC			100-120°C		
Skaropoulou et al. (2006)	PLC mortar	DTG			100-130°C	100-130°C	
Pipilikaki et al. (2008)	PLC mortar	DTG			130°C		
Vedalakshmi et al. (2008)	OPC concrete	DTG					465°C
Gao et al. (2010)	OPC concrete	DSC	83.2-104.2°C				429.6-449.1°C
Ou et al. (2011)	OPC paste	DTG	95°C	95°C		120°C	413°C
Patsikas et al. (2012)	White PLC mortar	DTG	130°C				450°C

2-5- Use of Ultrasonic Pulse Velocity (UPV) technique in studying concrete deterioration due to sulfate attack

Ultrasonic pulse velocity technique is one of the best-known non-destructive tests (NDT). It has been used as a reference in studying the characteristics of concrete structures. This technique can provide information about the internal condition of concrete, internal defects such as cracking and delamination, compressive strength, and

extent of deterioration (Toutanji-2000 and Yaman-2001). Typically, it gives some idea about the quality of concrete (Toutanji-2000).

Basically, this method is based on longitudinal wave pulse velocity and is popular among NDTs as it can be simply performed, and the test is cost effective (Komlos et al.-1996). To perform the test, a pair of transducers is used in contact with a concrete surface, and ultrasonic waves are sent from the sending transducer to the receiving one, and the duration of the process is measured. Accordingly, the UPV can be calculated by knowing the distance between the two transducers and the time of waves flight (Yaman-2001).

Hartshorn et al. (2001) studied 40x40x160 mm mortar samples, prepared with Portland-limestone cement and subjected to magnesium sulfate attack at 5°C and 20°C. The UPV test was performed on the long axis of the samples at specific periods of time during the course of a year. The results showed that the ultrasonic pulse velocity of the samples containing 35% limestone and immersed in magnesium sulfate solution slightly decreased until 220 days when severe deterioration at the end of the mortar prisms, made the test results inconsistent. The slight reduction in UPV in 220 days followed by inconsistency in the results was a sign of severe deterioration, which was confirmed by expansion and compressive strength tests as well as changes in mass of the samples.

Türkmen (2003) exposed the 10x20 cm cylindrical concrete samples to sodium sulfate and magnesium sulfate solutions for 400 days and reported that the samples in sulfate attack showed lower UPV than those cured in water. Likewise, the samples exposed to sulfates for 400 days had more porosity than the samples cured in limewater. Thus, UPV test was helpful in detecting sulfate deterioration in concrete samples

according to Türkmen (2003) results. Skaropoulou et al. (2009a) also reported a continuous reduction of UPV in 40x40x53 mm mortar samples immersed in magnesium sulfate solution during 5 years. Shannag et al. (2003) reported the same trend for 10 cm cubic concrete samples immersed in magnesium and sodium sulfate solutions.

2-6- Summary of background and gaps in the research field

Sulfate attack to concrete materials has been studied for many years. Nonetheless, due to its complexity there are still significant aspects of sulfate attack that need to be investigated. Thaumasite sulfate attack is one of the particular cases of sulfate attack that requires to be studied thoroughly, especially when PLCs are utilized. In addition, although ettringite sulfate attack is now a recognized problem in concrete durability, it is vital to study thaumasite sulfate attack along with ettringite sulfate attack to achieve a complete comprehension of their differences and the significance of each deterioration process.

According to the background of study in the field of sulfate attack, thaumasite sulfate attack is a serious problem that can cause severe damage to the concrete structures. This problem is intensified when Portland-limestone cements are used. Production and utilization of Portland-limestone cements are increasing in the world because of attentions to sustainable development and economic concerns; so, PLC is progressively becoming common in field practices everywhere in the world.

The introduction of Portland-limestone cement, containing up to 15% limestone filler, in the Canadian standard in 2008 is an indication of the interest in use of this kind of cement in Canada. Serious concerns about the performance of Portland-limestone cement in cold weather against sulfate attack make it difficult to use this kind of cement

in Canada as almost the whole country experiences long, cold winters. These concerns are reflected in the Canadian standard (CSA A23.1-09) by prohibition of the use of Portland-limestone cement in sulfate exposures. Accordingly, research on thaumasite sulfate attack to PLC and improvement of durability characteristics of this type of cement in sulfate attack, especially when thaumasite sulfate attack occurs, is of great significance.

It is well known that supplementary cementing materials are effective in developing durability of concrete against ettringite sulfate attack. Recently, some researchers have investigated the effect of SCMs on durability of mortar and concrete when the deterioration is governed by thaumasite sulfate attack. The positive effect of SCMs on resistance of cements against sulfate attack beside the weakness of PLC against thaumasite sulfate attack has led the Canadian standard, CSA A3001-10, to suggest minimum amounts of supplementary cementing materials to be added to Portland-limestone cement in order to achieve acceptable resistance. CSA A3001-10 suggests addition of 25% Type F fly ash, 40% slag, 15% metakaolin or a combination of 5% Type SF silica fume with 25% slag or 20% fly ash for moderate and high sulfate resistant Portland-limestone cements. It should be noted that these suggestions are the minimum action and do not guarantee resistance against TSA. In fact, the expansion limitations, presented in Table 2-3, should be achieved in order to use blended PLC in sulfate exposure.

Now, Portland-limestone cement is practically introduced by the Canadian standard and the necessary test for assessment of performance of this kind of cement is available. In addition, suggestions are made regarding addition of specific supplementary

cementing materials to Portland-limestone cements to achieve moderate sulfate resistant and high sulfate resistant blended Portland-limestone cement. Apparently, as these revisions are very recent, it is quite necessary to continue research on performance of PLC and blended PLC in order to evaluate the suggestions as well as limitations presented by the standard. With regards to the expansion limitations (CSA A3001-10), it is apparent that possibly they may change in the future, as the expansion limit for both moderate sulfate resistant blended PLC and high sulfate resistant blended PLC is the same. Moreover, considering the suggested amounts of SCMs, more study is necessary to evaluate these suggestions for different types of PLC produced in Canada. At this point there is a gap in research on the effect other kinds of SCMs on resistance of PLC against ettringite and thaumasite sulfate attack. Furthermore, there is a shortcoming in research on performance of ternary blends of Portland-limestone against ettringite as well as thaumasite sulfate attack. In this research, the mentioned shortcoming and gaps are addressed toward a contribution in research on ettringite and thaumasite sulfate attack to PLCs and improvement of durability sufficiency of PLCs using SCMs. Such contribution can help increasing utilization of Portland-limestone cements.

3- Experimental program and methods

As previously declared, the concentration of this research is on performance of Portland-limestone cements in sulfate exposure. According to the CSA A3000-08 standard (CSA-2008a), Portland-limestone cement is a class of cementitious material that may contain 5% to 15% inter-ground limestone. The CSA A3000-08 does not classify PLC as moderate or high sulfate resistant cement. As well, CSA A23.1-09 does not permit utilization of PLC in sulfate exposure. However, CSA A3000-10 (CSA-2010a) specifies expansion limits for high sulfate resistant blended Portland-limestone cement. Therefore, studying durability characteristics of Portland-limestone cements in sulfate environments, particularly when used in conjunction with supplementary cementing materials, is of significance, and can help to develop high sulfate resistant blended Portland-limestone cements.

In order to evaluate and compare performance of Portland-limestone cement in combination with different supplementary cementing materials exposed to sodium sulfate solutions at both 23°C and 5°C, expansion and mass change of mortar samples are studied as well as changes in visual condition. Additionally, compressive strength development of mortars prepared with blended PLC is studied at 5°C. Furthermore, UPV, DSC and XRD techniques are used in order to examine the mortar samples in thaumasite sulfate attack and study the development of deleterious compounds. The details of the materials and experiments are discussed in this chapter.

3-1- Materials

Two general use Portland-limestone cements (CSA Type: GUL), one provided by Ciment Québec, and the other one supplied by Joliette cement plant of Holcim Canada

are used in this study. The limestone contents of PLC from Ciment Québec and Holcim Canada were 10% and 13.5%, respectively. In this research, the PLC from Ciment Québec is designated as "L", and the one from Joliette cement plant is titled as "GUL". The chemical compositions and physical characteristics of Portland-limestone cements are presented in Table 3-1.

Table 3-1: Chemical composition and physical characteristics of the used PLCs in the research

		L – 10%L* Ciment Québec	**GUL – 13.5%L Holcim Canada**
Chemical composition			
SiO_2	%	18.40	19.00
Al_2O_3	%	4.60	4.10
Fe_2O_3	%	2.80	2.68
CaO	%	60.60	60.40
MgO	%	2.20	1.80
SO_3	%	3.90	3.05
K_2O	%	0.89	0.83
Na_2O	%	0.27	0.20
TiO_2	%	–––	0.15
Loss on Ignition	%	4.60	7.46
C_3S	%	61.00	70.00
C_2S	%	6.80	1.67
C_3A	%	7.30	6.30
C_4AF	%	8.60	8.16
Equivalent Alkalis	%	0.85	0.75
Physical characteristics			
Fineness - Blaine	m^2/kg	399	468
Retained on 45 μm sieve	%	10.5	10.8

*** L: Limestone**

In order to study the effect of supplementary cementing materials when added to Portland-limestone cement, a grade 80 slag from Stoney Creek plant of Lafarge in

Ontario, a Type F fly ash provided by Ciment Québec from Belledune plant in New Brunswick, as well as metakaolin, silica fume, and silica fume I (intermediate silica fume) all supplied by Ciment Québec were used. These SCMs are selected considering their availability in the region that makes their usage feasible for industrial purposes. The chemical composition of these SCMs is presented in Table 3-2.

Table 3-2: Chemical composition of the used SCMs in the research

		Fly ash (Type F)	Silica fume	Silica fume I	Metakaolin	Slag (grade 80)
SiO_2	%	47.34	83.75	81.05	61.45	38.60
Al_2O_3	%	18.80	1.81	1.17	29.23	9.90
Fe_2O_3	%	8.58	1.06	3.27	1.20	0.67
CaO	%	5.36	1.58	1.70	2.35	37.90
MgO	%	2.32	0.17	0.81	0.36	9.30
SO_3	%	0.75	0.05	0.08	0.19	3.00
K_2O	%	1.96	0.88	1.81	1.92	0.52
Na_2O	%	1.28	0.34	0.27	0.19	0.17
TiO_2	%	0.94	0.09	0.02	0.68	0.42
P_2O_5	%	0.22	0.08	0.07	0.03	–––
SrO	%	0.17	0.00	0.00	0.01	–––
Mn_2O_3	%	0.10	0.12	5.85	0.08	–––
Cr_2O_3	%	0.05	0.01	0.04	0.01	–––
ZnO	%	0.03	0.10	0.23	0.00	–––
Loss on Ignition	%	–––	9.09	2.65	2.31	–––
Equivalent Alkalis	%	2.57	0.92	1.46	1.45	0.51

In order to investigate performance of Portland-limestone cement in sulfate exposure when blended with the selected supplementary cementing materials, 23 cement blends are examined (Table 3-3). Blends number 1 through number 20 are prepared with the Portland-limestone cement containing 10% inter-ground limestone and blends number 21, 22, and 23 are made with the other Portland-limestone cement, which

contains 13.5% inter-ground limestone. According to the recommendations in the CSA A3001-10 standard, Portland-limestone cement can only be considered in sulfate environment when it conforms to the assigned expansions limits and contains a minimum of 25% Type F fly ash or 40% slag or 15% metakaolin or a combination of 5% Type SF silica fume with 25% slag or a combination of 5% Type SF silica fume with 20% Type F fly ash. The recommendations regarding the minimum SCM replacements are based on the limited research completed until the time of the standard publication. The PLC blends in this study are designed in order to evaluate the standard suggestions and to find new binary and ternary blends of PLC that can be categorized as high sulfate resistant blended Portland-limestone cement to be considered in later modifications of the standard.

Three blends of "L" are set to the CSA A3001-10 suggestions for addition of slag, fly ash and metakaolin, (L-40 Slag, L-25 FA, L-15 MK). In order to further refine the suggested limits of these SCMs, other blends are also set with 5% lower and higher than the suggested percentage levels. Silica fume is only mentioned in the standard at amount of 5% and in combination with slag or fly ash. Therefore, blends of "L" are studied solely with silica fume with percentages of 3%, 5%, and 8% toward evaluating effectiveness of this SCM on impeding sulfate attack to PLC. The same percentages are also studied for intermediate silica fume so that the performance of these two types of silica fumes would be compared in parallel. Moreover, owing to the fact that both slag and fly ash are effective on durability of cement in sulfate attack, and the standard does not have any suggestions for ternary blends of PLC containing these two SCMs, four ternary blends of PLC with slag and fly ash are devised (blends number 10, 11, 12, and 13). As slag possesses both cementing and pozzolanic characteristics, while Type F fly ash only has

pozzolanic characteristics, the percentage of slag in the blends is chosen higher than fly ash. CSA A3001-10 limits the amount of SCMs in ternary blends to 60%. Accordingly, a ternary blend was designed with 40% slag (the suggested percentage according to the standard) and 20% fly ash (blend number 13: L-40 Slag-20 FA). Three other ternary blends were also set by reducing amounts of slag and fly ash. With the purpose of verifying suggestions of the standard on addition of slag and fly ash that are the most used SCMs, binary blends of another type of Portland-limestone cement (GUL) with 40% slag and 25% fly ash are also set. It should be mentioned that samples number 20 and 21 are control samples prepared with each studied cement. Studying different replacement levels of Portland limestone cement with SCMs helps to find the efficient amount of SCMs regarding economic considerations, sustainable development issues, and durability factors.

As the standard suggestions for addition of SCMs is fairly new, evaluating the suggestions in more laboratory research tests with different types of PLC as well as studying new binary and ternary blends of PLC with SCMs would be helpful in improving performance of Portland-limestone cements in sulfate attack and to improve standard specifications for these types of cement.

Table 3-3: The studied blends of Portland-limestone cement

	Designation	PLC – Ciment Québec **(L)** %	Slag %	Fly ash Type F %	Silica fume %	Silica fume I %	Metakaolin %	PLC – Holcim **(GUL)** %
1	L-35 Slag	65	35					
2	L-40 Slag	60	40					
3	L-45 Slag	55	45					
4	L-20 FA	80		20				
5	L-25 FA	75		25				
6	L-30 FA	70		30				
7	L-3 SF	97			3			
8	L-5 SF	95			5			
9	L-8 SF	92			8			
10	L-25 Slag-10 FA	65	25	10				
11	L-30 Slag-10 FA	60	30	10				
12	L-35 Slag-15 FA	50	35	15				
13	L-40 Slag-20 FA	40	40	20				
14	L-3 SFI	97				3		
15	L-5 SFI	95				5		
16	L-8 SFI	92				8		
17	L-10 MK	90					10	
18	L-15 MK	85					15	
19	L-20 MK	80					20	
20	L Control	100						
21	GUL Control							100
22	GUL-40 Slag		40					60
23	GUL-25 FA			25				75

3-2- Expansion of mortars in sulfate attack

The sulfate resistance of blends of Portland-limestone cement is studied according to CSA A3004-C8 (2010). Both procedures for studying expansion of mortar samples in ettringite sulfate attack and thaumasite sulfate attack are applied. Standard mortar mixtures are prepared according to ASTM C305 (similar to CSA A3004-C1-2008c) and ASTM C109 (similar to CSA A3004-C2-2008d) with the blends of PLC presented in Table 3-3. Each mixture was proportioned as one part blended PLC and 2.75 parts standard graded sand, and the water to cement ratio was 0.485. Although the standard

indicates that the water to cement ratio should be changed to give constant flow, it was decided to keep the w/c constant. The constant w/c allows better comparison among the mixtures as well as avoids several trial mixtures to achieve the flow required. The constant w/c approach has been used by several researchers in the past (Ramezanianpour and Hooton, 2013b), likely for the same reasons. Blends of PLC with SCMs were manually prepared in the laboratory. For each mix, blended PLC was first prepared. For this purpose the desired amounts of PLC and SCM were obtained and hand mixed in a bowl. It should be mentioned that two types of the supplementary cementing materials used (SF and SFI) were not in powder form, therefore required ball-milling. These two SCMs were first ground to a Blaine fineness of ~1400 m^2/kg in the lab, then were hand mixed with PLC. Lastly, the prepared blended PLC, standard graded sand, and water were mixed by an electrical mixer in accordance to ASTM C109 and ASTM C305. Each blend required several batches to prepare sufficient number of samples. For each blend, 10 cubes (for finding when the compressive strength achieves 20 MPa) and 10 prisms were made in four batches. Prepared mortar was cast into metal cube molds of 50x50x50 mm as well as prisms molds of 25x25x285 mm. The molds were then put in 100% humidity containers, placed in an oven with temperature of 35 ± 3°C for 23 ± 0.5 hours. Afterwards, the mortar samples were demoulded and placed in saturated limewater at 23°C. At the time of demoulding, the compressive strength of two mortar cubes were tested according to ASTM C109 (or CSA A3004-C2) with the purpose of checking if the samples achieved the average compressive strength of 20 ± 1 MPa. The compressive strength measurements were followed daily until the average strength of mortar cubes reached 20 ± 1 MPa.

As for the CSA A3004-C8 procedure A (ettringite sulfate attack), once the companion mortar cubes attained the specified strength, the length of six mortar bars were measured with a digital comparator (Fig. 3-1) with the accuracy of 0.002 mm, and the length was defined as the initial length. The six mortar bars were then placed into two plastic containers (three bars in each one) with close-fitting lid containing 50 g/L sodium sulfate solution prepared with de-ionized water and anhydrous sodium sulfate. The mortar bars were placed on plastic rods in the containers so that the solution would engulf their whole perimeter. The volume of the solution was limited to 4 ± 0.5 times of the volume of the submerged mortar bars. The containers were then kept in the lab at temperature of 23 ± 2°C (Fig. 3-2).

In procedure B of the standard, which investigates thaumasite sulfate attack, when the companion mortar cubes reached the desired compressive strength, four mortar bars were first cooled to 5 ± 2°C. To do so, the bars were immersed in a precooled container of tap water in a refrigerator with temperature of 5 ± 2°C for 7 hours. It should be mentioned that the water container was placed in the refrigerator at least 7 hours prior to immersion of mortar bars. Subsequently, the initial length of mortar bars was measured, then they were immersed in 50 g/L sodium sulfate solution (Fig. 3-3), which was previously prepared and precooled in the refrigerator for at least 7 hours according to the CSA A3004-C8 standard. The same ratio of solution to the sample was conformed to as for the procedure A.

Following placing mortar bars in sodium sulfate solution, continuous length change measurements with the same comparator was carried out on mortar bars at 1, 2, 3, 4, 8, 13, 15 weeks followed by 4, 6, 9, 12, 15, 18, 21, and 24 months. After each

measurement, the sodium sulfate solution was renewed. The new solution was prepared at least 7 hours earlier, and stored at 5 ± 2°C or 23 ± 2°C in order to reach the desired test temperature for ettringite sulfate attack and thaumasite sulfate attack.

Fig. 3-1: Digital comparator used for the length change test – CSA A3004-C8

Fig. 3-2: Mortar samples immersed in sodium sulfate solution and stored at 23±2°C

Fig. 3-3: Mortar samples immersed in sodium sulfate solution and stored at 5±2°C

3-3- Mass change of mortar prisms

Although studying mass change of mortar samples is not mandated by the standard, it is studied along with the expansions on the same bars used for the length change study. Mass change in this study, is a sign of reactions occurring inside the mortar samples. It has been experienced that during the process of sulfate attack, mortar samples gain weight (Sotiriadis et al.-2012). When sulfate attack reactions take place, the resultants fill the voids inside the hydrated cement paste, which results in mass increase. Formation of ettringite, thaumasite and gypsum inside pores leads to expansions and crack propagation. Accordingly, mass increase can stop at certain points near failure and change to mass decrease due to disintegration. Lower increase in mass is a sign of resistance against formation of ettringite, thaumasite, and gypsum. Therefore, mass change is a sign of the progress of sulfate attack, and it can help to monitor and compare the resistance of different samples against formation of ettringite and thaumasite. In this

study, the mass change test was done along with the expansion test. For the test, the excess water on the surface of the mortar bars was removed using paper towel, then the samples were weighed.

3-4- Compressive strength and ultrasonic pulse velocity (UPV) of mortar samples in thaumasite sulfate attack

In order to evaluate the effect of thaumasite sulfate attack on mortar samples, compressive strength and UPV tests are also performed on selected blends from Table 3-3. The blends studied are presented in Table 3-4. The control blends are selected in addition to six other blends, each containing one of the supplementary cementing materials used in this research. The selection was made considering CSA A3001-10 and the 6-month expansion results of the mortar bars. As for slag and fly ash, the percentages recommended by CSA A3001-10 were selected. For metakaolin, although the standard recommends 15% addition of metakaolin, 20% addition was chosen as this sample was showing lower expansions in thaumasite sulfate attack. Regarding the binary blends containing SF and SFI and ternary blend containing slag and fly ash, the blends showing lower expansions at 6 months were selected.

Table 3-4: Blends of PLC used for compressive strength and UPV study

	Blend designation
1	L Control
2	GUL Control
3	L-40 Slag
4	L-25 FA
5	L-20 MK
6	L-40 Slag-20 FA
7	L-8 SF
8	L-8 SFI

Compressive strength is a criterion that indicates bonding and quality of concrete and mortar. During the process of thaumasite sulfate attack, mortar loses its cohesiveness and integrity, which directly affects its compressive strength. Thus, studying compressive strength of mortar samples during exposure to TSA can show their resistance. For this purpose, 50x50x50 mm standard cubic mortar samples are prepared according to ASTM C305 (Almost similar to CSA A3004-C1) and ASTM C109 (Almost similar to CSA A3004-C2) with PLC blends presented in Table 3-4. The same mixture proportions, procedure, and curing as for procedure B of CSA A3004-C8 for thaumasite sulfate attack was followed; the molds were put in 100% humidity containers, placed in an oven with temperature of 35 ± 3°C for 23 ± 0.5 hours. Then, the mortar samples were demoulded and placed in saturated limewater at 23°C. Later, when the mortar cubes achieved 20 ± 1 MPa strength, they were placed in 50 g/L sodium sulfate solution, which was previously prepared and precooled in the refrigerator for at least 7 hours. All the samples were placed in a refrigerator with temperature of 5 ± 2°C. The volume of the sodium sulfate solution was limited to 4 ± 0.5 times of the volume of the submerged mortar cubes, and the solution was renewed at the intervals suggested by CSA A3004-C8 for expansion measurements. The compressive strength of cubes was measured as per ASTM C109 (or CSA A3004-C2) after 28 days, 3, 6, 9, and 12 months of immersion in 5°C sodium sulfate solution. At each compressive strength test, two cubes were tested.

The ultrasonic pulse velocity test measures the velocity of ultrasonic waves passing through the sample. The wave's velocity is related to the density and integrity of the sample. Formation of cracks and defects inside the sample as well as disintegrations reduce the pulse velocity. Therefore, a periodic UPV measurement on specific samples

can reflect the changes that take place inside the sample. These changes can be due to hydration of cement that increases the density and pulse velocity or development of internal cracks and disintegration due to any deterioration mechanism, which reduces the UPV. This test, along with the compressive strength test shows the changes in the integrity of mortar samples during TSA. Studying compressive strength along with UPV has been practiced by other researchers (Türkmen-2003; Demirboğa et al.-2004; Khan et al.-2007). The UPV test results on cubic mortars during immersed in sodium sulfate solution can show the progress of TSA and the performance of the specified mix, and reinforce the results of the length changes of prismatic samples. In this research, the UPV test was performed according to ASTM C597 (ASTM-2002) on the same mortar cubes prepared for the compressive strength test using a Proceq Pundit+ lab device (Fig. 3-4). Three mortar cubes for each of the 8 blends of Table 3-4 were prepared, numbered, and cured with the other cubes prepared for compressive strength test. After attaining 20 ± 1 MPa strength, UPV was performed on the samples and was considered as the first day test, then they were immerged in 50 g/L sodium sulfate solution at 5 ± 2°C with other cubes prepared for compressive strength test. The same process of thaumasite sulfate attack including solution volume and solution change intervals was followed as for mortar bar samples prepared for the length change test. The ultrasonic test was performed on the numbered mortar cubes during a year at ages of 28 days, 3, 6, 7.5, 9, 10.5, 12, and 15 months of thaumasite sulfate attack. At each age of the test, the UPV device was first started and calibrated with the calibration rod. Afterwards, the samples' container was taken out of the refrigerator. Each mortar cube was taken out of the sodium sulfate solution, then immediately the transducers were put on two opposite sides, and when a

stable transit time was displayed on the device, the calculated ultrasonic pulse velocity was saved. For each cube, the same sides were used in the UPV test at all ages in order to keep the test results consistent. A couplant was applied on the surface of transducers to help the best contact with the surface of mortar samples. The couplant was easily removed from the surface of the mortar cubes and the transducers with paper towels and water after each test.

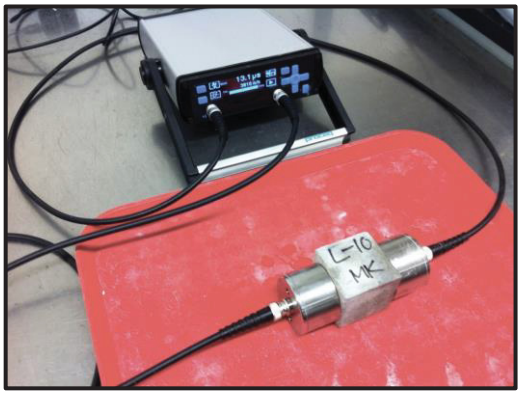

Fig. 3-4: Ultrasonic pulse velocity test on cubic mortar samples

3-5- Differential scanning calorimetry (DSC) on samples in thaumasite sulfate attack

Since detection of thaumasite in deteriorated mortar samples at 5°C was of significance, the DSC technique was implemented. This technique would help to identify presence of ettringite, thaumasite, and gypsum inside deteriorated samples. Mortar bars, which failed during TSA exposure, were processed at the date of failure. Small samples were then obtained from the disintegrated parts of the surface. The obtained samples were first air-dried at room temperature for at least 24 hours followed by hand grinding with a pestle to less than 75 microns. Afterwards, with the purpose of removing the physical water, they were kept in oven at temperature of 35°C – 40°C until they achieved a

constant weight. For the differential scanning calorimetry test, 7 to 10 mg of the each prepared powder sample was placed in a cell. Sealed aluminum cells were used with a small pinhole to allow for the escape of gases. The cell was placed in the test compartment of TA Instruments-2010 DSC apparatus beside an empty cell as the reference (Fig. 3-5 and Fig. 3-6). The DSC test was performed on the samples from 0°C to 550°C with heating rate of 5°C per minute under a flowing nitrogen environment. The temperature calibration of the device was made with pure Indium provided by TA Instruments. For each test, the computer connected to the DSC device would give a graph showing thermal peaks related to dehydration and decomposition of different compounds in the sample.

After two years (the time period that is defined by CSA A3001-10), those mortar bars, which did not fail were also taken for DSC. Samples were obtained from the surface of the sound mortar bars, and the same procedure for powder preparation and test was performed as explained.

Fig. 3-5: TA Instruments-2010 DSC apparatus

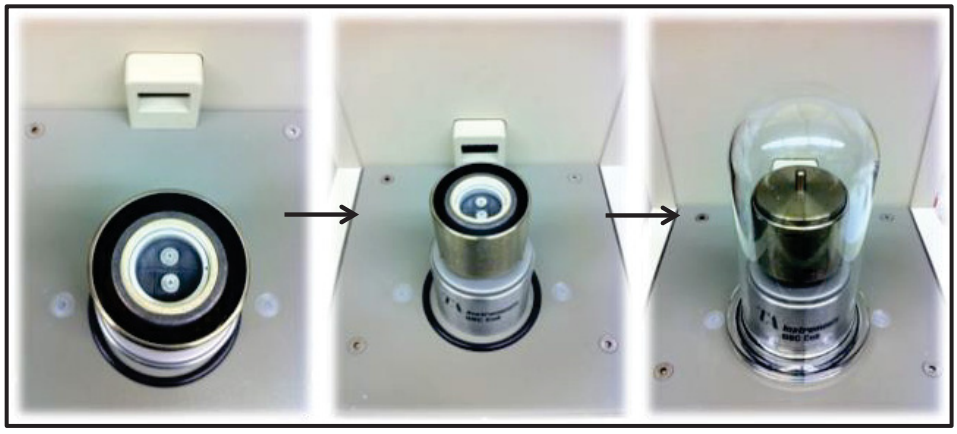

Fig. 3-6: Placing sample cell as well as reference cell in the DSC device

3-6- X-Ray Diffraction (XRD) test on samples in thaumasite sulfate attack

As mentioned before, differential scanning calorimetry was carried out for the compositional study of mortar samples affected by thaumasite sulfate attack. The results for a number of samples were not quite helpful, as distinctive peaks for thaumasite were not found. Regarding this issue, phase identification test using X-ray diffraction was performed on the mentioned samples as well as control samples. The same sample

preparation as for DSC test was followed. The only difference was in the powder particle sizes. In order to reach smoother XRD patterns, the samples were ground to less than 45 microns. The XRD equipment used for this purpose was a Philips PW1700 diffractometer system with copper radiation. The scan interval was 5-50° (2θ) with step sizes of 0.02° and time per step of 0.5 seconds.

4- Results

In this chapter, the data obtained from each test method explained in chapter 3 is presented in separate sections. The results are analyzed and discussed individually as well. The presentation of the results, analysis and discussions on each individual test has helped to better understand the properties of Portland-limestone cement and the effect of supplementary cementing materials when added to this type of cement. Relations between the tests are included in Chapter 5.

4-1- Expansion of mortar bars in sulfate attack

In this section, the results of the CSA A3004-C8 expansion tests are presented for both ettringite (23°C) and thaumasite (5°C) sulfate attack. The results for these two types of sulfate attack to blends of Portland-limestone cements are evaluated and discussed individually. The performance of blends of Portland-limestone cement is evaluated with regards to the CSA A3001-10 physical requirements for blended hydraulic cements. As mentioned earlier, this standard limits expansion of mortar bars tested according to CSA A3004-C8 in both ettringite and thaumasite sulfate attack in order to identify moderate and high sulfate resistant blended Portland-limestone cement.

According to CSA A3001-10, a blended Portland cement or a blended Portland-limestone cement is classified as a moderate sulfate resistant cement when the 6-month average expansion of mortar bars tested according to CSA A3004-C8-A (23°C) and the 18-month average expansion according to CSA A3004-C8-B (5°C) are less than 0.10%. For classifying blended Portland cement or blended Portland-limestone cement as a high sulfate resistant cement, the 6-month expansion limit at 23°C is lowered to 0.05%. Yet, the standard declares that if the expansion at 23°C after 6 months is greater than 0.05%,

but it is less than 0.10% after a year, the cement is considered to be passed. Besides, in procedure B of CSA A3004-C8 (5°C), "if the increase in expansion between 12 and 18 months exceeds 0.03%, the sulfate expansion at 24 months shall not exceed 0.10% in order for the cement to be deemed to have passed the sulfate resistance requirements". These requirements are summarized in Table 4-1.

Table 4-1: The CSA A3001-10 expansion limitations for mortar samples studied according to the CSA A3004-C8 sulfate attack test

	MSb and MSLb*	HSb and HSLb*	Reference
Maximum expansion at 6 months (%)	0.10	0.05§	CSA A3004-C8 Procedure A
Maximum expansion at 18 months (%)	0.10**	0.10**	CSA A3004-C8 Procedure B

* MSb stands for moderate sulfate resistant blended hydraulic cement
HSb stands for high sulfate resistant blended hydraulic cement
MSLb stands for moderate sulfate resistant blended Portland limestone cement
HSLb stands for high sulfate resistant blended Portland limestone cement
** If the increase in expansion between 12 and 18 months exceeds 0.03%, the sulfate expansion at 24 months shall not exceed 0.10% in order for the cement to be deemed to have passed the sulfate resistance requirement.
§ If the expansion is greater than 0.05% at 6 months but less than 0.10% at 1 year, the cement shall be considered to have passed.

4-1-1- Ettringite sulfate attack (23°C) – CSA A3004-A

The expansion measurements were carried out on mortar bars, immersed in sodium sulfate solution, after 1, 2, 3, 4, 8, 13, 15, 17, 26, 39, 52, 65, 78, 91, and 104 weeks. Table 4-2 presents the average expansion at some of the times; each average represents the mean of 6 mortar bars. For all blends, expansion increased during the 2-year study. None of the samples failed during this period of time. Therefore, the expansion results are available for all the blends. Expansion occurring in all blends was due to ettringite sulfate attack. During the process of conventional sulfate attack, gypsum and ettringite form due to the reaction of sulfate ions with the hydration products of

cement. Formation of gypsum and ettringite is known to be expansive. Therefore, it can result in surface deterioration and spalling of concrete and ultimately a total failure (Santhanam et al.-2001). The increase in the expansion of the samples during the course of two years is attributed to the progress of sulfate attack and formation of gypsum and ettringite. Continuous presence of sodium sulfate in the system (as the solution was renewed after each measurement) along with presence of calcium hydroxide and calcium aluminate hydrates (results of cement hydration) was in favor of formation of gypsum and ettringite, which led to a continual expansion.

Table 4-2: Expansion of CSA A3004-A mortar bars – Ettringite sulfate attack (23°C)

		Average expansion (%)				
		3 months	**6 months**	**12 months**	**18 months**	**24 months**
1	**L-35 Slag**	0.019	0.031	0.041	0.050	0.053
2	**L-40 Slag**	0.020	0.035	0.045	0.056	0.061
3	**L-45 Slag**	0.025	0.029	0.043	0.045	0.052
4	**L-20 FA**	0.032	0.036	0.050	0.055	0.061
5	**L-25 FA**	0.034	0.038	0.051	0.057	0.062
6	**L-30 FA**	0.019	0.023	0.036	0.041	0.046
7	**L-3 SF**	0.033	0.040	0.053	0.075	0.100
8	**L-5 SF**	0.024	0.034	0.048	0.057	0.063
9	**L-8 SF**	0.021	0.032	0.043	0.051	0.057
10	**L-25 Slag-10 FA**	0.026	0.033	0.039	0.043	0.047
11	**L-30 Slag-10 FA**	0.022	0.030	0.035	0.039	0.042
12	**L-35 Slag-15 FA**	0.017	0.023	0.029	0.029	0.032
13	**L-40 Slag-20 FA**	0.015	0.021	0.026	0.029	0.029
14	**L-3 SFI**	0.033	0.050	0.080	0.153	0.275
15	**L-5 SFI**	0.028	0.040	0.054	0.082	0.135
16	**L-8 SFI**	0.026	0.035	0.044	0.052	0.060
17	**L-10 MK**	0.023	0.030	0.053	0.063	0.083
18	**L-15 MK**	0.023	0.032	0.042	0.049	0.056
19	**L-20 MK**	0.019	0.024	0.029	0.036	0.036
20	**L Control**	0.019	0.047	0.146	0.324	0.569
21	**GUL Control**	0.030	0.097	0.288	0.511	0.799
22	**GUL-40 Slag**	0.013	0.029	0.042	0.048	0.050
23	**GUL-25 FA**	0.032	0.035	0.050	0.056	0.056

The average expansion of the mortar bars after 6, 12, and 24 months is also presented in Fig. 4-1, Fig. 4-2, and Fig. 4-3, respectively. Procedure A of CSA A3004-C8 has expansion limits of 0.10% and 0.05% for moderate sulfate resistant and high sulfate resistant blended PLC, respectively. According to Fig. 4-1, all tested blends of Portland-limestone cement other than the control sample prepared with GUL, have expanded less than the limit for high sulfate resistant blended Portland-limestone cement. Nonetheless, the expansion of "GUL Control" sample after 6 months is less than the limit for moderate sulfate resistance. As this sample shows expansion of 0.288% after a year (Table 4-2) it cannot be classified as high sulfate resistant PLC. All samples continued to expand beyond the six months.

Based on the results summarized in Table 4-2, the control samples (Samples No. 20 and 21) revealed the highest expansions amongst all the studied blends after 2 years immersion in sodium sulfate solution. Although both Portland-limestone cements (L and GUL) had nearly same C_3A contents, the "GUL Control" sample has expanded more than "L Control" sample. This can be attributed to the higher limestone content in GUL (13.5%) in comparison to L (10%). The higher limestone content means a lower cementing property, which weakens the hydrated cement matrix. This signifies the weakness of these cements against ettringite sulfate attack when compared to the blends of PLC with SCMs. According to Table 4-2, supplementary cementing materials have reduced expansions in conventional sulfate attack. When Portland-limestone cement is partially replaced with supplementary cementing materials, the amount of C_3A in the cementitious system is reduced; thus, the possibility of formation of ettringite is decreased. In addition, this replacement reduces the amount of calcium hydroxide in the

hydrated cement paste by reducing the amount of C_2S and C_3S in the system as well as developing pozzolanic reactions in the later stages of hydration. The reduction in the amount of calcium hydroxide in the hydrated cement matrix leads to reduction in the possibility of formation of gypsum and ettringite. Additionally, since supplementary cementing materials take part in pozzolanic reactions by reacting with calcium hydroxide in the hydrated cement matrix, secondary CSH gels are formed that reinforce the hydrated cement matrix. Evidently, the pozzolanic reactions reduce the porosity and permeability of the hydrated cement matrix. From this point of view, the SCMs are also effective in improving resistance against sulfate attack by reducing the chance of ingress of sulfate ions inside the hydrated cement matrix.

The results presented in Table 4-2, Fig. 4-1, Fig. 4-2, and Fig. 4-3 match to the mentioned positive effects of SCMs in mitigating problems due to sulfate attack. According to Fig. 4-1, all the blends of PLC have expanded less than the high sulfate resistance limit. Considering Fig. 4-1, Fig. 4-2, and Fig. 4-3, it can be inferred that generally at ages of 6 months, one year and two years, the samples prepared with supplementary cementing materials have expanded less than the control samples. Also, it could be found that for each type of supplementary cementing material, in most cases, the expansion is decreased when the amount of SCM is increased in the blend. This observation denotes the effectiveness of SCMs on impeding ettringite sulfate attack. Considering Fig. 4-3, the ternary PLC blend containing 40% slag and 20% fly ash had the lowest expansion after two years ettringite sulfate attack. This blend had 60% SCM, which was the highest amount among all the blends. Comparing expansion of this blend with expansion of the binary blends of “L” cement with slag and fly ash, the synergy of

slag and fly ash in a ternary blend of PLC can be inferred. Normally, slag reduces the workability of mortar while fly ash increases this property. Hence, when slag and fly ash are simultaneously used in a blend of cement, the prepared mortar can benefit from the pozzolanic and cementitious properties of slag as well as pozzolanic properties of fly ash (Type F) while it possesses a good flow that helps proper compaction.

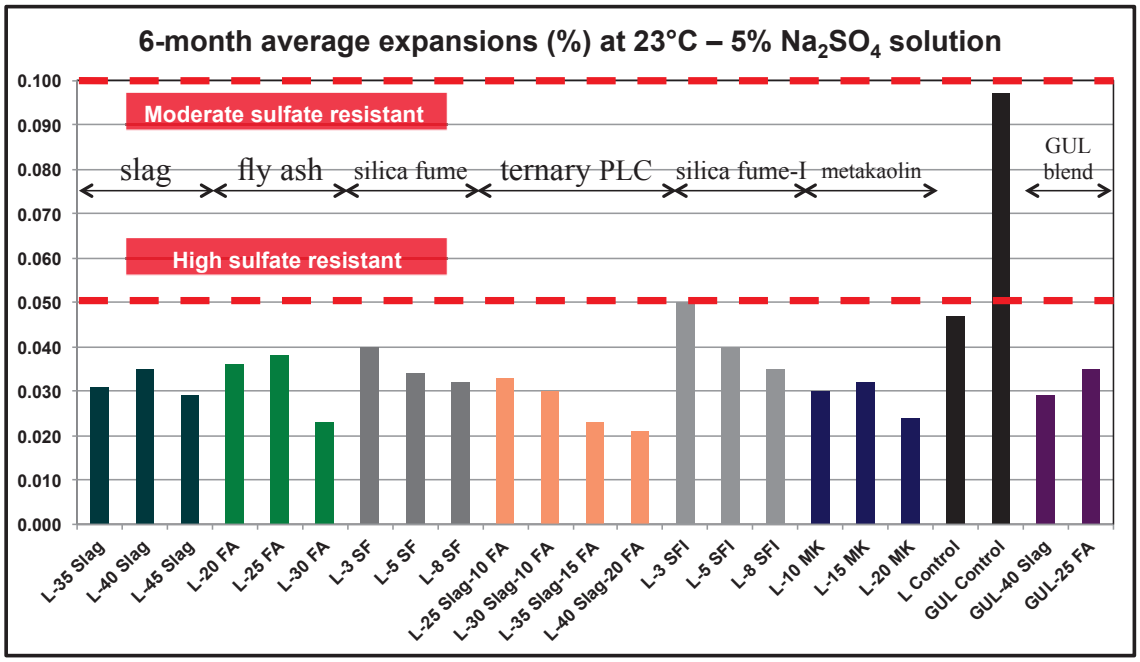

Fig. 4-1: Average expansion of CSA A3004-A mortar bars – 6-month ESA

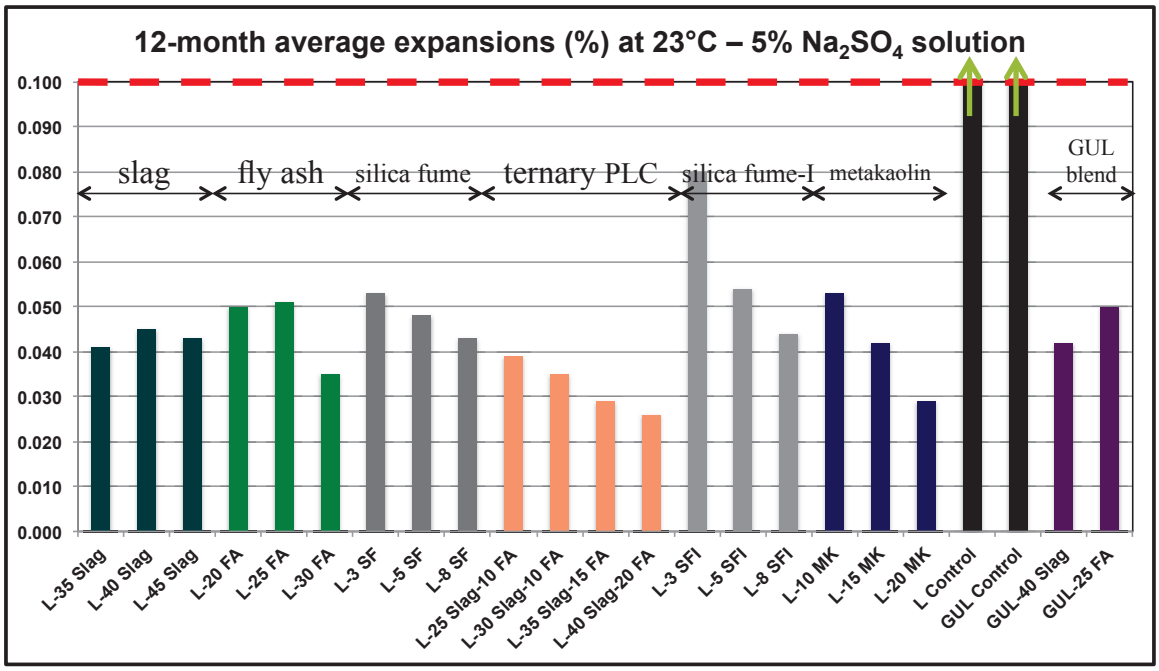

Fig. 4-2: Average expansion of CSA A3004-A mortar bars – 1-year ESA

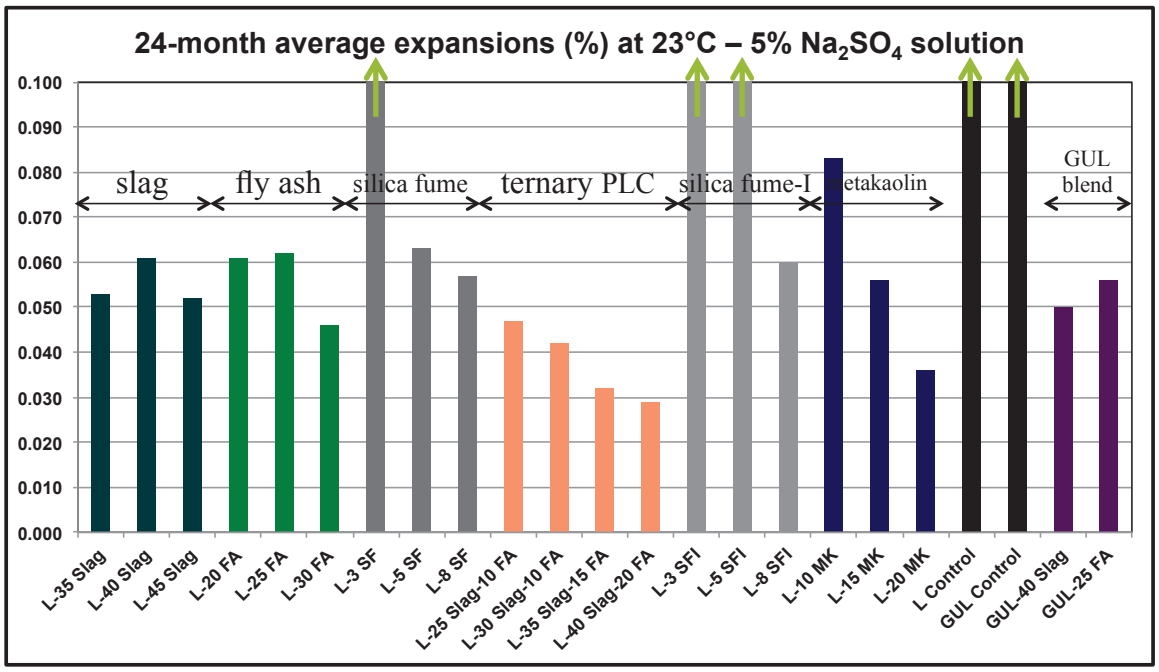

Fig. 4-3: Average expansion of CSA A3004-A mortar bars – 2-year ESA

Expansion in mortar bars can result in formation of cracks and distortion (curving), which ultimately results in total failure of the samples. Noticeable cracks and

distortion were found in mortar bars prepared with the two control blends of Portland-limestone cement. The distortion in mortar bars can be due to the deflection between the two supports of the mortar bars. It also can result from an uneven expansion inside the samples. In order to avoid such curving, the use of plastic grids as the support for mortar bars has been tried before in a similar study, and despite the use of such supports, curving was detected (Ramezanianpour-2013). As seen in Fig. 4-4, after 30 months of ettringite sulfate attack, cracks on the edges and at the end of the mortar bars of "GUL Control" and "L Control" were visible. The two mentioned blends had the highest expansions. After this period of time, the other blends containing SCMs were totally sound, and only very small longitudinal cracks were seen on "L-3 SFI" sample. In Fig. 4-4, an image of "L-40 Slag-20 FA" mortar bars, which showed the lowest expansion among the studied samples, is also presented. The mortar bars are completely sound and no sign of cracking is visible. Comparing these mortar bars with the control samples in Fig. 4-4, the positive effect of the SCMs on mortars in ettringite sulfate attack is more apparent. In Fig. 4-5, there is a closer look at the extent of cracks in "L Control" sample. The cracks are extensive and can finally cause failure in the mortar bars. According to the close visual study, the ettringite sulfate attack has not caused disintegration of the mortar bars.

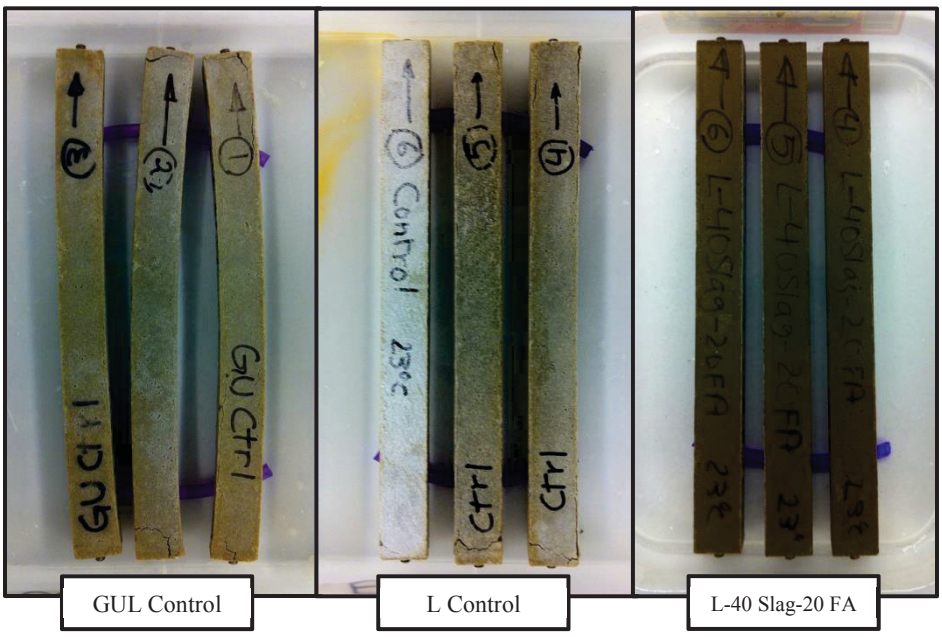

Fig. 4-4: Mortar bars after 30 months ettringite sulfate attack

Fig. 4-5: Formation of cracks on the edges and at the end of the control mortar bars due to ESA

4-1-2- Thaumasite sulfate attack (5°C) – CSA A3004-B

The average expansion of mortar bars tested in thaumasite sulfate attack as per CSA A3004-B is depicted in Table 4-3. The averages presented are the mean of 4 mortar bars. According to the standard procedure, the length change measurements were performed at ages of 1, 2, 3, 4, 8, 13, 15, 17, 26, 39, 52, 65, 78, 91, and 104 weeks, but in order to simply summarize the results, solely length changes at ages of 3, 6, 12, 18, and

24 months are reviewed in the table. All samples showed increasing expansions during the thaumasite sulfate attack test. The expansion along with the disintegration caused by severe thaumasite sulfate attack was followed by total failure in some of the samples as mentioned in the table. The expansions are due to thaumasite sulfate attack in which thaumasite is formed predominantly, but ettringite and gypsum are also formed. Formation of all these products is expansive, and results in deterioration. Since formation of thaumasite is associated with destruction of the CSH structure in the hydrated cement matrix, it has caused severe disintegration and failure in many of the studied blends during the 2-year thaumasite sulfate attack.

In the Table 4-3, the time to failure of the blends is also presented. The failure of a sample is considered the time in which the sample is broken or deteriorated in a way that performing the length change test is impossible. Although failure could have occurred at any time since the previous measurement, the time of failure is defined when a scheduled measurement was no longer possible. The failed samples were mostly disintegrated, fractured, or lost the cohesion to the measurement pins. The first to fail was blend No. 21, the "GUL Control" sample, which contained 13.5% ground limestone. The mortar bars failed after 17 weeks of immersion in sodium sulfate solution at 5°C. The other control sample, prepared with blend No. 20 (L Control) failed at 42 weeks. This type of cement contained 10% ground limestone. As the carbonate source is vital for thaumasite formation, the main reason for "GUL Control" to fail sooner than "L Control" is the higher limestone content. Compared to the "GUL Control" sample, addition of 40% slag or 25% fly ash to the Portland-limestone cement in blends No. 22 and 23, respectively, improved the performance in thaumasite sulfate attack by reducing the

expansion and delaying the failure time. Results for the blends No. 1 through 19, which contain the other PLC, presented in the Table 4-3, show that all blends containing Type F fly ash were deteriorated during this study. Also, "L-3 SF", "L-3 SFI", "L-5 SFI", "L-10 MK", and "L-15 MK" have failed. Those mixtures containing slag were generally intact until 24 months. According to the table, generally, increasing amounts of supplementary materials decreased expansion, but did not prevent failure in some cases.

Table 4-3: Expansion of CSA A3004-B mortar bars and time to failure – Thaumasite sulfate attack (5°C)

		Average expansion (%)					
		3 months	**6 months**	**12 months**	**18 months**	**24 months**	Time to failure (weeks)
1	**L-35 Slag**	0.010	0.025	0.047	0.173	0.518	Not failed
2	**L-40 Slag**	0.013	0.027	0.041	0.085	0.219	Not failed
3	**L-45 Slag**	0.019	0.027	0.039	0.045	0.055	Not failed
4	**L-20 FA**	0.036	0.086	**Failed**	**Failed**	**Failed**	52
5	**L-25 FA**	0.036	0.089	0.196	**Failed**	**Failed**	65
6	**L-30 FA**	0.025	0.047	**Failed**	**Failed**	**Failed**	52
7	**L-3 SF**	0.030	0.040	0.063	0.202	**Failed**	104
8	**L-5 SF**	0.025	0.037	0.047	0.056	0.091	Not failed
9	**L-8 SF**	0.026	0.036	0.046	0.046	0.051	Not failed
10	**L-25 Slag-10 FA**	0.025	0.034	0.048	0.064	0.110	Not failed
11	**L-30 Slag-10 FA**	0.023	0.031	0.044	0.084	0.178	Not failed
12	**L-35 Slag-15 FA**	0.020	0.028	0.038	0.044	0.048	Not failed
13	**L-40 Slag-20 FA**	0.019	0.024	0.035	0.037	0.038	Not failed
14	**L-3 SFI**	0.034	0.047	**Failed**	**Failed**	**Failed**	52
15	**L-5 SFI**	0.030	0.040	0.071	0.329	**Failed**	91
16	**L-8 SFI**	0.026	0.038	0.043	0.068	0.255	Not failed
17	**L-10 MK**	0.026	0.032	0.078	0.144	**Failed**	91
18	**L-15 MK**	0.024	0.036	0.104	**Failed**	**Failed**	78
19	**L-20 MK**	0.024	0.033	0.043	0.068	0.108	Not failed
20	**L Control**	0.015	0.038	**Failed**	**Failed**	**Failed**	42
21	**GUL Control**	0.376	**Failed**	**Failed**	**Failed**	**Failed**	17
22	**GUL-40 Slag**	0.007	0.025	0.111	0.435	**Failed**	91
23	**GUL-25 FA**	0.175	**Failed**	**Failed**	**Failed**	**Failed**	26

The average expansions of the studied blends of Portland-limestone cement at 18 months and 24 months are also presented in Fig. 4-6 and 4-7, respectively. As mentioned previously, the CSA A3001-10 limits the expansion of mortar bars, tested in accordance with CSA A3004-C8-B, to 0.10% at 18 months in order to achieve moderate or high sulfate resistant blended Portland-limestone cement. With respect to this mandate and Fig. 4-6, blends; "L-40 Slag", "L-45 Slag", "L-5 SF", "L-8 SF", "L-25 Slag-10 FA", "L-30 Slag-10 FA", "L-35 Slag-15 FA", "L-40 Slag-20 FA", "L-8 SFI", and "L-20 MK" expanded below the limit for sulfate resistant blended Portland-limestone cement. The CSA A3001-10 standard also limits the 24-month expansion to 0.10% for those samples, if their increase in expansion between 12 to 18 months exceeds 0.03%. If such limit is achieved, the cement would be classified as high sulfate resistant blended Portland-limestone cement. Considering the expansion data in Table 4-3, among the blends expanded less than 0.10% in 18 months, expansions of "L-40 Slag" and "L-30 Slag-10 FA" between 12 months and 18 months have exceeded 0.03%. According to Fig. 4.7, these two blends have expanded more than 0.10% after 24 months TSA as well, which means that they cannot be considered as high sulfate resistant blended PLC.

The effectiveness of supplementary cementing materials on resistance against thaumasite sulfate attack can be inferred from Table 4-3, Fig. 4-6, and Fig. 4-7. In Table 4-3, the positive effect of slag or fly ash addition to GUL cement is apparent, as they have delayed failure of the samples. For the first 20 blends containing the other type of PLC the same conclusion can be made since the blends containing SCMs are either not failed or failed later than the control sample (No. 20). The supplementary cementing materials studied are generally found more helpful in reducing expansion in TSA when

used in higher amounts in PLC blends. This can be observed in Fig. 4-6 and 4-7. In fact, in the studied binary and ternary blends of PLC, increases in the amount of slag, silica fume, silica fume I, metakaolin, and the combination of slag and fly ash (ternary blend) has decreased expansion. In both Fig. 4-6 and 4-7, the ternary Portland-limestone cement blend containing 40% slag and 20% fly ash showed the lowest expansion in TSA. Therefore, from the point of view of expansion, this sample resisted the best against thaumasite sulfate attack. Partially replacing Portland-limestone cement with supplementary cementing materials is beneficial from different aspects. Reactions related to formation of thaumasite are dependent to presence of carbonates. When PLC is partially replaced with SCM, the limestone content of the blended cement is reduced; therefore the extent of formation of thaumasite is reduced. Moreover, by addition of supplementary cementing materials the C_3A content of the blended PLC is lowered. So, formation of ettringite, which is an initiator for formation of thaumasite, is reduced. When formation of ettringite is decreased, the expansion and crack formation due to its development is decreased; accordingly, the resistance against thaumasite sulfate attack is improved, as the cement matrix is less affected and less permeable to ingress of sulfate ions that can result in formation of thaumasite inside the hydrated cement paste. Additionally, supplementary cementing materials reinforce the hydrated cement matrix by reacting with calcium hydroxide as a result of cement hydration, and forming secondary calcium silicate hydrate gels. This reinforcement improves the resistance against disintegrations occurred by formation of thaumasite. Besides, pozzolanic reactions and formation of secondary CSH gels reduce the porosity of the hydrated cement paste and increase its density. This results in a lower permeable concrete that can

better resist against thaumasite sulfate attack because the ingress of sulfate ions inside the hydrated cement paste is more difficult.

In order to achieve moderate sulfate resistant or high sulfate resistant blended PLC, the CSA A3001-10 standard declares that, the blended PLC shall contain at least 25% Type F fly ash, or 40% slag, or 15% metakaolin. Considering the results presented in Table 4-3, Fig. 4-6, and Fig. 4-7, the mentioned minimum amounts were not sufficient to promote the studied cements to high sulfate resistant blended PLC. Of course, when the SCM content was increased over the standard suggestions, the resistance was attained for slag and metakaolin containing blends, but none of the PLC blends containing the studied Type F fly ash achieved the standard limits for expansion. This can be due to the fact that typically fly ash is more chemically variable compared to slag and metakaolin. Considering these results and the fact that the standard recommendations are rather new, more experimental study on various PLC and SCMs is required to draw accurate suggestions for addition of supplementary cementing materials to Portland-limestone cement with the purpose of utilization in sulfate environments.

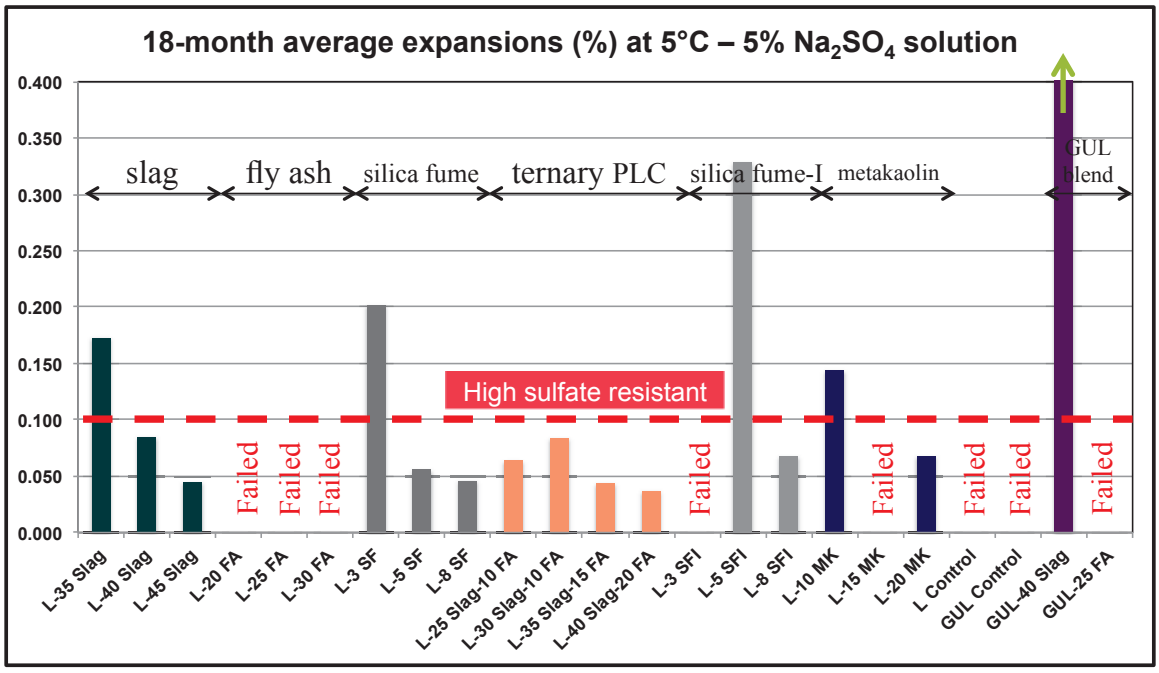

Fig. 4-6: Average expansion of CSA A3004-B mortar bars – 18-month TSA

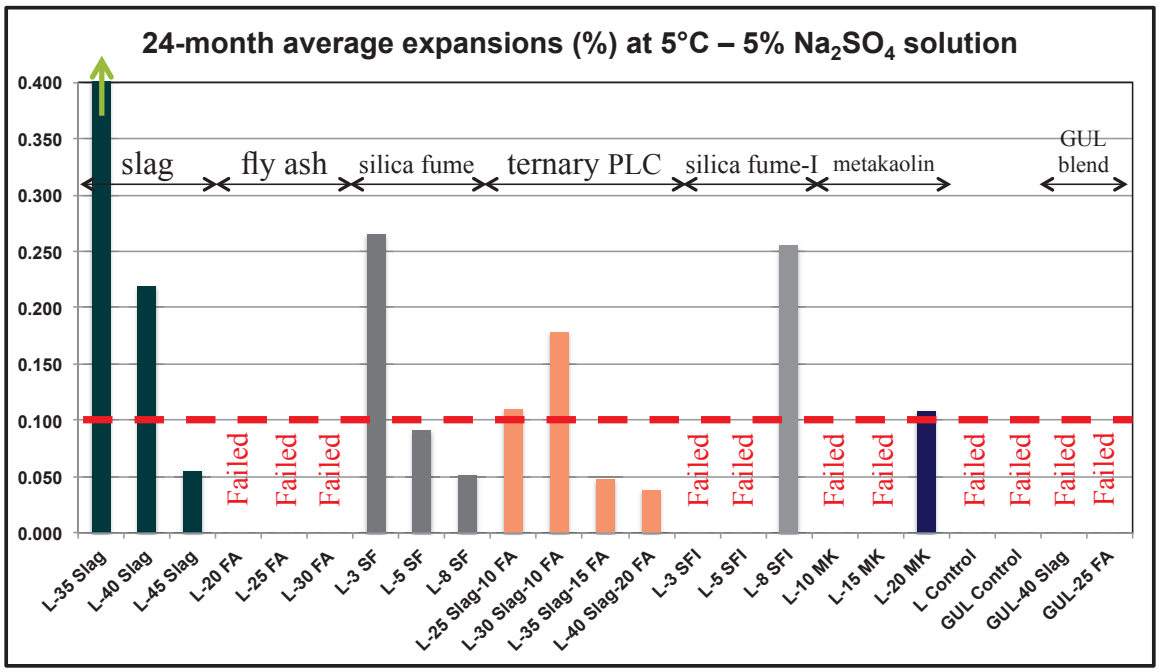

Fig. 4-7: Average expansion of CSA A3004-B mortar bars – 2-year TSA

As mentioned, some of the Portland-limestone cement blends qualified as high sulfate resistant blended PLC. The two-year average expansion of these blends in

thaumasite sulfate attack is presented in Fig. 4-8. While all the presented blends are high sulfate resistant blended PLC, there are noticeable differences in their expansions. Accordingly, considering expansion in CSA A3004-C8-B test as a criterion for resistance in TSA, the noted blends have different resistances. “L-40 Slag-20 FA”, which contained the highest amount of SCM, had the best performance against thaumasite sulfate attack. The worst performance from the point of view of expansion was related to “L-8 SFI”. It is clear that slag, when used in high percentages, had a key role on improving resistance in TSA. Silica fume also was quite effective in performance improvement of PLC, the intermediate silica fume (SFI) as expected was not as effective as silica fume. According to the figure, “L-8 SFI”, “L-25 Slag-10 FA”, and “L-20 MK” have passed the CSA A3001-10 expansion limit at some point after 18 months. Yet, they qualified as high sulfate resistant PLC as their expansion between 12 to 18 months was less than 0.03%. As clearly seen in Fig. 4-8, the rate of the length change for each blend changes as a function of time, and at older ages graph of some of the blends has shown an increased rate in length change. Such observation denotes that the mortar bars are getting close to the failure. The differences in the length change rate of the blends at particular ages also emphasize the differences in resistance against thaumasite sulfate attack. “L-40 Slag-20 FA” that had the lowest expansion in two years also showed the lowest length change rate at the last interval of expansion test amongst the other high sulfate resistant blended Portland-limestone cements.

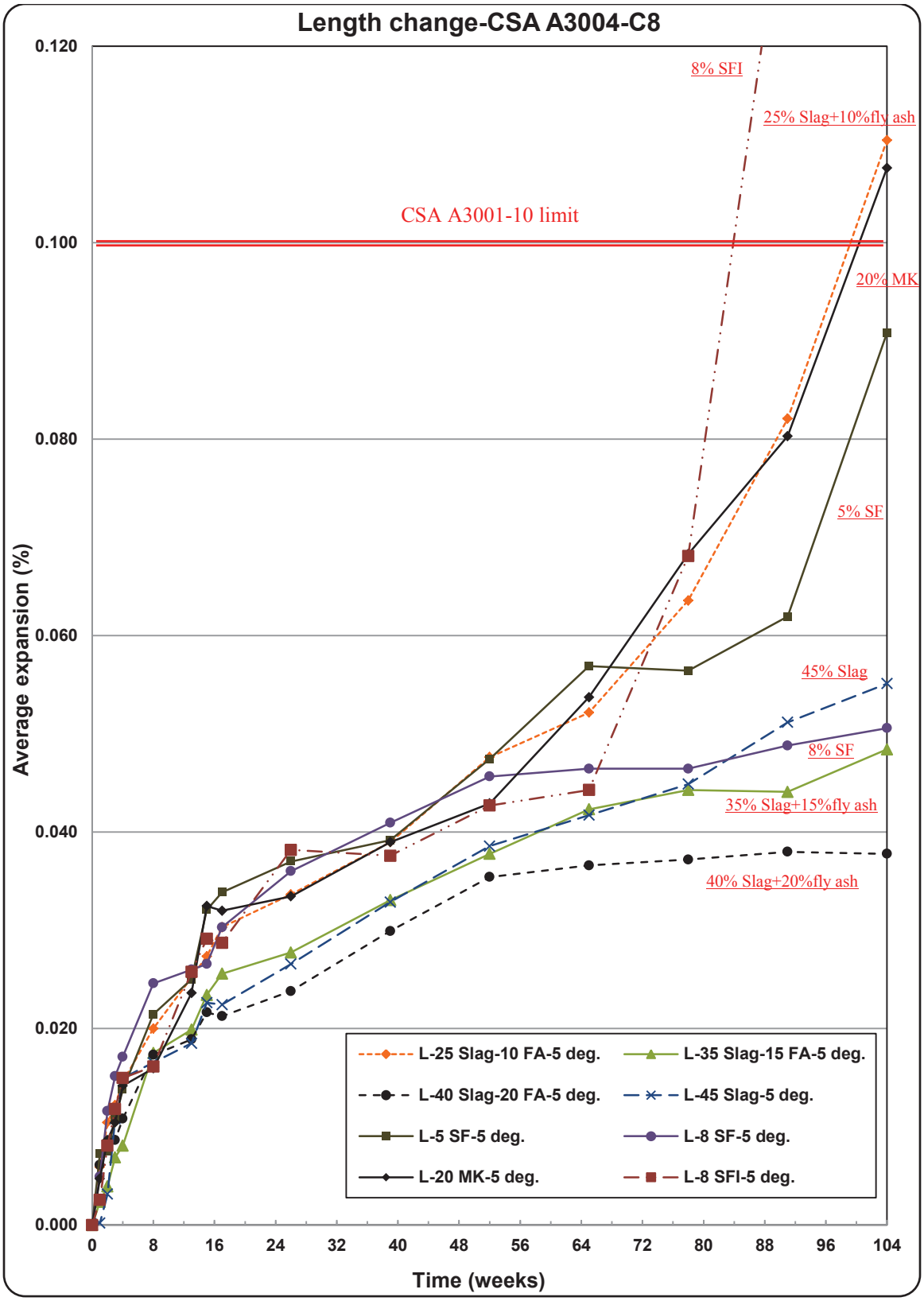

Fig. 4-8: Two-year average expansion of high sulfate resistant CSA A3004-C8 mortar bars in TSA

As previously mentioned, the mortar bars prepared with GUL cement (limestone content of 13.5%), were the first mortar samples to fail after only 17 weeks of immersion in 5% sodium sulfate solution at 5°C. The other Portland-limestone cement sample containing 10% ground limestone failed later after 42 weeks of thaumasite sulfate attack. The failure due to thaumasite sulfate attack was very extensive, and in addition to formation of cracks and mortar bars deformation, degradation and disintegration was occurred. The aggressiveness of thaumasite sulfate attack to the plain Portland-limestone cement can be seen in Fig. 4-9. After only 4 months of immersion of mortar bars in sodium sulfate solution at 5°C, the visible cracks were found on the edges and at the end sections of the samples as well as noticeable deformation because of expansion took place due to thaumasite sulfate attack. This was followed by decomposition of hydrated cement paste in later ages. As presented in Fig. 4-9, 7 months later the mortar bars were completely crumbled and disintegrated to a non-cohesive mush found on the base of the container. Such failure was also seen for the other control sample. The visual observations confirmed that deterioration due to thaumasite sulfate attack was quite extensive compared to the ettringite sulfate attack, and it was different from the point of view of type of failure since in addition to deformation and cracks, thaumasite sulfate attack resulted in decomposition of mortars.

Binary and ternary blends of PLC and SCMs visually exhibited greatly improved resistance to thaumasite sulfate attack in comparison to the control samples of plain PLC. Fig. 4-10 shows the mortar bars prepared with the blended Portland-limestone cement, which contains 5% and 8% silica fume I after 2 years of thaumasite sulfate attack. The deterioration due to thaumasite sulfate attack is apparent for both sets of mortar bars.

Although the one with higher SFI content reveals deterioration and mass loss on the edges and at the end, it is visually in a better condition and has not failed while the other sets of samples containing 5% SFI are fractured and lost much of the surface. The samples prepared with the other type of silica fume presented in Fig. 4-11 are relatively less damaged in the period of 2-year thaumasite sulfate attack. According to this figure, the increase in the silica fume content has improved the performance of mortar bars in TSA. Both "L-5 SF" and "L-8 SF" exhibited better visual condition in comparison to the corresponding mortar samples with SFI content. The differences in the two types of silica fume are the content of SiO_2, being greater in SF than SFI. CSA A3001-10 states that the classification of SF to be greater than 85%. The higher amounts of silicon create higher sulfate resistance.

The visual condition of samples prepared with 15% and 20% metakaolin is shown in Fig. 4-12. The mortar samples prepared with the PLC replaced with 15% metakaolin were broken and mainly lost the surface in thaumasite sulfate attack after two years. The other set of mortar bars showed a considerably better condition. Although some cracks formed on the edges, they looked fairly sound. Fig. 4-12 visually shows how the resistance of mortar bars is improved when the content of metakaolin in binary blend of PLC is increased from 15% to 20%. Slag containing mortar bars immersed in sodium sulfate solution at 5°C for 30 months are presented in Fig. 4-13. The increase in amount of slag has also improved the resistance against TSA. Deterioration in "L-35 Slag" mortars is visible in form of cracks and fracture. However, there are only small cracks on edges of "L-40 Slag" and the other set of mortar bars "L-45 Slag" is totally sound. Mortar samples of the ternary blends of PLC containing slag and fly ash after a 2-year

thaumasite sulfate attack can be observed in Fig. 4-14. Signs of TSA as cracks were visible in samples of “L-25 Slag-10 FA” and “L-30 Slag-10 FA”. Nevertheless, the other samples, which included higher amounts of slag and fly ash, were looking sound.

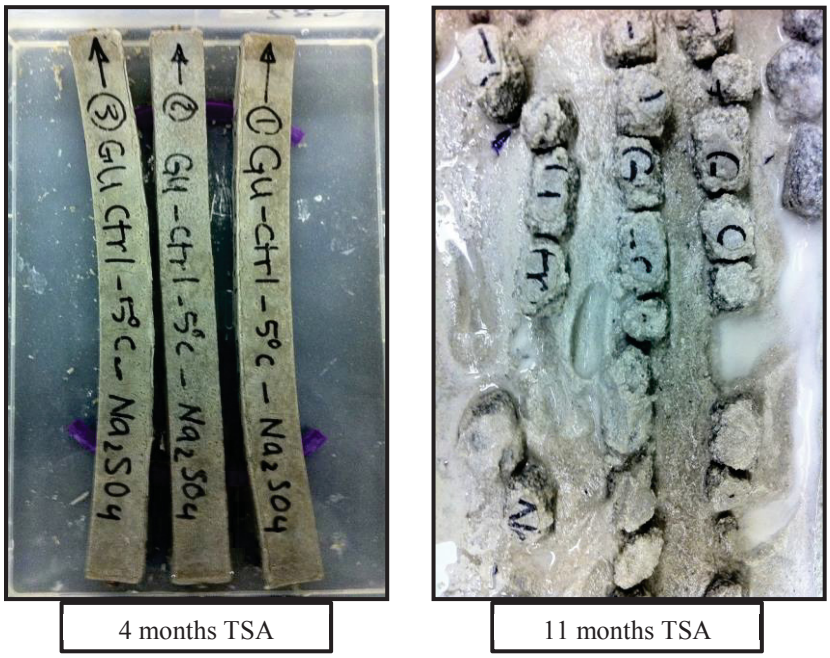

Fig. 4-9: Effect of thaumasite sulfate attack on plain Portland-limestone cement (GUL)

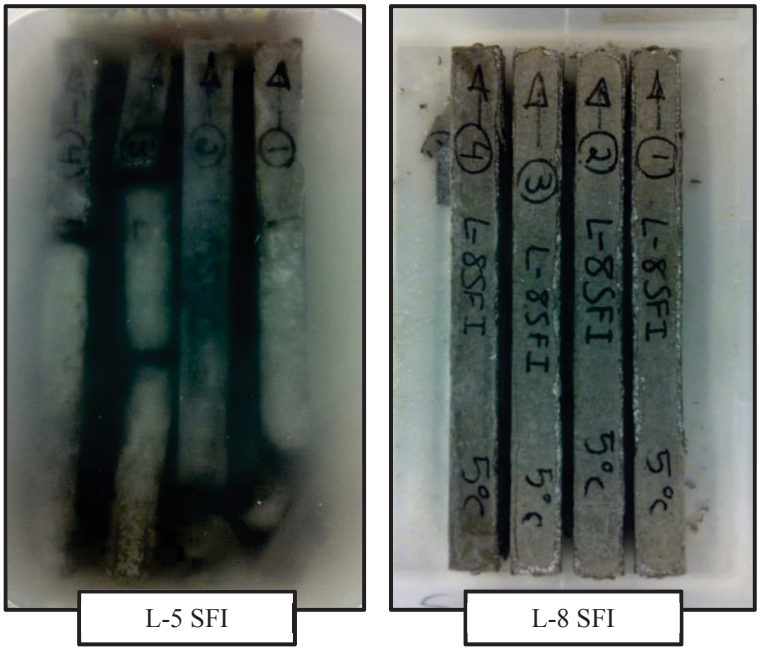

Fig. 4-10: 24-month thaumasite sulfate attack to mortar bars containing silica fume I

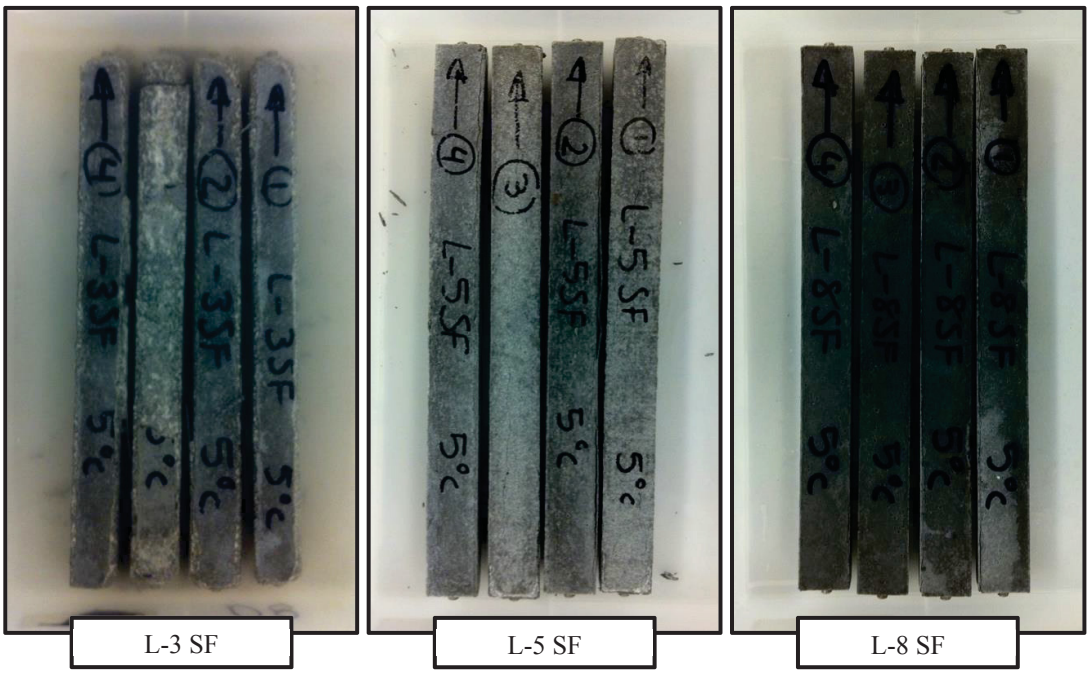

Fig. 4-11: 24-month thaumasite sulfate attack to mortar bars containing silica fume

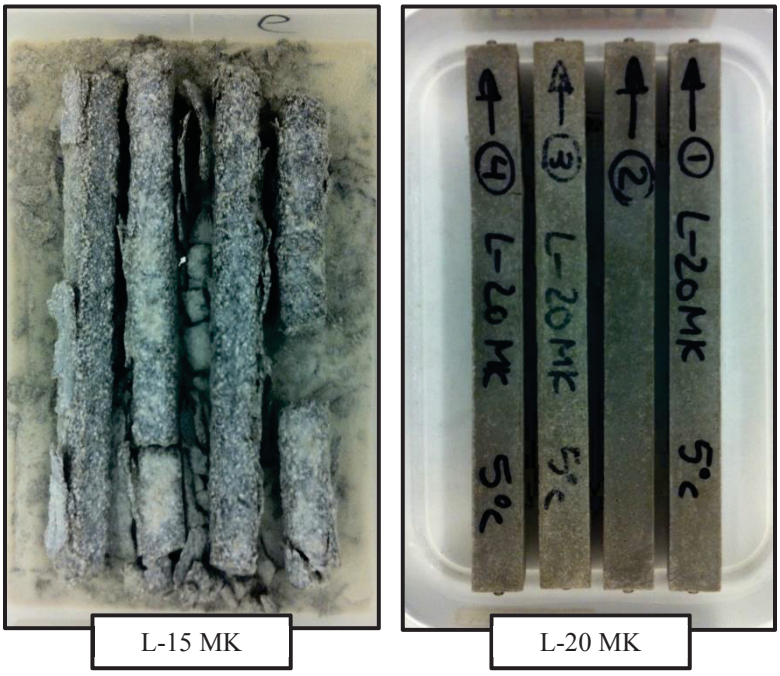

Fig. 4-12: 24-month thaumasite sulfate attack to mortar bars containing metakaolin

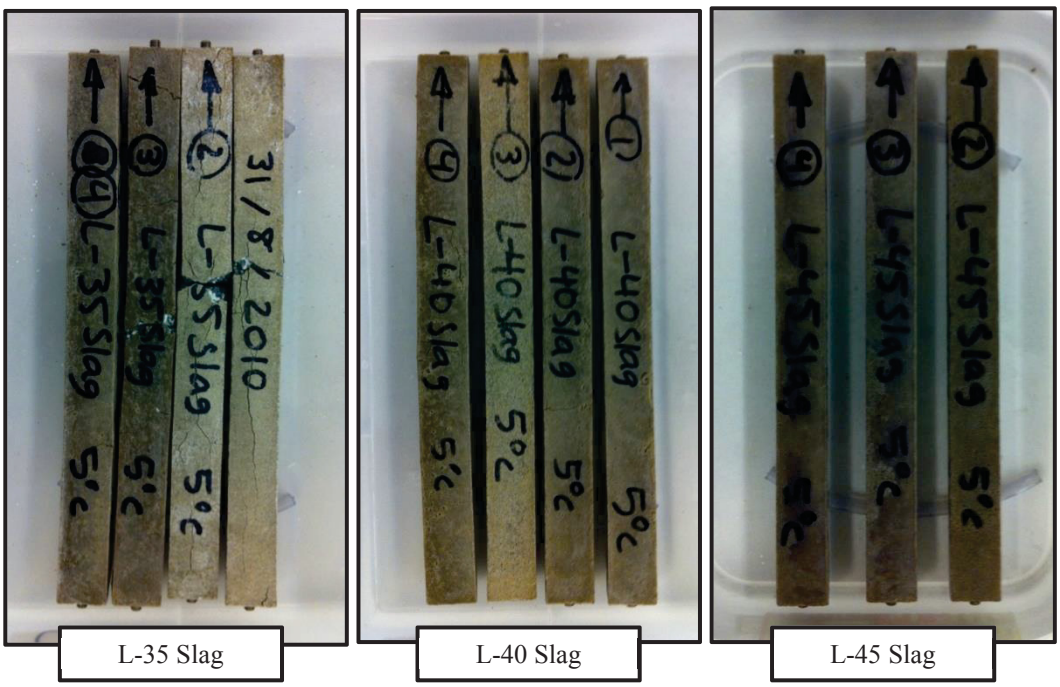

Fig. 4-13: 30-month thaumasite sulfate attack to mortar bars containing slag

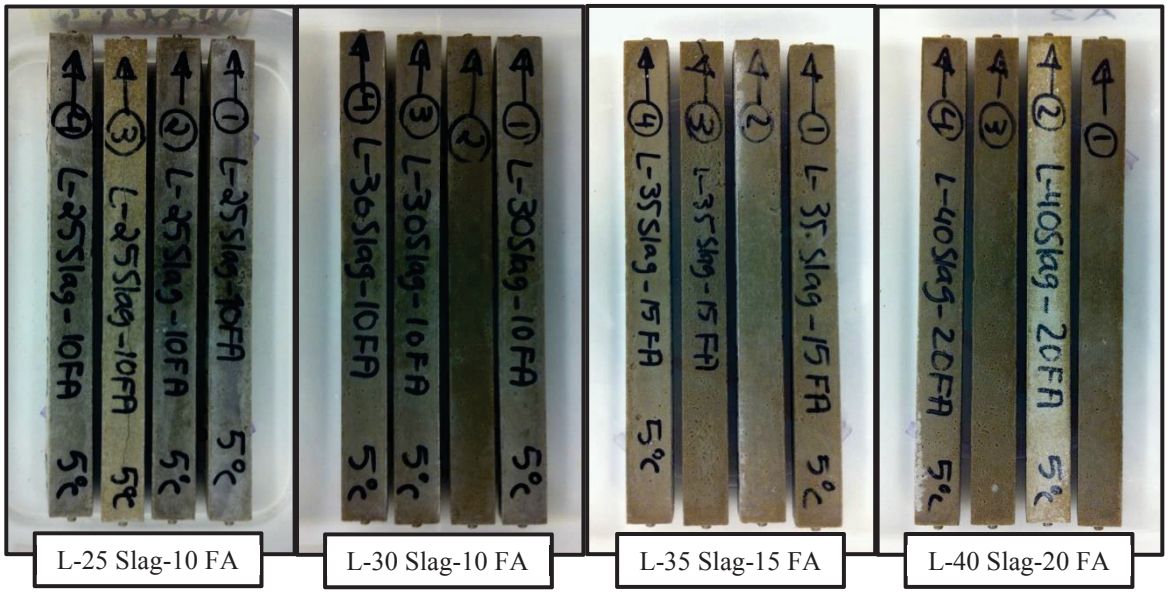

Fig. 4-14: 24-month thaumasite sulfate attack to mortar bars containing slag and fly ash

4-1-3- Sulfate resistant blends of Portland-limestone cement (CSA A3001-10)

Certainly, the main purpose for studying expansion of mortar bars in sulfate attack is to verify whether a specific cement can be considered as a sulfate resistant

cement or not. In order to classify the studied blends as moderate or high sulfate resistant blended PLC, according to CSA A3001-10, the 6- and 12-month expansion in ettringite sulfate attack as well as the 12-, 18-, and 24-month expansion in thaumasite sulfate attack is required. The mentioned data is presented in Table 4-4. As explained earlier, the Canadian standard requires expansions lower than 0.05% and 0.10% after 6 months of exposure to ESA for high sulfate resistant blended PLC (HSLb) and moderate sulfate resistant blended PLC (MSLb), respectively. In case a PLC blend overpasses the expansion limit for HSLb after 6 months, yet shows expansion less than 0.10% after 12 months, it can be deemed as HSLb. Thus, for ettringite sulfate attack study, 6-month and 12-month results are essential. According to the standard, the limits for TSA are stricter. HSLb or MSLb mortar prisms must have average expansions of 0.10% or less after 18 months of TSA. Such samples also must expand lower than 0.03% between 12 months and 18 months of exposure, and if they do not satisfy this requirement, the 18-month expansion limit shifts to 24-month. Accordingly, in general, the 12-, 18-, and 24-month expansion in TSA is required for assessment of sulfate resistance of the studied blends. The required data is presented Table. 4-4, and the status of the blends from the viewpoint of sulfate resistance is determined. Only 8 of the 23 studied blends qualified as HSLb, and none of the other blends could be considered as MSLb.

Table 4-4: Studying sulfate resistance of PLC blends – CSA A3001-10

		Average expansion (%)					
		ESA (23°C)		TSA (5°C)			Sulfate resistance
		6 months	12 months	12 months	18 months	24 months	
1	L-35 Slag	0.031	0.041	0.047	0.173	0.518	----
2	L-40 Slag	0.035	0.045	0.041	0.085	0.219	----
3	L-45 Slag	0.029	0.043	0.039	0.045	0.055	HSLb*
4	L-20 FA	0.036	0.050	Failed	Failed	Failed	----
5	L-25 FA	0.038	0.051	0.196	Failed	Failed	----
6	L-30 FA	0.023	0.035	Failed	Failed	Failed	----
7	L-3 SF	0.040	0.053	0.063	0.202	Failed	----
8	L-5 SF	0.034	0.048	0.047	0.056	0.091	HSLb
9	L-8 SF	0.032	0.043	0.046	0.046	0.051	HSLb
10	L-25 Slag-10 FA	0.033	0.039	0.048	0.064	0.110	HSLb
11	L-30 Slag-10 FA	0.030	0.035	0.044	0.084	0.178	----
12	L-35 Slag-15 FA	0.023	0.029	0.038	0.044	0.048	HSLb
13	L-40 Slag-20 FA	0.021	0.026	0.035	0.037	0.038	HSLb
14	L-3 SFI	0.050	0.080	Failed	Failed	Failed	----
15	L-5 SFI	0.040	0.054	0.071	0.329	Failed	----
16	L-8 SFI	0.035	0.044	0.043	0.068	0.255	HSLb
17	L-10 MK	0.030	0.053	0.078	0.144	Failed	----
18	L-15 MK	0.032	0.042	0.065	Failed	Failed	----
19	L-20 MK	0.024	0.029	0.043	0.068	0.108	HSLb
20	L Control	0.047	0.146	Failed	Failed	Failed	----
21	GUL Control	0.097	0.288	Failed	Failed	Failed	----
22	GUL-40 Slag	0.029	0.042	0.111	0.435	Failed	----
23	GUL-25 FA	0.035	0.050	Failed	Failed	Failed	----

***HSLb: High sulfate resistant blended Portland-limestone cement**

4-2- Mass changes of mortar bars in sulfate attack

Mass change of mortar bars is studied along with the length changes, and at the same intervals as for length changes study. Despite the fact that there is not any standard specified limitation for mass change of mortar samples in sulfate attack, examining this property along with the length change is helpful toward studying development of gypsum, ettringite, and thaumasite in the course of sulfate attack. In this section, changes in mass of the CSA A3004-C8 mortar bars in process of ettringite sulfate attack and thaumasite sulfate attack are reviewed separately.

4-2-1- Ettringite sulfate attack (23°C)

Average mass of the mortar samples was measured along with length change tests. Therefore, the mass change data was obtained periodically during the two-year sulfate attack study. The mass changes of mortar bars immersed in sodium sulfate solution at 23°C after 3, 6, 12, 18 and 24 months is presented in Table 4-5. For all samples, continuous mass increase was found during ettringite sulfate attack. The mass increase, which is found in all samples, is a sign of formation of gypsum and ettringite. The average mass gain of the mortar bars in ettringite sulfate attack after 24 months is presented in Fig. 4-15. The binary blends containing slag and the ternary ones containing slag and fly ash demonstrated the lowest mass gain. This indicated that these blends were more resistant against formation of ettringite and gypsum in comparison to the other blends. In Fig. 4-15 it is clear that the control blends had the highest mass gains due to ESA. Accordingly, addition of the studied supplementary cementing materials improved the resistance of the PLC blends against ettringite sulfate attack. This figure also suggests that generally for each SCM, an increase in the amount of the SCM leads to a decrease in mass gain. In other words, increase in amount of SCM in the PLC blends has mainly improved resistance against ettringite sulfate attack.

Table 4-5: Mass changes of mortar bars – Ettringite sulfate attack (23°C)

		Average mass change (%)				
		3	**6**	**12**	**18**	**24**
1	**L-35 Slag**	0.4	0.5	0.7	0.8	0.9
2	**L-40 Slag**	0.5	0.5	0.7	0.8	1.0
3	**L-45 Slag**	0.4	0.5	0.6	0.7	0.8
4	**L-20 FA**	0.7	0.9	1.2	1.4	1.5
5	**L-25 FA**	0.7	0.9	1.2	1.3	1.4
6	**L-30 FA**	0.7	0.9	1.1	1.2	1.2
7	**L-3 SF**	0.8	1.0	1.4	1.7	1.9
8	**L-5 SF**	0.7	0.9	1.3	1.6	1.8
9	**L-8 SF**	1.0	1.1	1.4	1.8	1.9
10	**L-25 Slag-10 FA**	0.4	0.5	0.8	0.9	1.1
11	**L-30 Slag-10 FA**	0.5	0.6	0.7	0.9	1.0
12	**L-35 Slag-15 FA**	0.4	0.5	0.5	0.7	0.8
13	**L-40 Slag-20 FA**	0.3	0.3	0.6	0.8	1.1
14	**L-3 SFI**	1.0	1.4	1.8	2.1	2.5
15	**L-5 SFI**	0.7	0.9	1.4	1.7	2.0
16	**L-8 SFI**	0.6	0.8	1.2	1.6	1.8
17	**L-10 MK**	0.7	1.0	1.2	1.5	1.7
18	**L-15 MK**	0.7	0.8	1.0	1.2	1.3
19	**L-20 MK**	0.7	0.7	0.9	1.0	1.0
20	**L Control**	0.6	0.9	1.5	2.1	2.9
21	**GUL Control**	0.9	1.4	1.9	2.6	3.5
22	**GUL-40 Slag**	0.3	0.4	0.6	0.6	0.7
23	**GUL-25 FA**	0.8	1.0	1.3	1.5	1.5

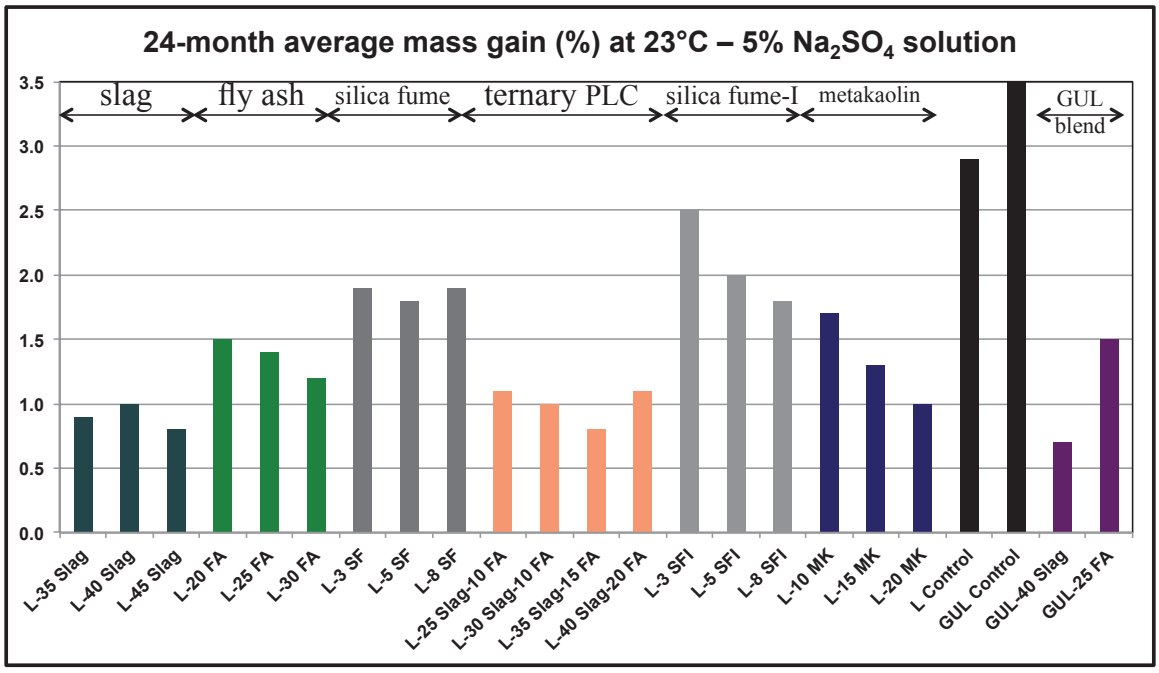

Fig. 4-15: Average mass changes of mortar bars – 2-year ettringite sulfate attack

4-2-2- Thaumasite sulfate attack (5°C)

The mass change of the mortar bars during thaumasite sulfate attack was also investigated. The result's trend was similar to those of ettringite sulfate attack. Mass changes at ages of 3, 6, 12, 18, and 24 months are summarized in Table 4-6. As gypsum, ettringite, and thaumasite are formed, a mass increase is detected in all mortar samples. However, since mortar is softened and disintegrated, especially when it is close to the total failure, a mass loss can be found in some of the samples. This phenomenon was observed for "L-3 SF", "L-8 SFI", and "L-10 MK". Other samples were either not approaching failure, or had failed before the next measurement could be done. The lowest mass gain after 24 months according to Table 4-5 was 0.9% related to "L-40 Slag-20 FA". Therefore, from the point of view of mass changes, this sample performed the best against thaumasite sulfate attack. The mass gain of this sample after 24 months was equal of the mass gain of the control sample (sample No. 20) after only 3 months of TSA.

It should be noted that "L-40 Slag-20 FA" also had the lowest expansion in thaumasite sulfate attack. Comparing the mass gain results of the studied blends after 24 months, the samples "L-45 Slag", "L-35 Slag-15 FA", and "L-8 SFI" performed very well.

Fig. 4-16 compares the average mass changes of mortar bars after 6 months of thaumasite sulfate attack. The later results are not presented in the graph as at the later ages a large number of the samples had failed and could not be shown in a graph. The lowest mass increases were for binary PLC blends containing slag or ternary blends containing slag and fly ash. This demonstrates effectiveness of the mentioned blends on slowing the process of thaumasite sulfate attack. These blends of PLC also showed the lowest mass increases in ettringite sulfate attack. According to Fig. 4-16, it is also inferred that in general, increase in the content of each SCM in the PLC blend has led to a decrease in the mass gain, which indirectly shows improvement in performance of samples in thaumasite sulfate attack.

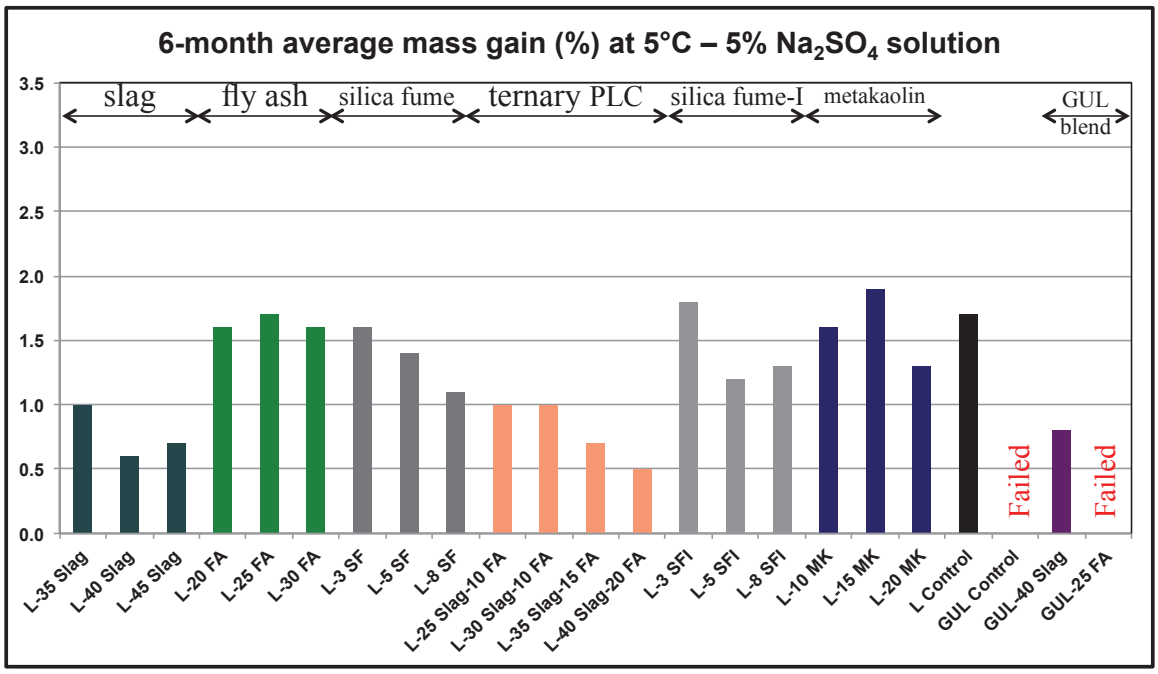

Fig. 4-16: Average mass changes of mortar bars – 6-month thaumasite sulfate attack

Table 4-6: Mass changes of mortar bars – Thaumasite sulfate attack (5°C)

		Average mass change (%)				
		3	**6**	**12**	**18**	**24**
1	**L-35 Slag**	0.5	1.0	1.4	2.3	3.6
2	**L-40 Slag**	0.4	0.6	0.9	1.2	1.6
3	**L-45 Slag**	0.6	0.7	1.0	1.1	1.3
4	**L-20 FA**	1.0	1.6	Failed	Failed	Failed
5	**L-25 FA**	0.9	1.7	3.3	Failed	Failed
6	**L-30 FA**	0.9	1.6	Failed	Failed	Failed
7	**L-3 SF**	1.2	1.6	2.5	-1.3	-4.5
8	**L-5 SF**	1.1	1.4	2.1	2.8	3.8
9	**L-8 SF**	0.9	1.1	1.5	1.9	2.2
10	**L-25 Slag-10 FA**	0.6	1.0	1.5	2.3	2.8
11	**L-30 Slag-10 FA**	0.6	1.0	1.4	1.8	2.3
12	**L-35 Slag-15 FA**	0.5	0.7	0.9	1.1	1.4
13	**L-40 Slag-20 FA**	0.3	0.5	0.7	0.8	0.9
14	**L-3 SFI**	1.2	1.8	Failed	Failed	Failed
15	**L-5 SFI**	0.7	1.2	2.3	3.1	Failed
16	**L-8 SFI**	0.9	1.3	2.1	3.1	1.3
17	**L-10 MK**	1.0	1.6	-5.8	-22.7	Failed
18	**L-15 MK**	1.1	1.9	3.0	Failed	Failed
19	**L-20 MK**	1.0	1.3	1.7	1.8	2.0
20	**L Control**	0.9	1.7	Failed	Failed	Failed
21	**GUL Control**	1.8	Failed	Failed	Failed	Failed
22	**GUL-40 Slag**	0.4	0.8	1.3	Failed	Failed
23	**GUL-25 FA**	1.2	Failed	Failed	Failed	Failed

4-3- Compressive strength of mortar cubes in thaumasite sulfate attack

The effect of the process of thaumasite sulfate attack was also studied by the changes in compressive strength of 5x5x5 cm mortar cubes. CSA A3004-C8-B requires such cubes to determine when to immerse mortar prisms for length change; there is no requirement to monitor compressive strength after this stage in the standard. The mortar cubes were immersed in 5% sodium sulfate solution at 5 ± 2°C after they attained

20 ± 1 MPa strength. Not all 23 mixtures were investigated; one mixture representing each supplementary material was investigated. The average compressive strength of 2 mortar cubes at the first day of immersion in sodium sulfate solution, after 28 days, 3 months, 6 months, 9 months, and 12 months of thaumasite sulfate attack is presented in Fig. 4-17. When mortar samples are immersed in sodium sulfate solution at 5°C, their compressive strength is affected by two opposite processes. First of all, as water is available in the system, and the mortar samples are freshly made, cement reacts with water, and due to the hydration, the compressive strength will increase. In addition, when supplementary cementing materials are used, pozzolanic reactions cause increases in the strength over time. Moreover, formation of gypsum and ettringite due to sulfate attack increases the strength at initial stages of the attack since gypsum and ettringite fill the cement paste pores. On the other hand, as thaumasite sulfate attack takes place and progresses, cracks and degradation in the mortar samples occur that cause reduction in the strength of the samples, which eventually results in total failure. Accordingly, the mortar samples can show increase in strength initially, and when the thaumasite sulfate attack develops to a certain stage that is prior to serious deterioration, the compressive strength decreases.

According to Fig. 4-17, the control samples ("L Control" and "GUL Control") were the first ones to show reduction in strength. Considerable strength reduction after six months of thaumasite sulfate attack was observed in these samples. The other blends containing supplementary cementing materials other than those prepared with SF and SFI showed increases in strength during a year of thaumasite sulfate attack. The blends of Portland-limestone cement with SF or SFI showed only a slight reduction in compressive

strength during the last three months. Maintaining the compressive strength when affected by thaumasite sulfate attack is a sign of resistance. From this point of view, the addition of supplementary cementing materials to PLC has been significantly effective on improving the resistance of mortar samples in thaumasite sulfate attack.

Table 4-7 summarizes the relative strength of the mortar samples prepared with each blend to the corresponding compressive strength at the first day. "GUL Control" samples failed in less than a year of thaumasite sulfate attack. "L Control" samples showed the lowest relative strength after a year of thaumasite sulfate attack among the studied blends. This confirms that addition of supplementary cementing materials improved the performance of PLC. Samples of "L-40 Slag", "L-40 Slag-20 FA", and "L-8 SF" achieved more than two times of the average compressive strength of their first day of immersion in sodium sulfate attack at 5°C. "L-40 Slag" and "L-40 Slag-20 FA" attained such strength due to the fact that they contained a large amount of SCM, and pozzolanic reactions could help increasing in compressive strength at older ages. "L-8 SF" also achieved such high compressive strength because silica fume is a highly reactive supplementary cementing material due to its fineness and its large content of SiO_2. Overall, all the mortar samples made with supplementary cementing materials notably maintained strength when subjected to thaumasite sulfate attack for a course of one year. The results reveal the extent of effectiveness of the studied supplementary cementing materials with the selected PLC replacement percentage on performance of Portland-limestone cement when exposed to cold sulfate environment. In a similar study, Qu and Zhang (2012) found that, compared to the control samples, the ternary blends of PLC containing 15% fly ash and 25% slag were more resistant against TSA from the

viewpoint of maintaining the compressive strength in a course of one year. All the mortar samples in their study showed strength loss due to their high limestone content (30%) and exposure to magnesium sulfate solution, which is more aggressive than sodium sulfate solution.

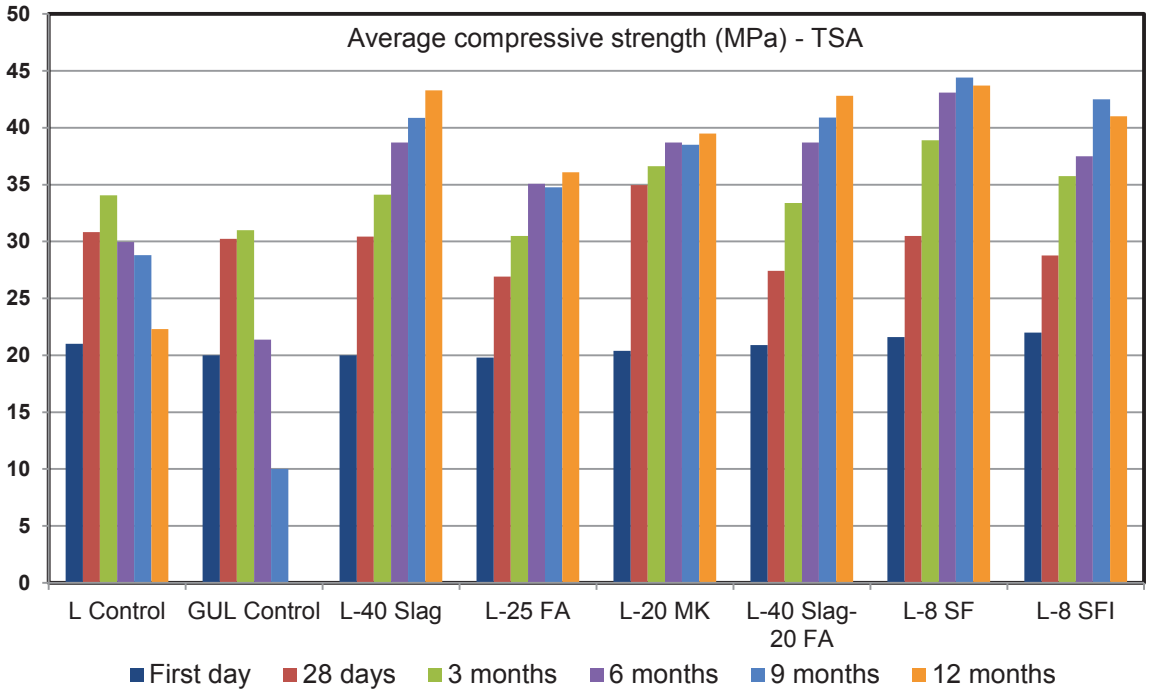

Fig. 4-17: Average compressive strength of mortar cubes during a year of thaumasite sulfate attack

Table 4-7: The percentage of compressive strength in comparison to the first day of TSA

	First day	28 days	3 months	6 months	9 months	12 months
L Control	100	147	162	143	137	106
GUL Control	100	151	155	107	50	Failed
L-40 Slag	100	152	171	194	204	217
L-25 FA	100	136	154	177	176	182
L-20 MK	100	171	180	190	189	194
L-40 Slag-20 FA	100	131	160	185	196	205
L-8 SF	100	141	180	200	206	202
L-8 SFI	100	131	162	170	193	186

4-4- Ultrasonic pulse velocity test on mortar cubes in thaumasite sulfate attack

The Ultrasonic pulse velocity test (ASTM C597) was performed on 5x5x5 cm mortar cubes immersed in 5% sodium sulfate solution at 5°C. The thaumasite sulfate attack procedure and condition was similar to the CSA A3004-C8-B procedure for mortar prisms. The effect of thaumasite sulfate attack on changes in pulse velocity through the mortar samples was studied for 15 months. Since the ultrasonic pulse velocity passing through a mortar sample is directly related to the sample's density, compactness, and integrity, a continuous measurement of UPV on each set of mortar samples shall explain the changes occur inside the samples. The mortar cubes, when achieving a compressive strength of 20 ± 1 MPa, were tested by the UPV device, then immersed in 5% sodium sulfate solution at 5 ± 2°C. The solution was renewed at the same ages as specified in CSA A3004-C8 for mortar prisms. The UPV measurement at the first day test was followed by tests at 28 days, and 3, 6, 7.5, 9, 10.5, 12, and 15 months. Since this is a non-destructive test, measurements were performed on the same samples over time to decrease variability.

Theoretically, in a continuous UPV measurement on mortars prepared and cured in standard condition, an increase in the test results can be found until a certain age. This increase is due to hydration of cement that increases density of hydrated cement paste and decreases the volume of pores. If supplementary cementing materials are added to cement, pozzolanic reactions would further increase the velocity of waves passing through a mortar sample as pozzolanic reactions contribute to formation of secondary CSH gel and decreasing the hydrated cement paste pores. When mortar samples are

immersed in sodium sulfate solution, the mentioned process will take place since water is available in the system, similar to that observed for compressive strength. In addition to the hydration and pozzolanic reactions, sulfate attack reactions take place. At the initial stage of sodium sulfate attack, formation of gypsum and ettringite inside the cement paste pores reduces the porosity and increases the density of mortar sample, which leads to an increase in UPV. At later ages, the thaumasite sulfate attack results in reduction in UPV as it triggers crack formation and softening of the cement paste. Accordingly, during the process of sulfate attack to freshly prepared mortar samples, increase in ultrasonic pulse velocity may be detected followed by a decrease in UPV that finally will progress to total failure of the mortar sample.

In Fig. 4-18, the average UPV results through the 15-month study on mortar cubes are presented. At the earlier ages, all samples showed an increase in UPV due to cement hydration and formation of ettringite and gypsum through hydrated cement pores. As the thaumasite sulfate attack progressed, the two control samples were the first ones to show reductions in UPV. The "GUL Control" and the "L Control" samples showed reduction in UPV after 3 months and 6 months, respectively. Softening of the hydrated cement paste during thaumasite sulfate attack was the main reason for reduction in UPV. "GUL Control" contained 13.5% ground limestone while "L Control" contained 10% ground limestone by weight. The higher content of limestone filler in samples of "GUL Control" caused quicker deterioration due to thaumasite sulfate attack. The other studied samples containing supplementary cementing materials normally showed better performance in 15-month thaumasite sulfate attack in comparison to the "L Control" sample from the perspective of ultrasonic pulse velocity results. Partial replacement of

PLC with supplementary cementing materials has reduced the probability and the extent of formation of thaumasite. Furthermore, SCMs have reduced the porosity of the mortar samples and increased the density that has led to an increase in density of the mortar samples. The density increase has also reduced permeability, and improved resistance of mortar samples in TSA. Consequently, the mentioned improvements are clear when the average UPV results are compared with the control sample. From the viewpoint of ultrasonic pulse velocity, according to Fig. 4-17, "L-40 Slag" and "L-40 Slag-20 FA" performed the best against thaumasite sulfate attack through a course of 15 months. The mentioned samples did not show any reduction in average UPV. "L-20 MK" also performed well in TSA considering this test. Compared to the mentioned blends, mortar samples prepared with blends of PLC containing 25% fly ash, or 8% SF, or 8% SFI did not show a good resistance against TSA.

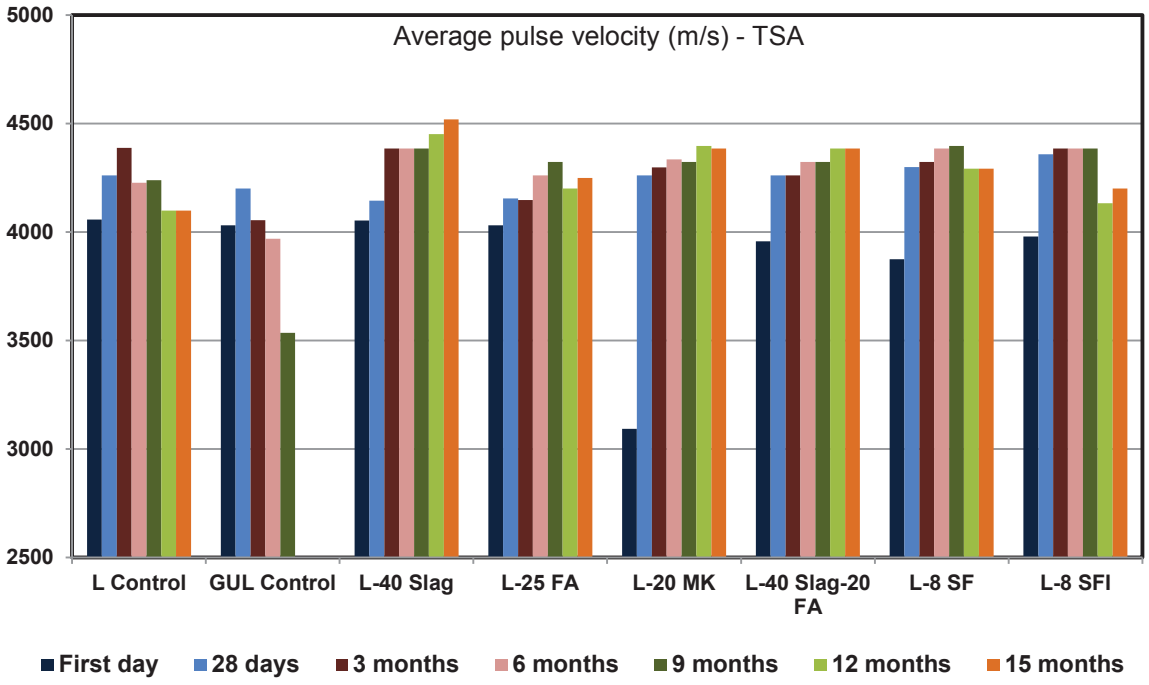

Fig. 4-18: Average UPV of mortar cubes during 15 months of thaumasite sulfate attack

The visual condition of mortar cubes prepared for the UPV test and immersed in sodium sulfate solution is outlined in Fig. 4-19. The control samples ("L Control" and "GUL Control") showed the worst physical condition. The "GUL Control" cubes were severely deteriorated, and had lost the surface completely. The "L Control" cubes were in better condition compared to the "GUL Control" samples. The mortar cubes prepared with "L Control", lost the edges. Also, some parts of the surfaces of the cubes were about to be removed due to thaumasite sulfate attack as seen in the figure. This visual observation is in agreement with the results of ultrasonic pulse velocity technique. As mentioned previously, "GUL Control" contained higher amount of limestone filler than "L Control". The higher limestone content has caused more severe damage since carbonates are a main base for development of thaumasite sulfate attack reactions. Considering Fig. 4-19, the "L-40 Slag" and "L-40 Slag-20 FA", which showed the best performance when tested with UPV, showed no sign of deterioration during 12 months of thaumasite sulfate attack. The other blends of PLC with supplementary cementing materials were found to have visual signs of deterioration in thaumasite sulfate attack. The samples of "L-25 FA", "L-20 MK", "L-8 SF", and "L-8 SFI" showed cracks on the edges and some mass loss on the corners and the edges. Amongst these samples, the "L-25 FA" mortar cubes were more deteriorated.

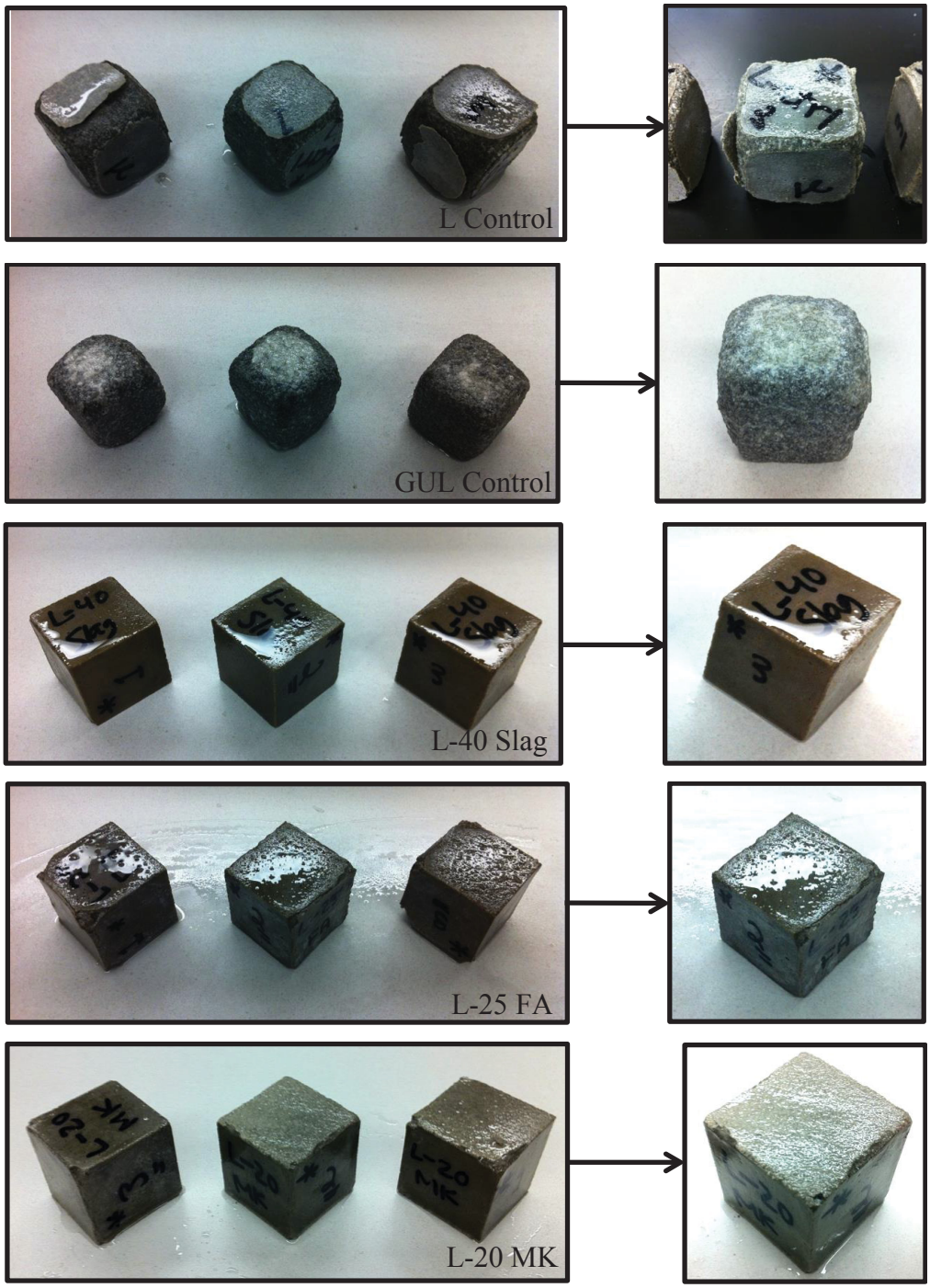

Fig. 4-19: Mortar cubes after 12 months thaumasite sulfate attack

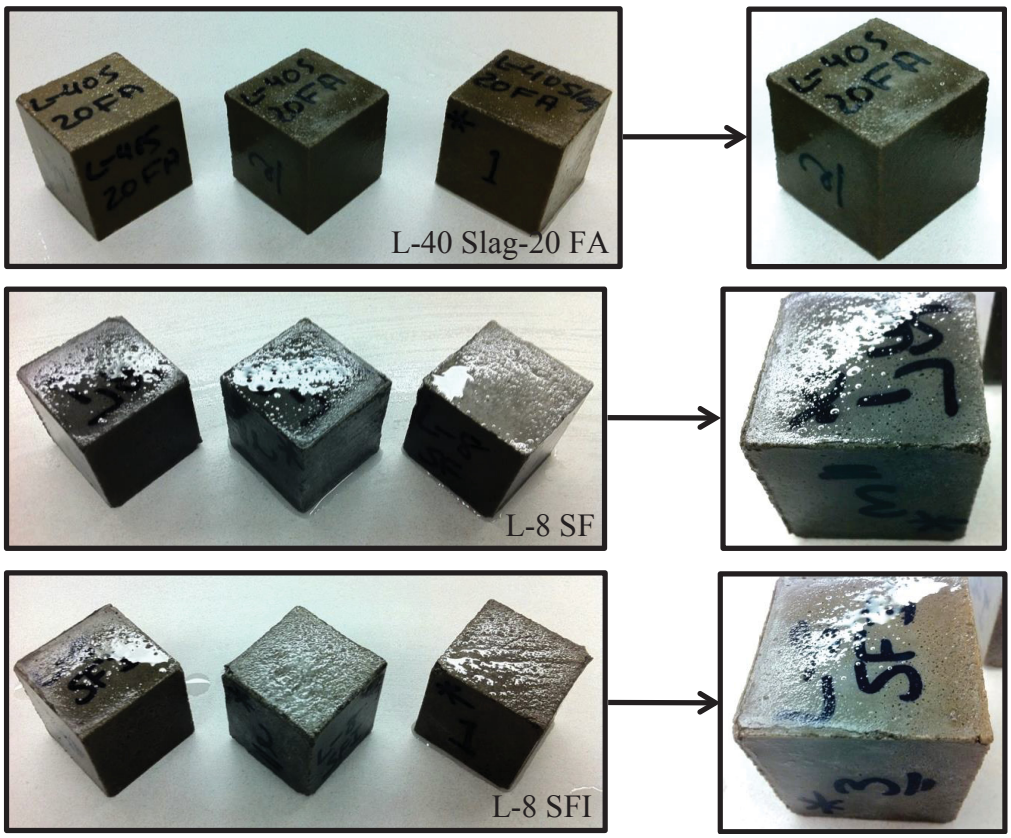

Fig. 4-19: Mortar cubes after 12 months thaumasite sulfate attack (Continued)

4-5- Differential scanning calorimetry of mortar samples in thaumasite sulfate attack

Differential scanning calorimetry (DSC) was used in order to verify formation of thaumasite in mortar samples immersed in 5% sodium sulfate solution at 5°C. The test was performed on mortar samples from all 23 blends. Samples for the DSC test were obtained from the surface of the samples when the mortar bars failed during thaumasite sulfate attack. Of course, mortar bars corresponding to a number of blends did not fail during the length change test. As mentioned in chapter 3 for experiments, DSC samples were also obtained from the surface of these mortar bars after 2 years of exposure. According to the literature review on thermal analysis techniques, presented in chapter 2, and the summarized available results in Table 2-7, generally the ettringite dehydration

temperature peak is found in the range of 80°C to 105°C, the peak for calcium silicate hydrate gel is observed between 95°C and 105°C, the thaumasite peak is detected between 100°C and 130°C, and the range of gypsum peak is 100°C to 145°C. This review as well as the comments by the experts on field of thermal analysis was the base for analysis of the DSC results obtained in this research.

Firstly, in order to evaluate the DSC results and find the normal peaks that may occur in a hydrated cement paste, two sets of mortars from the studied PLCs ("L" and "GUL") were prepared and cured in saturated limewater for 90 days. Then, samples were taken from the surface of mortar cubes, and prepared for the DSC tests. The results are presented in Fig. 4-20 and Fig. 4-21. The DSC graphs show heat flow in unit of Watts per gram of samples as function of temperature in 0°C to 550°C range. For "GUL Control" and "L Control", distinct thermal peaks at 89°C and 88°C are found, respectively. These peaks are attributed to ettringite and CSH. It should be noted that in DSC, it is possible that the corresponding peaks of each compound overlap each other and consequently only one peak appears in DSC curve. Similar results were found by Sha et al. (1999). Reaction between C_3A and gypsum in cement in presence of water results in formation of ettringite. In both samples, a small shoulder is detected at 133°C and 134°C, respectively, for "GUL Control" and "L Control" samples, which could be attributed to gypsum and/or calcium carboaluminate. Naturally, a hydrated cement paste contains a large amount of calcium hydroxide. The large distinct peaks at 438°C and 435°C for "GUL Control" and "L Control", respectively, are attributed to $Ca(OH)_2$ dehydroxylation.

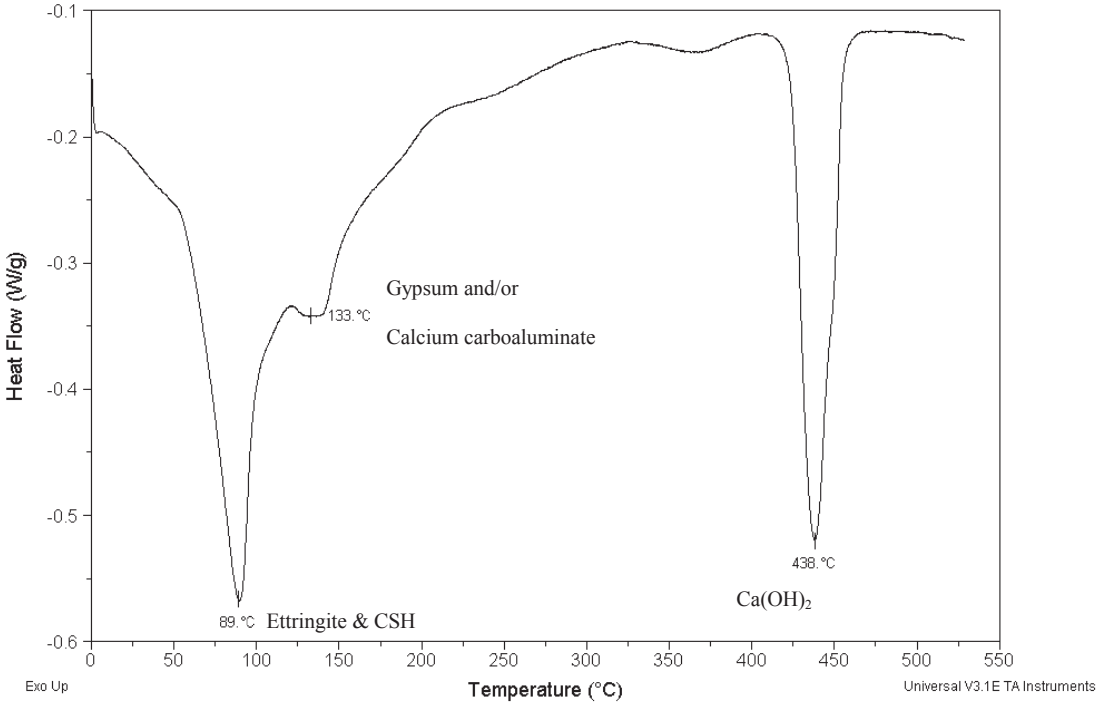

Fig. 4-20: DSC graph of "GUL Control" sample cured in saturated limewater for 90 days

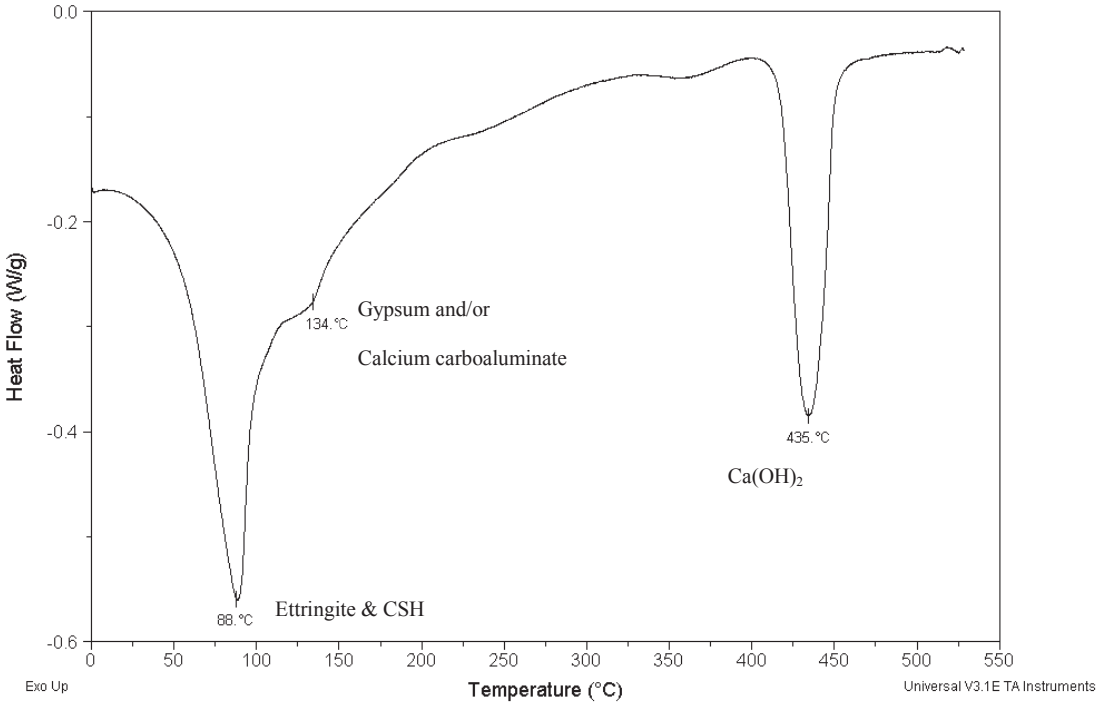

Fig. 4-21: DSC graph of "L Control" sample cured in saturated limewater for 90 days

Considering the above-mentioned tests carried out on control samples hydrated in limewater, the DSC test was performed on all 23 blends of Portland-limestone cement. The results are presented in Fig. 4-22 through Fig. 4-29. It should be mentioned that the test was carried out from 0°C to 550°C, but since no peaks were detected after 200°C, the graphs are bounded from 0°C to 200°C. The only peak higher than 200°C that could have been detected in the deteriorated samples was for calcium hydroxide around 435°C. Evidently, such a peak was not detected in any of the deteriorated samples tested with DSC as calcium hydroxide was completely consumed during pozzolanic reactions as well as reactions associated to formation of gypsum, ettringite, and thaumasite.

Fig. 4-22 presents DSC results for the mortar samples containing "GUL" Portland-limestone cement and its blends with fly ash and slag. Single peaks at 92°C, 100°C, and 95°C respectively, correspond to ettringite and CSH dehydration. A peak at 111°C for "GUL Control" represents thaumasite dehydration. The same peak was found for "GUL-25 FA". For "GUL-40 Slag", thaumasite was detected at 113°C. Although "GUL-25 FA" and "GUL-40 Slag" remained in sulfate exposure for a longer time, the intensity of their thaumasite peaks are lower than "GUL Control", which indicates the improvement of resistance against thaumasite sulfate attack. The peak at 125°C for the binary blends was related to gypsum dehydration. However, such a peak was not found in "GUL Control" sample. The identification of gypsum and ettringite in the blend samples suggests that even though the mode of sulfate attack was TSA, ettringite and gypsum were formed during the deterioration process. This is a natural phenomenon since as presented in chapter 2 and reviewed in the previous literature, gypsum and ettringite form during the process of thaumasite sulfate attack. In the "GUL Control" sample due to the

severity of the thaumasite sulfate attack, gypsum is consumed to form ettringite that is a base for formation of thaumasite either by functioning as a nucleation site or by reacting to form thaumasite (Köhler et al.-2006). In the other blends, because the amount of carbonates is lower (cement is partially replaced with SCM), the extent of reactions is lower than in the control sample so a part of gypsum remains in the system. The DSC graph for the other control sample (L Control) in Fig. 4-23 also shows formation of thaumasite in the 42-week TSA study. Peaks at 89°C, 111°C, and 123°C are detected relating to dehydration of ettringite and CSH, thaumasite, and gypsum, respectively. Accordingly, thaumasite sulfate attack has occurred. Presence of gypsum in quite large amount is because of the reactions of large amounts of calcium hydroxide with sulfate ions. At later ages, gypsum can take part in formation of ettringite, which can help further formation of thaumasite as discussed in the literature review (Eq. 2-8).

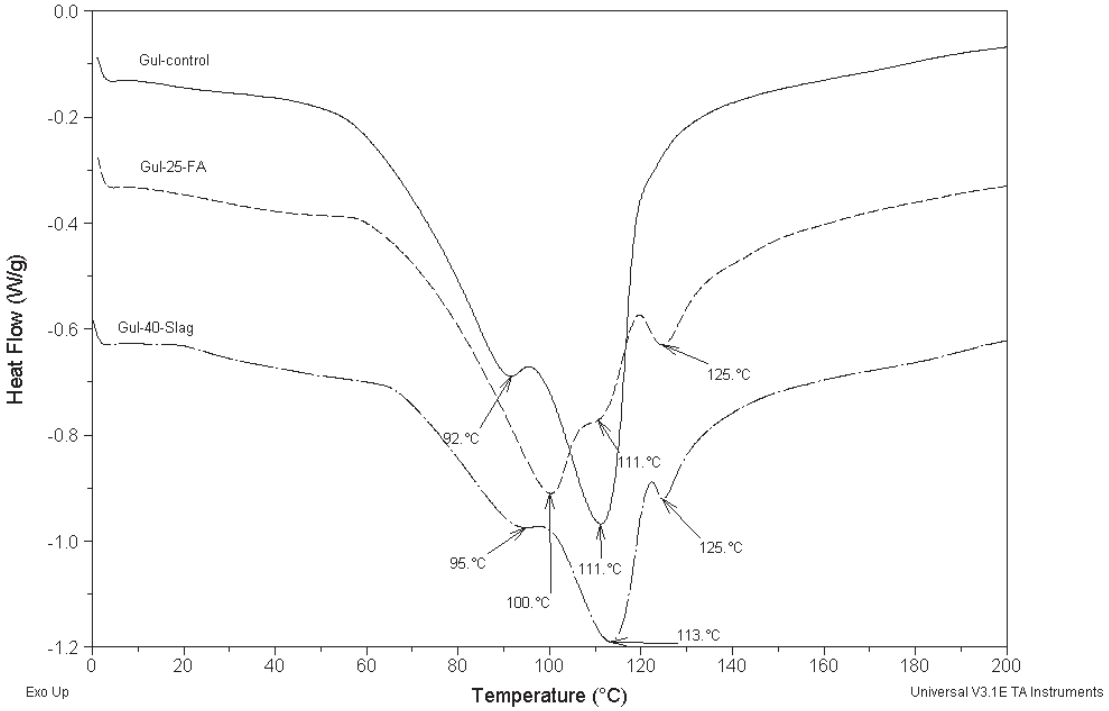

Fig. 4-22: DSC graph of "GUL Control" (failed after 17 weeks), "GUL-25 FA" (failed after 26 weeks), and "GUL-40 Slag" (failed after 91 weeks) at the time of failure in thaumasite sulfate attack

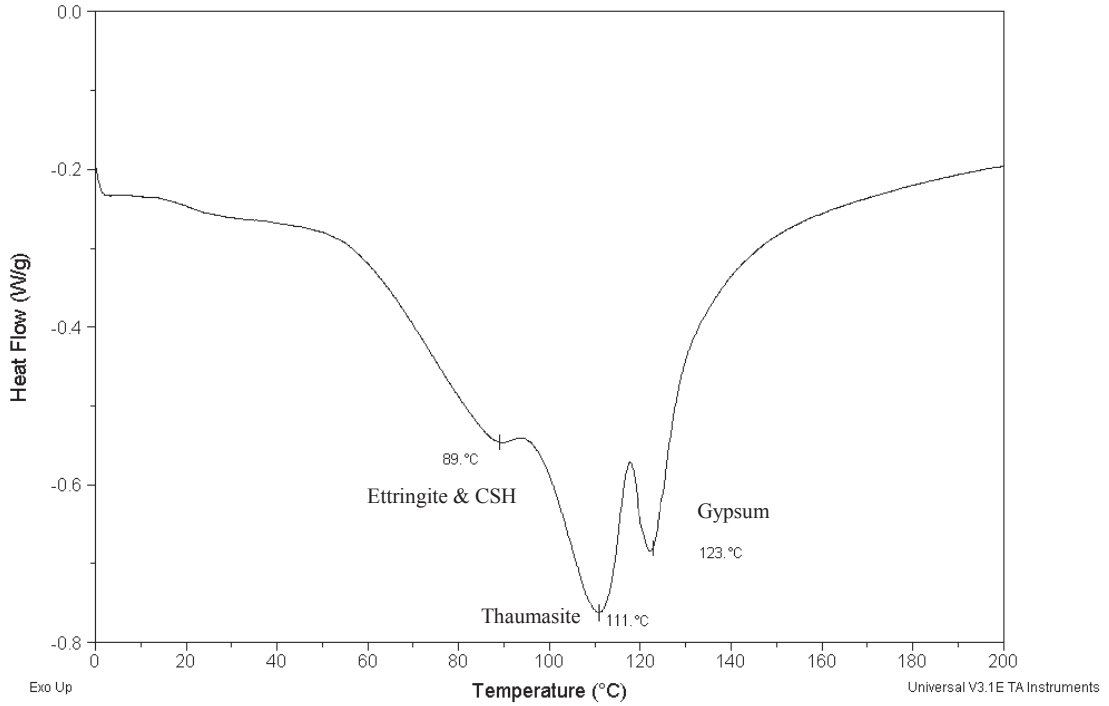

Fig. 4-23: DSC graph of "L Control" sample at the time of failure in TSA (42 weeks)

Formation of thaumasite was also found in mortar samples of binary blends of Portland-limestone cement containing slag, immersed in 5% sodium sulfate solution at 5°C for two years. In Fig. 4-24, peaks at 119°C, 113°C, and 111°C are attributed to thaumasite. Since the samples were tested at the same age, the intensity of their peaks can be compared. It is clearly seen that increase in the amount of slag in the samples has led to a decrease in the intensity of thaumasite peak. An increase in the amount of slag has reduced the amount of carbonates, which are vital reactants towards formation of thaumasite; therefore, the amount of the formed thaumasite is decreased. For the blends of PLC and slag, small peaks related to gypsum are found at 129°C, 126°C, and 125°C. In addition, a single peak for ettringite and calcium silicate hydrate is characterized at 105°C, 96°C, and 98°C for "L-35 Slag", "L-40 Slag", and "L-45 Slag", respectively. It is remarkable that, although the cement content is reduced when the slag content is increased, the CSH peak is intensified with increase in the amount of slag. This is directly related to pozzolanic reactions and secondary CSH formation.

In Fig. 4-25, the DSC results are outlined for fly ash containing mortar samples. A peak related to dehydration of thaumasite is found for all samples. This peak is at 113°C for "L-20 FA" and "L-25 FA" and at 110°C for "L-30 FA". The graph suggests that an increase in the amount of fly ash resulted in a decrease in the peak intensity as in blends with slag. Although, "L-25 FA" was kept in sodium sulfate solution 3 months longer than "L-20 FA", its thaumasite peak intensity was weaker. In the figure, peaks at 99°C, and 101°C are due to concurrent dehydration of CSH and ettringite. Moreover, peaks indicating gypsum are detected at 125°C, 128°C, and 122°C. Similar to the slag

containing mortars, the increase in the content of fly ash has increased the CSH content of the blends of PLC with fly ash.

Ternary blends of Portland-limestone cement containing slag and fly ash were also tested with the DSC technique. Fig. 4-26 includes the resulting graphs. As previously mentioned, none of the CSA A3004-C8 mortar bars failed during the two-year thaumasite sulfate attack study. Samples were obtained from the surface of the corresponding mortar bar of each ternary blend at the end of the two-year study. All the samples showed peaks for CSH and ettringite. The peak was at 94°C for both "L-25 Slag-10 FA" and "L-40 Slag-20 FA". For the other samples "L-30 Slag-10 FA" and "L-35 Slag-15 FA", this peak was placed at 100°C. Regarding the formation of thaumasite, "L-25 Slag-10 FA" that had lowest content of SCM among the ternary blends, showed a peak at 110°C. In the DSC graphs of "L-30 Slag-10 FA" and "L-35 Slag-15 FA", presence of thaumasite was only indicated as a shoulder at 112°C and 111°C, respectively. This observation clearly confirms the effect of combination of slag and fly ash on improvement of the performance of mortar samples in TSA. Remarkably, the DSC graph of "L-40 Slag-20 FA", which had the highest amount of SCMs did not show any peak or shoulder related to thaumasite for the two-year old samples immersed in sodium sulfate solution at 5°C. This result is of significance, and shows effectiveness of slag and fly ash when added to Portland-limestone cement in large quantities on impeding thaumasite sulfate attack and formation of destructive thaumasite. Weak peaks related to gypsum were also found in the ternary blends at 124°C, 125°C, and 120°C. The source of gypsum is the reactions of calcium hydroxide with sodium sulfate ions.

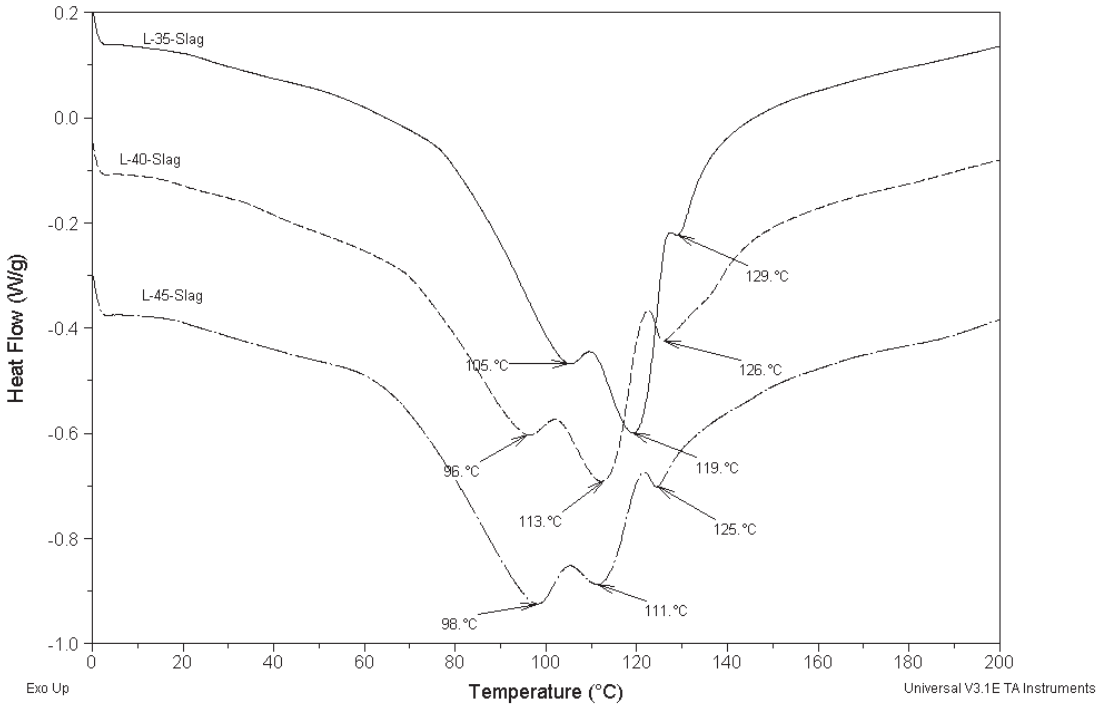

Fig. 4-24: DSC graph of blends of PLC with slag after two years of thaumasite sulfate attack

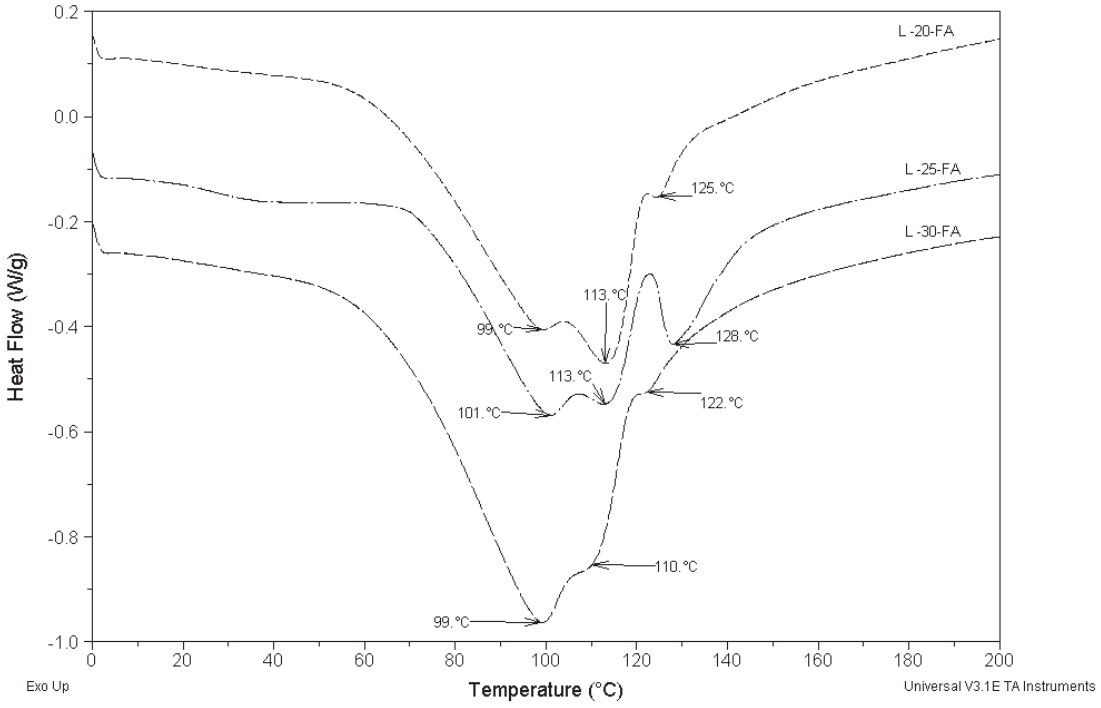

Fig. 4-25: DSC graph of blends of PLC with fly ash in TSA at the time of failure ("L-20 FA": 52 weeks, "L-25 FA": 65 weeks, and "L-30 FA: 52 weeks)

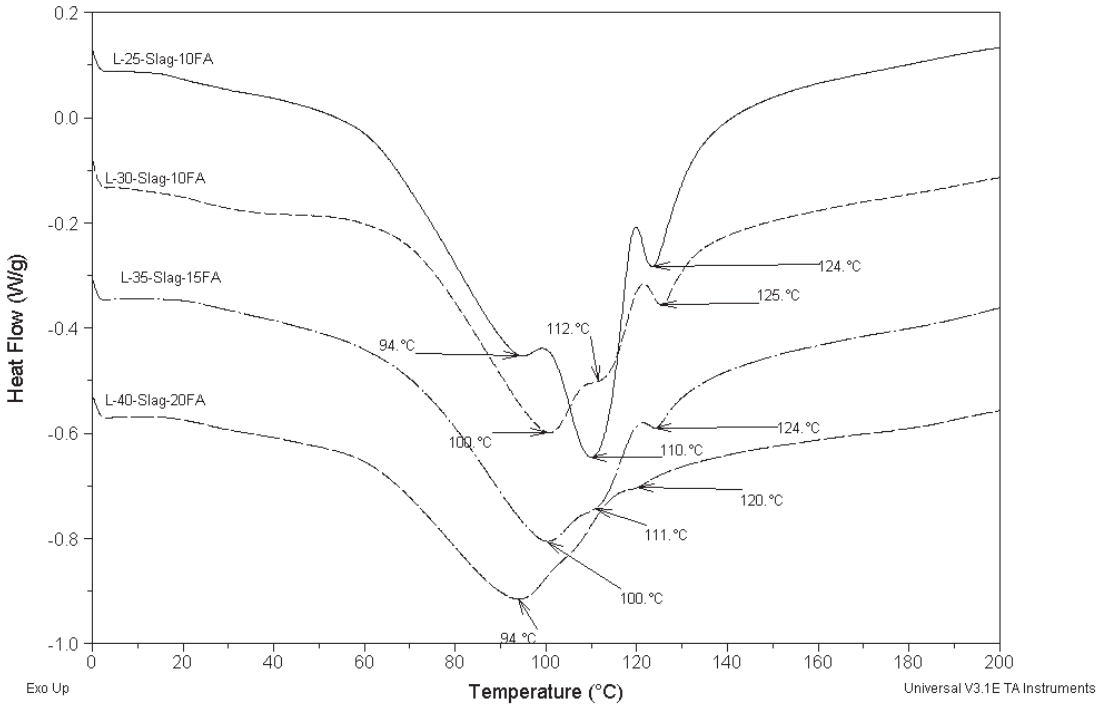

Fig. 4-26: DSC graph of ternary blends of PLC containing slag and fly ash after two years of thaumasite sulfate attack

The mortar samples containing binary blends of Portland-limestone cement and silica fume were subjected to thermal analysis. Samples for the DSC technique were obtained from the surface of the samples immersed in sodium sulfate solution for two years since none of the samples failed earlier. The results are presented in Fig. 4-27. Ettringite and CSH are found as single peaks at 98°C, 104°C, 99°C for "L-3 SF", "L-5 SF", and "L-8 SF", respectively. The graphs confirm formation of thaumasite on the surface of the CSA A3004-C8 mortar bars. Peaks relating to thaumasite in the samples of "L-3 SF", "L-5 SF", and "L-8 SF" are found at 112°C, 116°C, 113°C, respectively. The strength of the peak corresponding to the dehydration of thaumasite is reduced when the silica fume content of the sample is increased. "L-8 SF" shows the weakest thaumasite dehydration peak, which admits that addition of silica fume has reduced the possibility of

its formation in two years of TSA. The DSC graphs suggest presence of gypsum in two of the samples with peaks at 126°C and 128°C. For "L-5 SF" a thermal peak for gypsum is not found. According to the previous research in thermal analysis, outlined in Table 2-7, thermal peaks for gypsum and thaumasite may overlap. In addition, it should be noted that, for "L-5 SF", the thaumasite peak is 3°C to 4°C higher than the two other samples. Furthermore, the DSC curve for "L-5 SF" shows a shoulder after 116°C. Consequently, it is possible that for this sample, thaumasite and gypsum peaks have overlapped. Considering the fact that in thaumasite sulfate attack, gypsum is initially formed from reactions between calcium hydroxide and sulfate ions, then it contributes in formation of ettringite, and ettringite itself takes part in formation of thaumasite, presence of gypsum would be a sign indicating that thaumasite sulfate attack was not at its extreme stage.

Fig. 4-28 presents DSC graphs for SFI containing samples. According to the figure, "L-3 SFI" at the time of failure at 52 weeks, showed a peak at 114°C for dehydration of thaumasite and a small peak probably corresponding to gypsum at 133°C. A separate peak showing ettringite and CSH was not found in the analysis. The peak at 114°C strength may be due to combination of ettringite and thaumasite. The sample obtained from "L-5 SFI", which failed after 91 weeks indicates a peak at 97°C corresponding to ettringite and CSH. According to the figure, thaumasite is also found in the sample, which confirms process of TSA. The thaumasite peak was located at 113°C as well as the gypsum peak at 126°C. After two years of thaumasite sulfate attack, thaumasite was found in samples taken from the surface of "L-8 SFI". The corresponding peak is at 118°C as seen in the figure. This samples also has a peak at 102°C denoting dehydration of ettringite and CSH, and a peak at 129°C related to gypsum.

Thermal analysis results obtained from DSC on samples of metakaolin containing mortars are summarized in Fig. 4-29. Sample containing 10% metakaolin (L-10 MK) showed presence of ettringite/CSH, thaumasite, and gypsum at the time of failure located at 103°C, 114°C, and 126°C, respectively. In the tested sample from "L-15 MK" after 78 weeks of thaumasite sulfate attack a shoulder at 114°C represented dehydration of thaumasite. For this sample a peak at 104°C related to ettringite and CSH was also found. The two-year old samples of "L-20 MK" did not indicate a peak for thaumasite at the common range in this study. It is possible that because of presence of limited amount of thaumasite in the sample in addition to presence of large amount of ettringite due to metakaolin's large quantity content of aluminates, the CSH/ettringite peak that usually occurs in the range of 80°C-105°C, has shifted to a higher temperature and possibly overlapped thaumasite peak.

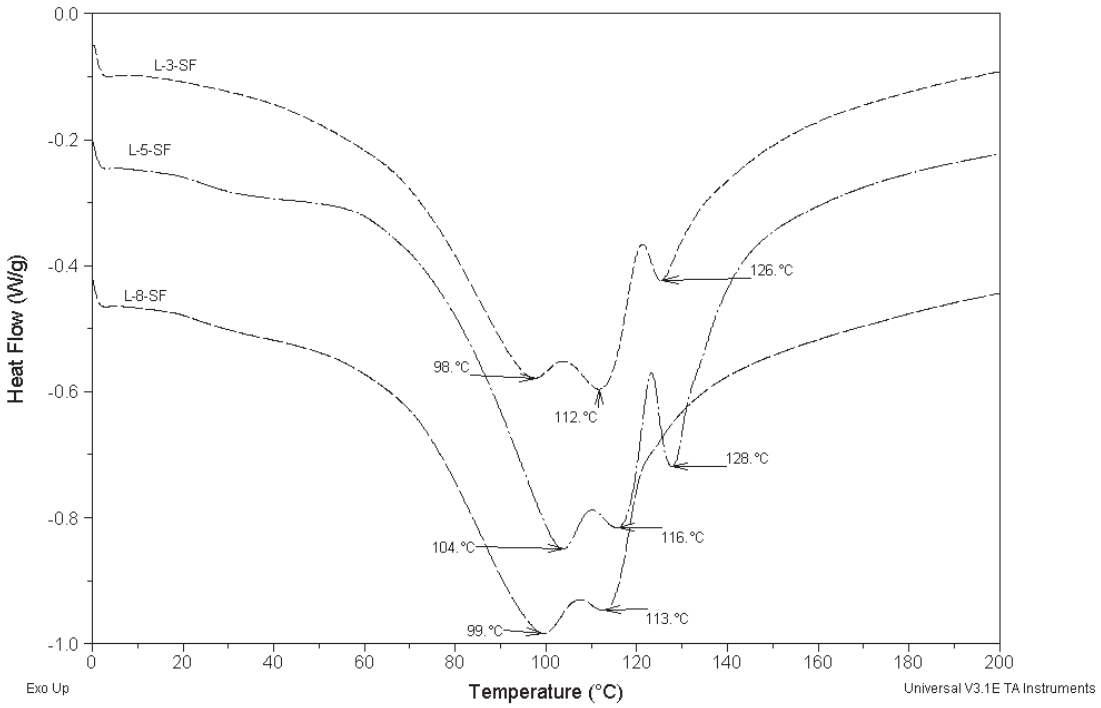

Fig. 4-27: DSC graph of blends of PLC with silica fume after two years of thaumasite sulfate attack

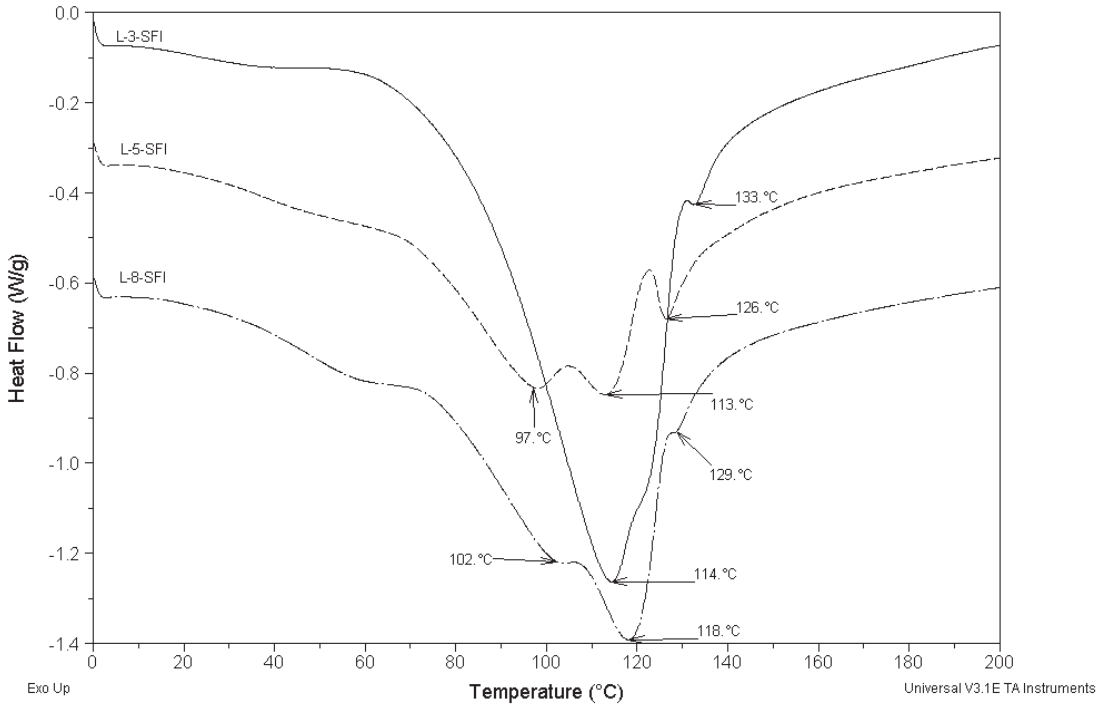

Fig. 4-28: DSC graph of blends of PLC with silica fume I in TSA ("L-3 SFI": failed in 52 weeks, "L-5 SFI": failed in 91 weeks, and "L-8 SFI": not failed in two years)

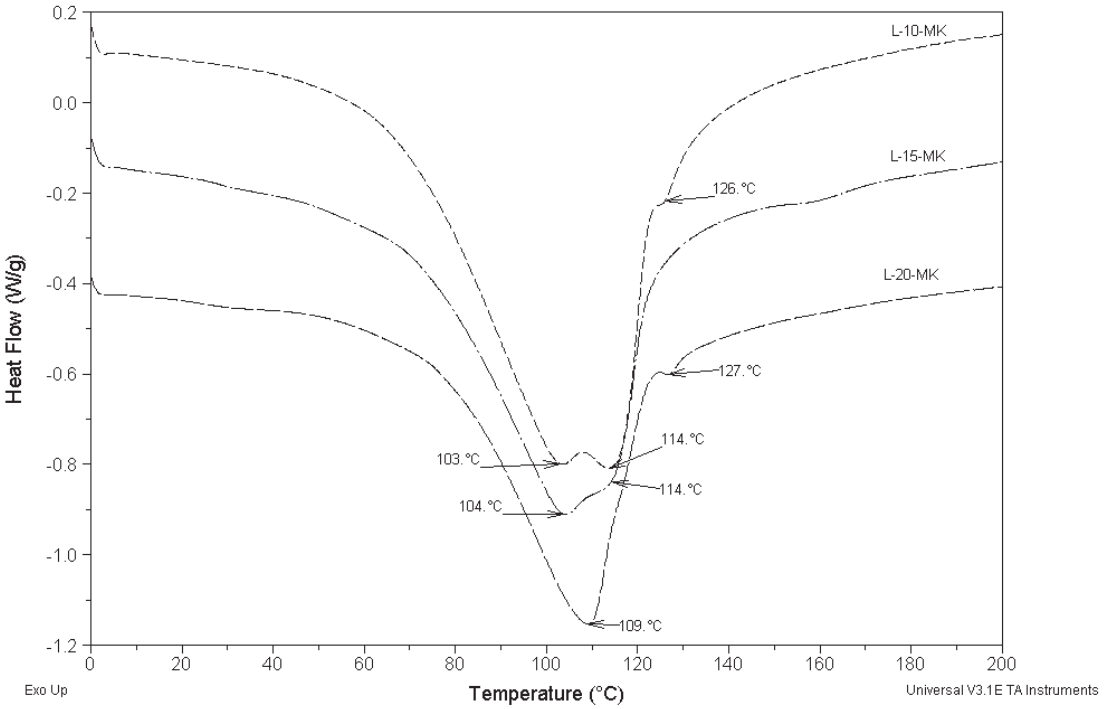

Fig. 4-29: DSC graph of blends of PLC with metakaolin in TSA ("L-10 MK": failed in 91 weeks, "L-15 MK": failed in 78 weeks, and "L-20 MK": not failed in two years)

Subsequently, it can be inferred from the obtained and analyzed DSC results that the mode of failure in all failed samples was thaumasite sulfate attack. Even though a number of samples had not failed at the test time, formation of thaumasite was confirmed on their surface. Thaumasite sulfate attack occurred at different stages for the samples. It was found that addition of supplementary cementing materials could delay formation of thaumasite. Additionally, SCMs reduced amount of thaumasite formed in mortar samples. Overall, thermal peaks corresponding to each compound were quite close for all samples, and fell in the temperature range found in the literature. Table 4-8 summarizes the results of the DSC study. In this table the temperature of the detected thermal peaks are presented and can be compared with the peak temperature range found in the previous thermal analysis studies. According to the table, ettringite and CSH were found in single peaks ranging from 88°C to 105°C. Thaumasite dehydration peak was found from 110°C to 119°C falling in the range of previous studies (100-130°C). As well, gypsum peak in the samples tested with DSC was characterized from 120°C to 134°C. Calcium hydroxide as explained before was only detected in two samples cured in limewater at peaks of 435°C and 438°C.

Basically, tests with differential scanning calorimetry technique can face errors and be misleading. The mass of powder samples tested in this technique is very small. It is probable that they misrepresent the real composition. The process of thaumasite sulfate attack and the extent of formation of thaumasite can differ point to point on a mortar bar. Thus, taking samples from different locations of a single sample can cause variation and confusion. Additionally, as the thermal peaks of ettringite, thaumasite, and gypsum are quite close, sometimes it is impossible to attain separate peaks corresponding to each of

the mentioned materials. Consequently, the results should be cautiously interpreted. The DSC results for a number of samples were not as convincing as the others. Therefore, X-ray diffraction test was employed to further study the mentioned samples. The problem cases are listed as follows:

- According to Fig. 4-22, "GUL-25 FA" showed only a shoulder representing dehydration of thaumasite, while due to its extent of deterioration it was expected to find a more intense peak.

- Considering Fig. 4-24, thaumasite peak for "L-35 Slag" was at 119°C that was slightly higher than 113°C and 111°C, which were found for the other slag containing samples.

- "L-3 SFI" did not show a peak for ettringite as seen in Fig. 4-28. Also, "L-8 SFI" indicated a peak for thaumasite at 118°C, which was marginally higher than the other samples.

- In Fig. 4-29, for "L-15 MK" only a shoulder was denoting the dehydration of thaumasite, and the graph for "L-20 MK" only had a unique peak at 109°C, and there was not any separate peak in this graph for ettringite, thaumasite, and gypsum.

- In addition to the mentioned samples, the control sample and the binary blend containing 45% slag were also studied with XRD technique for comparison.

Table 4-8: Comparison of the DSC peaks with the literature (°C)

		Ettringite	C-S-H	Thaumasite	Gypsum	$Ca(OH)_2$
	Temperature range in the literature	**80-105**	**95-105**	**100-130**	**100-145**	**420-480**
	Temperature range observed in this study	88-105		110-119	120-134	435-438
90 days curing in limewater	**L Control**	88		N.D.*	134	435
	GUL Control	89		N.D.	133	438
Thaumasite sulfate attack	**L-35 Slag**	105		119	129	N.D.
	L-40 Slag	96		113	126	N.D.
	L-45 Slag	98		111	125	N.D.
	L-20 FA	99		113	125	N.D.
	L-25 FA	101		113	128	N.D.
	L-30 FA	99		110	122	N.D.
	L-3 SF	98		112	126	N.D.
	L-5 SF	104		116	N.D.	N.D.
	L-8 SF	99		113	128	N.D.
	L-25 Slag-10 FA	94		110	124	N.D.
	L-30 Slag-10 FA	100		112	125	N.D.
	L-35 Slag-15 FA	100		111	124	N.D.
	L-40 Slag-20 FA	94		N.D.	120	N.D.
	L-3 SFI	N.D.		114	133	N.D.
	L-5 SFI	97		113	126	N.D.
	L-8 SFI	102		118	129	N.D.
	L-10 MK	103		114	126	N.D.
	L-15 MK	104		114	N.D.	N.D.
	L-20 MK	N.D.		N.D.	N.D.	N.D.
	L Control	89		111	123	N.D.
	GUL Control	92		111	N.D.	N.D.
	GUL-40 Slag	95		113	125	N.D.
	GUL-25 FA	100		111	125	N.D.

***N.D.: Not detected (no peak)**

4-6- X-ray diffraction test on mortar samples in thaumasite sulfate attack

Phase identification of the mortar samples deteriorated in thaumasite sulfate attack was carried out with X-ray diffraction. As previously mentioned, the DSC results for a number of samples were not quite satisfactory. Powder samples with particle sizes of less than 45μ were acquired from the surface of the CSA A3004-C8 mortar bars at the age of failure. If a set of mortar bars had not failed in two years, the sample was obtained from the surface of the mortar bars after two years. In addition to the noted blends in section 4-5 that required XRD, the control samples ("GUL Control" and "L Control") and "L-45 Slag" were also tested for better evaluation of the results. The results are presented in Fig. 4-30 through Fig. 4-34.

According to Fig. 4-30, the phases identified in samples of "GUL Control" and "GUL-25 FA" at failure were thaumasite, gypsum, and ettringite. The presence of thaumasite and the intensity of peaks confirm that as it was expected, the governing mode of attack was thaumasite sulfate attack. For both samples, thaumasite had the strongest peak. Accordingly, the amount of thaumasite was the highest. Detection of ettringite and gypsum peaks was normal. Since during thaumasite sulfate attack gypsum and ettringite are formerly formed to initiate development of thaumasite, identification of gypsum and ettringite verified the occurrence of TSA. Although "GUL Control" was tested with XRD at lesser age than "GUL-25 FA", its identified thaumasite peak was stronger. Thus, partial replacement of Portland-limestone cement with fly ash reduced the amount of thaumasite formed. It should be noted that in the DSC analysis for "GUL Control" gypsum was not characterized while in the XRD analysis peaks for gypsum were identified. Also, DSC analysis of "GUL-25 FA" showed a weak peak related to

thaumasite; however the XRD analysis confirmed relatively intense peaks corresponding to thaumasite.

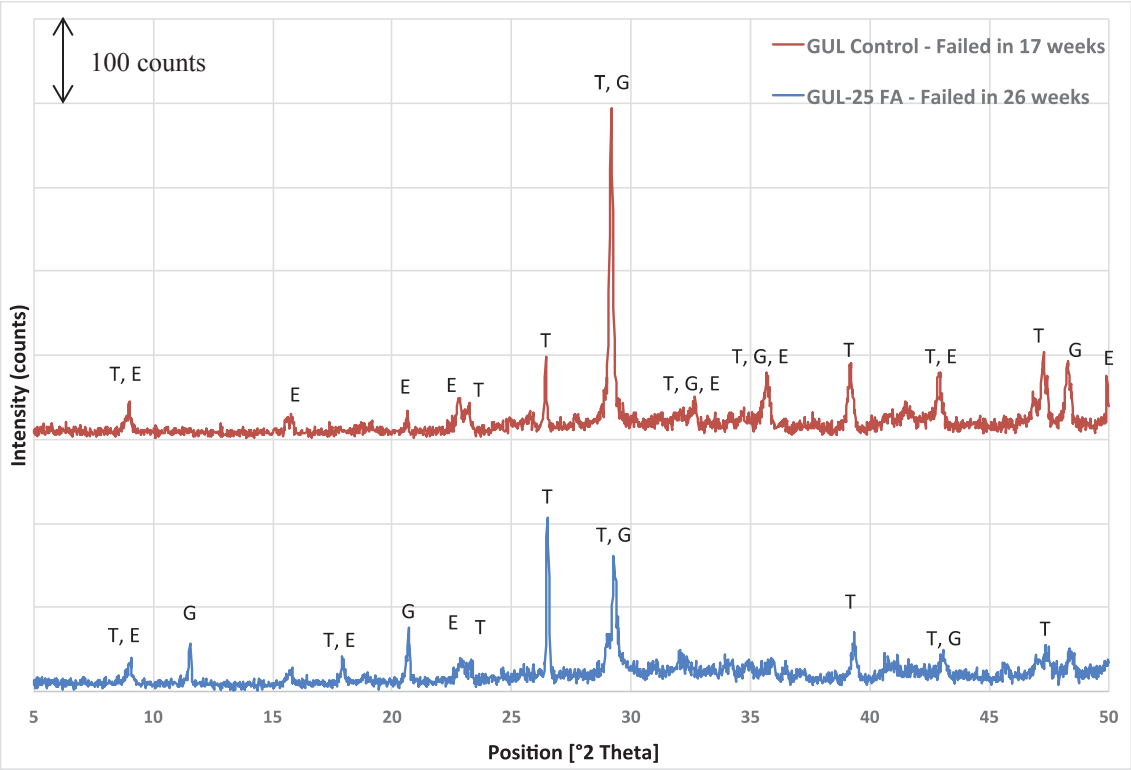

Fig. 4-30: XRD analysis of "GUL Control" and "GUL-25 FA" in TSA
(E: Ettringite – G: Gypsum – T: Thaumasite)

Fig. 4-31 presents the XRD analysis for "L Control" sample. The main identified phases are thaumasite, ettringite, gypsum, and quartz. The presence of thaumasite, ettringite, and gypsum confirmed thaumasite sulfate attack occurrence. Identification of quartz was due to the process of powder sample preparation. As for powder sample preparation cut sections of mortar samples were crushed in several stages to achieve a fine powder, in the finally prepared sample; crushed sand could be present. Presence of gypsum was due to the fact that calcium hydroxide was completely reacted with sulfate ions and gypsum was formed. Of course, a portion of gypsum was consumed in reactions

associated with formation of ettringite. Thaumasite was detected in several peaks. The intense peak related to thaumasite, ettringite, and gypsum at around 29 (°2 Theta) confirmed severe TSA. Such a peak was also seen for "GUL Control" in Fig. 4-30.

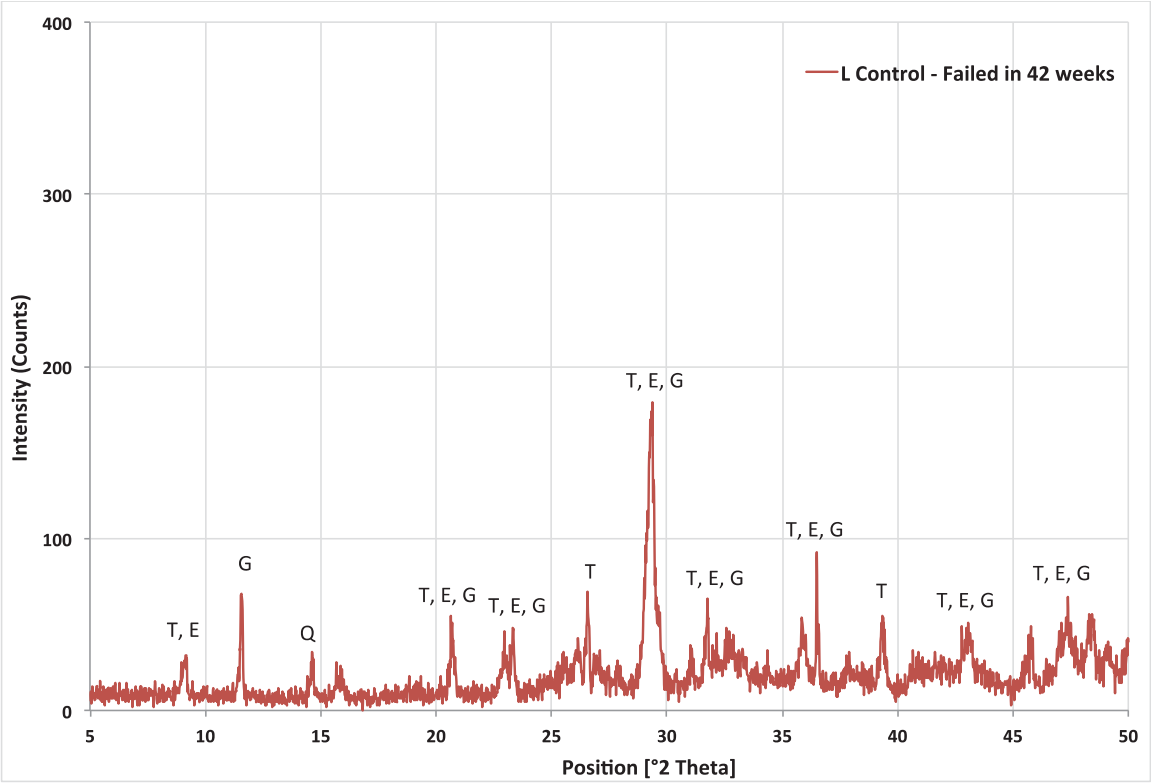

Fig. 4-31: XRD analysis of "L Control" in TSA
(E: Ettringite – G: Gypsum – Q: Quartz – T: Thaumasite)

The XRD analysis of samples obtained from surface of "L-35 Slag" and "L-45 Slag" mortar bars after 2-year thaumasite sulfate attack are shown in Fig. 4-32. The principal peaks are related to gypsum, ettringite, thaumasite, and quartz. As mentioned, identification of quartz was due to presence of crushed sand inside the analyzed powder sample. For both samples, the intensity of the peaks related to gypsum, ettringite, and thaumasite was quite low. The replacement of PLC with slag resulted in a better

performance against TSA, and development of lower amounts of thaumasite, ettringite, and gypsum. It was interesting that increase in the content of slag noticeably reduced the intensity of the peaks corresponding to ettringite, gypsum, and thaumasite. Therefore, lower amounts of the noted materials were formed in "L-45 Slag" that verifies the higher resistance of this blend of Portland-limestone cement against thaumasite sulfate attack.

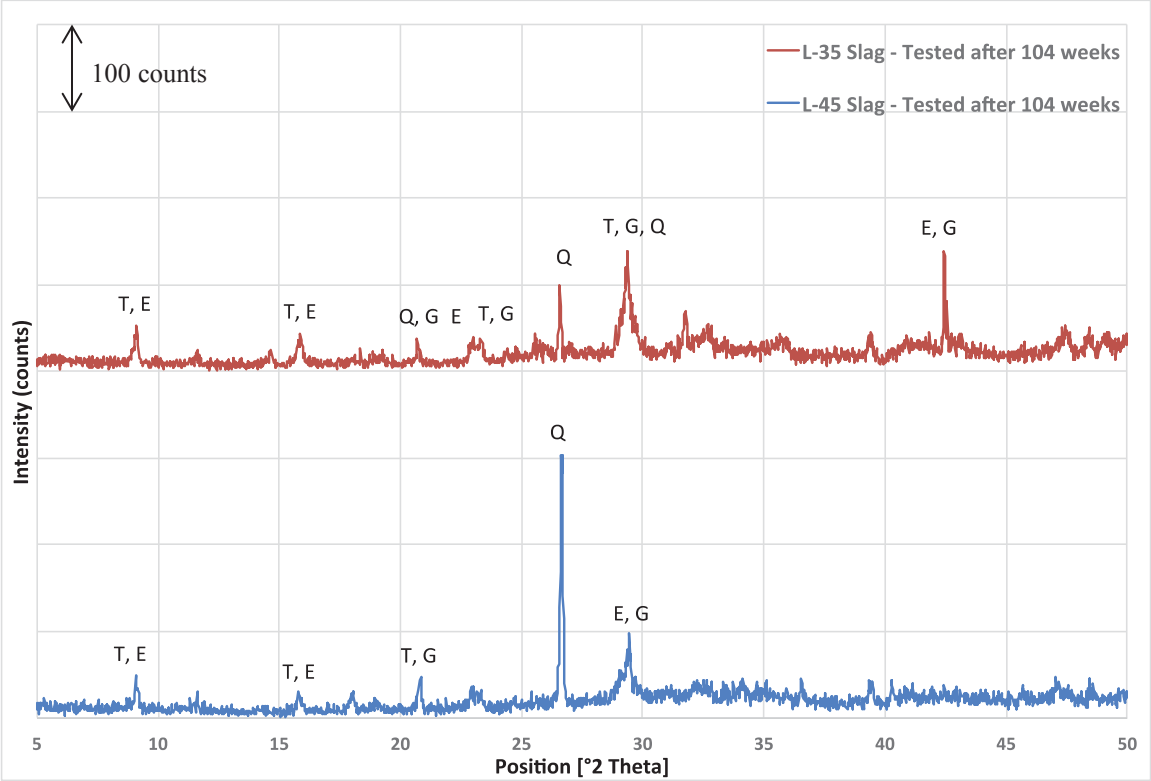

Fig. 4-32: XRD analysis of "L-35 Slag" and "L-45 Slag" in TSA
(E: Ettringite – G: Gypsum – Q: Quartz – T: Thaumasite)

In Fig. 4-33, the XRD analysis of "L-3 SFI" and "L-8 SFI" are presented. Thaumasite sulfate attack was confirmed by identification of thaumasite in both samples. "L-3 SFI" failed after a year in TSA. The highest XRD peak of this sample was for thaumasite. In addition to thaumasite, ettringite, gypsum, and quartz were found in the

sample. The XRD analysis complemented the DSC analysis of "L-3 SFI" by identifying ettringite that was not found in DSC analysis. The CSA A3004-C8 mortar bars of "L-8 SFI" did not fail in two years; however, on their surface thaumasite, gypsum, and ettringite were apparently detected as seen in Fig. 4-33. The highest XRD peak was characterized for thaumasite and gypsum together. Smaller peaks solely representing ettringite, gypsum, and thaumasite were also detected. For this sample, the uncertainty about thaumasite detection in DSC analysis was resolved by finding peaks of thaumasite in the XRD result.

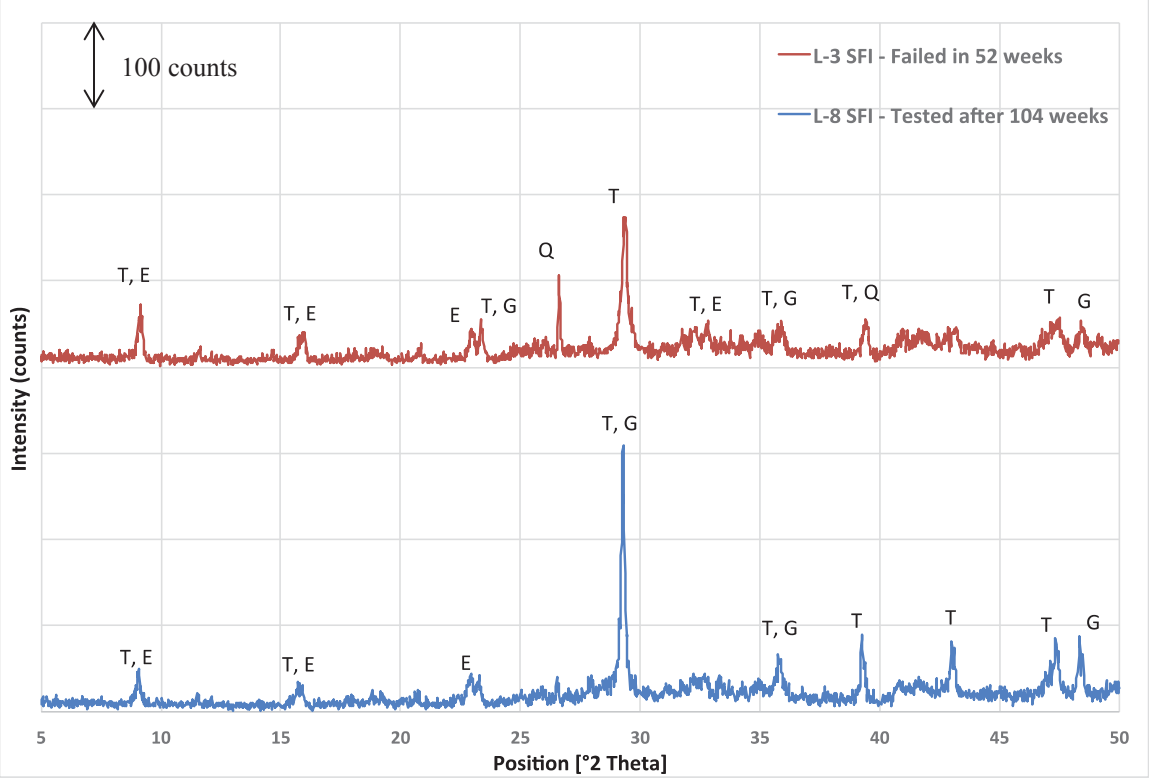

Fig. 4-33: XRD analysis of "L-3 SFI" and "L-8 SFI" in TSA
(E: Ettringite – G: Gypsum – Q: Quartz – T: Thaumasite)

The XRD analysis results of "L-15 MK" and "L-20 MK" tested after 18 months and 24 months, respectively, can be found in Fig. 4-34. Thaumasite was found in the samples and its peak intensity was higher than ettringite. So, the type of attack as expected was thaumasite sulfate attack. The DSC analysis of both samples was not satisfactory; yet, the XRD analysis could help to characterize thaumasite sulfate attack. "L-15 MK" when tested with DSC, did not show presence of gypsum, and only depicted a shoulder representing thaumasite; however, with the XRD analysis, gypsum as well as thaumasite were detected. The DSC analysis of "L-20 MK" was even more problematic as distinctive peaks of thaumasite, ettringite, and gypsum were not found. Nevertheless, in the XRD analysis, the mentioned materials were found on the surface of the "L-20 MK" CSA A3004-C8 mortar bars confirming that even though the mortar bars were effectively resisting against thaumasite sulfate attack, formation of thaumasite occurred on the surface of the samples.

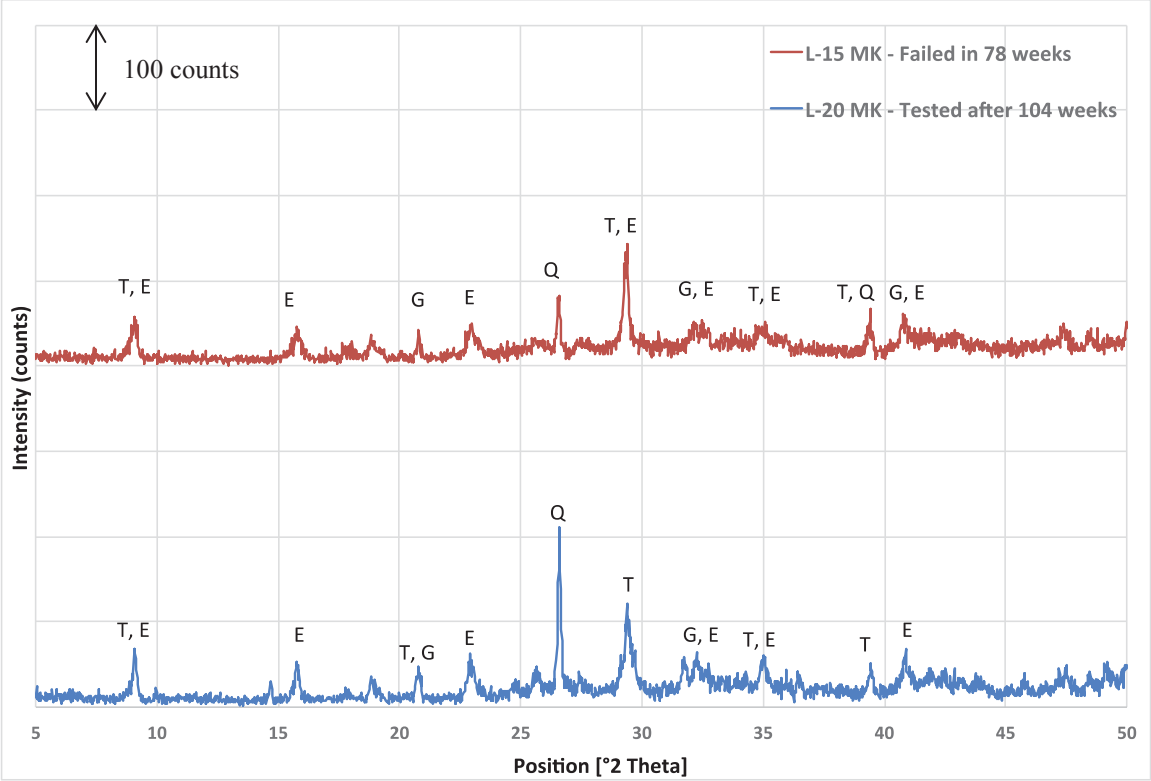

Fig. 4-34: XRD analysis of "L-15 MK" and "L-20 MK" in TSA

(E: Ettringite – G: Gypsum – Q: Quartz – T: Thaumasite)

5- Discussion

The results of the research were independently presented and discussed in the previous chapter. Commonly, there can be correlations between different tests' results in a research project that would improve understanding of the whole concept and help to draw more precise conclusions. Moreover, different tests can complement each other and shed light on the dark points. With regards to this fact, in this section, a more detailed study is presented on the test results. Also, the results of different tests are studied along with each other. In addition, where available, the results are compared with other published studies in the field. Consequently, efforts are made through the discussions to implement accurate conclusions.

5-1- Rate of expansion of CSA A3004 mortar bars in ettringite sulfate attack

The detailed change in mortar bars' expansions during two years of ettringite sulfate attack is shown in Fig. 5-1 through Fig. 5-7. According to the mentioned figures, control samples had the highest expansions compared to the PLC blends. Due to their high expansion, the average length changes at final ages are not seen in the figures to maintain scale, but are noted. In Fig. 5-1, it is seen that addition of 25% fly ash or 40% slag to the GUL cement has significantly reduced the expansion of mortar prisms in ESA. It can be inferred from the figure that in regard to the expansion, both blends of Portland-limestone cement had nearly similar performances, while the blend containing 40% slag had slightly lower expansion than the one with 25% fly ash. For "GUL Control" it is seen that after 13 weeks the rate of expansion increased and stayed roughly constant during the remaining test duration. The two other samples also had a constant rate of expansion, which was noticeably lower than the control sample.

In Fig. 5-2 to Fig. 5-7, for all blends it is clearly perceived that the addition of the studied supplementary cementing materials has considerably decreased expansions. Moreover, the increase in the amount of each type of SCM in the blends of PLC has resulted in a decrease in expansion. According to the figures, "L Control" showed an increase in the rate of expansion during the first year of ESA study, followed by an approximately constant rate of expansion. It is interesting that such an increase in expansion rate is also seen for some blends of PLC with relatively lower SCM contents. The PLC blend containing 10% metakaolin showed an increase in the rate of expansion in Fig. 5-3, and when compared with the other metakaolin blends, it expanded more at the final ages. This observation confirms that deterioration is affecting this sample at later ages than the control sample, but at sooner ages than the other metakaolin blends. Such observation was also made for "L-3 SF" in Fig. 5-4 and "L-3 SFI" and "L-5 SFI" in Fig. 5-5. Other blends of PLC with SCMs, as seen in the figures, had expansion but with low constant rates. Such low constant expansion rate was especially observed for the binary PLC blends containing slag or ternary PLC blends with slag and fly ash (Fig. 5-6 and Fig. 5-7).

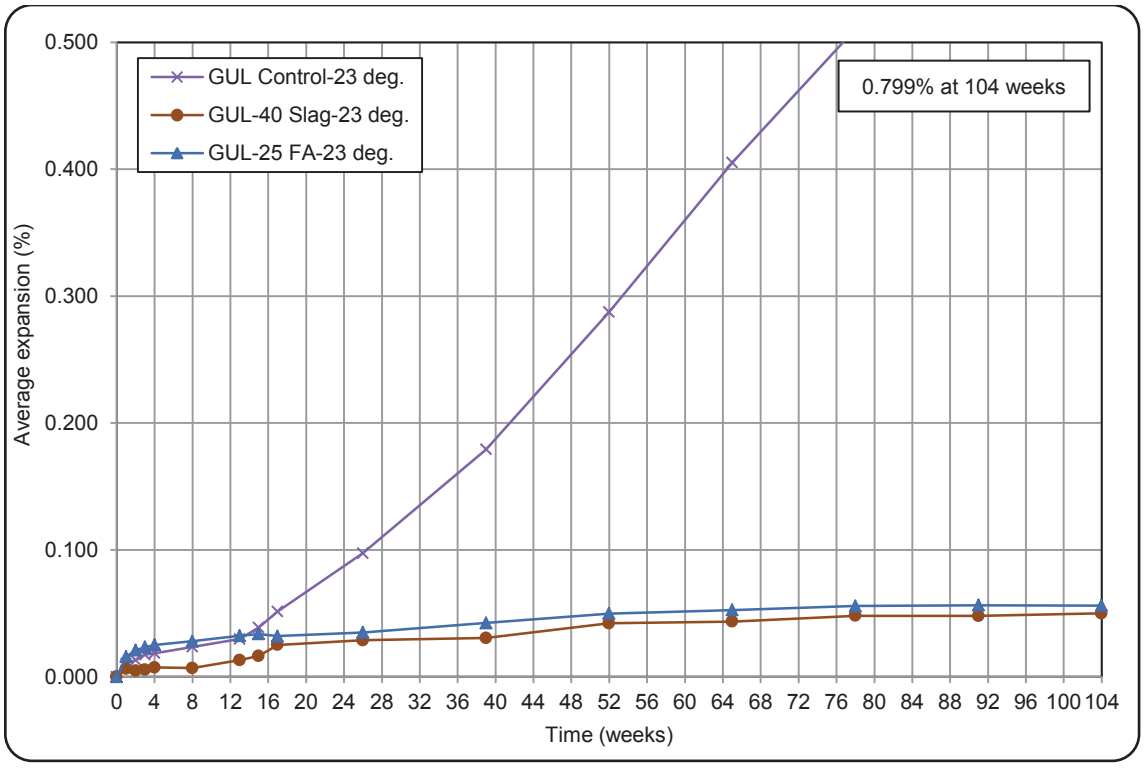

Fig. 5-1: Expansion of CSA A3004-C8-A mortar bars in a 2-year ESA – GUL cement

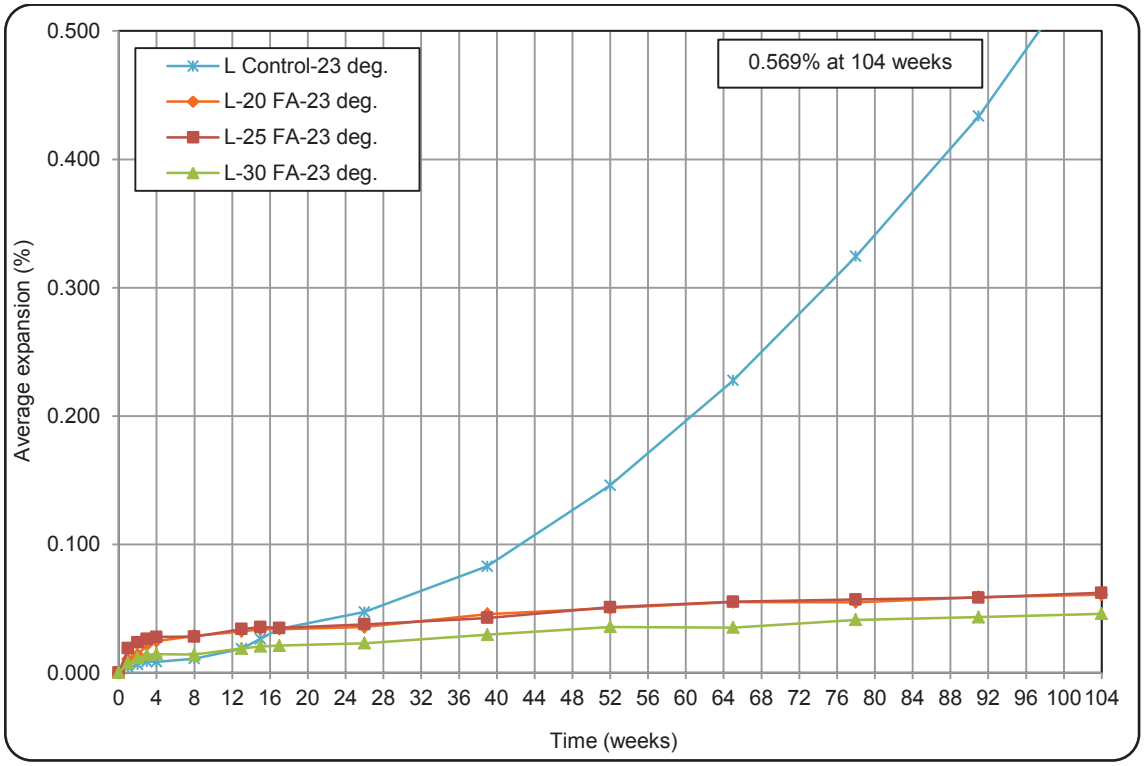

Fig. 5-2: Expansion of CSA A3004-C8-A mortar bars in a 2-year ESA – Fly ash blends

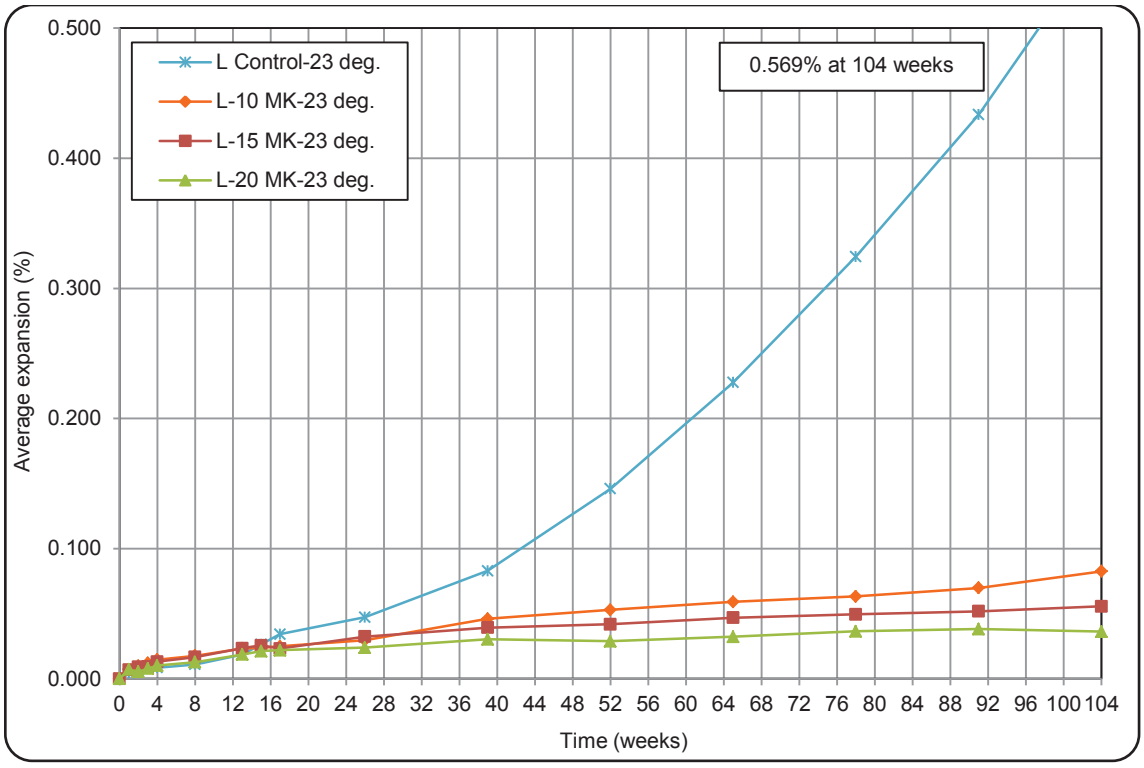

Fig. 5-3: Expansion of CSA A3004-C8-A mortar bars in a 2-year ESA – Metakaolin blends

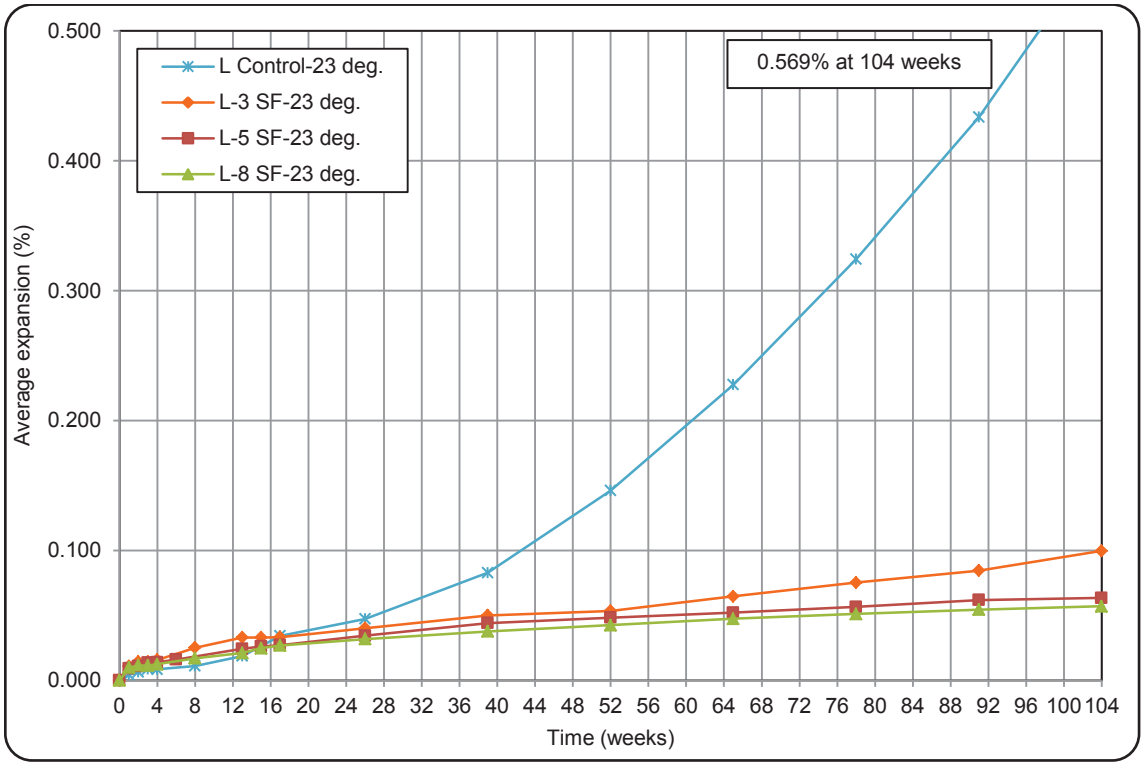

Fig. 5-4: Expansion of CSA A3004-C8-A mortar bars in a 2-year ESA – Silica fume blends

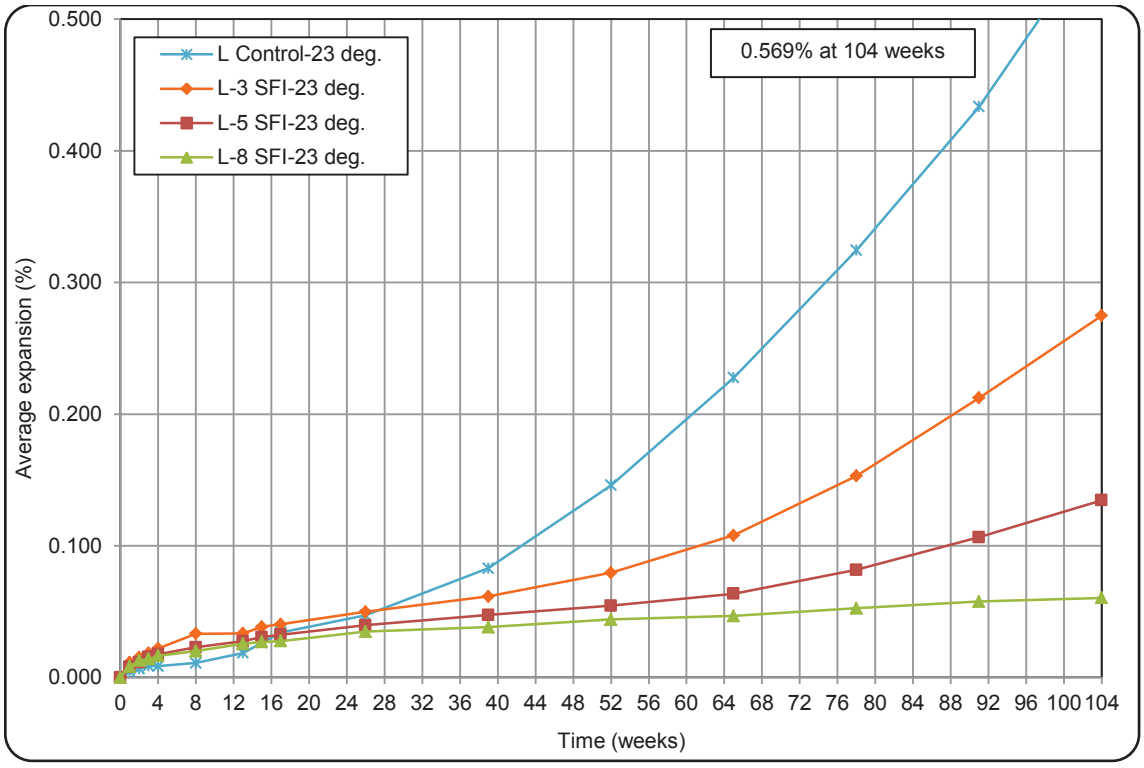

Fig. 5-5: Expansion of CSA A3004-C8-A mortar bars in a 2-year ESA – Silica fume I blends

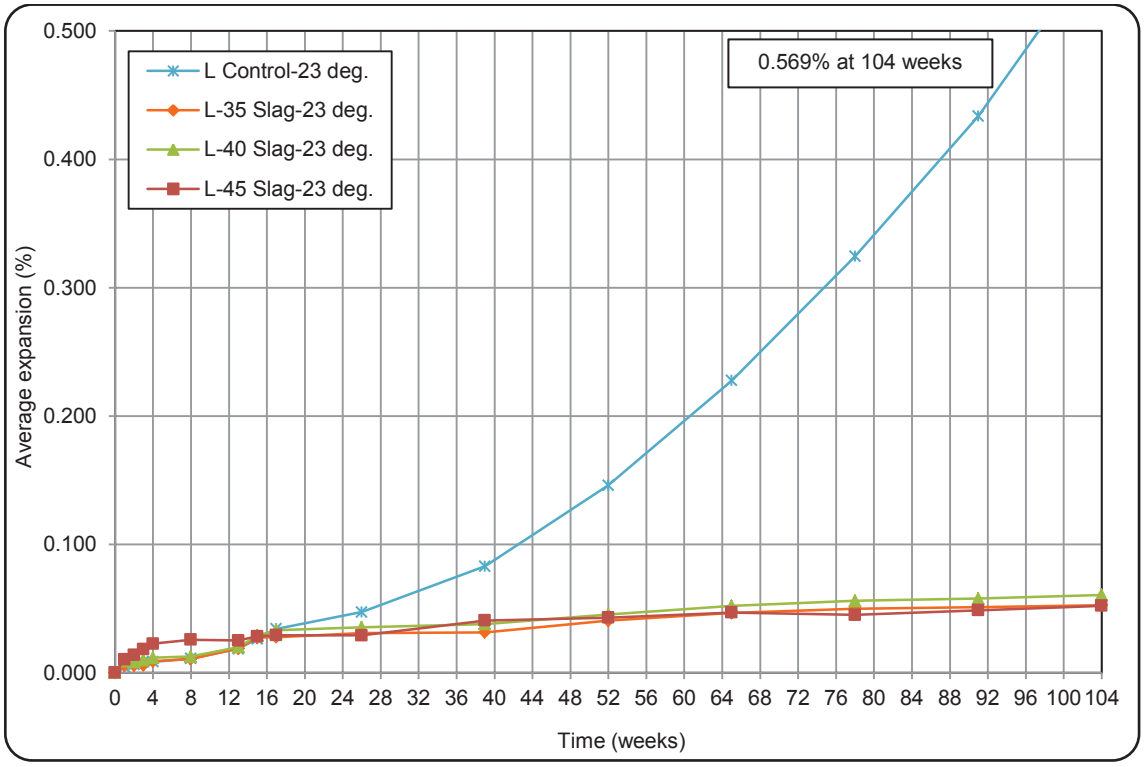

Fig. 5-6: Expansion of CSA A3004-C8-A mortar bars in a 2-year ESA – Slag blends

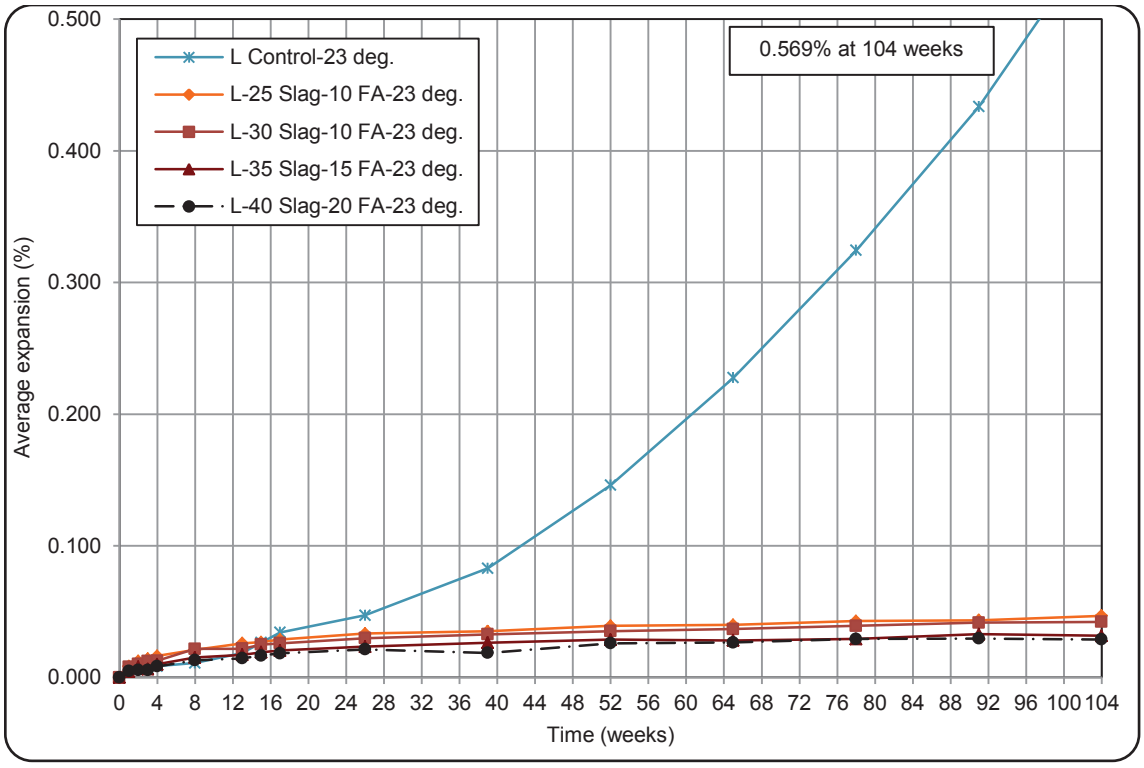

Fig. 5-7: Expansion of CSA A3004-C8-A mortar bars in a 2-year ESA – Slag & fly ash blends

5-2- Rate of expansion of CSA A3004 mortar bars in thaumasite sulfate attack

The two-year expansion of mortar bars in thaumasite sulfate attack is outlined in Fig. 5-8 through Fig. 5-14. Since a number of samples failed during the study, their corresponding curves are discontinued in the relevant figures. Considering all figures, it is apparent that the control samples had the highest expansions in TSA. In Fig. 5-8, "GUL Control", which failed at 17 weeks and had the highest expansion of 1.098%, failed as the first sample. This figure implies that, unlike ettringite sulfate attack, addition of type F fly ash to PLC at 25% has not been effective for resistance against TSA. The blend containing 40% slag had a better performance from the point of view of expansion, yet this blend did not last for two years as well. Fig. 5-8 suggests that the expansion rates of the three samples increased near the failure ages compared to the initial test days.

In Fig. 5-9 to Fig. 5-14, the effect of addition of different types of SCMs on TSA is clearly understood. In general, all the studied SCMs have reduced the mortar bars' expansion in TSA, and an increase in the amount of SCMs has decreased expansion. According to Fig. 5-13, "L-35 Slag" expanded more than 0.500% after two years while not failing. This expansion was higher than the failure expansion of metakaolin containing blends (Fig. 5-10), "L-3 SF" (Fig. 5-11), and SFI containing blends (Fig. 5-12). This observation denotes that slag containing PLC blends can resist TSA disintegration more than the mentioned blends. The expansion of the control sample as seen in the figures, had an abrupt rate increase after 26 weeks and before failure. For all the failed blends in Fig. 5-9, Fig. 5-11, and Fig. 5-12 such increase in expansion rate was found. The increase in the expansion rate was also seen in some of the survived lasted blends in thaumasite sulfate attack. "L-5 SF" showed an increase in the length change rate in the last 3 months of the study according to Fig. 5-11, while "L-8 SF" had a constant low rate of expansion. In Fig. 5-12, continuous increase in expansion rate was found for "L-8 SFI". Such continuous increase in the length change rate was also seen for "L-35 Slag" and "L-40 Slag" in Fig. 5-13, yet not for "L-45 Slag", which suggests that this sample would fail later than the other two, and was more resistant against TSA. In addition, Fig. 5-14 suggests that "L-25 Slag-10 FA" and "L-30 Slag-10 FA" had increase in the rate of expansion after 65 weeks (15 months), but the other two ternary blends with higher contents of slag and fly ash had a constant low expansion rate during the two-year TSA that confirms their improved resistance in thaumasite sulfate attack.

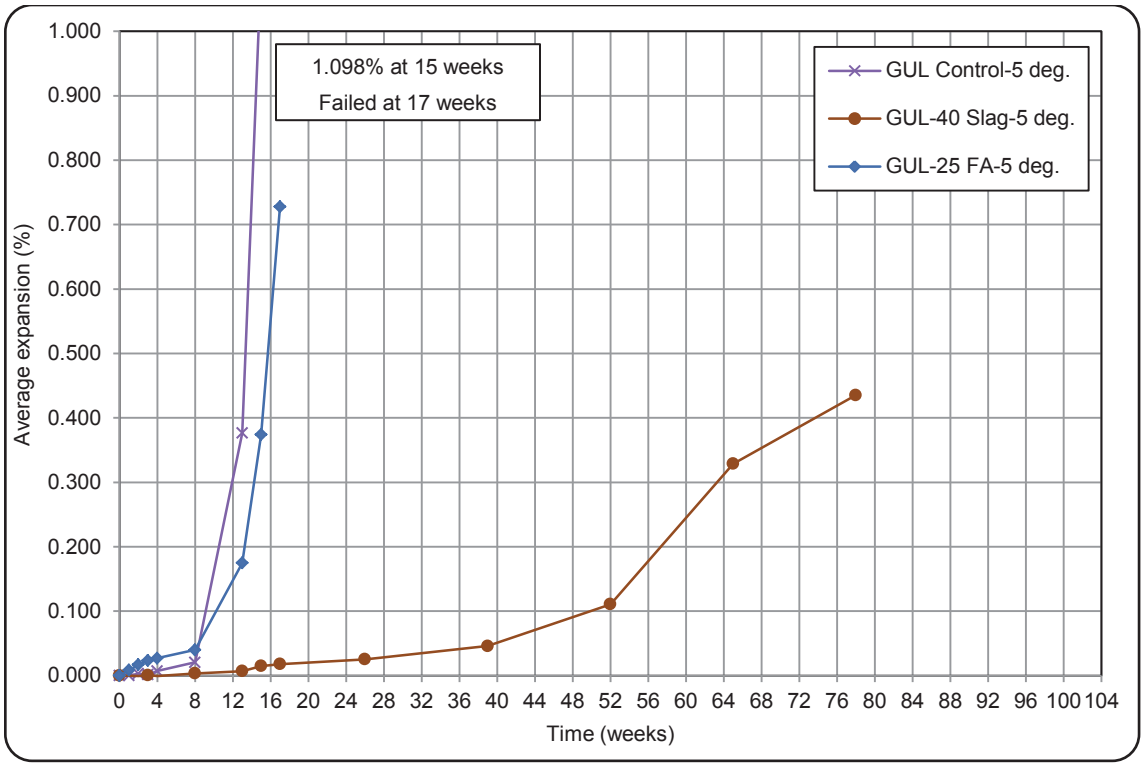

Fig. 5-8: Expansion of CSA A3004-C8-B mortar bars in a 2-year TSA – GUL cement

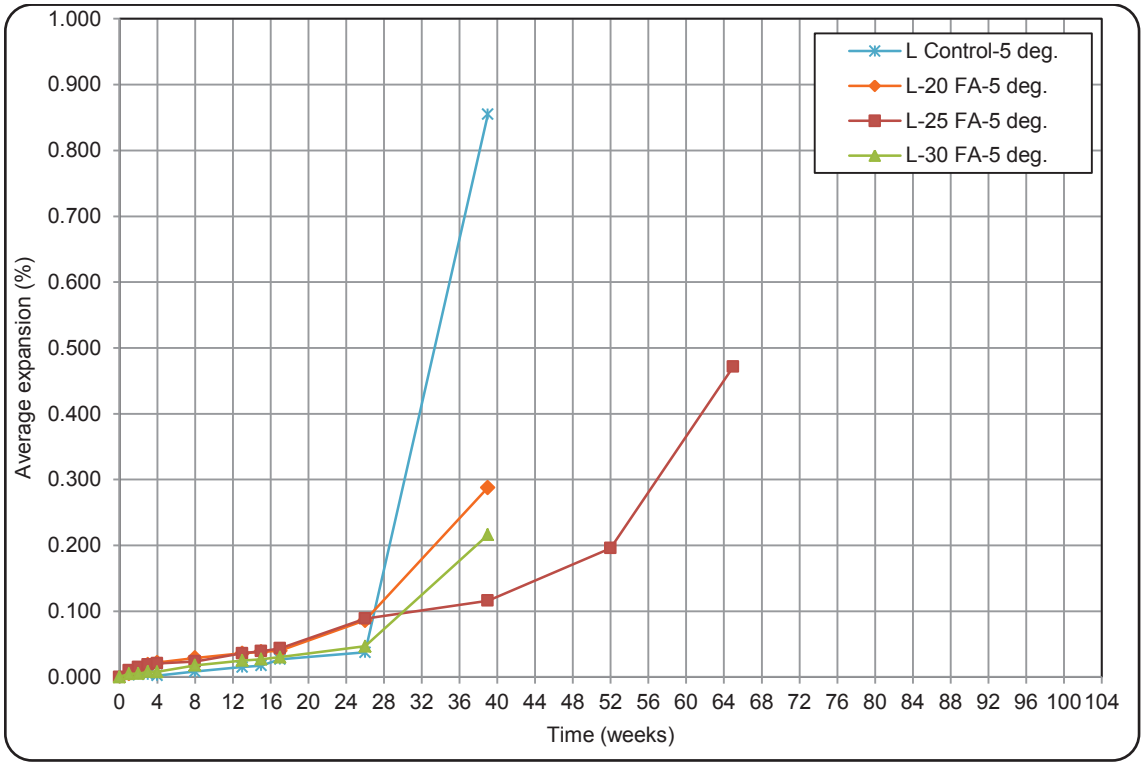

Fig. 5-9: Expansion of CSA A3004-C8-B mortar bars in a 2-year TSA – Fly ash blends

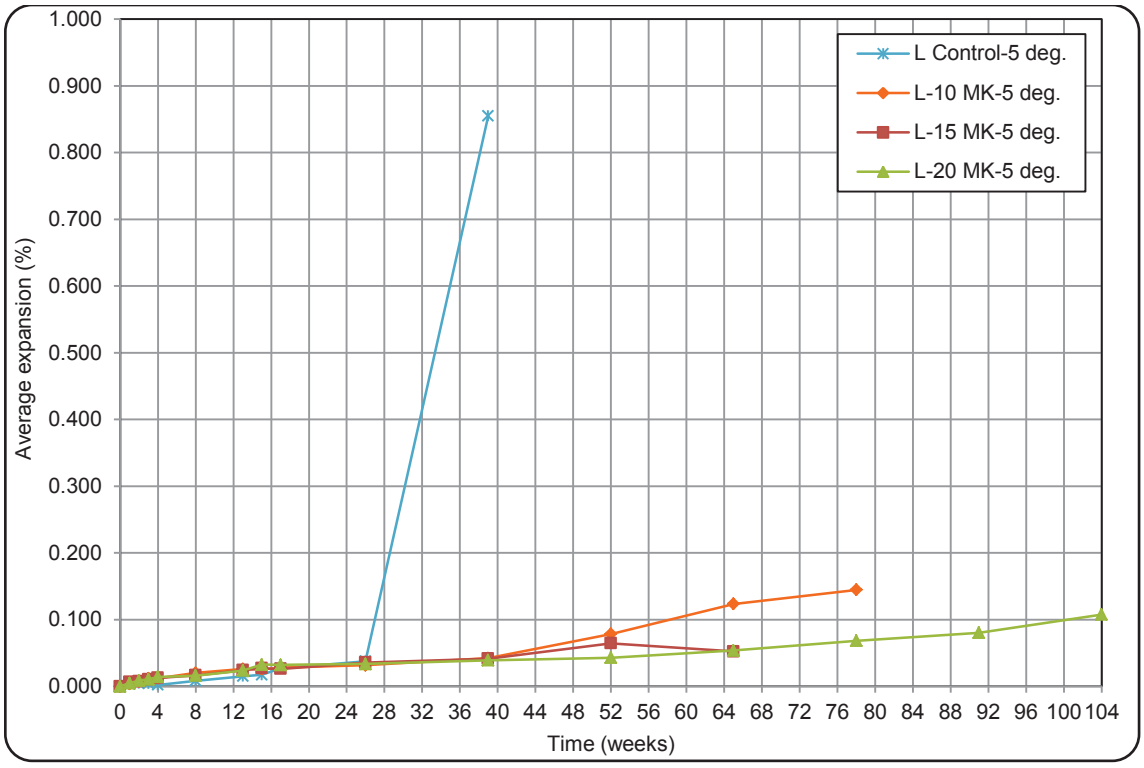

Fig. 5-10: Expansion of CSA A3004-C8-B mortar bars in a 2-year TSA – Metakaolin blends

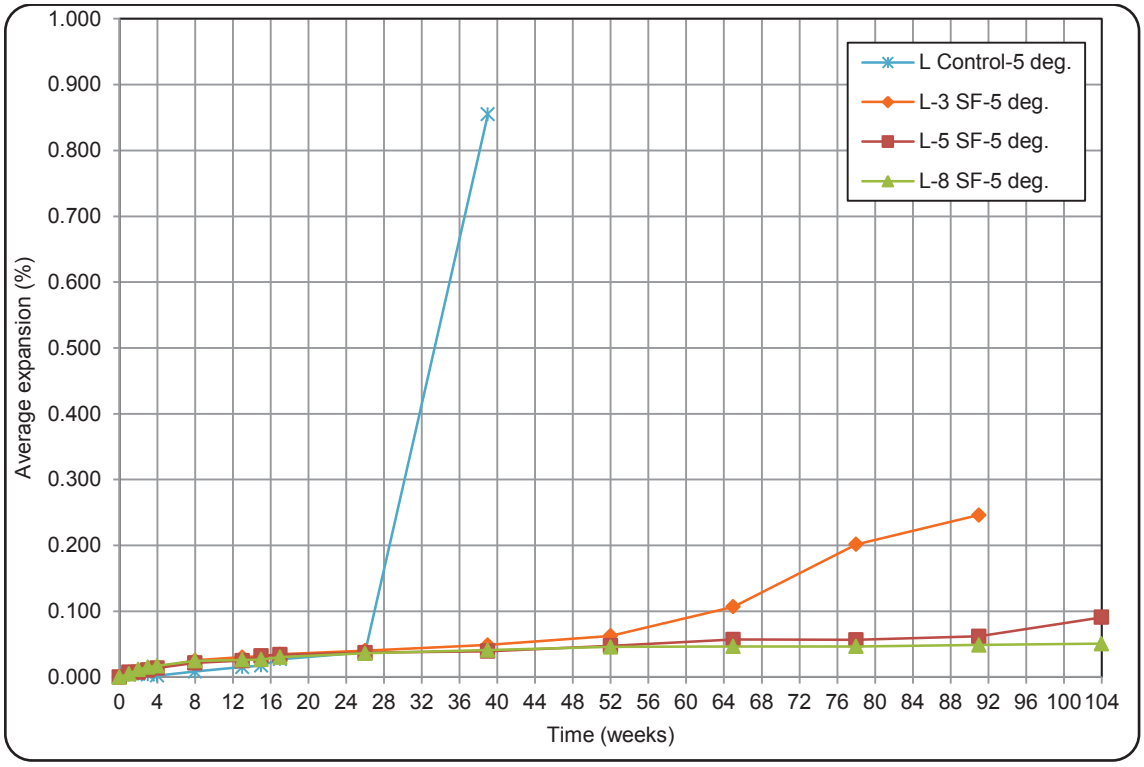

Fig. 5-11: Expansion of CSA A3004-C8-B mortar bars in a 2-year TSA – Silica fume blends

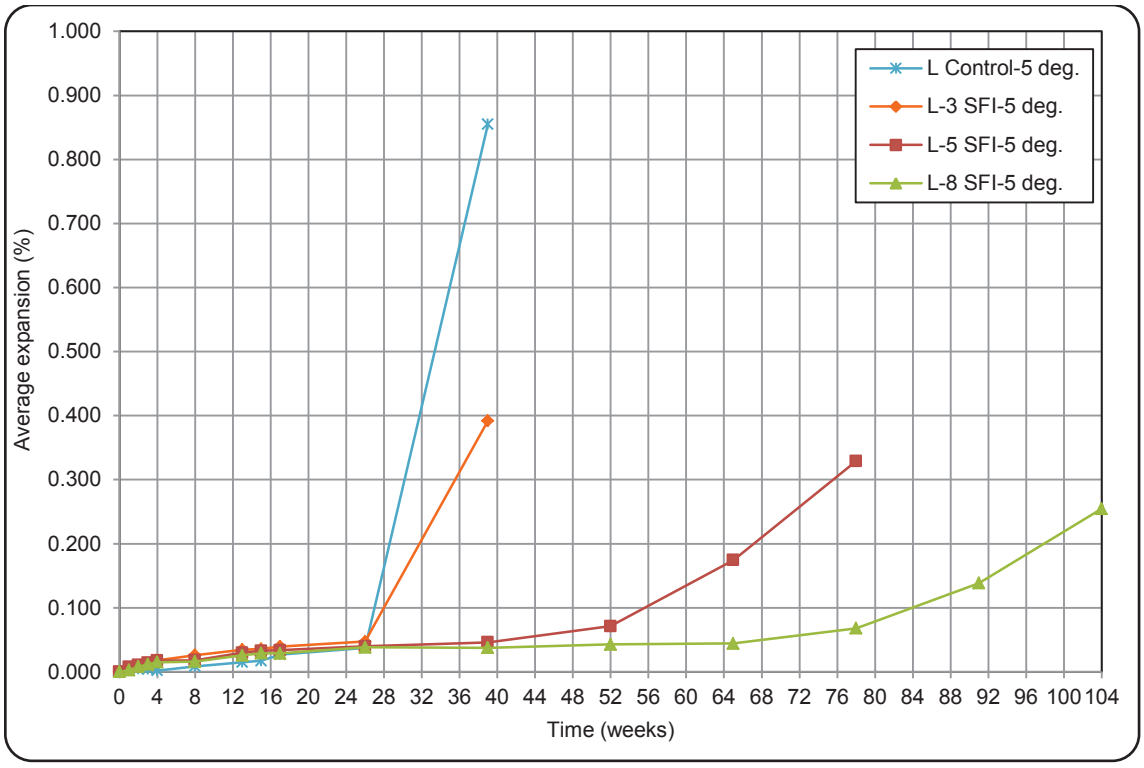

Fig. 5-12: Expansion of CSA A3004-C8-B mortar bars in a 2-year TSA – Silica fume I blends

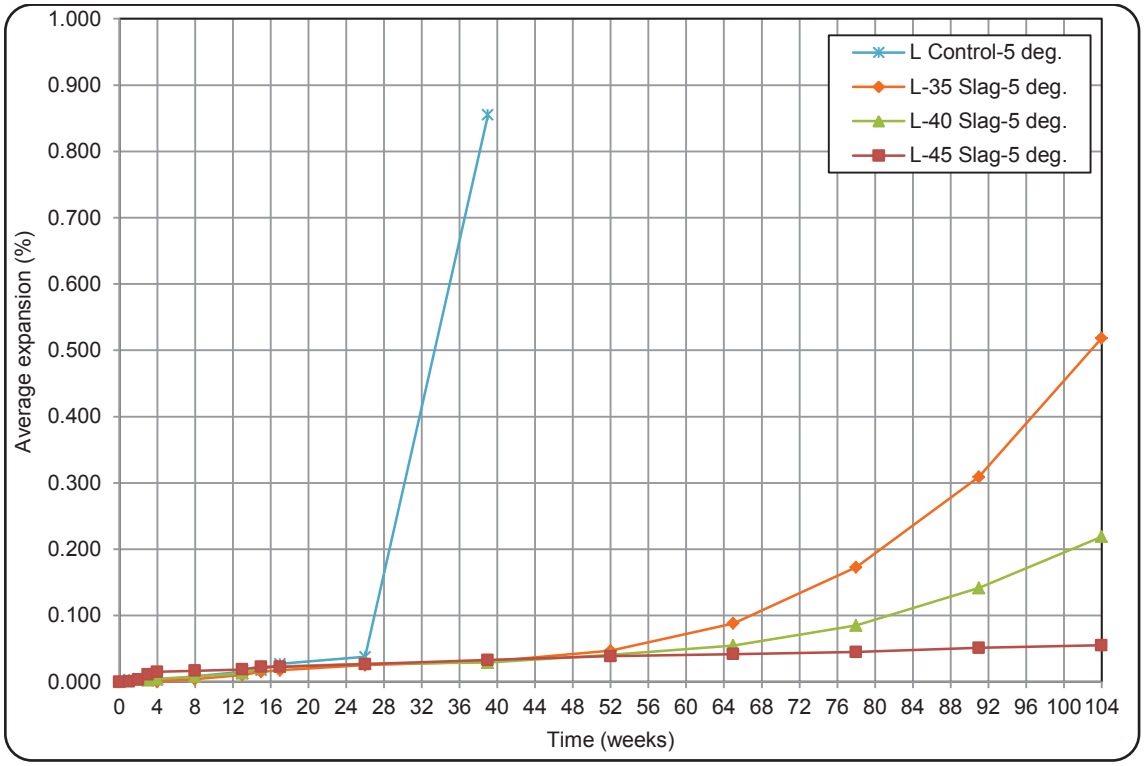

Fig. 5-13: Expansion of CSA A3004-C8-B mortar bars in a 2-year TSA – Slag blends

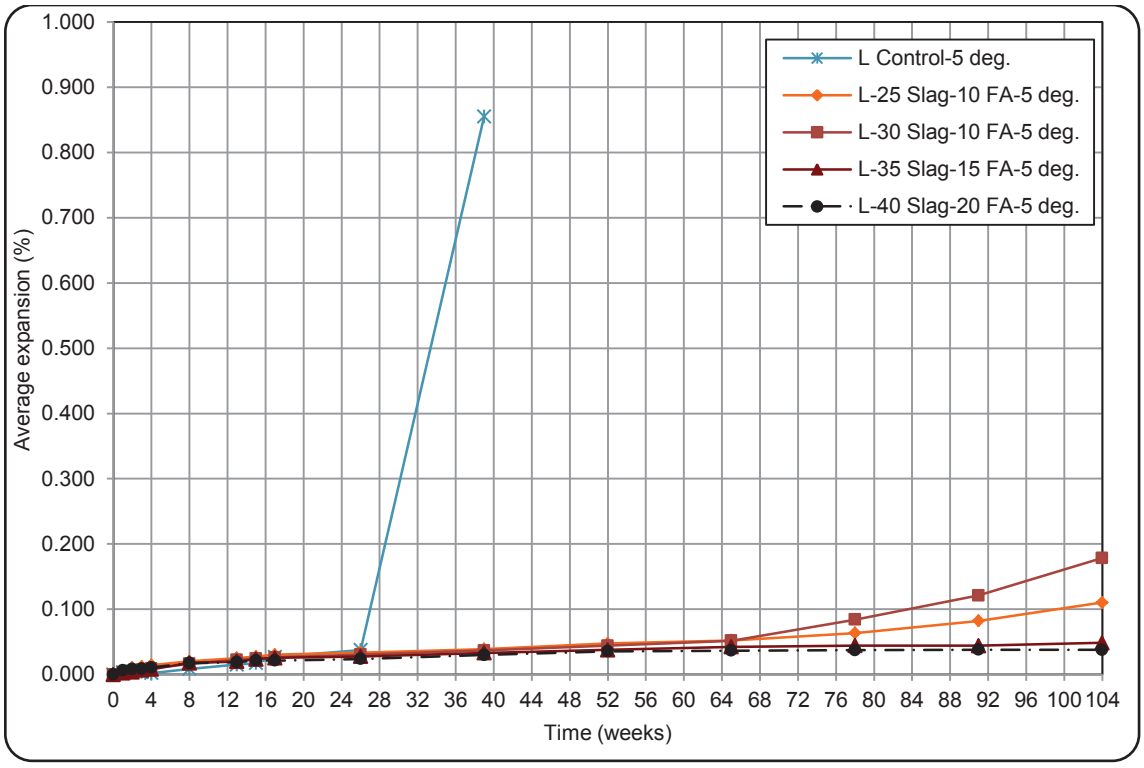

Fig. 5-14: Expansion of CSA A3004-C8-B mortar bars in a 2-year TSA – Slag & fly ash blends

5-3- Comparing expansion of CSA A3004-C8 mortar bars in sulfate attack with other studies

Considering the fact that Portland-limestone cement is recently introduced in Canada by CSA A3001-08, and the standard specification for evaluating this category of cement was devised and modified in 2010 (CSA A3004-C8 and CSA A3001), currently there are very limited published studies on performance of PLC in sulfate attack as per CSA A3004-C8 standard. One of the published studies is a research on the performance of the general use cement when partially replaced with different amounts of ground limestone, which was recently completed by Ramezanianpour (2012) in University of Toronto under supervision of Dr. Hooton. The focus of the research was on the effect of slag as a supplementary cementing material on limestone containing cements. In this section, the CSA A3004-C8 results of slag containing mortar bars as well as control ones

obtained in the present research at Concordia University are compared with the published data from Ramezanianpour (2012). The compared blends are presented in Table 5-1. As seen in the table, the limestone contents of the samples are fairly close. The slag contents are ranged from 30% to 50%.

Table 5-1: The compared blends of Portland-limestone cement

	Designation	Limestone content (%)	Slag content (%)
	L Control	10	0
	L-35 Slag	10	35
	L-40 Slag	10	40
	L-45 Slag	10	45
	GUL Control	13.5	0
	GUL-40 Slag	13.5	40
Ramezanianpour (2012)	GUL11-Control	11	0
	GUL11-30%Slag	11	30
	GUL11-50%Slag	11	50
	GUL13-Control	13	0
	GUL13-30%Slag	13	30
	GUL13-50%Slag	13	50

In Fig. 5-15, the CSA A3004-C8-A results of control and slag containing mortar bars are compared. The dashed lines are the results by Ramezanianpour (2012). According to the figure, the control samples from both studies expanded significantly more than the blends containing slag. All the results of the blends of slag and limestone cement showed very low expansions after two years of exposure, which indicated a considerable resistance against ettringite sulfate attack. Among the samples prepared with slag, the ones which contained 50% slag expanded noticeably lower than the other blends. According to this figure, although the cement and slag used in the two studies

were chemically different, Portland-limestone cement blends containing 30% to 45% slag had very close expansions after 2 years of ettringite sulfate attack.

The results of the thaumasite sulfate attack study on PLC blends with slag as per CSA A3004-C8-B are compared with the literature in Fig. 5-16. Obviously, the control samples have expanded faster and to larger extents compared to the blends of slag. According to the CSA A3001-10, only PLC blends containing 45% and 50% slag would be specified as high sulfate resistant blended PLC. The results presented in Fig. 5-16 can be classified in 3 categories of high range expansion, moderate range expansion, and low range expansion. The control samples were in the high range expansion category. They all showed large expansions in only a few months of exposure, followed by quick failure. Different blends of PLC, presented in Fig. 5-16, containing 30%, 35%, and 40% slag can be characterized as moderate range expansion blends. These samples did not fail after two years; however, they did not expand within the standard limit. The blends containing 45% and 50% did not expand more than the standard limit for high sulfate resistant blended PLC. In fact, they showed very low expansions after two years of TSA, which indicates that they can be classified in low range expansions.

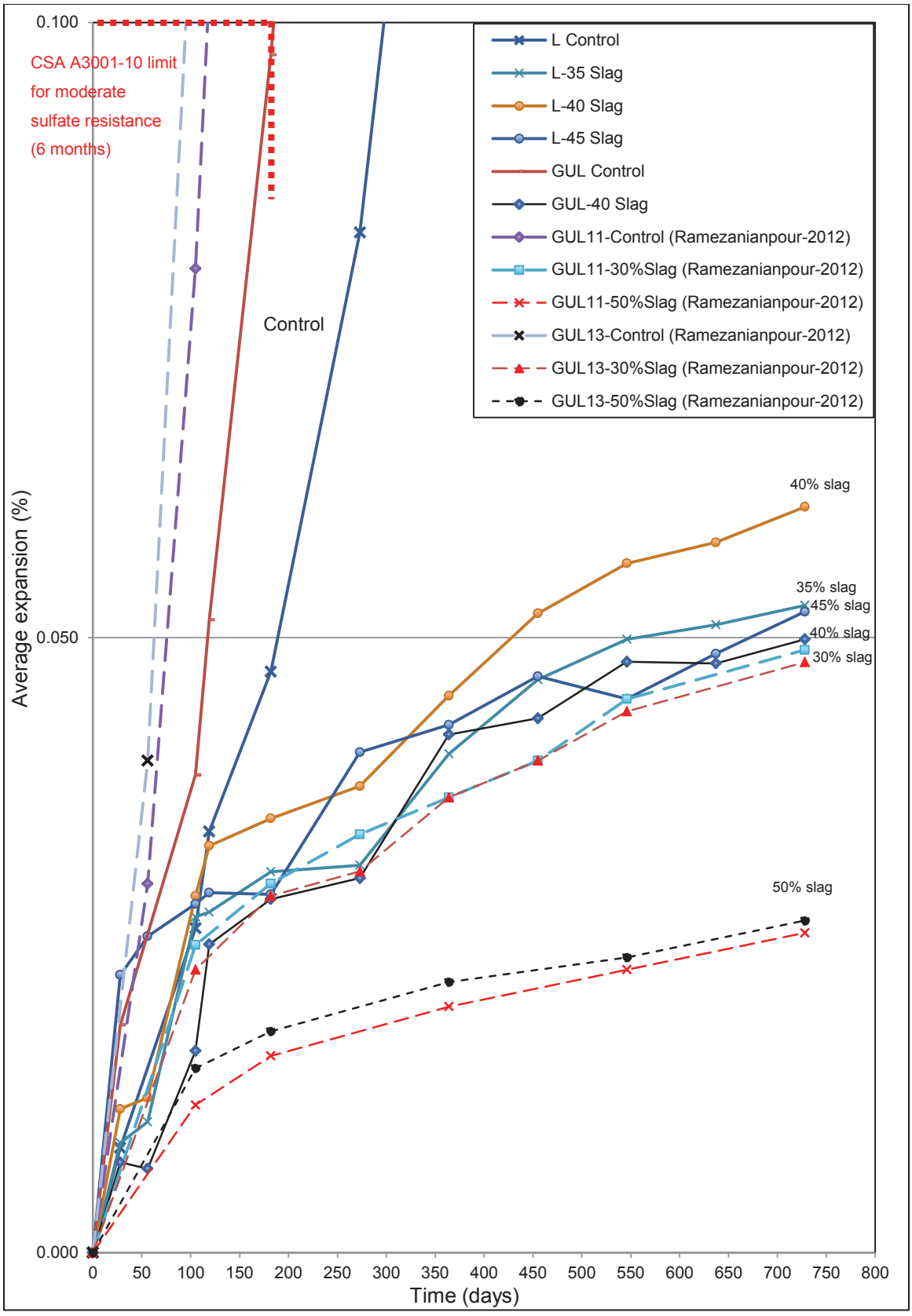

Fig. 5-15: Expansion of slag containing mortar bars in ettringite sulfate attack – CSA A3004-C8-A

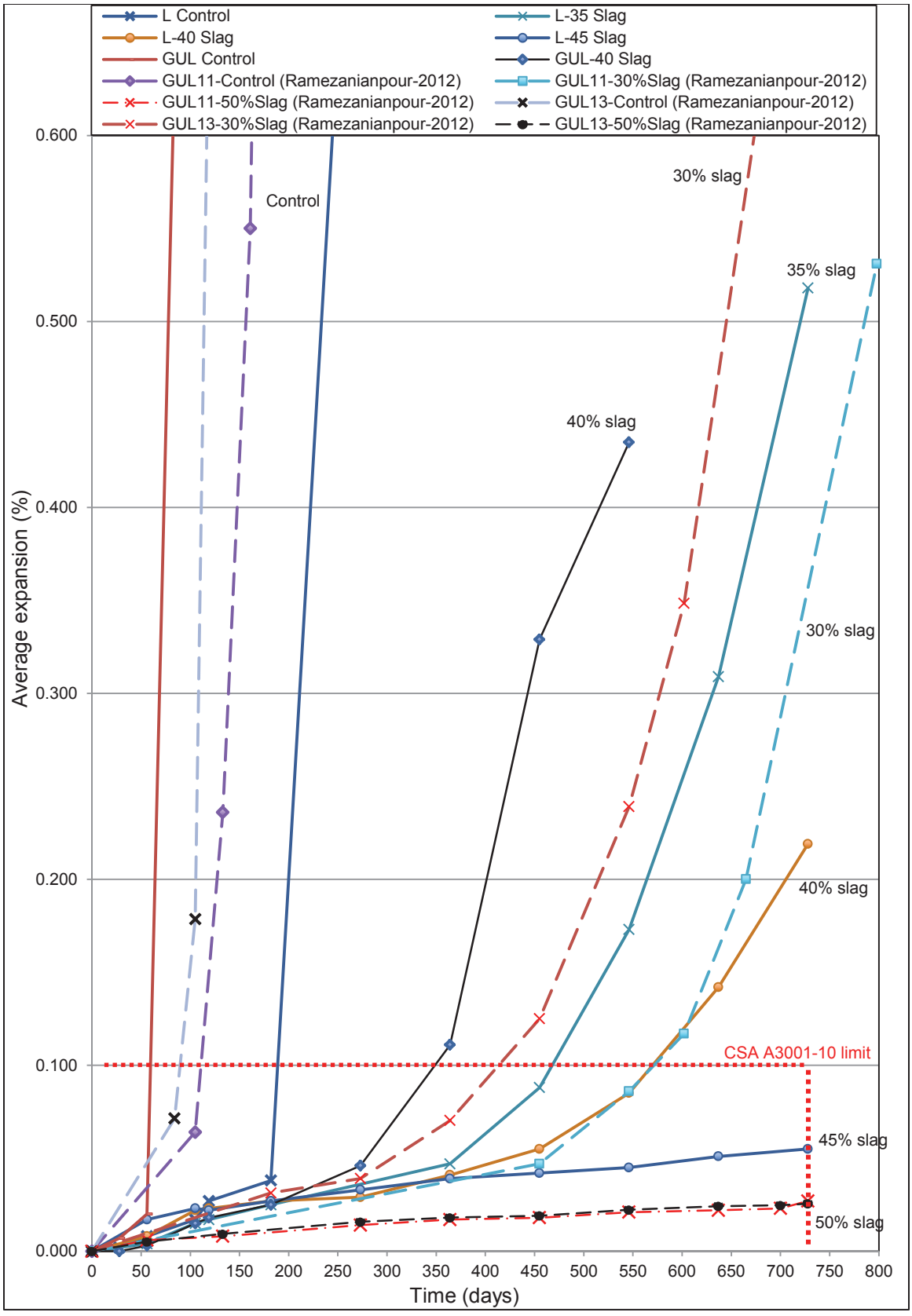

Fig. 5-16: Expansion of slag containing mortar bars in thaumasite sulfate attack – CSA A3004-C8-B

5-4- Mass change of CSA A3004 mortar bars in ettringite sulfate attack

The average mass changes of mortar bars in ettringite sulfate attack for two years are shown in Fig. 5-17 to Fig. 5-23. Continuous mass increases for all samples were observed due to formation of gypsum and ettringite during the exposure to sodium sulfate solution. The control samples of PLC showed more mass increases after two years of exposure than the blends of Portland-limestone cement. It should be mentioned that at early ages the mass change results were different than the older ages. Generally, at initial stages of the exposure, the average mass change of the control sample was not the highest since at that stage the pozzolanic reactions had not taken place; therefore, the PLC blend mortars were more affected by sulfate attack. However, at later stages, along with the progress of pozzolanic reactions, the mortars' resistance was improved, and as seen in the figures their mass increase was lower than the control sample. According to Fig. 5-17 through 5-23, the rate of mass increase for all samples, especially the blends containing supplementary cementing materials, was higher at earlier ages than the older ages. During exposure, the mortars' pores are gradually filled with gypsum and ettringite as well as secondary CSH gel; thus, the rate of mass gain decreases. Overall, the rate of mass gain of the PLC blends was lower than the control sample. As was visually observed, noticeable cracks formed in the control mortar bars during the exposure. The cracks opened up new spaces for formation of gypsum and ettringite; thus, they resulted in higher mass gain rate.

In Fig. 5-17, the mass change of samples prepared with GUL is shown. Addition of slag and fly ash was effective on reducing the mass increase, which indicates the improvement in resistance against formation of ettringite and gypsum during the

exposure to sodium sulfate solution. “GUL-40 Slag” had the lowest mass increase therefore the highest resistance in ettringite sulfate attack. According to Fig. 5-18, the mortar samples prepared with combination of PLC and fly ash were nearly similar in the mass change results. The one contained the highest amount of fly ash showed the lowest mass increase (L-30 FA). This blend also had the lowest expansion among the blends of PLC and fly ash (Fig. 5-2). Accordingly, in ettringite sulfate attack it had the best performance.

Studying Fig. 5-19, addition of metakaolin to PLC reduced the mass gain rate. The increase in the amount of metakaolin also decreased the mass change rate and the total mass gain. This observation was in accordance with the expansion results in Fig. 5-3 in which the increase in the amount of metakaolin decreased the expansion. Fig. 5-20 shows that in ettringite sulfate attack, the studied blends of PLC and SF had reduced the mass gain compared to the control samples. Their mass changes results were very close, similar to the expansion results presented in Fig. 5-4. According to Fig. 5-21, SFI blends’ mass gains were fairly close to the control sample. Although SFI was not as effective as the other SCMs on reducing the mass gain due to ESA, the increase in SFI content noticeably decreased the mass gain. The same positive effect was seen for their expansion results in ESA (Fig. 5-5); the PLC blend’s expansion was considerably decreased when the SFI content was changed from 3% to 8%.

The binary blends of PLC and slag or the ternary blends of PLC, slag, and fly ash performed very well from the viewpoint of mass changes. Considering Fig. 5-22 and Fig. 5-23, all mentioned blends had about one third of the average mass gain of the control mortar sample after 2 years of ESA. It can be inferred from both figures that

compared to the control sample, the mentioned blends effectively resisted against ESA. Similar results were remarked for the expansion results outlined in Fig. 5-6 and Fig. 5-7.

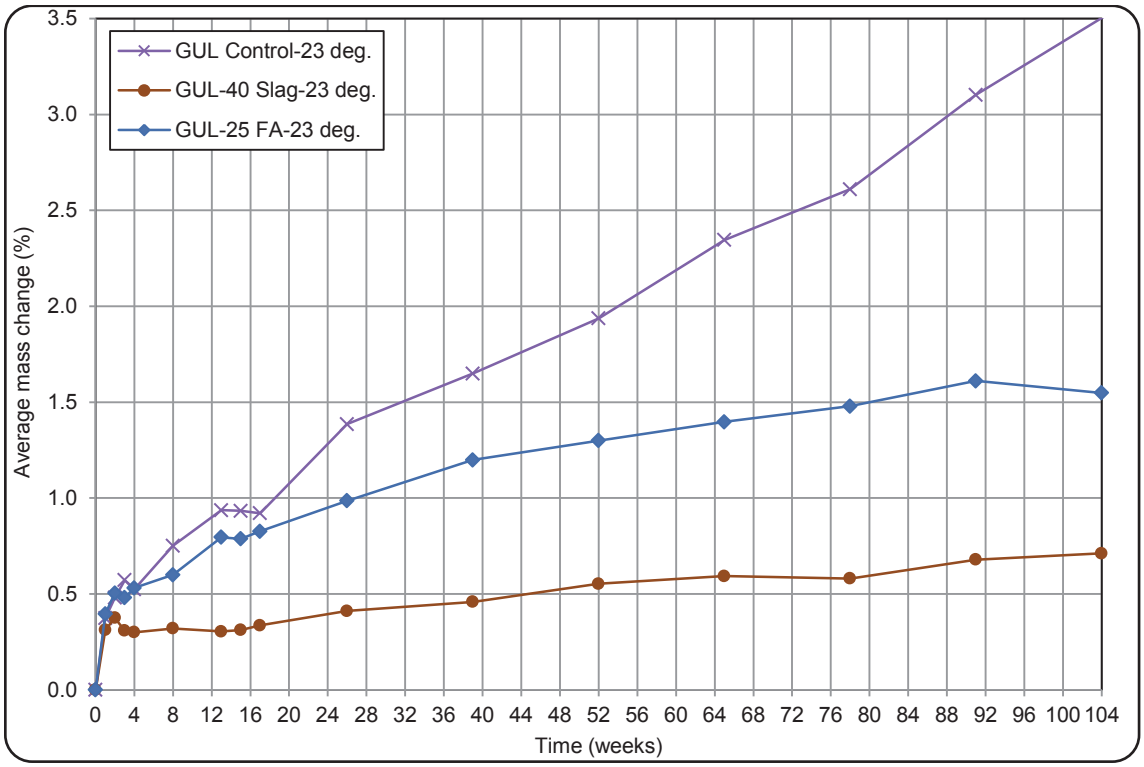

Fig. 5-17: Mass change of CSA A3004-C8-A mortar bars in a 2-year ESA – GUL cement

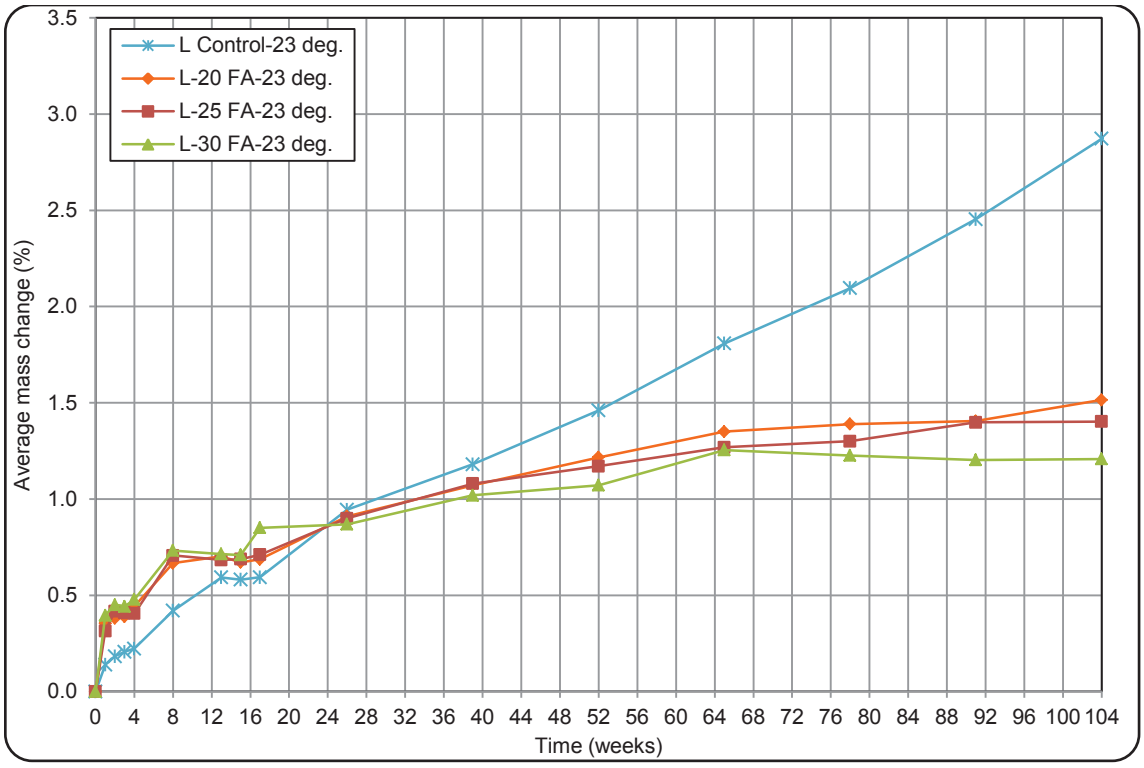

Fig. 5-18: Mass change of CSA A3004-C8-A mortar bars in a 2-year ESA – Fly ash blends

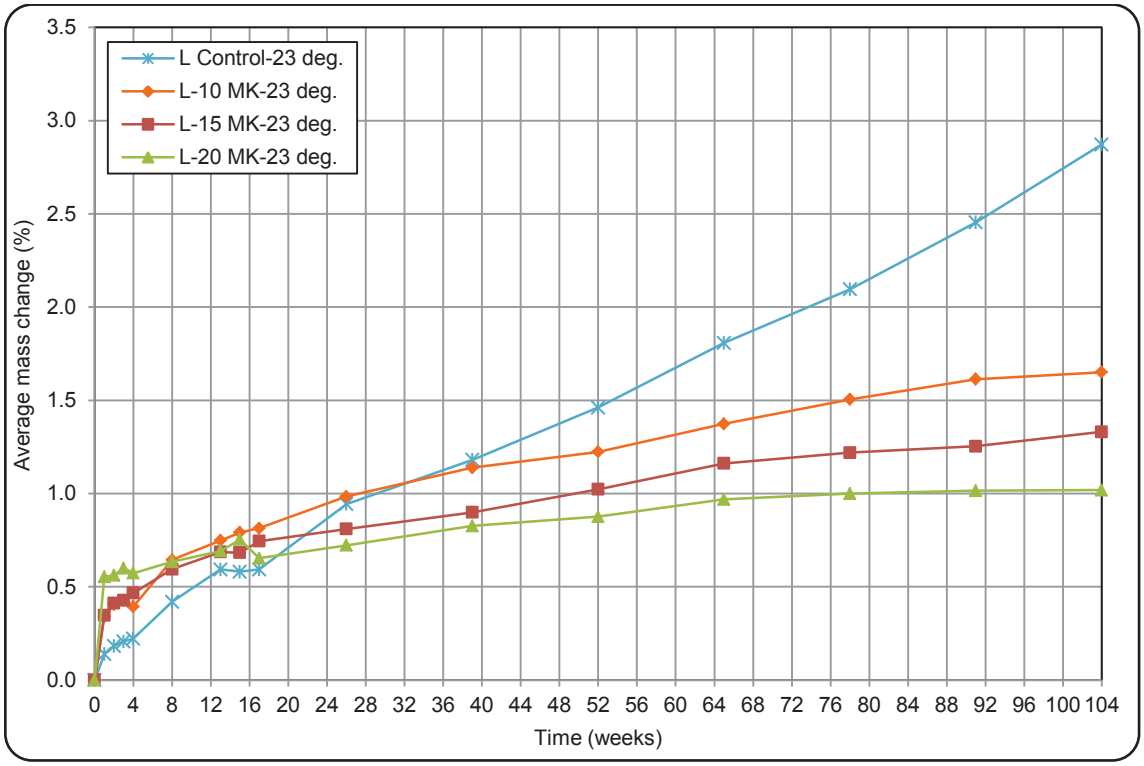

Fig. 5-19: Mass change of CSA A3004-C8-A mortar bars in a 2-year ESA – Metakaolin blends

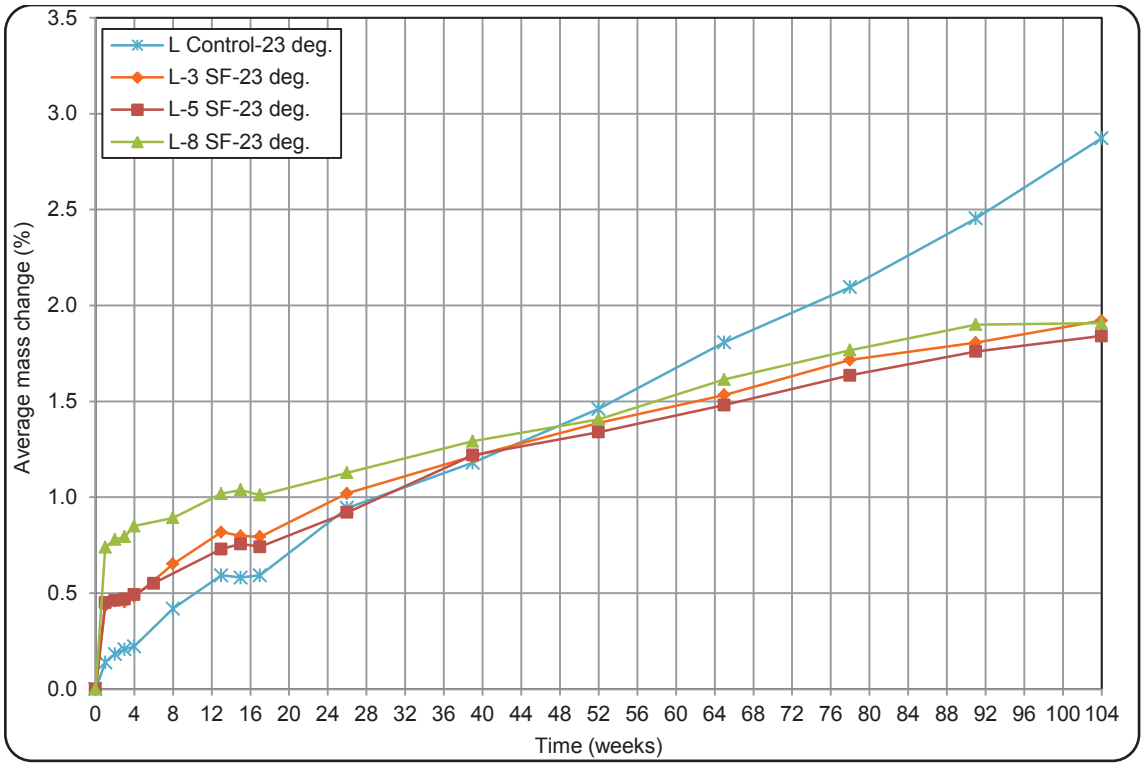

Fig. 5-20: Mass change of CSA A3004-C8-A mortar bars in a 2-year ESA – Silica fume blends

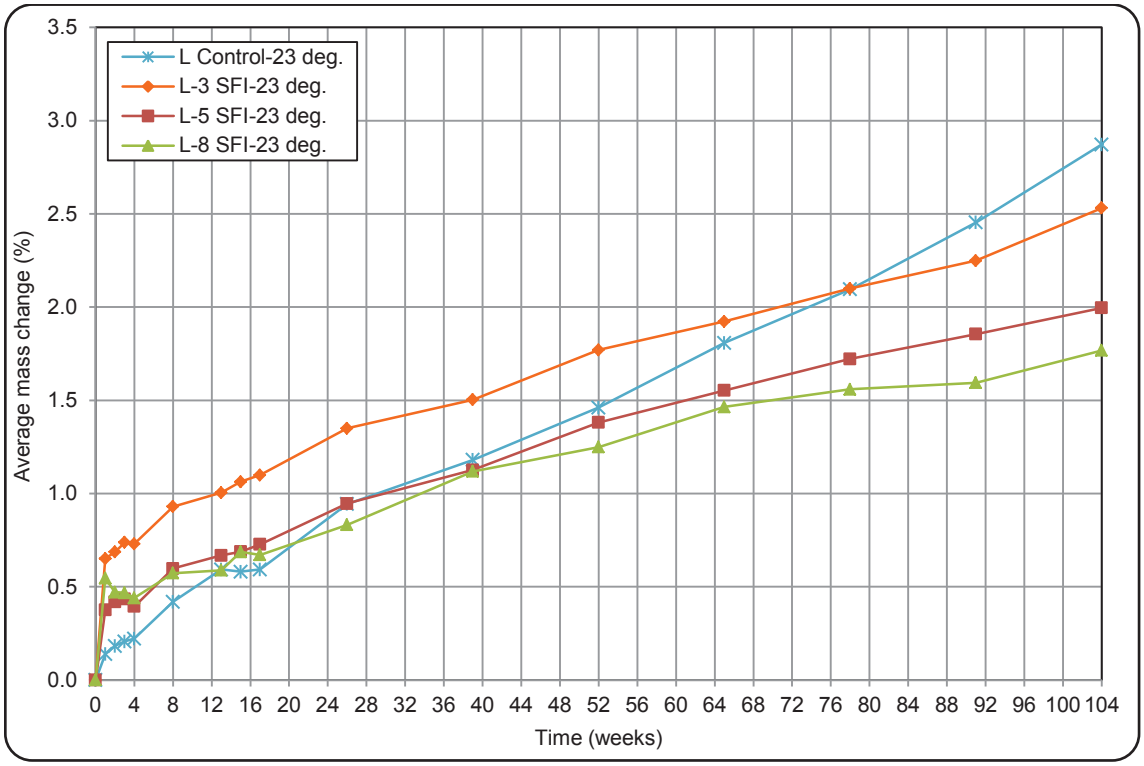

Fig. 5-21: Mass change of CSA A3004-C8-A mortar bars in a 2-year ESA – Silica fume I blends

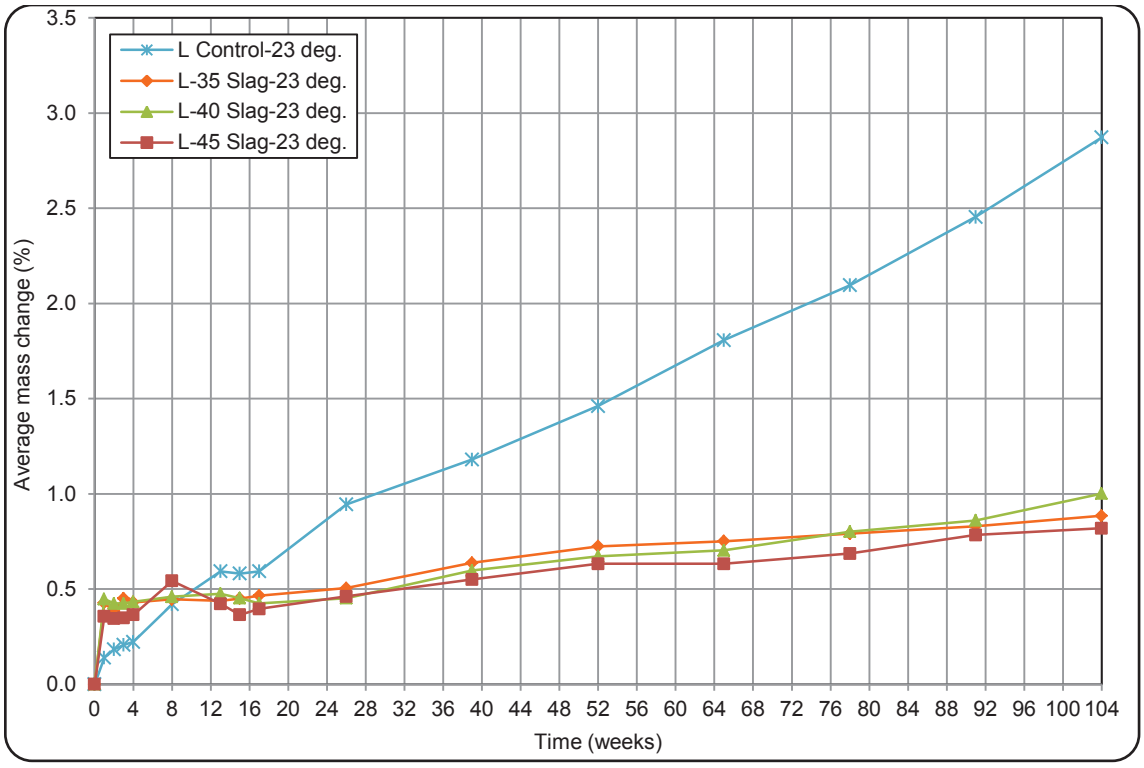

Fig. 5-22: Mass change of CSA A3004-C8-A mortar bars in a 2-year ESA – Slag blends

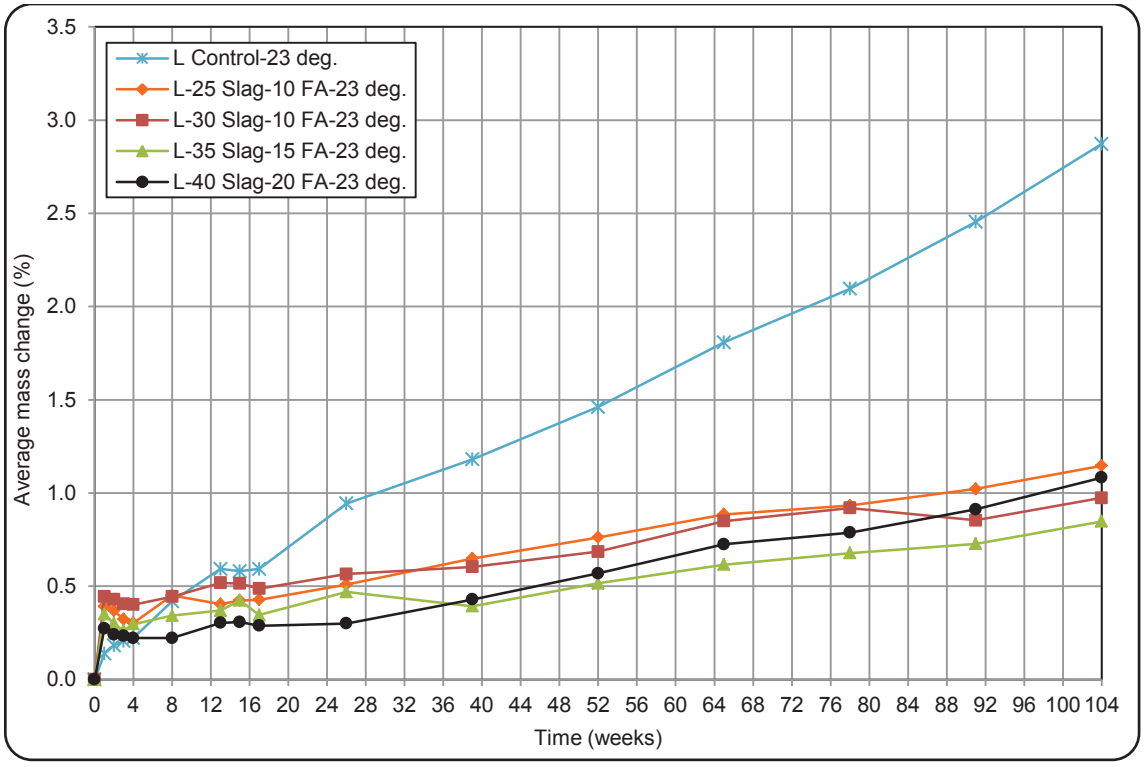

Fig. 5-23: Mass change of CSA A3004-C8-A mortar bars in a 2-year ESA – Slag & fly ash blends

5-5- Mass change of CSA A3004 mortar bars in thaumasite sulfate attack

The mass changes of mortar prisms during the two years of thaumasite sulfate attack are presented in Fig. 5-24 through Fig. 5-30. A number of curves are discontinued in the figures corresponding the failed samples during the study. During this study, unlike ettringite sulfate attack, mass loss was observed. Such observation was due to the severity of thaumasite sulfate attack compared to ettringite sulfate attack. According to Fig. 5-24, addition of slag and fly ash reduced the mass gain, therefore increased resistance in TSA. Similar to the mass loss results in ESA (Fig. 5-17), addition of 40% slag to GUL cement was more effective than addition of 25% fly ash. The fact that replacement of GUL with 40% slag was more effective than its replacement with 25% fly ash was also clearly seen in expansion results in TSA presented in Fig. 5-8

The mass changes of fly ash containing blends in TSA were quite similar to the control sample as seen in Fig. 5-25. However, the fly ash blends could last longer before failure. The expansion results of these samples were also the same, and the mortar bars prepared with the fly ash blends expanded with almost the same rate as the control sample for the first 6 months (Fig. 5-9). Accordingly, addition of the studied type F fly ash to PLC was not desirably helpful in improving the resistance against TSA. Metakaolin containing mortar samples also experienced considerable mass gains as seen in Fig. 5-26. “L-10 MK” and “L-15 MK” had mass gains followed by considerable mass loss due to losing the surfaces (surface deterioration of L-15 MK is presented in Fig. 4-12). These two samples failed during the two-year study. “L-20 MK” also had considerable mass gain, but its rate of mass gain decreased after 4 months and as it was

explained in the results section, it resisted very well against TSA and was categorized as high sulfate resistant blended PLC.

Fig. 5-27 presents the mass changes of PLC blends containing silica fume. "L-3 SF" showed mass loss after a year of TSA. This sample failed during the study unlike the other two blends of PLC and SF. It can be inferred from the figure that an increase in the silica fume content has decreased the mass gain. Similar performance considering length changes in TSA was previously discussed according to Fig. 5-11. According to Fig. 5-28, compared to the control sample, the rate of mass gain decreased when 5% or 8% SFI were added to PLC. A similar decrease in the expansion when SFI content was increased was discussed previously according to Fig. 5-12. The mass loss seen in Fig. 5-28 for "L-5 SFI" and "L-8 SFI" was due to TSA deterioration that caused surface removal (the deterioration is seen in Fig. 4-10).

From the viewpoint of the mass changes, the binary blends of PLC containing slag and the ternary ones containing a combination of slag and fly ash had a better resistance to TSA compared to the other PLC blends. According to the mass change results presented in Fig. 5-29 and Fig. 5-30, the mentioned blends had lower mass increases than the control sample. In both figures it is clearly seen that the increase in the amount of SCM has decreased the mass gain, which remarks increase in the resistance against TSA. The increase in the SCM content also has decreased the mass gain rate, which denotes slower rate of formation of gypsum, ettringite, and thaumasite in the mortar samples. Fig. 5-29 shows that the mass gain rate of "L-35 Slag" increased after a year of exposure, that was due to an increase in the pace of TSA in the mortar sample. Interestingly, this sample also showed an increase in its expansion rate at the same age

according to Fig. 5-13. Formation of cracks caused deeper ingress of sulfate ions and formation of larger amounts of thaumasite, ettringite, and gypsum. Such mass gain rate increase was also detected for "L-40 Slag" at a later age (21 months). "L-45 Slag" showed the lowest mass gain in Fig. 5-29 confirming its lowest expansion reported in Fig. 5-13. Considering Fig. 5-30 it is evident that "L-25 Slag-10 FA" and "L-30 Slag-10 FA" had higher mass gain rate than "L-35 Slag-15 FA" and "L-40 Slag-20 FA" due to lower SCM contents. "L-40 Slag-20 FA", which had the highest content of SCM showed the lowest mass increase in TSA implying its resistance. This sample had the lowest expansion in TSA as well (Fig. 5-14).

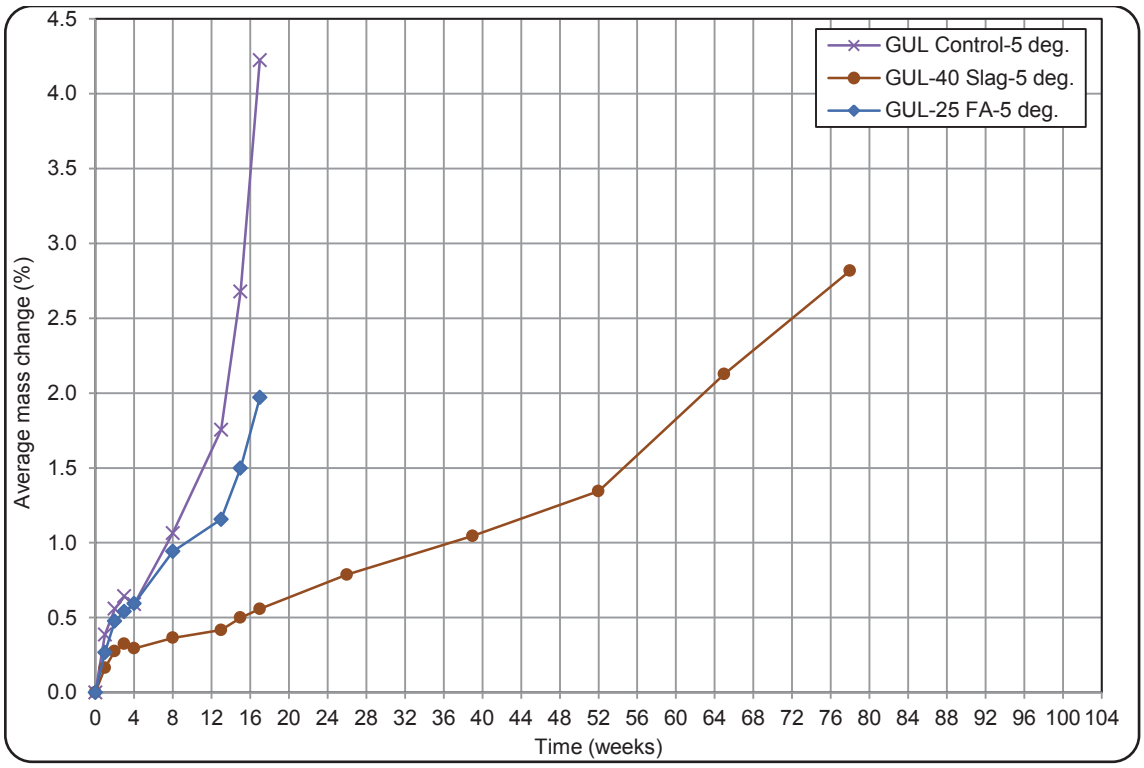

Fig. 5-24: Mass change of CSA A3004-C8-B mortar bars in a 2-year TSA – GUL cement

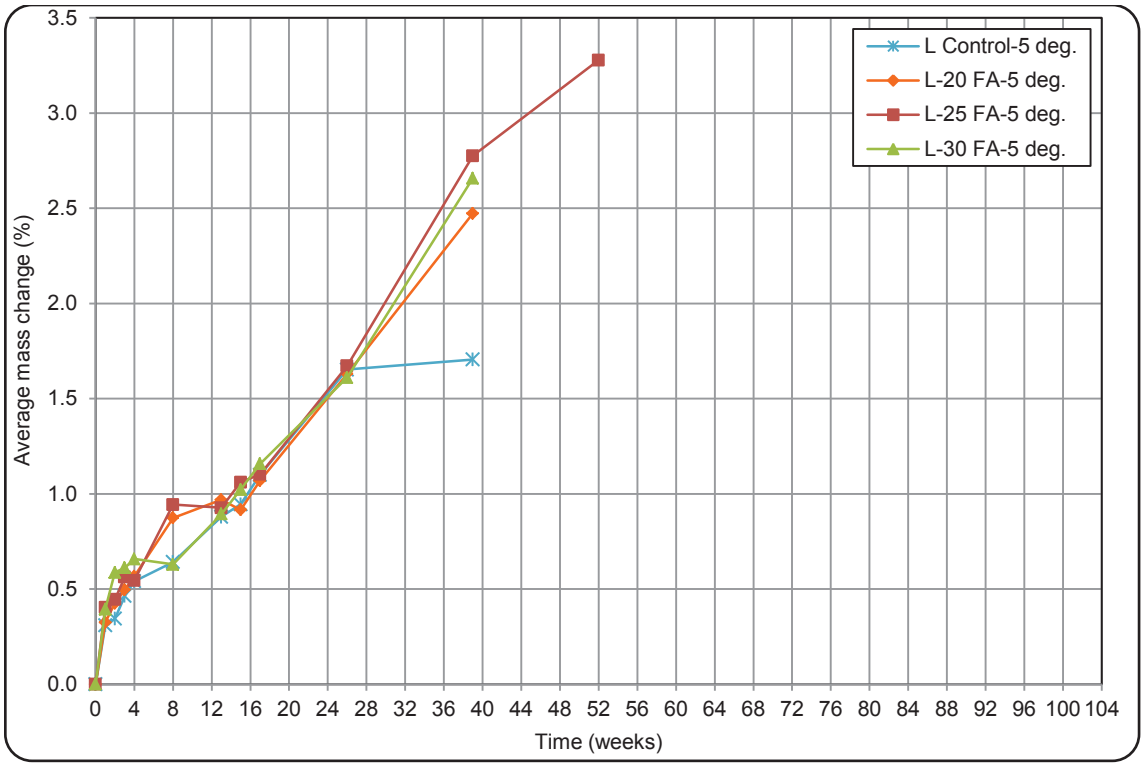

Fig. 5-25: Mass change of CSA A3004-C8-B mortar bars in a 2-year TSA – Fly ash blends

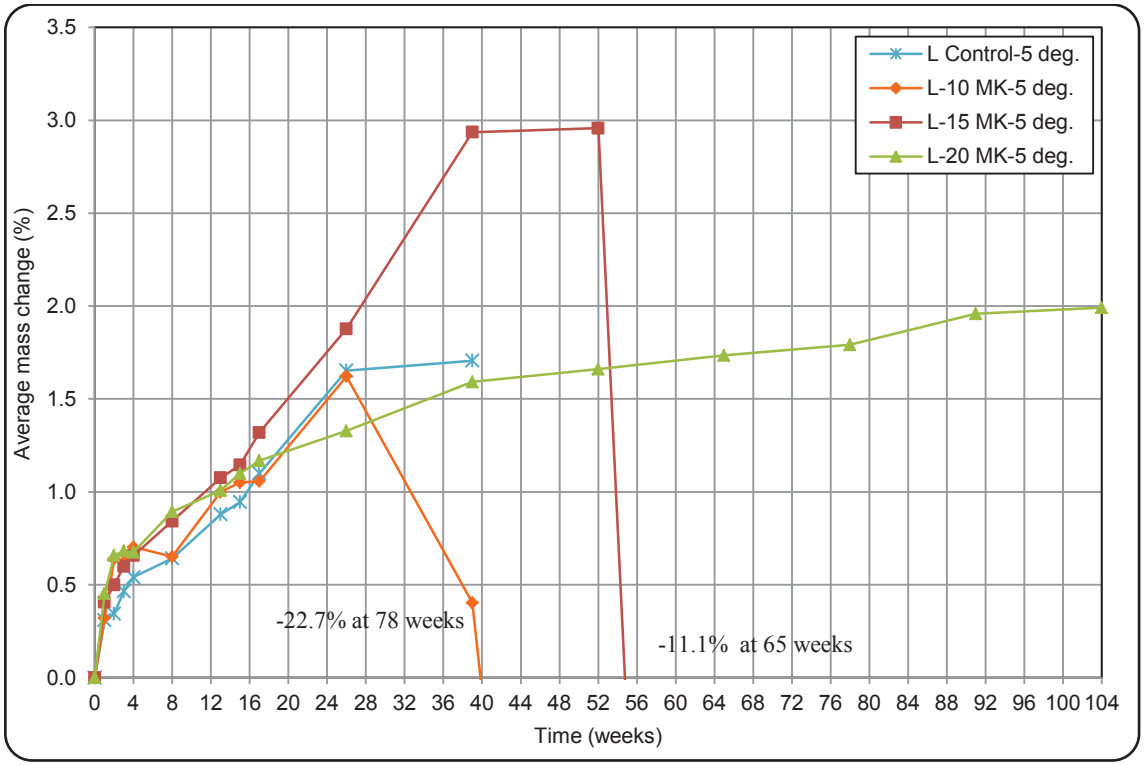

Fig. 5-26: Mass change of CSA A3004-C8-B mortar bars in a 2-year TSA – Metakaolin blends

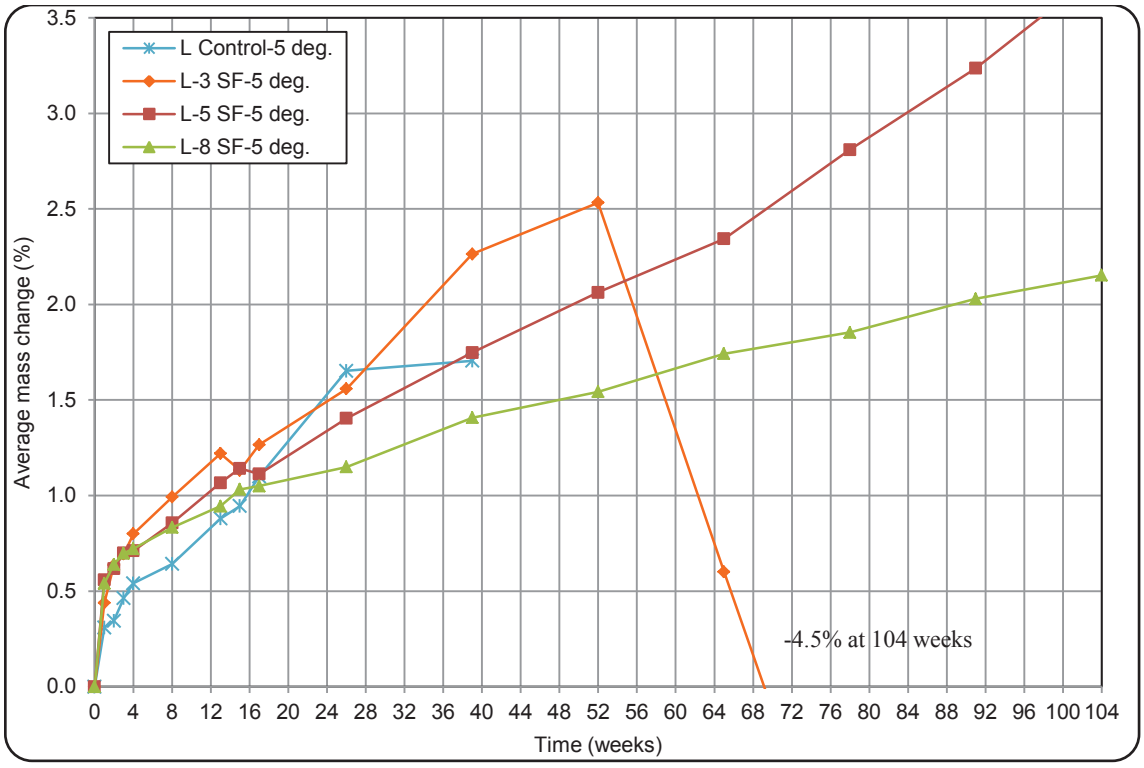

Fig. 5-27: Mass change of CSA A3004-C8-B mortar bars in a 2-year TSA – Silica fume blends

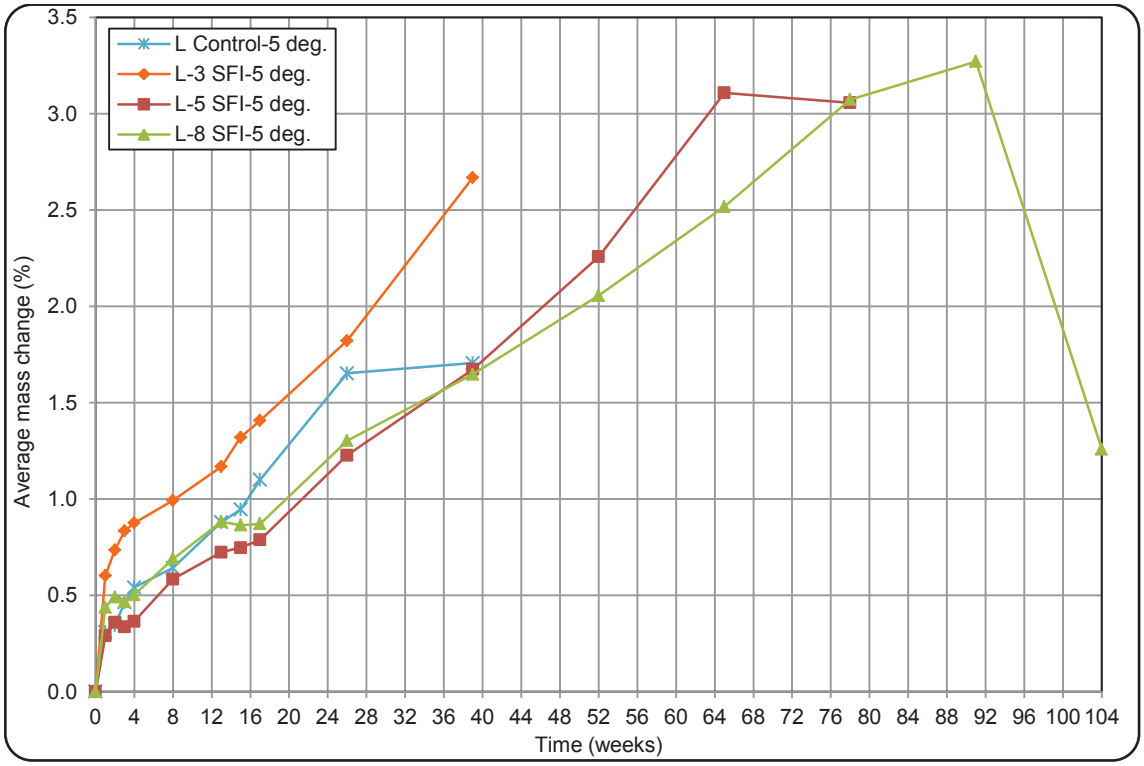

Fig. 5-28: Mass change of CSA A3004-C8-B mortar bars in a 2-year TSA – Silica fume I blends

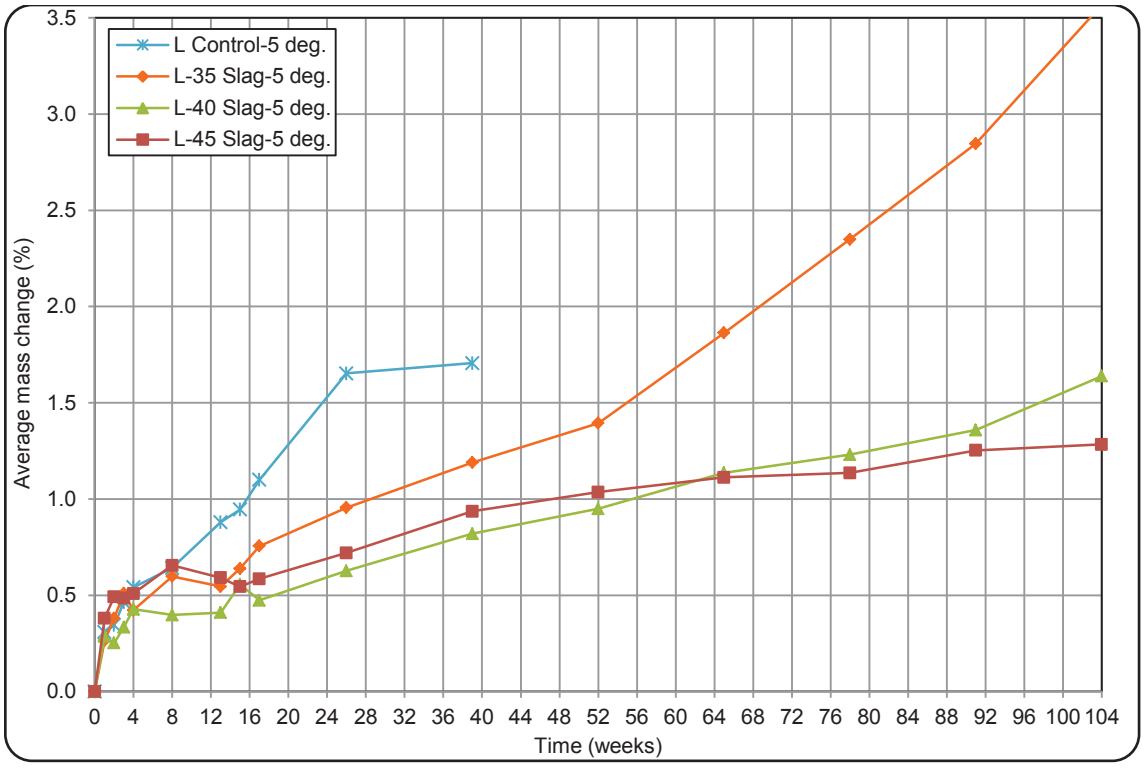

Fig. 5-29: Mass change of CSA A3004-C8-B mortar bars in a 2-year TSA – Slag blends

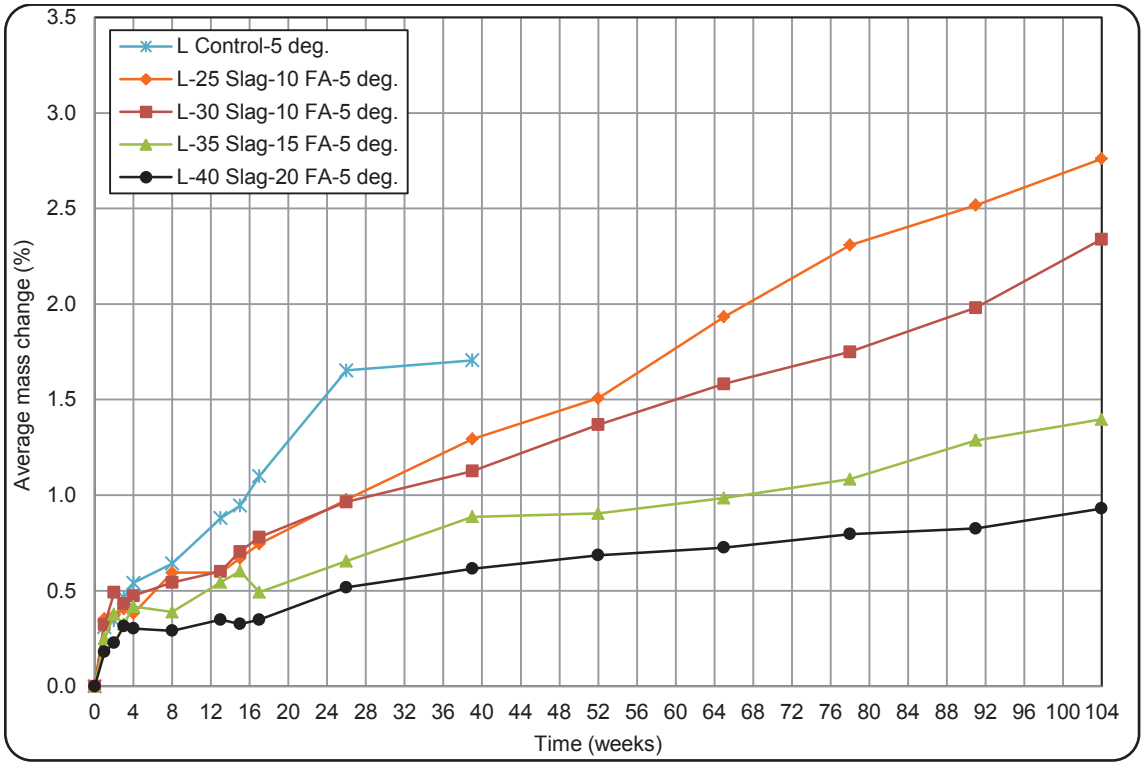

Fig. 5-30: Mass change of CSA A3004-C8-B mortar bars in a 2-year TSA – Slag & fly ash blends

5-6- Comparing average expansion and average mass changes of CSA A3004-C8 mortar bars

As previously stated, length change of mortar prisms was studied along with mass changes during the sulfate attack study. It was observed that the mortar samples initially gained mass in sulfate attack, which was followed by mass loss when deterioration developed in mortar samples. Such mass loss was observed in a number of samples in TSA during the two-year study, while in ESA only mass increase was found in mortar samples, as this deterioration process is less detrimental than TSA. According to the results, mortar bars had expansion during both processes of sulfate attack. The cause for both expansion and mass gain is gypsum, ettringite, and thaumasite formation inside the hydrated cement paste; accordingly, there can be a correlation between average expansion and average mass gain of the CSA A3004-C8 mortar bars. In Fig. 5-31, the average expansion of all blends is plotted over the average mass gain in ettringite sulfate attack according to the results at 3, 6, 12, 18, and 24 months. According to the figure, there is a good correlation between the expansion and mass gain of the mortar prisms in ettringite sulfate attack. The increase in length has been along with the increase in mass of the mortar samples. Fig. 5-32 demonstrates the relationship of expansion and mass changes of mortar prisms after 3, 6, 12, 18, and 24 months of thaumasite sulfate attack. In this figure, the negative mass changes (losses) are not presented. Generally, as seen in the figure, the increase in length has been associated with the increase in mass. However, there is not a good correlation as for ettringite sulfate attack between the results. The main reason for such observation lies in the nature of TSA that is more aggressive than ESA and in the considerable diversity in performance of the studied blends. In TSA, in

addition to expansion in the deterioration process, CSH removal occurs. During the course of two years thaumasite sulfate attack, many mortar samples started to deteriorate and lost the total integrity. This resulted in a discontinued mass gain, while the expansion was still occurring. Moreover, as explained and presented in the results section, there was a significant difference in the performance of mortar samples containing different types of SCMs. Such difference was even found in the samples with different contents of a single type of SCM. Accordingly, the correlation between the whole expansion and mass change data was not as good as the ettringite sulfate attack. However, when the correlation between the average expansion and the average mass change of the blends was studied separately, the results were completely different. In general, very good correlation was found between the average expansion and the average mass change results, as seen in Fig. 5-33 through Fig. 5-42. When studied separately, each blend showed even better correlation between expansion and mass change results according to Table 5-2.

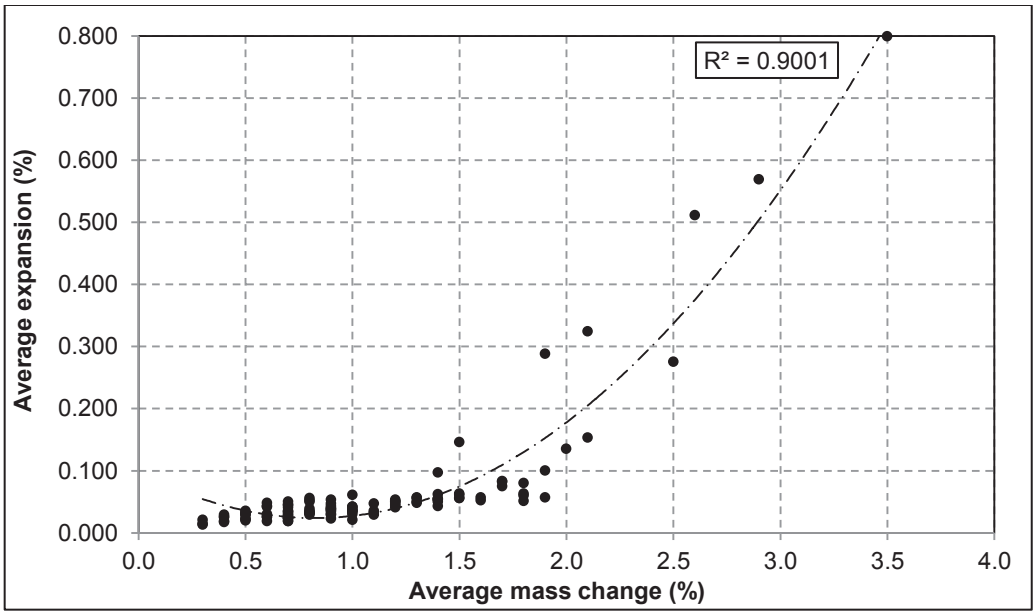

Fig. 5-31: Average expansions versus average mass changes of CSA A3004-C8 mortar bars at ages of 3, 6, 12, 18, and 24 months in ettringite sulfate attack (23°C)

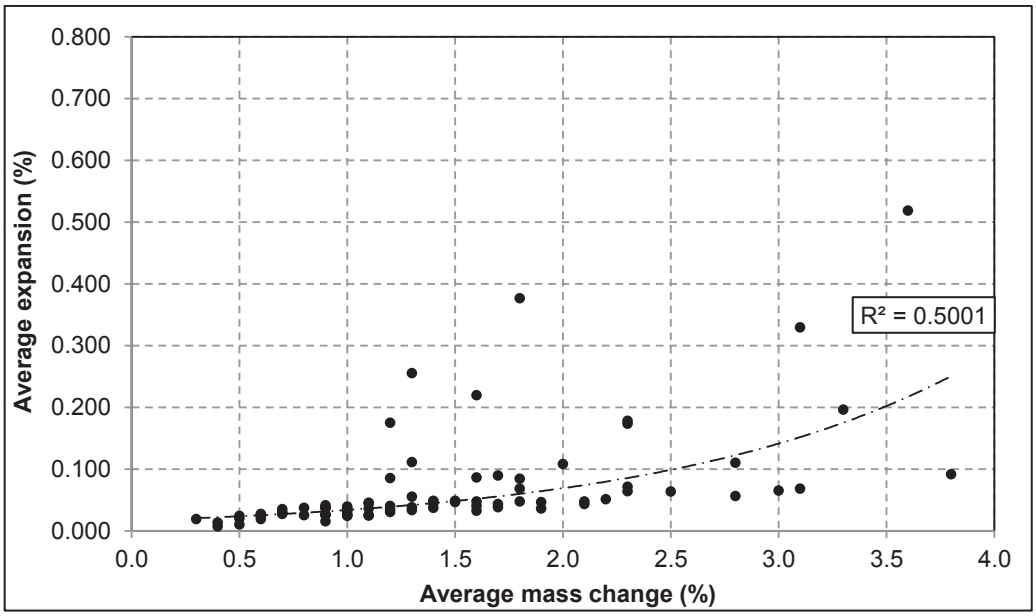

Fig. 5-32: Average expansions versus average mass changes of CSA A3004-C8 mortar bars at ages of 3, 6, 12, 18, and 24 months in thaumasite sulfate attack (5°C)

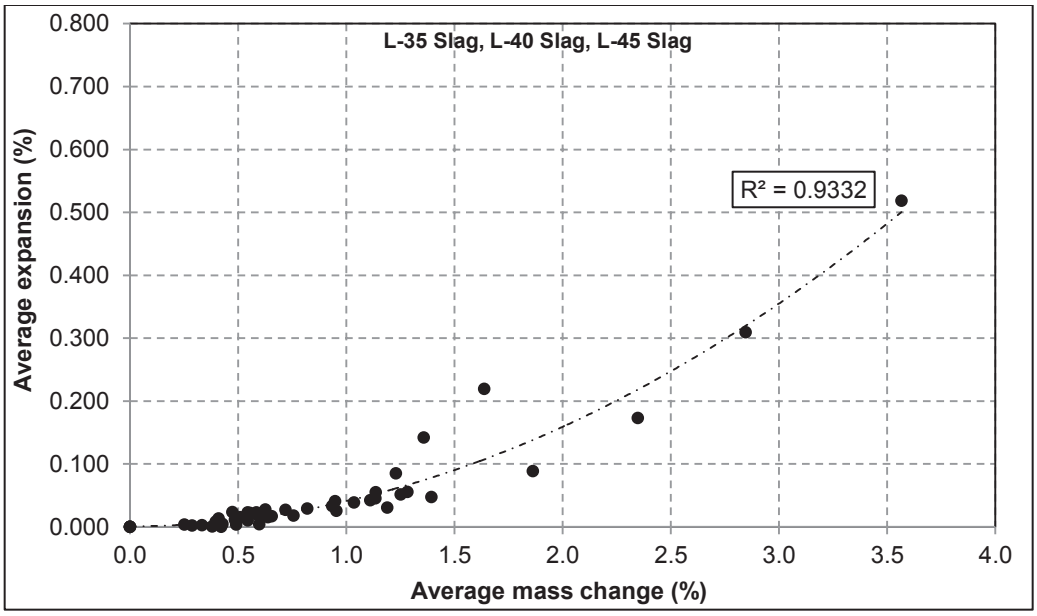

Fig. 5-33: Average expansions versus average mass changes of CSA A3004-C8 mortar bars containing slag during 24 months of thaumasite sulfate attack (5°C)

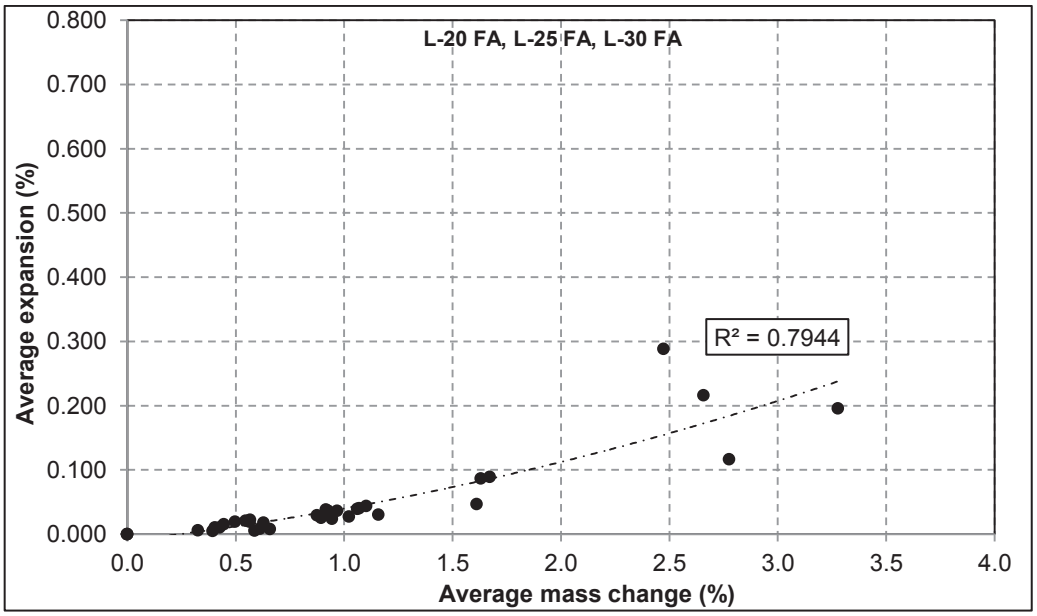

Fig. 5-34: Average expansions versus average mass changes of CSA A3004-C8 mortar bars containing fly ash during 24 months of thaumasite sulfate attack (5°C)

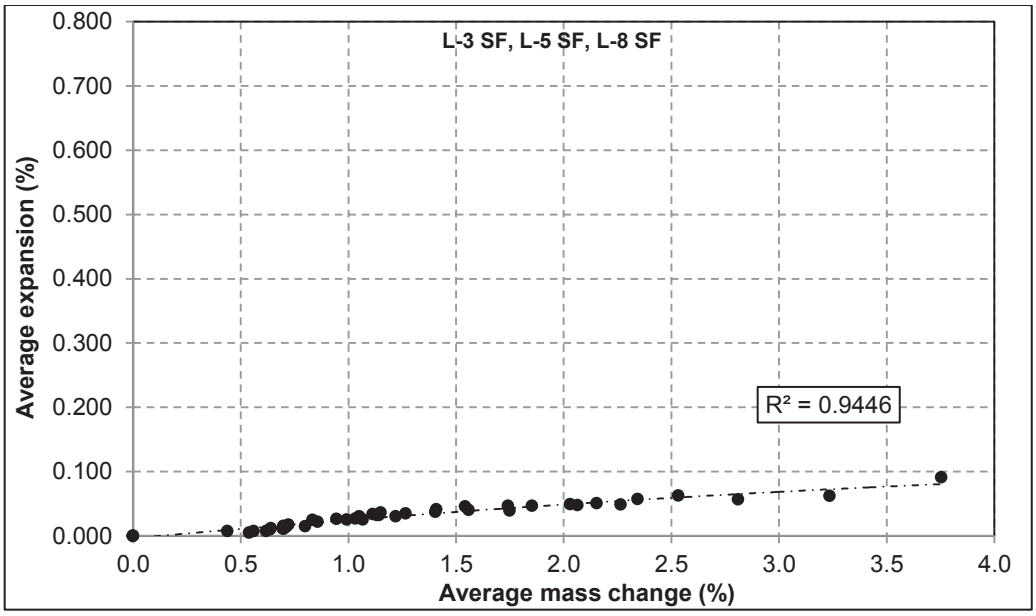

Fig. 5-35: Average expansions versus average mass changes of CSA A3004-C8 mortar bars containing silica fume during 24 months of thaumasite sulfate attack (5°C)

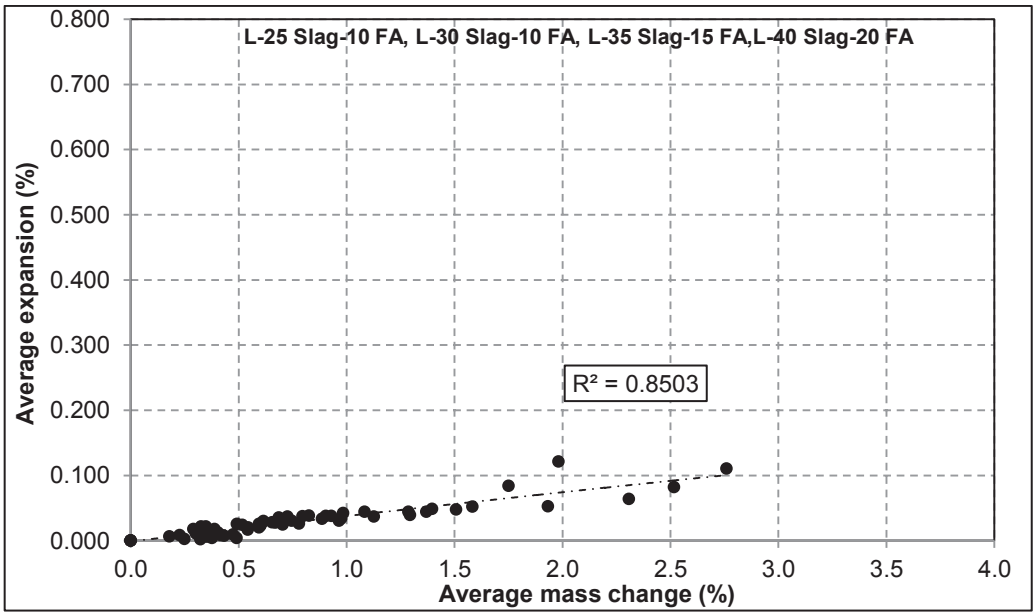

Fig. 5-36: Average expansions versus average mass changes of CSA A3004-C8 mortar bars containing ternary blends of PLC during 24 months of thaumasite sulfate attack (5°C)

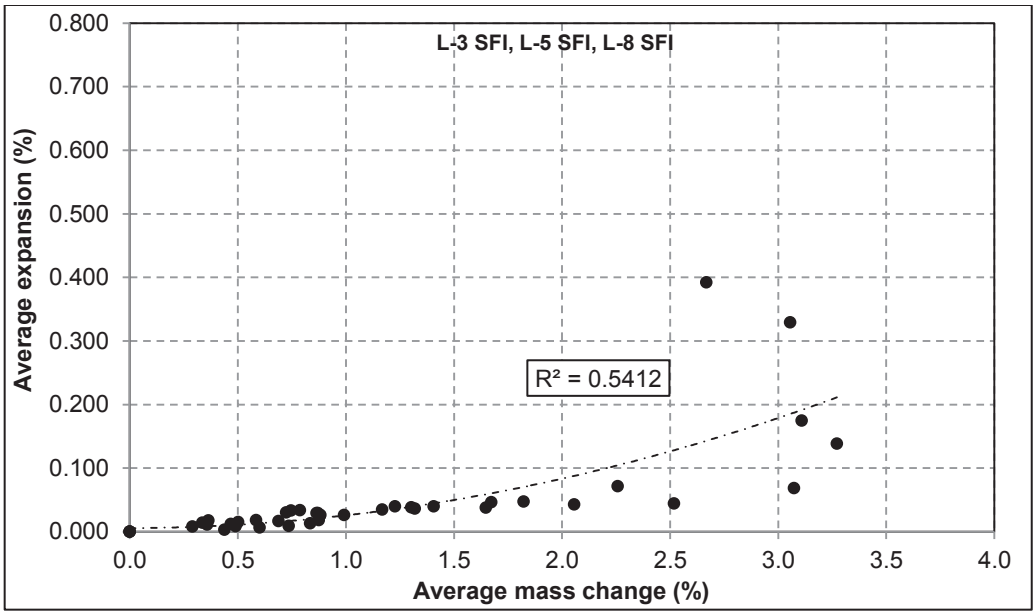

Fig. 5-37: Average expansions versus average mass changes of CSA A3004-C8 mortar bars containing silica fume I during 24 months of thaumasite sulfate attack (5°C)

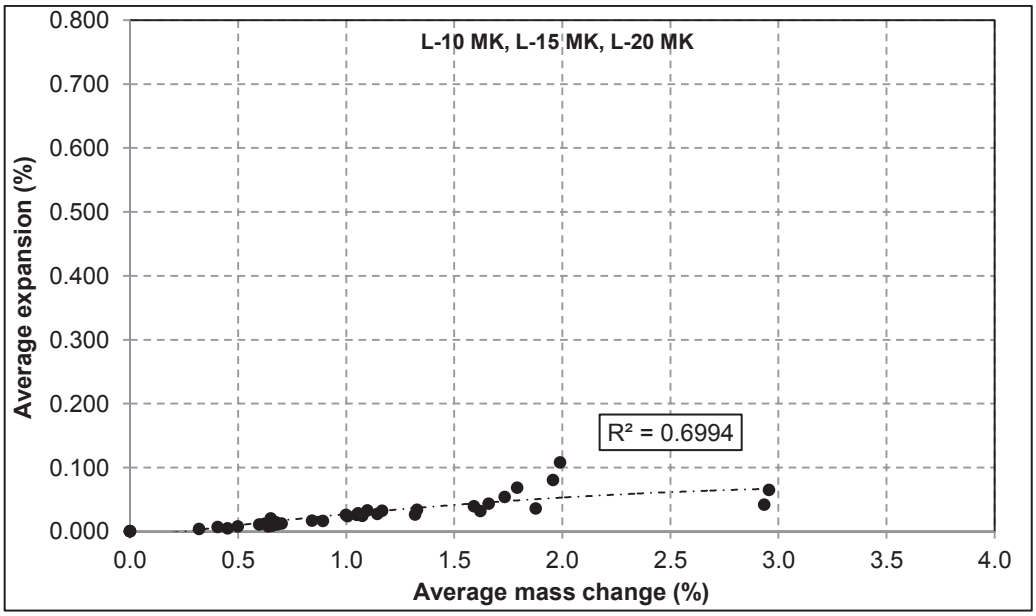

Fig. 5-38: Average expansions versus average mass changes of CSA A3004-C8 mortar bars containing metakaolin during 24 months of thaumasite sulfate attack (5°C)

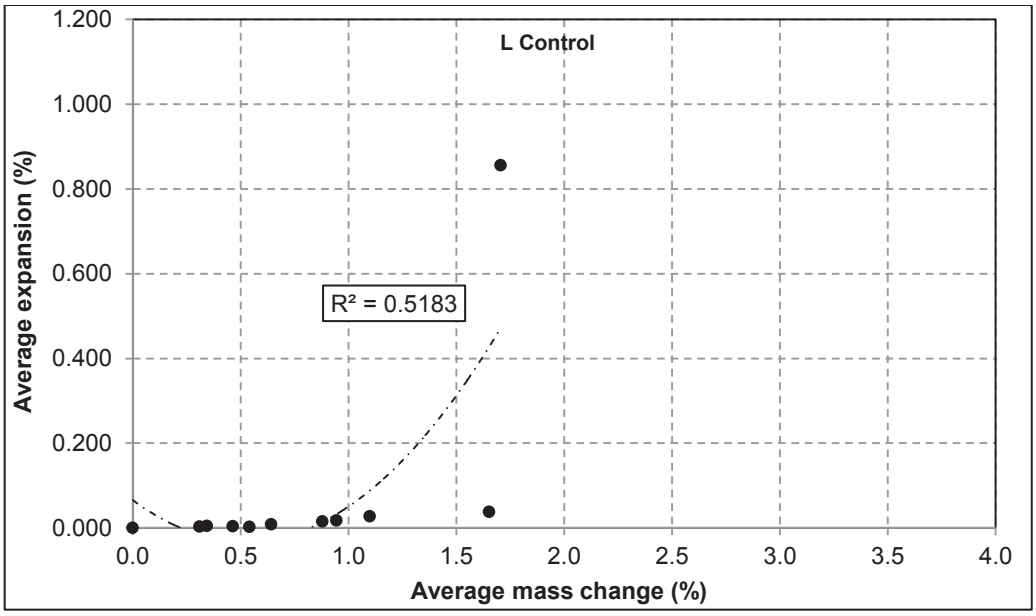

Fig. 5-39: Average expansions versus average mass changes of CSA A3004-C8 mortar bars containing "L" cement during 24 months of thaumasite sulfate attack (5°C)

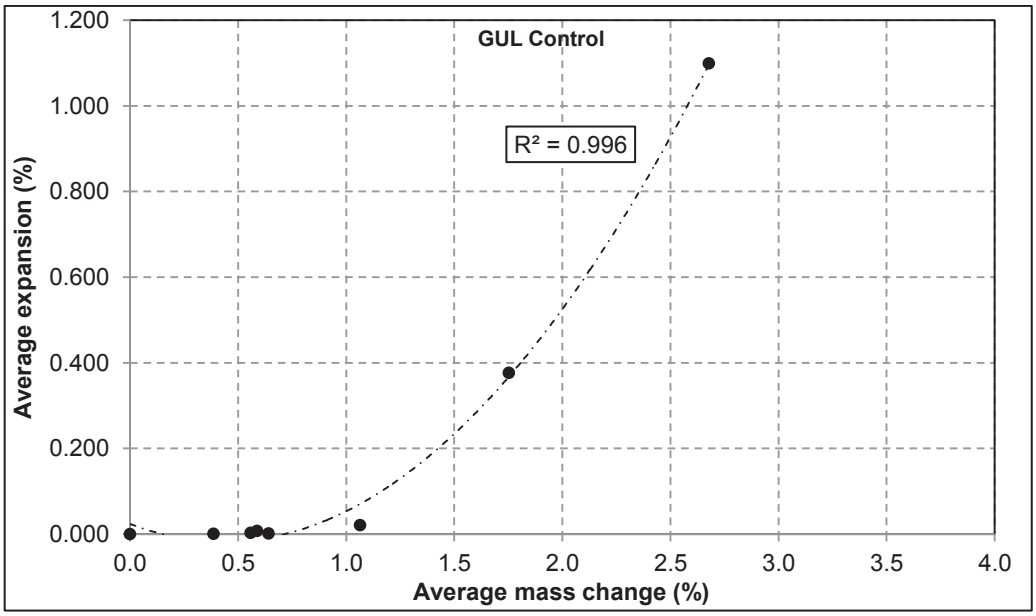

Fig. 5-40: Average expansions versus average mass changes of CSA A3004-C8 mortar bars containing "GUL" cement during 24 months of thaumasite sulfate attack (5°C)

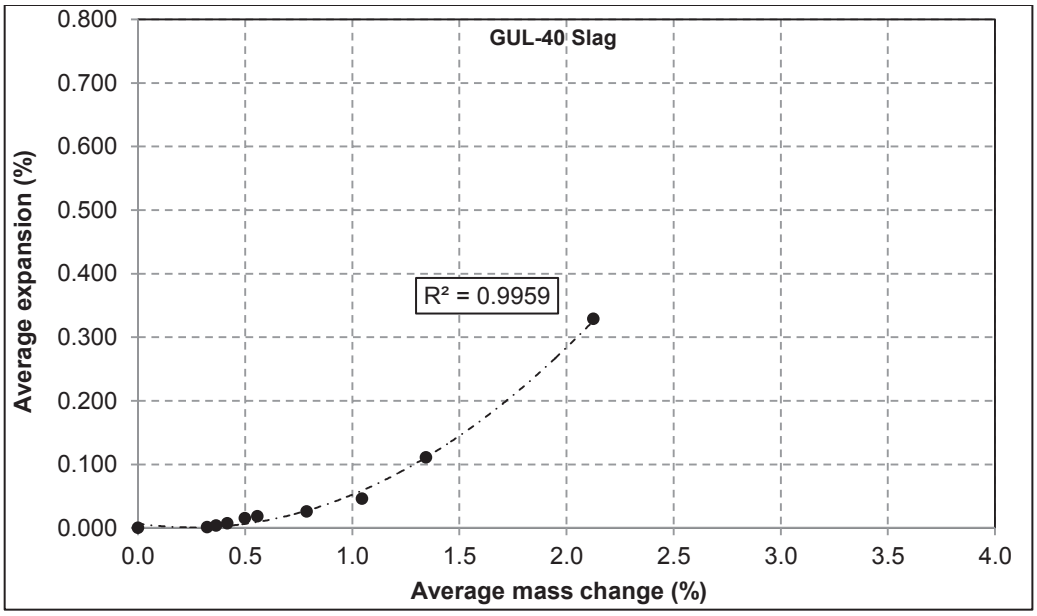

Fig. 5-41: Average expansions versus average mass changes of CSA A3004-C8 mortar bars containing "GUL-40 Slag" during 24 months of thaumasite sulfate attack (5°C)

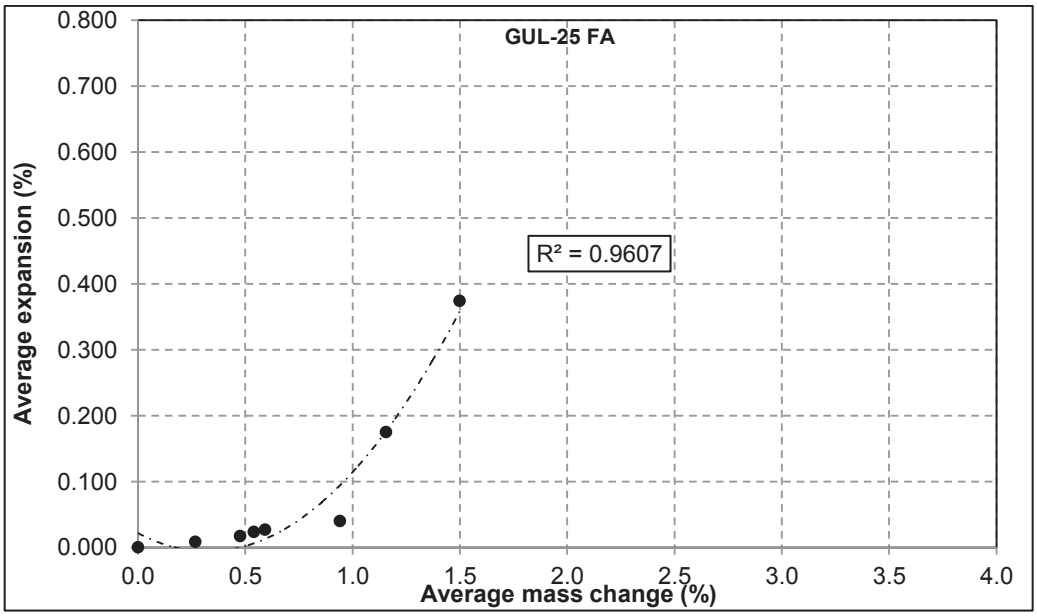

Fig. 5-42: Average expansions versus average mass changes of CSA A3004-C8 mortar bars containing "GUL-25 FA" during 24 months of thaumasite sulfate attack (5°C)

Table 5-2: Correlation between the average expansion and the average mass change of each studied blend of PLC in TSA

	Sample	Correlation coefficient (R^2)		Sample	Correlation coefficient (R^2)
1	L-35 Slag	**1.00**	13	L-40 Slag-20 FA	**0.93**
2	L-40 Slag	**0.96**	14	L-3 SFI	**0.93**
3	L-45 Slag	**0.93**	15	L-5 SFI	**0.83**
4	L-20 FA	**0.98**	16	L-8 SFI	**0.82**
5	L-25 FA	**0.96**	17	L-10 MK	**0.86**
6	L-30 FA	**0.98**	18	L-15 MK	**0.92**
7	L-3 SF	**0.96**	19	L-20 MK	**0.91**
8	L-5 SF	**0.95**	20	L Control	**0.52**
9	L-8 SF	**0.95**	21	GUL Control	**1.00**
10	L-25 Slag-10 FA	**0.95**	22	GUL-40 Slag	**1.00**
11	L-30 Slag-10 FA	**0.94**	23	GUL-25 FA	**0.96**
12	L-35 Slag-15 FA	**0.92**			

5-7- Combination of ultrasonic pulse velocity and compressive strength tests

The ultrasonic pulse velocity and compressive strength tests on cubic mortar samples immersed in sodium sulfate solution at 5°C were studied independently in the results section. During the tests, it was observed that the changes in UPV and compressive strength were correlated in someway. In Fig. 5-43 to Fig. 5-50 the results are combined and compared. The coordination between the two tests' results is clearly perceived.

In Fig. 5-43 the combined compressive strength and UPV results on "GUL Control" mortar samples is presented. Both results have similar trends. Initially, the compressive strength and pulse velocity of the mortar samples in TSA increased up to a certain age followed by a considerable reduction. The reduction in compressive strength was observed at 26 weeks, and the decrease in UPV was detected at 13 weeks. Similar

results were observed for the other control sample as seen in Fig. 5-44. The reduction in compressive strength and UPV were found at 26 weeks.

Unlike the control sample, “L-40 Slag” did not show reduction in strength or UPV in one year of thaumasite sulfate attack. According to Fig. 5-45, both tests’ results were in agreement and showed continuous increase. Such statement can also be made for “L-40 Slag-20 FA” and “L-20 MK” considering Fig. 5-46 and Fig. 5-47, respectively. “L-25 FA” also presented corresponding trends for strength and UPV changes up to 39 weeks in Fig. 5-48. After this age the UPV showed reduction, but such trend was not found in strength. Such observation was also made for the “GUL Control” sample in which UPV decrease was occurred sooner than strength decrease. This can be due to the fact that pulse velocity is more sensitive to formation of cracks than compressive strength as perpendicular cracks are less effective on compressive strength than the parallel ones.

The combined compressive strength and UPV results of “L-8 SF” and “L-8 SFI” are shown in Fig. 5-49 and Fig. 5-50, respectively. Compressive strength and UPV in both blends had similar trends. The increase in the results was followed by a reduction at the age of 52 weeks.

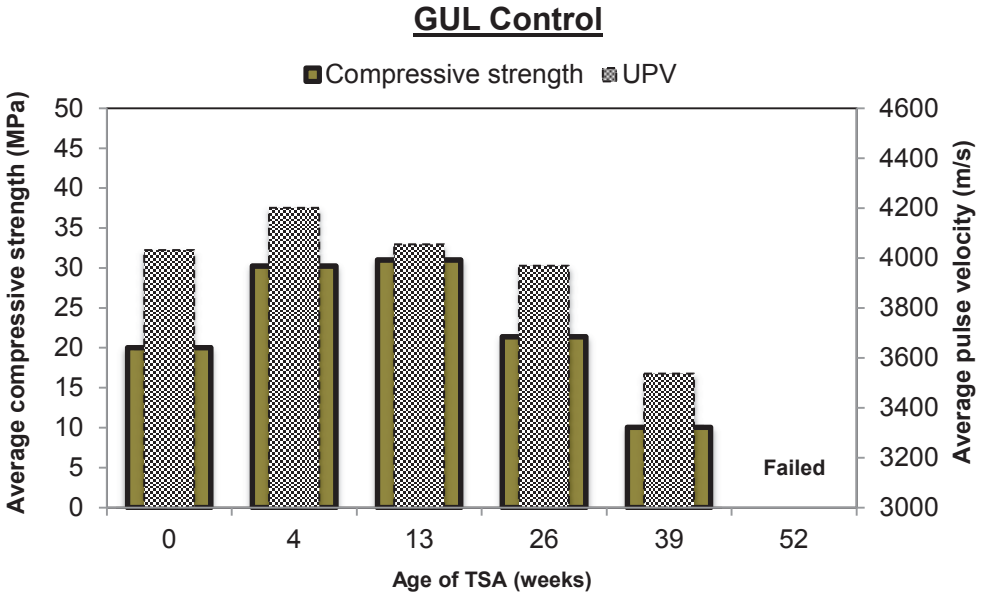

Fig. 5-43: Compressive strength and UPV of "GUL Control" mortar cubes in TSA

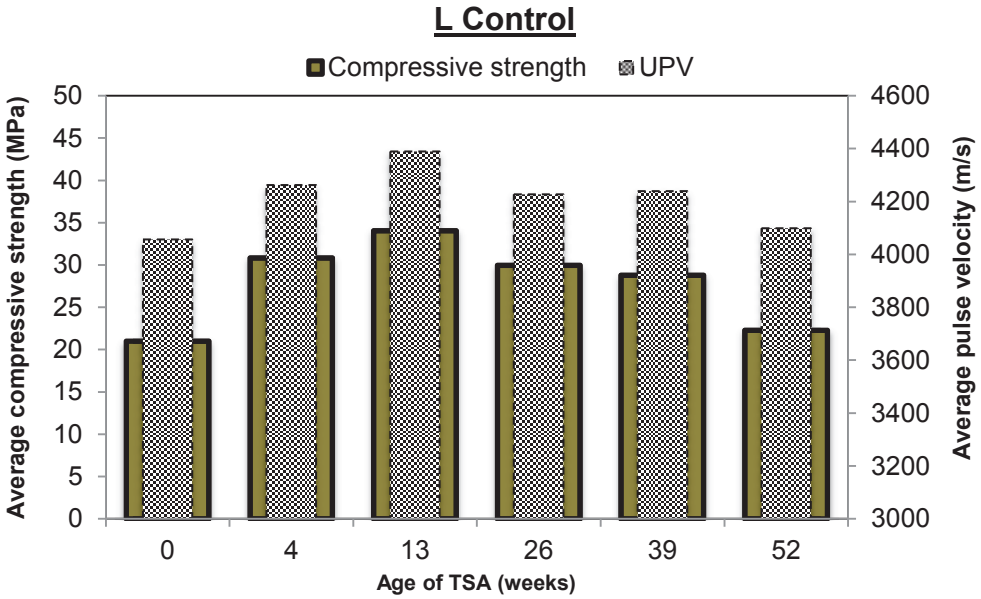

Fig. 5-44: Compressive strength and UPV of "L Control" mortar cubes in TSA

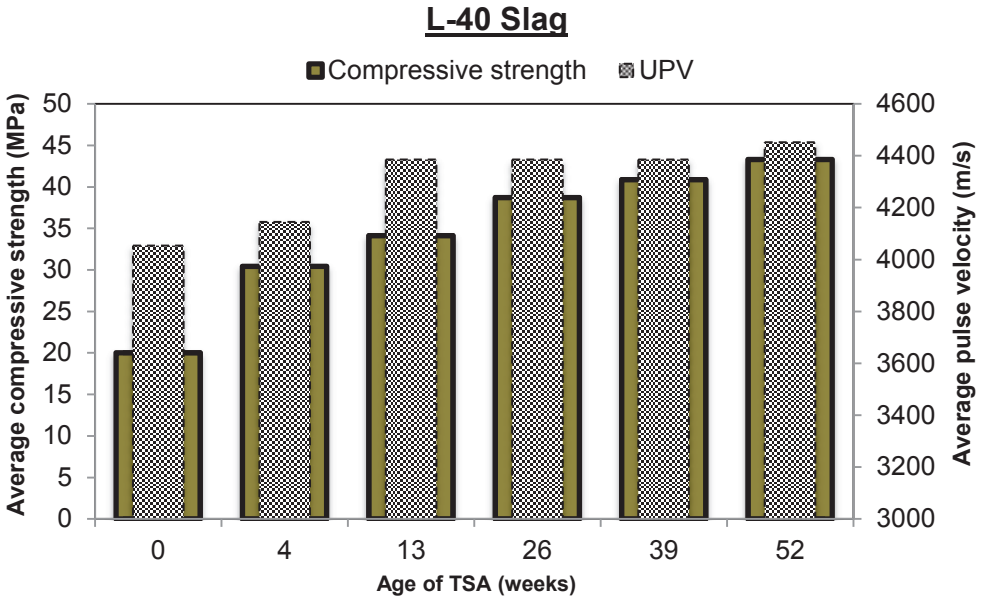

Fig. 5-45: Compressive strength and UPV of "L-40 Slag" mortar cubes in TSA

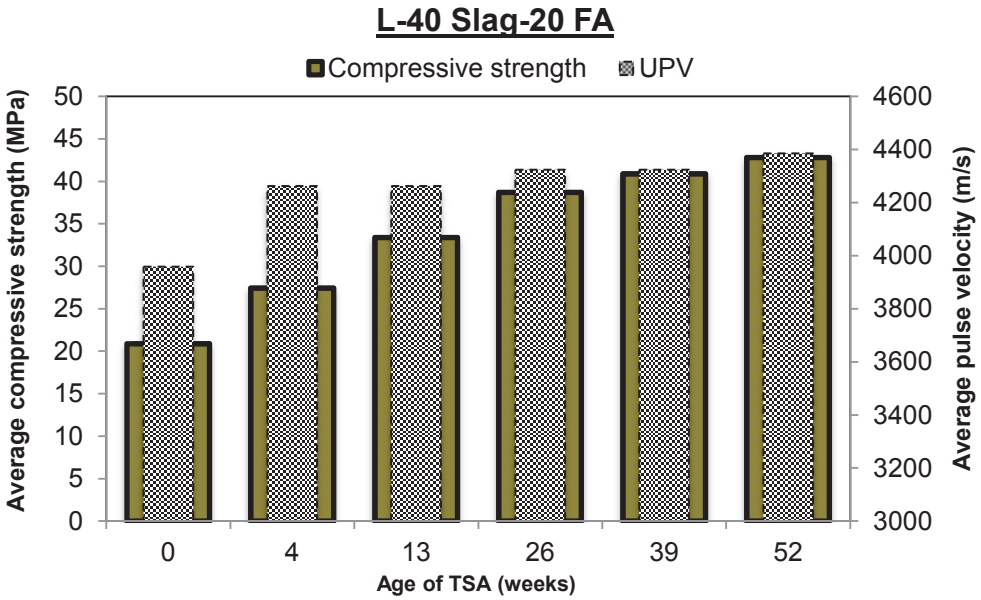

Fig. 5-46: Compressive strength and UPV of "L-40 Slag-20 FA" mortar cubes in TSA

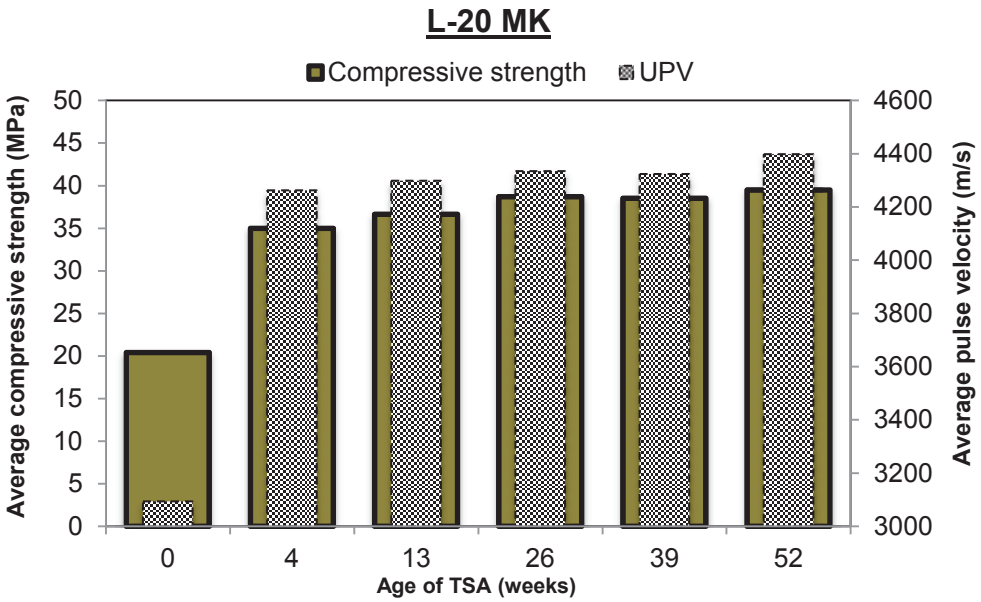

Fig. 5-47: Compressive strength and UPV of "L-20 MK" mortar cubes in TSA

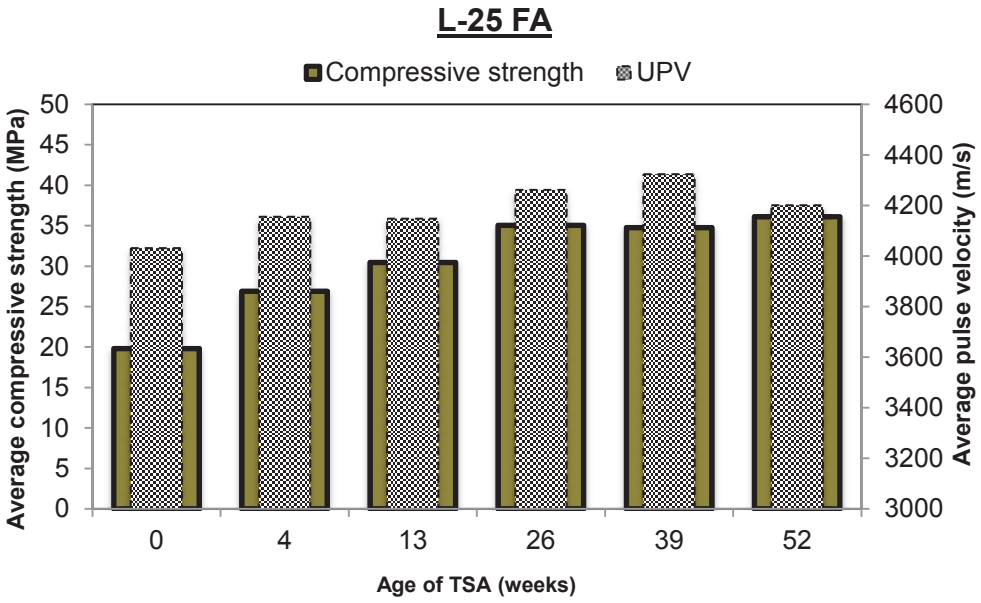

Fig. 5-48: Compressive strength and UPV of "L-25 FA" mortar cubes in TSA

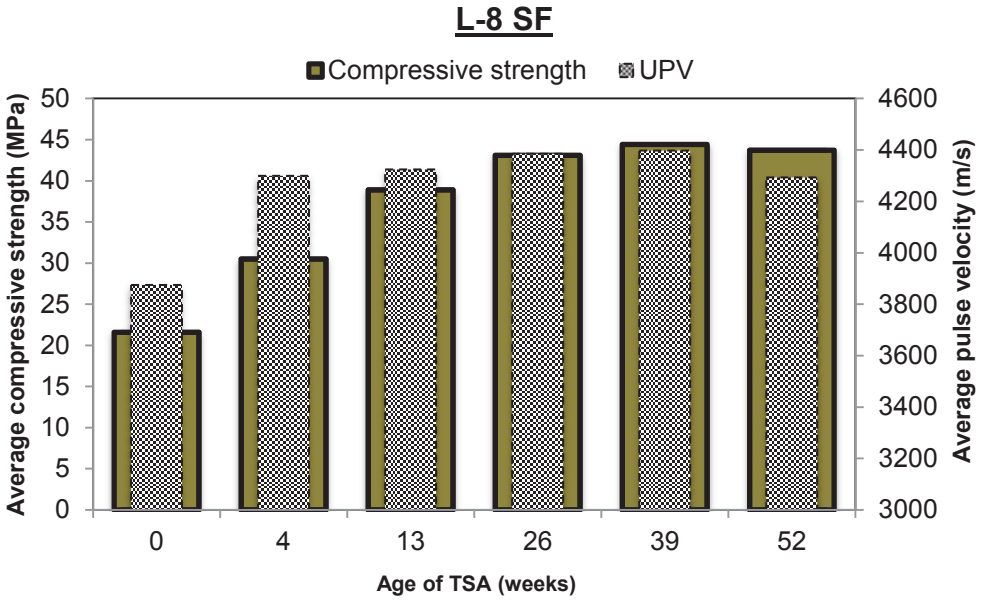

Fig. 5-49: Compressive strength and UPV of "L-8 SF" mortar cubes in TSA

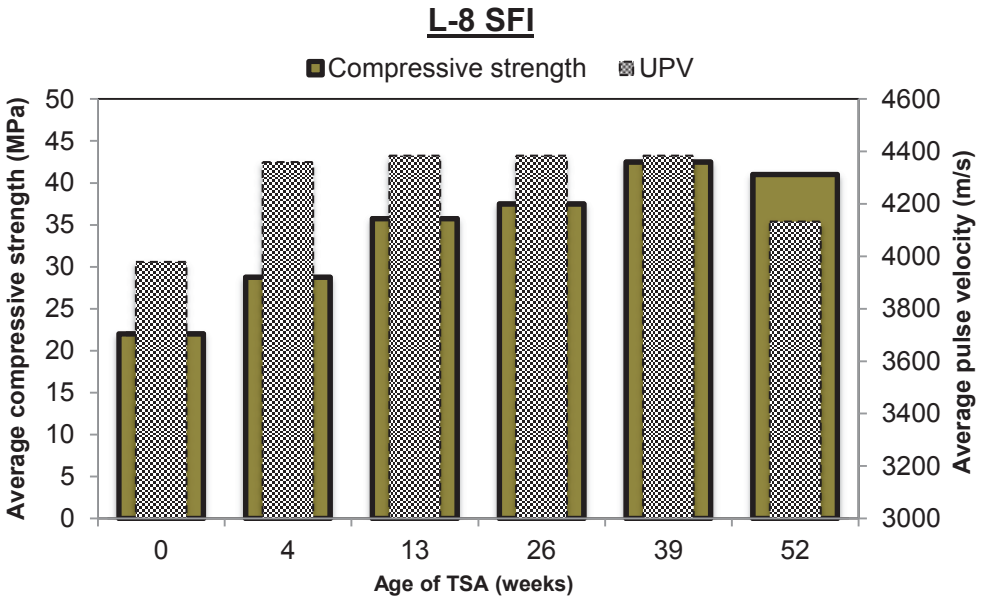

Fig. 5-50: Compressive strength and UPV of "L-8 SFI" mortar cubes in TSA

The correlation between the average compressive strength and the average UPV of mortar cubes is studied in Fig. 5-51. All data obtained from the two tests are outlined in the graph. It was found that there is a good exponential correlation between

compressive strength (f'_c) and ultrasonic pulse velocity (v). Such an exponential correlation was also reported by Trtnik et al. (2009) through a research on predicting compressive strength by the UPV technique for concrete prepared with plain Portland cement as well as slag cement. Demirboğa et al. (2004) also reported exponential correlation between the compressive strength and the UPV of concrete samples containing slag, fly ash, and a mixture of both when cured in limewater. Neither of these studies investigated samples subjected to deterioration. Generally, increase in compressive strength is accompanied with increase in UPV that is also understood from the figure. The mentioned correlation verifies the simultaneous study of compressive strength and UPV on mortars during the sulfate attack study, and it approves the UPV test as a nondestructive test for investigating the extent of the deterioration on mortar samples instead of the compressive strength test.

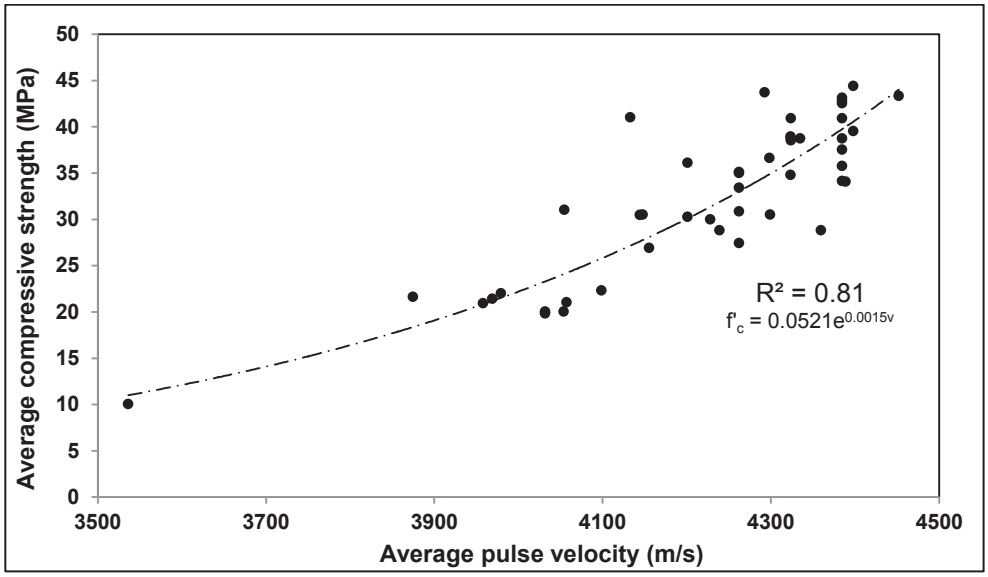

Fig. 5-51: Relationship between the average compressive strength and the average UPV of mortar cubes during a year of TSA

5-8- Complementing DSC with XRD results

As it was discussed in the results section, the DSC technique used in order to characterize ettringite, gypsum, and thaumasite in the deteriorated mortar samples did not give distinct peaks corresponding to the mentioned compounds for all samples. Therefore, the XRD technique was employed in a supplementary study. In the following section, the DSC and XRD results for these samples are discussed and it is explained that how the XRD test results has supplemented the DSC study.

- GUL-25 FA

Considering the fact that mortar samples prepared with this PLC blend weakly resisted against thaumasite sulfate attack, it was expected that thaumasite would be characterized in samples taken from this sample for DSC. As seen in Fig. 4-22, for "GUL Control" and "GUL-40 Slag" distinct peaks corresponding the dehydration of thaumasite were found, but for "GUL-25 FA", such a peak was not detected. However, in the XRD test result presented in Fig. 4-30, strong distinct peaks for thaumasite were found confirming occurrence of thaumasite formation.

- L-35 Slag

In Fig. 4-24, when the thermograph of "L-35 Slag" is compared with the other blends containing 40% and 45% slag, it seems that its thermal peaks are shifted a few degrees higher. For this sample, the thaumasite dehydration peak was detected at 119°C, which was a few degrees higher than the two other blends. The uncertainty about formation of thaumasite was solved when XRD test was performed. The XRD analysis on "L-35 Slag" and "L-45 Slag" confirmed that similar to "L-45 Slag", "L-35 Slag" had peaks related to thaumasite dehydration. The XRD analysis verified that the thermal peak at 119°C for "L-35 Slag" was related to thaumasite.

- L-3 SFI and L-8 SFI

By considering the DSC thermographs for SFI containing samples in Fig. 4-28, it can be inferred that no thermal peak related to ettringite and CSH was observed for "L-3 SFI". Besides, for "L-8 SFI" the thaumasite dehydration peak was found at 118°C, a few degrees higher than the average degree corresponding to the other samples. The XRD analysis presented in Fig. 4-33 complemented the DSC results. According to this analysis, ettringite was detected in XRD peaks related to "L-3 SFI" sample. In addition, for "L-8 SFI", thaumasite peaks were distinctly detected. Accordingly, combination of both tests results in Fig. 4-28 and Fig. 4-33, confirmed formation of ettringite and thaumasite in both studied mortar samples.

- L-15 MK and L-20 MK

The DSC results of "L-15 MK" and "L-20 MK" shown in Fig. 4-29 were not satisfying. "L-15 MK" did not have a peak related to thaumasite, and only a shoulder at 114°C was detected for thaumasite in this sample. The "L-20 MK" DSC result was quite confusing as in the temperature range of ettringite, CSH, and thaumasite dehydration, only one thermal peak at 109°C was found. Accordingly, it was impossible to assuredly characterize ettringite and thaumasite in deteriorated mortar samples of "L-20 MK". The XRD analysis depicted in Fig. 4-34 was helpful in describing the results. According to this figure, thaumasite is found in the "L-15 MK" deteriorated mortar sample. In addition, gypsum that was not found in this sample's DSC thermograph is found in small quantities according to the XRD analysis. Considering the XRD analysis in Fig. 4-34, the samples obtained from the surface of "L-20 MK" mortar bars, also contained ettringite, thaumasite, and gypsum.

According to the discussion on comparing both DSC and XRD analysis, it can be declared that the XRD analysis has successfully supplemented the DSC analysis.

6- Conclusions and contributions

In this chapter, the conclusions of the present research are summarized. As well, the contributions of the research conclusions are included.

6-1- Conclusions

1. All mortar bars prepared with the studied blends of Portland-limestone cement showed continuous expansion when immersed in sodium sulfate solution at 23°C (ESA) and 5°C (TSA) due to the formation of gypsum, ettringite, and thaumasite.

2. Considering the expansion and mass change results as well as the visual inspections, the thaumasite sulfate attack (5°C) was found significantly more aggressive than ettringite sulfate attack (23°C).

3. After a two-year sulfate attack study, performed in accordance with CSA A3004-C8, mortars prepared with the blends of Portland-limestone cement and the studied SCMs (slag, Type F fly ash, metakaolin, silica fume, and silica fume I) and exposed to ESA, showed notably reduced expansions as well as expansion rates, compared to the control samples. In the exposure to TSA, addition of any of all the studied SCMs also improved the performance of PLC blends from the viewpoint of expansion and expansion rate, but not all of them prevented failure. Additionally, for each type of the SCMs, in general, an increase in the content of SCM in the PLC blend resulted in an improved resistance against ettringite sulfate attack as well as thaumasite sulfate attack (less expansion in mortar bars). Therefore, the studied supplementary cementing materials improved the

resistance of mortar samples to ESA and TSA when added to Portland-limestone cement as well as when increased in their amount of addition.

4. The mortar bars containing the ternary blends (PLC + slag + fly ash) had an improved performance from the viewpoint of expansion in ESA and TSA compared to the binary blends of PLC-slag and PLC-fly ash. This was attributed to the synergy of slag and fly ash. Beside its contribution in pozzolanic reactions and its effect on reduction of carbonates and calcium hydroxide of the hydrated PLC blend, fly ash improves the workability of mortar and therefore improves its compaction. On the other hand, slag contributes in cementing reactions at early ages, pozzolanic reactions at later ages, and reduction of carbonates and calcium hydroxide inside the hydrated cement paste. Consequently, in addition to their pozzolanic advantages, slag and fly ash complement each other's characteristics. The other advantage of the ternary blends compared to the binary ones was the higher SCM content of "L-35 Slag-15 FA" and "L-40 Slag-20 FA".

5. The ternary blend of PLC containing 40% slag and 20% fly ash (L-40 Slag-20 FA) that had the highest content of SCM amongst the studied blends, showed the lowest expansion and the lowest expansion rate among all blends after two years of ettringite sulfate attack as well as thaumasite sulfate attack, denoting its considerable resistance to sulfate attack compared to the other blends.

6. Considering the CSA A3001-10 mandate for sulfate resistant blended PLC and the expansion of the mortars in ESA and TSA, “L-45 Slag”, “L-5 SF”, “L-8 SF”, “L-25 Slag-10 FA”, “L-35 Slag-15 FA”, “L-40 Slag-20 FA”, “L-8 SFI”, and “L-20 MK” can be considered as high sulfate resistant blended Portland-limestone cements. CSA A3001-10 mandates the addition of at least 25% type F fly ash, or 40% slag, or 15% metakaolin in order to achieve moderate sulfate resistant or high sulfate resistant blended PLC. The present study showed that the mentioned minimum amounts were not sufficient for achieving a high sulfate resistant blended PLC. It should be mentioned that when the SCM content was increased over the standard suggestions for slag and metakaolin, the required resistance was reached, but none of the blends containing type F fly ash expanded below the standard limits. In fact, although the Type F fly ash effectively improved the PLC resistance against ESA, its blends in TSA failed during their immersion in sodium sulfate solution at 5°C.

7. In ettringite sulfate attack, the rate of the expansion of the control samples was considerably higher than for the samples of the PLC blends with SCMs. Furthermore, with the progress of this attack, the expansion rate increased. Such an increase first occurred for the control samples, and it was considerably higher than the other samples. Among the PLC blends, during the two-year ESA, “L-10 MK”, “L-3 SF”, “L-3 SFI”, and “L-5 SFI” showed increases in the expansion rate. The other blends that had higher SCM contents did not show such increases and expanded with an almost constant rate during the two-year study. Among the

PLC blends, the binary ones containing slag and the ternary ones containing slag and fly ash had the lowest expansion rates. In thaumasite sulfate attack, the control samples also had higher expansion rates compared to the PLC blends. During the TSA exposure, an abrupt increase in the expansion rate occurred before the failure. Among the studied blends, during the two-year TSA, "L-8 SF", "L-45 Slag", "L-35 Slag-15 FA", and "L-40 Slag-20 FA" did not show an increased expansion rate; accordingly, they demonstrated the best resistance against TSA. This was also evidenced by the expansion and mass change results.

8. The visual inspection of the mortar bars in ESA showed noticeable cracks and distortion in the control samples while the binary and ternary PLC blends were totally sound. The visual shape of the samples was in agreement with the CSA A3004-C8-A expansion results. According to the visual observations, while deterioration due to ESA and TSA caused formation of cracks and curving, this was followed by disintegration and removal of the CSH matrix only for the case of TSA. Deteriorated mortar samples at the ultimate stage of failure in TSA were transformed to a non-cohesive mass. This kind of deterioration has also been reported in previous research (Higgins and Crammond-2003, Ramezanianpour and Hooton-2013b). The aggressiveness of TSA compared to ESA can be better understood when taking to the account that the "GUL Control" failed after only 17 weeks of TSA while this sample did not fail in the two-year ESA study (104 weeks). The visual condition of the mortar samples in TSA was in agreement with the expansion results. Overall, the visual assessments confirmed the improvement

in the resistance of PLC mortars in ESA and TSA when supplementary cementing materials were used.

9. After two years of thaumasite sulfate attack, amongst the sulfate resistant blends, "L-45 Slag", "L-8 SF", "L-35 Slag-15 FA", and "L-40 Slag-20 FA" had noticeably lower expansions. These samples also had the lowest mass increases. This emphasizes the effectiveness of slag and silica fume on mitigating the deterioration due to TSA.

10. In ettringite sulfate attack after two years, the control samples had the highest mass increase. This implies that addition of SCMs reduced formation of gypsum and ettringite, and is in agreement with the expansion results. Moreover, the rate of mass gain for all samples in ESA decreased when SCMs were added to PLC, implying the improvement in their resistance. Furthermore, in general, the increase in the amount of each SCM decreased the mass increase. The binary blends containing slag and the ternary ones containing a combination of slag and fly ash had the lowest mass gain. In thaumasite sulfate attack reduction in the mass gain with the increase in the content of SCM was also observed. In this attack to the binary blends of PLC and slag and the ternary blends of PLC, slag, and fly ash, when the SCM content was increased the mass gain rate and the total mass gain decreased, which showed a clear improvement in the resistance. In TSA, the mortar samples of the ternary blend, which contained 40% slag and 20%

fly ash, had the lowest mass gain in TSA, indicating its improved resistance against formation of gypsum, ettringite, and thaumasite.

11. The mass gain in the ESA conformed to the expansions in the two-year study; the samples with higher expansions had higher mass gains with very good overall correlation for all mixtures. In TSA, such a correlation was only detected within results for each SCM type. This was attributed to the nature of the two deterioration processes. In sodium sulfate attack at 23°C, only expansion in the cement paste occurs, but at 5°C due to cement paste removal mass loss to a huge extent may also occur.

12. There was a very good polynomial correlation between the average expansions and the average mass changes of the mortar samples in the sulfate attack study. Therefore, investigating mass changes along with expansions is helpful in better understanding the performance of mortars in sulfate attack.

13. The studied supplementary cementing materials, when added to PLC, significantly improved the resistance of mortars against thaumasite sulfate attack by maintaining the compressive strength during a one-year exposure to TSA. The control sample prepared with plain PLC lost a significant portion of its strength during that period.

14. Based on the UPV results, the studied SCMs improved the resistance of PLC by delaying the UPV reduction. During a 15-month TSA study on mortar cubes, "L-40 Slag" and "L-40 Slag-20 FA" performed very well by not showing any UPV reduction. These mortar cubes, when visually inspected, did not show any sign of deterioration. Other mixtures showed UPV reduction, particularly those showing greater expansion and visual signs of damage.

15. The compressive strength and the UPV of mortar cubes in TSA changed with similar trends. The test results showed an increase, which was followed by a reduction in some samples during one year of exposure. The other samples did not show a decrease in the compressive strength in a year due to their improved performance. These samples would demonstrate the reduction in the compressive strength and the UPV at later ages after one year. Additionally, there was a reasonable exponential correlation between compressive strength and UPV results. Such a correlation was previously reported in other research.

16. As evidenced by the DSC and XRD study, the mode of sulfate attack to all samples immersed in sodium sulfate solution at 5°C was thaumasite sulfate attack. Formation of gypsum, ettringite, and thaumasite was detected in all the failed CSA A3004-C8 mortar bars in the TSA study. As well, when the surface of the remaining mortar bars after two years was tested, presence of gypsum, ettringite, and thaumasite was confirmed. It should be mentioned that due to its resistance, "L-40 Slag-20 FA" was the only mortar sample, which did show

presence of thaumasite on its surface during the TSA study. This sample also showed the best resistance to sulfate exposure at 5°C considering the expansion, mass changes, compressive strength, and UPV results.

17. According to the DSC results, in the mortar samples, containing similar SCM type and tested at similar ages, an increase in the SCM content caused a decrease in the amount of thaumasite formed during the sulfate exposure at 5°C.

18. The DSC peak related to the dehydration of ettringite/CSH ranged from 88°C to 105°C, the peak for thaumasite dehydration was from 110°C to 119°C for different samples, and the DSC peaks characterized for gypsum were found between 120°C and 134°C. In XRD, presence of these compounds was confirmed indicating the appropriateness of the selected peak temperatures.

19. The differential scanning calorimetry (DSC) was found quite reliable in investigating TSA to samples of Portland-limestone blends.

20. Overall, the findings of this research indicate that although the performance of Portland-limestone cement in thaumasite sulfate attack is extremely weak, addition of specific types of supplementary cementing materials in adequate amounts may improve its resistance against TSA as high sulfate resistant blended Portland-limestone cement. In addition, current recommendations regarding the minimum required replacement levels of SCMs might be too low in some cases.

The recommended amounts are: 40% for slag, 25% for Type F fly ash, and 15% for metakaolin, while this research found that these amounts were not sufficient for achieving a high sulfate resistant blended PLC. However, when 45% slag or 20% metakaolin were added to PLC, the required resistance was reached. Additionally, the present research offers 8% silica fume addition in a binary blend of PLC as well as including 40% slag + 20% fly ash or 35% slag + 15% fly ash in a ternary blend of PLC in order to achieve high sulfate resistant blended PLC.

6-2- Contributions

1. PLC is a recently introduced category of cement in the North America, and according to the literature its performance in sulfate attack is questioned, especially in cold weather. Thus, it is necessary to continue studies on this type of cement in sulfate exposure. The present research is a comprehensive study on the performance of PLC produced in Canada in both ESA and TSA. It has given a valuable perspective of the performance of blends of PLC in sulfate attack when replaced in different percentages with available SCMs in Canada. Almost everywhere in Canada experiences long cold winters; therefore, PLC cannot be practical unless its performance in TSA is improved. This research showed the contribution of different types of SCMs on improvement of PLC resistance against sulfate attack in a comprehensive study.

2. Additionally, the CSA A3001-10 recommendations for use of SCMs in PLC blends were evaluated and it was found that further research is absolutely necessary on the high sulfate resistant blended PLC. Moreover, ternary blends of

PLC were introduced in this research as high sulfate resistant blended PLC. Thus, it was an effective step forward making PLC practical. Increasing the usage of PLC will improve sustainable development and helps moving forward greening the concrete industry.

3. In addition, the present experimental work evaluated mass change, compressive strength, and UPV tests as complements of the expansion test. New horizons are now established for reinforcing the CSA A3004-C8 and devising new improved methods for evaluating resistance of different types of cements in sulfate exposure.

4. Lastly, this research employed differential scanning calorimetry on 23 different mortar samples affected by thaumasite sulfate attack. This technique has not been employed in such an extent for studying TSA. It is well understood from the results that DSC is a reliable technique for detecting formation of gypsum, ettringite, and thaumasite. It can be used instead of XRD or as a supplement. Moreover, intervals for dehydration peaks of gypsum, ettringite, and thaumasite were established which improves the knowledge in the field.

7- Recommendations

1. Considering the present research results and the nature of sulfate attack, investigating the porosity and absorption of mortar samples along with the CSA A3004-C8 standard test would be helpful in studying resistance of different cement types against ESA and TSA. In fact, during the process of sulfate attack, sulfate ions penetrate into the hydrated cement paste, and gypsum, ettringite, and thaumasite are formed in its voids. Therefore, porosity and absorption measurement may help to evaluate the possible resistance against sulfate attack. Such a study can help to develop standard limitations regarding the porosity and absorption of mortar samples in order to develop sulfate resistant cements. As the current CSA standard is extremely time consuming, introducing new criteria for high sulfate resistant cements, which involves porosity and absorption measurements would be of great help. Of course, chemistry of the cement or blended cement has effect on the process of ESA and TSA. In light of this, it looks possible to devise an expansion test together with a porosity and/or absorption measurement. In such case, a dual limit could be specified; a porosity and/or absorption measurement can be preformed at a certain time after casting (for instance at the time of immersion in the sulfate solution), and the expansion test can be devised for shorter test periods.

2. As it was clearly seen in the present research, the mass changes of the CSA A3004-C8 mortar samples had a very good correlation with the expansion results, and it was quite helpful in understanding the performance of mortars in

sulfate attack. Accordingly, the mass change test is recommended to be added to CSA A3004-C8, at least as a noncompulsory procedure. This test is simple and can be easily done at the time of length change test. With further studies on expansion and mass changes of mortar samples, it will be possible to introduce limitations for mass gain and mass loss of the mortar samples.

3. In the sulfate attack test as per CSA A3004-C8 (Also ASTM C1012), before the exposure starts, the mortar samples are cured in limewater until they achieve the compressive strength of 20 ± 1 MPa. This results in different curing times for different types of cement blends. Considering the fact that the standard purpose is to introduce moderate and high sulfate resistant cements to be used in construction, and curing is an extremely important factor that affects the concrete properties, it is essential to keep the curing process explained in the standard as close as possible to the field practices. Noting that usually the curing process in the field is regardless of the cement blend type, it will be more realistic if a unique reasonable curing period is assigned for all samples tested in accordance with the standard. In such case, the comparison between the cement blends would be more accurate and more realistic. It should also be taken to the account that, pozzolanic blends need longer curing until attaining 20 ± 1 MPa, and such curing may not be applied in the field. As an instance, blends of PLC and Type F fly ash need a considerable long curing for a good performance when fly ash is used in large quantities. This can cause problems because a pozzolanic blend can be considered

of better performance compared to a plain cement sample in the lab, while due to insufficient curing period in the field project, it fails the expectations.

4. Another critical difference between the CSA (or ASTM) sulfate attack test and the field practice is the sulfate attack condition. Mortar samples are continuously immersed in sulfate solution during the ESA or TSA standard procedure. Yet, the concrete structures exposed to sulfate ions are usually in a wetting/drying situation. In such case, carbonation may occur on the concrete surface. The carbonated concrete will be more susceptible to TSA. Moreover, during a wetting/drying cycle, in addition to the chemical sulfate attack reactions, physical sulfate crystallization may cause deterioration. In further research, the effect of wetting/drying can be studied especially on TSA in order to improve the standard procedure for sulfate attack. Similar research on concrete cylinders partially submerged in sulfate solution has been performed in ESA (Hartell et al.-2011).

5. The present research showed that the recommendation by CSA A3001-10 for the minimum amounts of slag (40%), fly ash (25%), and metakaolin (15%) to be added to PLC in order to achieve a high sulfate resistant blended PLC needs to be revised by further research on different types of PLC available in Canada. The present research showed that 5% increase in the percentage of slag and metakaolin added to PLC improved the performance of a type of PLC to high sulfate resistant blended PLC. For fly ash, considering its variability, increases in its addition to PLC did not help achieving sulfate resistance. The standard does

not have any recommendations for Type CI and CH fly ash that can be considered in further studies. Moreover, regarding the results of the present research, further studies may concentrate on the performance of ternary blends of PLC in TSA. Considering the fact that fly ash improves the workability of concrete while metakaolin reduces this characteristic, and the successful performance of the ternary PLC blend containing slag and fly ash in this work, studying the performance of ternary PLC blends prepared with a combination of fly ash and metakaolin is recommended. For a new study, PLC blends containing 15% MK + 20% FA, 20% MK + 25% FA, and 25% MK + 30% FA can be taken into account.

6. Unfortunately, the expansion limitations for high and moderate sulfate resistant blended cements in TSA (CSA A3004-C8-B) assigned by CSA A3001-10 are similar. Further research on performance of mortars in TSA is required for a revision and differentiating moderate and high sulfate resistant blended cements.

7. Finally, it should be considered that with sufficient studies on wetting/drying cycles and porosity or absorption measurements, which are recommended in this section, CSA A3004-C8-B can be revised later. As discussed previously, the standard limits for expansion of CSA A3004-C8-B mortar bars is assigned for 18 months that in some cases may be extended to 24 months; in fact, this test is considerably time consuming. It looks reasonably necessary to whether increase the rate of sulfate attack in the test or change the criterion for evaluating sulfate

resistance. For the former, the recommended wetting/drying cycle can be helpful, and for the latter combining a shorter period expansion study (as an instance: 6 months) with the early age porosity and/or absorption measurement would be applicable. Accordingly, the mandate for sulfate resistance could be a combination of porosity at sometime at the early ages (e.g. 7 days) and the 6-month expansion. Definitely, for accomplishing such mandate several experimental studies has to be done to compare the current standard limits with the proposed ones.

8- References

Abdelrazig, B., Main, S., & Nowell, D. (1992). Hydration studies of modified OPC pastes by differential scanning calorimetry and thermogravimetry. *Journal of Thermal Analysis and Calorimetry, 38*(3), 495-504.

ASTM. (2002). ASTM C597, “Standard test method for pulse velocity through concrete”. ASTM International.

ASTM. (2004a). ASTM C150, “Standard specification for Portland cement". ASTM International.

ASTM. (2004b). ASTM C1012, “Standard test method for length change of hydraulic-cement mortars exposed to a sulfate solution”. ASTM International.

ASTM. (2006). ASTM C452, “Standard test method for potential expansion of Portland-cement mortars exposed to sulfate”. ASTM International.

ASTM. (2007). ASTM C150, "Standard specification for Portland cement". ASTM International.

ASTM. (2008a). ASTM C595 “Standard specification for blended hydraulic cements”. ASTM International.

ASTM. (2008b). ASTM C1157, “Standard performance specification for hydraulic cement”. ASTM International.

ASTM. (2012). ASTM C595 “Standard specification for blended hydraulic cements”. ASTM International.

Barker, A., & Hobbs, D. (1999). Performance of Portland-limestone cements in mortar prisms immersed in sulfate solutions at 5 C. *Cement and Concrete Composites, 21*(2), 129-137.

Bellmann, F., & Stark, J. (2007). Prevention of thaumasite formation in concrete exposed to sulphate attack. *Cement and Concrete Research, 37*(8), 1215-1222.

Bellmann, F., & Stark, J. (2008). The role of calcium hydroxide in the formation of thaumasite. *Cement and Concrete Research, 38*(10), 1154-1161.

Bensted, J., & Varma, S. P. (1974). Studies of thaumasite—Part II. *Silicates Industriel, 39*(1), 11-19.

Bensted, J. (1999). Thaumasite—background and nature in deterioration of cements, mortars and concretes. *Cement and Concrete Composites, 21*(2), 117-121.

Berra, M., & Baronio, G. (1987). Thaumasite in deteriorated concretes in the presence of sulphates. *ACI Special Publication, 100*

Bickley, J., Hemmings, R., Hooton, R., & Balinski, J. (1994). Thaumasite related deterioration of concrete structures. *ACI Special Publication, 144*

Bickley, J. A. (1999). The repair of arctic structures damaged by thaumasite. *Cement and Concrete Composites, 21*(2), 155-158.

BRE Special Digest. (2001). Concrete in aggressive ground. *Building Research Establishment*, Watford, UK.

Brueckner, R., Williamson, S., & Clark, L. (2012). Rate of the thaumasite form of sulfate attack under laboratory conditions. *Cement and Concrete Composites, 34*(3), 365-369.

Report of the Thaumasite Expert Group. (1999). The thaumasite form of sulfate attack: Risks, diagnosis, remedial works and guidance on new construction. *Department of the Environment, Transport and the Regions*.

Crammond, N. (2003). The thaumasite form of sulfate attack in the UK. *Cement and Concrete Composites, 25*(8), 809-818.

Crammond, N., Collett, G., & Longworth, T. (2003). Thaumasite field trial at shipston on stour: Three-year preliminary assessment of buried concretes. *Cement and Concrete Composites, 25*(8), 1035-1043.

Crammond, N., & Nixon, P. (1993). Deterioration of concrete foundation piles as a result of thaumasite formation. *Proceedings of the 6th International Conference on Durability of Building Materials and Components, , 1* 295-305.

CSA. (2008a). CSA A3000, “Cementitious materials compendium”. Canadian Standards Association.

CSA. (2008b). CSA A3001, “Cementitious materials for use in concrete”. Canadian Standards Association.

CSA. (2008c). CSA A3004-C1, “Standard practice for mechanical mixing of hydraulic cement mortars and test method for determination of flow”. Canadian Standards Association.

CSA. (2008d). CSA A3004-C2, “Test method for determination of compressive strengths”. Canadian Standards Association.

CSA. (2009). A23.1 - Concrete materials and methods of concrete construction. Canadian Standards Association.

CSA. (2010a). CSA A3000, “Cementitious materials compendium”. Canadian Standards Association.

CSA. (2010b). CSA A3001, “Cementitious materials for use in concrete”. Canadian Standards Association.

CSA. (2010c). CSA A3004-C8, “Test method for determination of expansion of blended hydraulic cement mortar bars due to external sulphate attack”. Canadian Standards Association.

Demirboğa, R., Türkmen, İ., & Karakoc, M. B. (2004). Relationship between ultrasonic velocity and compressive strength for high-volume mineral-admixtured concrete. *Cement and Concrete Research, 34*(12), 2329-2336.

Eriksen, K. (2003). Thaumasite attack on concrete at Marbjerg waterworks. *Cement and Concrete Composites, 25*(8), 1147-1150.

Erlin, B., & Stark, D. C. (1966). Identification and occurrence of thaumasite in concrete a discussion for the 1965 HRB symposium on aggressive fluids. *Highway Research Record,*

European Committee for Standardization. (2000). EN 197-1, “Cement – part 1”, composition, specifications and uniformity criteria for common cements.

Gao, R., Li, Q., Zhao, S., & Yang, X. (2010). Deterioration mechanisms of sulfate attack on concrete under alternate action. *Journal of Wuhan University of Technology-Materials and Science Edition, 25*(2), 355-359.

Gemelli, E., Lourenci, S., Folgueras, M., & Camargo, N. (2004). Assessment of industrial wastes in mortar layers deposited on stainless steel sheets of sinks. *Cerâmica, 50*(316), 336-344.

Ghrici, M., Kenai, S., & Said-Mansour, M. (2007). Mechanical properties and durability of mortar and concrete containing natural pozzolana and limestone blended cements. *Cement and Concrete Composites, 29*(7), 542-549.

Gonzalez, M., & Irassar, E. (1998). Effect of limestone filler on the sulfate resistance of low C_3A Portland cement. *Cement and Concrete Research, 28*(11), 1655-1667.

Hartell, J. A., Boyd, A. J., & Ferraro, C. C. (2011). Sulfate attack on concrete: Effect of partial immersion. *Journal of Materials in Civil Engineering, 23*(5), 572-579.

Hartshorn, S., Sharp, J., & Swamy, R. (1999). Thaumasite formation in Portland-limestone cement pastes. *Cement and Concrete Research, 29*(8), 1331-1340.

Hartshorn, S., Swamy, R., & Sharp, J. (2001). Engineering properties and structural implications of Portland limestone cement mortar exposed to magnesium sulphate attack. *Advances in Cement Research, 13*(1), 31-46.

Higgins, D., & Crammond, N. (2003). Resistance of concrete containing GGBS to the thaumasite form of sulfate attack. *Cement and Concrete Composites, 25*(8), 921-929.

Hime, W. G., & Mather, B. (1999). "Sulfate attack," or is it? *Cement and Concrete Research, 29*(5), 789-791.

Hooton R. D. (2010) "A Review of Different Forms of Sulfate Attack", *presentation*, University of Toronto, Department of Civil Engineering.

Hooton, R., Nokken, M., & Thomas, M. (2007). Portland-limestone cement: State-of-the-art report and gap analysis for CSA A3000. *Cement Association of Canada Research and,*

Hooton, R., Ramezanianpour, A., & Schutz, U. (2010). Decreasing the clinker component in cementing materials: Performance of Portland-limestone cements in concrete in combination with supplementary cementing materials. *Concrete Sustainability Conference, National Ready Mixed Concrete Association, Tempe, AZ, USA*

İnan Sezer, G. (2012). Compressive strength and sulfate resistance of limestone and/or silica fume mortars. *Construction and Building Materials, 26*(1), 613-618.

Khan, S. R., Noorzaei, J., Kadir, M., Waleed, A., & Jaafar, M. (2007). UPV method for strength detection of high performance concrete. *Structural Survey, 25*(1), 61-73.

Köhler, S., Heinz, D., & Urbonas, L. (2006). Effect of ettringite on thaumasite formation. *Cement and Concrete Research, 36*(4), 697-706.

Komlos, K., Popovics, S., Nürnbergerova, T., Babal, B., & Popovics, J. (1996). Ultrasonic pulse velocity test of concrete properties as specified in various standards. *Cement and Concrete Composites, 18*(5), 357-364.

Long, G., Xie, Y., Deng, D., & Li, X. (2011). Deterioration of concrete in railway tunnel suffering from sulfate attack. *Journal of Central South University of Technology, 18*(3), 881-888.

Longworth, T. (2003). Contribution of construction activity to aggressive ground conditions causing the thaumasite form of sulfate attack to concrete in pyritic ground. *Cement and Concrete Composites, 25*(8), 1005-1013.

Ma, B., Gao, X., Byars, E. A., & Zhou, Q. (2006). Thaumasite formation in a tunnel of Bapanxia dam in western china. *Cement and Concrete Research, 36*(4), 716-722.

Matthews, J. D. (1994). Performance of limestone filler cement concrete. *In Euro-Cements – Impact of ENV 197 on Concrete Construction, (Ed. R. K. Dhir and M. R. Jones)*, E&FN Spon, London, 113-147.

Mehta, P. K. (2002). Greening of the concrete industry for sustainable development. *Concrete International,* 23-28.

Mingyu, H., Fumei, L., & Mingshu, T. (2006). The thaumasite form of sulfate attack in concrete of Yongan dam. *Cement and Concrete Research, 36*(10)

Mulenga, D., Stark, J., & Nobst, P. (2003). Thaumasite formation in concrete and mortars containing fly ash. *Cement and Concrete Composites, 25*(8), 907-912.

Neville, A. M., & Brooks, J. J. (1987). *Concrete technology*

Oberholster, R., Du Toit, P., & Pretorius, J. (1984). Deterioration of concrete containing a carbonaceous sulphide-bearing aggregate. *Proceedings of the 6th International Conference on Cement Microscopy,* 360-373.

Ou, Z. H., Ma, B. G., & Jian, S. W. (2011). Comparison of FT-IR, thermal analysis and XRD for determination of products of cement hydration. *Advanced Materials Research, 168*, 518-522.

Patsikas, N., Katsiotis, N., Pipilikaki, P., Papageorgiou, D., Chaniotakis, E., & Beazi-Katsioti, M. (2012). Durability of mortars of white cement against sulfate attack in elevated temperatures. *Construction and Building Materials, 36*, 1082-1089.

Pipilikaki, P., Papageorgiou, D., Teas, C., Chaniotakis, E., & Katsioti, M. (2008). The effect of temperature on thaumasite formation. *Cement and Concrete Composites, 30*(10), 964-969.

Qu, G., & Zhang, A. (2012). Influence of temperature on the resistance to sulfate attack of limestone filler concrete. *Revista Română De Materiale/Romanian Journal of Materials, 42*(4), 381-386. (in English)

Ramezanianpour, A. M. (2012). (PhD, University of Toronto). *Sulfate Resistance and Properties of Portland-Limestone Cements,*

Ramezanianpour, A. M., & Hooton, R. D. (2013a). Sulfate resistance of Portland-limestone cements in combination with supplementary cementitious materials. *Materials and Structures, 46*(7), 1061-1073.

Ramezanianpour, A. M., & Hooton, R. D. (2013b). Thaumasite sulfate attack in Portland and Portland-limestone cement mortars exposed to sulfate solution. *Construction and Building Materials, 40*, 162-173.

Révay, M., & Gável, V. (2003). Thaumasite sulphate attack at the concrete structures of the Ferenc Puskás stadium in Budapest. *Cement and Concrete Composites, 25*(8), 1151-1155.

Romer, M., Holzer, L., & Pfiffner, M. (2003). Swiss tunnel structures: Concrete damage by formation of thaumasite. *Cement and Concrete Composites, 25*(8), 1111-1117.

Santhanam, M., Cohen, M. D., & Olek, J. (2001). Sulfate attack research – whither now? *Cement and Concrete Research, 31*(6), 845-851.

Santhanam, M., Cohen, M. D., & Olek, J. (2003a). Effects of gypsum formation on the performance of cement mortars during external sulfate attack. *Cement and Concrete Research, 33*(3), 325-332.

Santhanam, M., Cohen, M. D., & Olek, J. (2003b). Mechanism of sulfate attack: A fresh look: Part 2. Proposed mechanisms. *Cement and Concrete Research, 33*(3), 341-346.

Schmidt, M. (1992). Cement with interground additives--capabilities and environmental relief: II. *ZKG International, Edition B, 45*(6), 296-301.

Schneider, M., Romer, M., Tschudin, M., & Bolio, H. (2011). Sustainable cement production – present and future. *Cement and Concrete Research, 41*(7), 642-650.

Scrivener, K., & Skalny, J. (2002). Internal sulphate attack and delayed ettringite formation. *Rilem Proceedings PRO 35, Proc. of the International Rilem TC 186-ISA Workshop,* 4-6.

Scrivener, K. L., & Young, J. F. (1997). *Mechanisms of chemical degradation of cement-based systems: Proceedings of the materials research society's symposium on mechanisms of chemical degradation of cement-based systems, Boston, USA, 27-30 November 1995* Taylor & Francis.

Senhadji, Y., Mouli, M., Khelafi, H., & Benosman, A. S. (2010). Sulfate attack of Algerian cement-based material with crushed limestone filler cured at different temperatures. *Turkish Journal of Engineering and Environmental Science, 34*, 131-143.

Sha, W., O'Neill, E., & Guo, Z. (1999). Differential scanning calorimetry study of ordinary Portland cement. *Cement and Concrete Research, 29*(9), 1487-1489.

Shannag, M., & Shaia, H. A. (2003). Sulfate resistance of high-performance concrete. *Cement and Concrete Composites, 25*(3), 363-369.

Sharp, J. H. (2006). Surely we know all about cement–don't we?. *Advances in Applied Ceramics, 105*(4), 162-174.

Schmidt, M., Middendorf, B., & Singh, N. B. (2010). Blended Cements. *Portland Cement Association*, Modern Cement Chemistry, Chapter 10, SP409, Skokie, Illinois, USA.

Shi, C., Wang, D., & Behnood, A. (2012). Review of thaumasite sulfate attack on cement mortar and concrete. *Journal of Materials in Civil Engineering, 24*(12), 1450-1460.

Skalny, J., Marchand, J., & Odler, I. (2002). *Sulfate attack on concrete* Spon Press London.

Skaropoulou, A., Kakali, G., & Tsivilis, S. (2006). A study on thaumasite form of sulfate attack (TSA) using XRD, TG and SEM. *Journal of Thermal Analysis and Calorimetry, 84*(1), 135-139.

Skaropoulou, A., Tsivilis, S., Kakali, G., Sharp, J., & Swamy, R. (2009a). Long term behavior of Portland limestone cement mortars exposed to magnesium sulfate attack. *Cement and Concrete Composites, 31*(9), 628-636.

Skaropoulou, A., Tsivilis, S., Kakali, G., Sharp, J., & Swamy, R. (2009b). Thaumasite form of sulfate attack in limestone cement mortars: A study on long term efficiency of mineral admixtures. *Construction and Building Materials, 23*(6), 2338-2345.

Smallwood, I., Wild, S., & Morgan, E. (2003). The resistance of metakaolin (MK)–Portland cement (PC) concrete to the thaumasite-type of sulfate attack (TSA)—Programme of research and preliminary results. *Cement and Concrete Composites, 25*(8), 931-938.

Sotiriadis, K., Nikolopoulou, E., & Tsivilis, S. (2012). Sulfate resistance of limestone cement concrete exposed to combined chloride and sulfate environment at low temperature. *Cement and Concrete Composites, 34*(8), 903-910.

Tennis, P., Thomas, M., & Weiss, W. (2011). State-of-the-art report on use of limestone in cements at levels of up to 15%–SN3148. *Portland Cement Association, Skokie, IL, USA*

Thomas, M., & Hooton, R. (2010). The durability of concrete produced with Portland-limestone cement: Canadian studies-SN3142. *Portland Cement Association, Skokie, IL, USA,*

Thomas, M., Rogers, C., & Bleszynski, R. (2003). Occurrences of thaumasite in laboratory and field concrete. *Cement and Concrete Composites, 25*(8), 1045-1050.

Torres, S., Sharp, J., Swamy, R., Lynsdale, C., & Huntley, S. (2003). Long term durability of Portland-limestone cement mortars exposed to magnesium sulfate attack. *Cement and Concrete Composites, 25*(8), 947-954.

Toutanji, H. (2000). Ultrasonic wave velocity signal interpretation of simulated concrete bridge decks. *Materials and Structures, 33*(3), 207-215.

Trtnik, G., Kavčič, F., & Turk, G. (2009). Prediction of concrete strength using ultrasonic pulse velocity and artificial neural networks. *Ultrasonics, 49*(1), 53-60.

Tsivilis, S., Kakali, G., Skaropoulou, A., Sharp, J., & Swamy, R. (2003). Use of mineral admixtures to prevent thaumasite formation in limestone cement mortar. *Cement and Concrete Composites, 25*(8), 969-976.

Türkmen, İ. (2003). Influence of different curing conditions on the physical and mechanical properties of concretes with admixtures of silica fume and blast furnace slag. *Materials Letters, 57*(29), 4560-4569.

Vedalakshmi, R., Sundara Raj, A., & Palaniswamy, N. (2008). Identification of various chemical phenomena in concrete using thermal analysis. *Indian Journal of Chemical Technology, 15*(4), 388-396.

Vuk, T., Gabrovšek, R., & Kaučič, V. (2002). The influence of mineral admixtures on sulfate resistance of limestone cement pastes aged in cold $MgSO_4$ solution. *Cement and Concrete Research, 32*(6), 943-948.

Yaman, I. O., Inci, G., Yesiller, N., & Aktan, H. M. (2001). Ultrasonic pulse velocity in concrete using direct and indirect transmission. *ACI Materials Journal, 98*(6), 450-457.

Zelić, J., Krstulović, R., Tkalčec, E., & Krolo, P. (1999). Durability of the hydrated limestone-silica fume Portland cement mortars under sulphate attack. *Cement and Concrete Research, 29*(6), 819-826.

Zhang, F., Ma, B., Wu, S., & Zhou, J. (2011). Effect of fly ash on TSA resistance of cement-based material. *Journal of Wuhan University of Technology-Material Science Edition, 26*(3), 561-566.